U.PORTO
FEUP FACULDADE DE ENGENHARIA
UNIVERSIDADE DO PORTO

The Effect of Biofilm Formation on Recombinant Protein Expression

A Dissertation presented to the
UNIVERSITY OF PORTO
for the degree of Doctor in
Chemical and Biological Engineering
by

Luciana Calheiros Gomes

Supervisor: Prof. Filipe J. Mergulhão
Co-supervisor: Prof. Luís F. Melo

Lepabe
Laboratory for Process Engineering, Environment, Biotechnology and Energy

LEPABE – Laboratory for Process Engineering, Environment, Biotechnology and Energy
Department of Chemical Engineering
Faculty of Engineering, University of Porto
October, 2016

COMPETE 2020
PORTUGAL 2020
UNIÃO EUROPEIA
Fundo Europeu de Desenvolvimento Regional
FCT
Fundação para a Ciência e a Tecnologia

“Para ser grande, sê inteiro: nada
Teu exagera ou exclui.
Sê todo em cada coisa. Põe quanto és
No mínimo que fazes.”

Ricardo Reis

Acknowledgments

I would like to express my sincere gratitude to my supervisor Prof. Filipe Mergulhão for the personal and scientific guidance throughout my studies. I also would like to thank his pertinent suggestions and criticisms, as well as the invaluable trust, availability and encouragement. The knowledge I gained from him, in both academic and non-academic matters, has been precious and will definitely be crucial to my future career.

I am also grateful to my co-supervisor Prof. Luís de Melo and to Prof. Manuel Simões for having always showed a constant cooperation and support.

I would like to thank to Dr. João Miranda and Dr. José Araújo from the Centro de Estudos de Fenómenos de Transporte (CEFT) group for the numerical simulations.

I would like to acknowledge the PhD scholarship (SFRH/BD/80400/2011) from Fundação para a Ciência e Tecnologia (FCT), who funded this study.

To all those in the Department of Chemical Engineering and LEPABE, I would like to express my sincere thanks for providing good working facilities.

To Prof. Gabriel Monteiro and Dr. Romain Briandet, I am grateful for receiving me so well in their research groups in the Institute for Bioengineering and Biosciences (iBB) in Instituto Superior Técnico (IST), and INRA in AgroParisTech, respectively.

To all my LabE007 and E008 colleagues, with special thanks to Ana Luísa, Anabela, Andreia, Catarina and Sílvia Fontenete, who were with me during all these years. I also would like to thank to Joana Moreira and Carla Ferreira for being always ready to help me.

To Sofia, Sílvia Andrade and Joana Serra from iBB, my sincere gratitude for sharing knowledge in molecular biology and helping me with the PCR “stuff”. To Julien Deschamps from INRA, I acknowledge the technical assistance with CLSM imaging. To Daniel Carvalho, I would like to thank for helping in image processing with ImageJ.

I would like to thank to my family, especially to my parents and my brother for the patience and unconditional support. To João P., I thank for all the optimism and love. Thank you for believing in my skills and in a bright future!

Last but not least, I would like to thank to all my friends, especially to Ju, Carla, Vera, Pedro’s and Chiote, for the good times that we always had together.

Thank you!

Scientific outputs

The results presented in this thesis are partially published/submitted in:

Papers in peer-reviewed journals

Gomes LC, Moreira JMR, Miranda JM, Simões M, Melo LF, Mergulhão FJ. 2013. Macroscale *versus* microscale methods for physiological analysis of biofilms formed in 96-well microtiter plates. Journal of Microbiological Methods. 95:342-349. (doi: 10.1016/j.mimet.2013.10.002) (**Chapter 4**)

Gomes LC, Moreira JMR, Teodósio JS, Araújo JDP, Miranda JM, Simões M, Melo LF, Mergulhão FJ. 2014. 96-well microtiter plates for biofouling simulation in biomedical settings. Biofouling. 30:535-546. (doi: 10.1080/08927014.2014.890713) (**Chapter 3**)

Gomes LC, Moreira JMR, Simões M, Melo LF, Mergulhão FJ. 2014. Biofilm localization in the vertical wall of shaking 96-well plates. Scientifica, vol. 2014, Article ID 231083, 6 pages. (doi: 10.1155/2014/231083) (**Chapter 4**)

Gomes LC, Carvalho D, Briandet R, Mergulhão FJ. Temporal variation of recombinant protein expression in *Escherichia coli* biofilms analysed at single-cell level. Process Biochemistry. 51: 1155-1161. (doi:10.1016/j.procbio.2016.05.016) (**Chapter 7**)

Gomes LC, Mergulhão FJ. Heterologous protein production in *Escherichia coli* biofilms: a non-conventional form of high cell density cultivation. Process Biochemistry (accepted). (**Chapter 5**)

Gomes LC, Mergulhão FJ. Effects of antibiotic concentration and nutrient medium composition on *Escherichia coli* biofilm formation and GFP expression. FEMS Microbiology Letters (submitted). (**Chapter 6**)

Book chapters

Gomes LC, Araújo PA, Teodósio JS, Simões M, Mergulhão FJ. 2014. The Effect of Plasmids and Other Biomolecules on the Effectiveness of Antibiofilm Agents. In: Rumbaugh K.P., Ahmad I, editors. Antibiofilm Agents. Berlin: Springer-Verlag, p. 161-174.

Other publications (abstracts in international conferences)

Gomes LC, Moreira JMR, Teodósio JS, Araújo JDP, Miranda JM, Simões M, Melo LF, Mergulhão FJ. 2012. Microtiter plates for biofilm formation in biomedical settings. Biofilms 5, Paris.

Gomes LC, Araújo PA, Teodósio JS, Simões M, Mergulhão FJ. 2013. The effect of plasmids and other biomolecules on the effectiveness of antibiofilm agents. Eurobiofilms 2013, Ghent.

Gomes LC, Moreira JMR, Simões M, Melo LF, Mergulhão FJ. 2013. SEM as a powerful tool to analyse the heterogeneity of biofilms formed in 96-well microtiter plates. International Multidisciplinary Microscopy Congress - INTERM 2013, Antalya.

Gomes LC, Moreira JMR, Araújo JDP, Miranda JM, Simões M, Melo LF, Mergulhão FJ. 2014. Medical biofilms easily simulated in 96-well microtiter plates. International Conference on Antimicrobial Research - ICAR 2014, Madrid.

Gomes LC, Moreira JMR, Araújo JDP, Miranda JM, Simões M, Melo LF, Mergulhão FJ. 2014. Use of 96-well microtiter plates to reproduce medical biofilms. Biofilms 6, Vienna.

Gomes LC, Melo LF, Mergulhão FJ. 2015. The effect of recombinant protein expression on *Escherichia coli* biofilm formation and resistance. 8th Conference on Recombinant Protein Production - RPP8, Mallorca.

Abstract

Bacterial biofilms are usually known for their negative effects, but they can also be applied on the industrial-scale production of added-value products such as bioethanol, organic acids and enzymes. The main goal of this thesis was to assess the potential of *Escherichia coli* biofilms to produce a model heterologous protein, the enhanced green fluorescent protein (eGFP), from a recombinant plasmid. Besides being an excellent model for biofilm studies, *E. coli* is one of the favourite hosts for recombinant protein expression. Versatile genetic tools are available for high-level protein expression in this Gram-negative bacterium, where expression induction is simple and cost-effective. Two biofilm formation platforms were used in this work, the 96-well microtiter plate for screening purposes and a flow cell for long-term biofilm formation assays.

Microtiter plates are one of the most commonly used biofilm formation platforms. However, hydrodynamic conditions inside those plates are poorly understood and therefore computational fluid dynamics (CFD) was used to determine the shear rate distribution in 96-well microtiter plates for different orbital diameters and shaking frequencies. Numerical simulations indicated that the 96-well microtiter plate is a powerful platform for biofilm formation and that the hydrodynamic conditions inside their wells are able to simulate those found in a variety of applications, including biomedical scenarios, if the right operating conditions are used. Although the macroscale techniques used (crystal violet and resazurin) did not reveal bulk differences on the amount and metabolic state of sessile cells when comparing shaking with static conditions, scanning electron microscopy (SEM) showed that biofilm deposition and morphology was not uniform and that the biofilm characteristics correlate strongly with local shear strain rates along the wall of the well. The higher shear rates below the interface were associated with the formation of dispersed aggregates containing cells of smaller size, while a decrease in the shear rate values resulted in a homogeneous distribution of single cells of larger size. A differential crystal violet (CV) staining method was also used to determine the spatial location of biofilms in microtiter plates. The results

obtained by this novel method and by SEM reinforce the need to complement macroscale approaches with a microscale analysis of biofilms.

The interaction between heterologous protein production and biofilm formation was first assessed on *E. coli* JM109(DE3) cells transformed with plasmid pFM23 for eGFP expression, using as control a strain harbouring the same plasmid backbone but lacking the *eGFP* gene (plasmid pET28A). Results showed that biofilm formation was enhanced for the eGFP-producing strain. Furthermore, it was found that the specific protein production from biofilm cells was about 30 fold higher than in planktonic state and that the volumetric productivity is already within the range that can be obtained by conventional high cell density cultures (HCDCs), even before optimization of cultivation conditions.

Recombinant protein production is dependent on many factors, including the composition of the culture medium. Increasing the kanamycin (selection marker) concentration had a modest effect on the specific eGFP production of biofilm cells, but the change of diluted medium (DM) to lysogeny broth (LB) led to increased eGFP expression in both planktonic and sessile states (20 fold and 2 fold, respectively). Single-cell scale analysis of the biofilms has shown that eGFP expression was highly heterogeneous and that this heterogeneity increased with time. Biofilm analysis by confocal microscopy revealed that this heterogeneity is probably due to the fact that expressing cells are located in the upper layers of the biofilm where oxygen penetration readily occurs. Concerning chemical induction by isopropyl-β-D-thiogalactoside (IPTG), it was observed that the inducer increased the eGFP levels in biofilm cells when compared to the non-induced culture and that the expression profile was not associated with the gene dosage. It was also established that the biofilm environment enhances plasmid retention. Additionally, biofilm analysis at single-cell scale revealed that the producing capacity of the biofilm system is limited by the low percentage of eGFP-expressing cells. The indentification of this bottleneck enables the further design of optimization strategies to increase the potential of *E. coli* biofilms for recombinant protein production.

Keywords: Biofilm*; Escherichia coli*; microtiter plate; hydrodynamics; plasmid; recombinant protein production; enhanced green fluorescent protein; flow cell.

Resumo

Os biofilmes bacterianos são geralmente conhecidos pelos seus efeitos negativos, embora sejam também aplicados na produção de produtos de valor acrescentado à escala industrial, como o bioetanol, ácidos orgânicos e enzimas. O objetivo principal desta tese foi avaliar o potencial dos biofilmes de *Escherichia coli* na produção de um modelo de proteína heteróloga, a proteína verde fluorescente melhorada (em inglês "enhanced green florescent protein" ou eGPF), a partir de um plasmídeo recombinante. Além de ser um excelente modelo para estudos de biofilme, a *E. coli* é um dos hospedeiros preferidos para a expressão de proteínas recombinantes. Ferramentas genéticas versáteis estão disponíveis para a elevada expressão de proteínas nesta bactéria Gram-negativa, onde a indução da expressão é simples e de baixo custo. Neste trabalho foram usadas duas plataformas para a formação de biofilme, a microplaca de 96 poços para rastreio e uma célula de fluxo para ensaios longos de formação de biofilme.

As microplacas são uma das plataformas de formação de biofilme mais utilizadas. Contudo, desconhece-se as condições hidrodinâmicas dentro dessas placas, pelo que a dinâmica de fluídos computacional (em inglês "computational fluid dynamics" ou CFD) foi usada para determinar a distribuição da taxa de deformação (em inglês "shear strain rate") em microplacas de 96 poços sujeitas a diferentes diâmetros de orbital e frequências de agitação. As simulações numéricas indicaram que a microplaca de 96 poços é uma plataforma poderosa para a formação de biofilme e que as condições hidrodinâmicas dentro dos seus poços são capazes de simular os biofilmes encontrados em diferentes locais, incluindo cenários biomédicos, se forem selecionadas as condições operacionais adequadas. Embora as técnicas à macroescala utilizadas (violeta de cristal e resazurina) não tenham revelado diferenças na quantidade e estado metabólico das células sésseis comparando condições de agitação com condições estáticas, a microscopia eletrónica de varrimento (em inglês "scanning electron microscopy" ou SEM) mostrou que a deposição e morfologia do biofilme não foi uniforme e que as suas características se correlacionam fortemente com taxas de deformação locais ao longo da parede do poço. As taxas de deformação mais elevadas encontradas abaixo da interface estão associadas à formação

de agregados dispersos contendo células de tamanho mais pequeno, enquanto uma diminuição nos valores da taxa de deformação resultou numa distribuição homogénea de células individuais de tamanho maior. Um método de coloração diferencial com violeta de cristal foi também usado para determinar a localização espacial dos biofilmes nas microplacas. Os resultados obtidos por este novo método e por microscopia eletrónica de varrimento reforçam a necessidade de complementar as abordagens à macroescala com uma análise à escala micro dos biofilmes.

A interação entre a produção da proteína heteróloga e a formação de biofilme foi avaliada em primeiro lugar em células de *E. coli* JM109(DE3) transformadas com o plasmídeo pFM23 para a expressão de eGFP, utilizando como controlo uma estirpe que contém um plasmídeo com os mesmos elementos, mas ao qual falta o gene da eGFP (plasmídeo pET28A). Os resultados mostraram que a formação de biofilme foi superior para a estirpe produtora de eGFP. Verificou-se também que a produção específica de proteína nas células do biofilme foi cerca de 30 vezes maior do que nas células planctónicas em estado estacionário, e que a produtividade volumétrica está já dentro da gama que pode ser obtida com culturas convencionais de elevada densidade celular (em inglês "high cell density cultures" ou HCDCs), mesmo sem otimização das condições de cultura.

A produção de proteína recombinante depende de muitos fatores, incluindo a composição do meio de cultura. Aumentar a concentração de canamicina (marcador de seleção) teve um efeito modesto na produção específica de eGFP nas células do biofilme, mas a mudança do meio diluído (DM) para o meio lisogénico (em inglês "lysogeny broth" ou LB) conduziu a um aumento da expressão de GFP nos estados planctónico e séssil (20 e 2 vezes mais, respetivamente). A análise dos biofilmes à escala celular mostrou que a expressão de eGFP foi altamente heterogénea e que esta heterogeneidade aumentou com o tempo. A análise do biofilme por microscopia confocal revelou que a heterogeneidade se deve provavelmente ao facto de as células que expressam estarem localizadas nas camadas mais externas do biofilme em que a penetração do oxigénio é facilitada. No que diz respeito à indução química com isopropil-β-D-tiogalactosídeo (IPTG), observou-se que o indutor aumentou os níveis de eGFP nas células do biofilme quando comparado com a cultura não induzida e que o perfil de expressão não está relacionado com a dosagem génica. Foi também estabelecido que o biofilme promove a retenção do plasmídeo. Além disso, a análise do biofilme à escala celular revelou que a capacidade de produção do sistema de biofilme é limitada pela baixa percentagem de células que

expressam eGFP. A identificação desta limitação permite o posterior desenho de estratégias de otimização de modo a aumentar o potencial dos biofilmes de *E. coli* na produção de proteínas recombinantes.

Palavras-chave: Biofilme; *Escherichia coli*; microplaca; hidrodinâmica; plasmídeo; produção de proteína recombinante; proteína verde fluorescente melhorada; célula de fluxo.

Table of contents

List of figures

Chapter 2

Chapter 3

Chapter 4

Chapter 6

Chapter 7

Chapter 8

Chapter 9

List of tables

Chapter 8

Nomenclature

Abbreviations

AFM	atomic force microscopy
AFU	arbitrary fluorescent unit
ATP	adenosine triphosphate
BCA	bicinchoninic acid protein
cDNA	complementary DNA
CCD	charge-coupled device
CFD	computational fluid dynamics
CFU	colony forming unit
CLSM	confocal laser scanning microscopy
C_T	cycle threshold
CV	crystal violet
DAPI	4’,6-diamidino-2-phenylindole
DM	diluted medium
DNA	deoxyribonucleic acid
eGFP	enhanced green fluorescent protein
EPS	extracellular polymeric substances
ESEM	environmental scanning electron microscopy
FISH	fluorescence *in situ* hybridization
GFP	green fluorescent protein
HCDC	high cell density culture
HMDS	hexamethyldisilazane
IPTG	isopropyl-β-D-thiogalactoside

LB	lysogeny broth
OCT	optical coherence tomography
OD	optical density
pDNA	plasmid DNA
PCN	plasmid copy number
PI	propidium iodide
PNA	peptide nucleic acid
PS	polystyrene
PVC	polyvinyl chloride
Q-cell	quiescent cell
RNA	ribonucleic acid
RNAP	RNA polymerase
RT-PCR	real time-polymerase chain reaction
SD	standard deviation
SEM	scanning electron microscopy
TEM	transmission electron microscopy
TVS	total volatile solids
UTI	urinary tract infection
UV	ultraviolet
VBNC	viable but non-culturable cell
VBNE	viable but non-expressing cell
VOF	volume of fluid

Symbols

a_f	specific surface area in a dynamic well (L^{-1})
a_i	specific surface area in a stationary well (L^{-1})
A	coupon area (L^2)
A_w	wetted area for a dynamic well (L^2)

A_{wi}	wetted area for a stationary well (L^2)
C	bulk IPTG concentration ($M\ L^{-3}$)
d	hydraulic diameter (L)
d_0	shaking diameter (L)
D	well diameter (L)
D_{aq}	diffusion coefficient ($L^2\ T^{-1}$)
DR	dilution rate (T^{-1})
F	volumetric flow rate ($L^3\ T^{-1}$)
h	maximum height of interface (L)
H	well height (L)
K_m	external mass transfer coefficient ($L\ T^{-1}$)
$\dot{n}$	mass transfer rate ($M\ T^{-1}$)
Re	Reynolds number (-)
Sc	Schmidt number (-)
Sh	Sherwood number (-)
t	time (T)
V	volume of flow cell system (L^3)
θ	surface angle (º)
τ	average residence time (T)

1.

Introduction

1.1. Relevance and motivation

Biofilms are communities of microbial cells that grow on living or inert surfaces and surround themselves with secreted polymers. Bacterial biofilms are often unwanted since they can cause water contamination in potable distribution systems (Simões et al. 2010a), infection or clogging of medical devices (Bryers 2008), contamination of household products and food preparations (Bridier et al. 2015), and biofouling of heat exchange systems (Pogiatzis et al. 2015). Nevertheless, biofilms can find application in processes as diverse as the production of industrial chemicals like ethanol, butanol and lactic acid (Qureshi et al. 2005, Qureshi et al. 2004), bioremediation (Edwards & Kjellerup 2013, Singh et al. 2006), wastewater treatment (Nicolella et al. 2000), and even generation of electricity in microbial fuel cells (Cristiani et al. 2013).

The field of recombinant protein production has historically focused on bacteria growing in liquid culture. However, the natural state for many bacteria is not to grow in liquid culture, but rather living as a community attached to a surface. Recombinant protein production in biofilms has been studied in the context of waste biodegradation (Bryers & Huang 1995, Venkata Mohan et al. 2009), but this approach could also be advantageous for the biosynthesis of pharmaceutical intermediates and catalysts for the food industry.

The Gram-negative bacterium *Escherichia coli* is a preferred host for the production of recombinant proteins (Mergulhão et al. 2004b, Sanchez-Garcia et al. 2016) due to its fast growth at high cell densities, minimal nutrient requirements, well-known genetics and the availability of a large number of cloning vectors and mutant host strains (Baneyx 1999). *E. coli* has the ability to accumulate many recombinant proteins to at least

20% of the total cell protein content (Pines & Inouye 1999) and, in some cases, to translocate them from the cytoplasm to the periplasm (Mergulhão et al. 2005). Despite its natural inability to perform some post-translational modifications like glycosylation (Rosano & Ceccarelli 2014) and its limited secretion capacity (Folch et al. 1957, Mergulhão et al. 2005), *E. coli* remains at the forefront of the expression systems used for the production of many recombinant proteins. For example, among marketed biopharmaceuticals for antitumoral therapies, 69% are produced in *E. coli* against only 26% produced in mammalian cells (Sanchez-Garcia et al. 2016).

Recombinant protein expression in *E. coli* biofilms was pioneered by Huang et al. (1993, 1994a, 1995) who have compared the production of β-galactosidase in *E. coli* DH5α planktonic and biofilm cells. These authors found that the recombinant protein was successfully produced in biofilm cells, although at low level than in planktonic cells (Bryers & Huang 1995, Huang et al. 1993). Much later, O'Connell et al. (2007) have described the first system for high level heterologous protein production in *E. coli* biofilm cells using a pUC-based vector for the expression of enhanced green fluorescent protein (eGFP). It has been shown that the biofilm environment enhanced the production of eGFP when compared to planktonic cells. Additionally, continuous biofilm cultures for heterologous protein production were beneficial for retention of plasmid-bearing cells when compared to chemostats (O'Connell et al. 2007). Despite the enormous potential of this expressing system, this subject remains largely unexplored.

In a previous work, our research group showed that the presence of the non-conjugative plasmid pET28A in *E. coli* JM109(DE3) cells increased biofilm formation under turbulent flow conditions when compared to a non-transformed strain (Teodósio et al. 2012a). Having established this, it is pertinent to ask if the additional metabolic load imposed by the introduction of an eGFP-coding cassette into this plasmid has a further impact on biofilm formation.

The role of plasmids in bacterial biofilms is likely much more complex than what is observed in homogeneous batch cultures (Cook & Dunny 2014). Recombinant protein expression in biofilms is probably highly heterogeneous and may allow for the development of subgroups within the biofilm population that are specifically poised to react to different environments and stimuli. By performing single-cell analysis during biofilm development, one can better understand the physiology of biofilm cells and optimize the operational factors that can lead to a higher specific production of recombinant proteins by these cells with potential industrial application.

1.2. Objectives and outline

The main objective of this thesis was to assess the potential of *E. coli* biofilms to express a model heterologous protein, the eGFP, from a recombinant plasmid. Two biofilm formation platforms were used for this purpose - flow cells and agitated microtiter plates. Microtiter plates were used essentially for screening purposes due to their high throughput. Flow cells were used for long-term assays and both platforms were used in controlled hydrodynamic conditions.

For expression studies, plasmid pFM23 was used (Mergulhão et al. 2004a). This vector has the backbone of plasmid pET28A, harbouring the T7 promoter for the cytoplasmic production of eGFP, which can be induced by the non-hydrolysable lactose analogue isopropyl-β-D-thiogalactoside (IPTG). Since heterologous protein production is dependent on several cultivation factors, the influence of antibiotic concentration (used to maintain the selective pressure), nutrient medium composition and IPTG induction on eGFP expression and biofilm formation was evaluated. This study was complemented by a single-cell analysis technique to provide information on the fluorescent protein distribution in individual cells, which may be important for bioprocess monitoring, particularly when using biofilms that are known to be highly heterogeneous. The final purpose of this work was to identify cellular bottlenecks in biofilm systems, enabling the development of efficient strategies to increase the production of heterologous proteins in sessile cells.

This thesis is outlined as follows:

Chapter 2 is a brief literature review describing the state of the art pertaining to this thesis.

In the following two chapters, a detailed characterization of the hydrodynamic conditions inside the biofilm platform used for screening purposes - the 96-well microtiter plate - was made.

In **Chapter 3**, the influence of hydrodynamic conditions and nutrient concentration on *E. coli* biofilm formation in the 96-well microtiter plate was assessed. Computational fluid dynamics (CFD) was performed to characterize the hydrodynamics inside the wells of a 96-well microtiter plate under different orbital shaking conditions, as well as to define the operational conditions to be used in order to simulate relevant biomedical scenarios where biofilms develop. It was also intended to verify if the microtiter plate can reproduce the shear forces experienced in a flow cell operated under turbulent regime.

In **Chapter 4**, macroscale and microscale methods were used to study the impact of hydrodynamic conditions on the location and amount of biofilms formed on the vertical walls of 96-well plates. A new method was developed by combining the high throughput features of the common crystal violet (CV) staining with the determination of the spatial localization of the biofilm without the use of expensive equipment such as scanning electron microscopes.

After this initial hydrodynamic characterization, the following studies on the impact of *E. coli* biofilm formation on recombinant protein production were performed in a flow cell system.

Chapter 5 evaluates the potential of *E. coli* JM109(DE3) biofilm cells to express a model protein (eGFP) from a recombinant plasmid (plasmid pFM23). This strain was compared with a control strain containing the same plasmid backbone but lacking the *eGFP* gene (vector pET28A). The fluorescence of eGFP enabled the analysis of recombinant protein expression levels in both planktonic and biofilm cells.

In **Chapter 6**, the influence of culture conditions - antibiotic concentration and nutrient medium composition - on the expression of the heterologous protein in biofilms was assessed. *E. coli* JM109(DE3) cells transformed with plasmid pFM23 were used. This vector contains a kanamycin resistance gene. The 96-well microtiter plate was used for the initial screening of kanamycin concentrations. Then, a flow cell system was used to expose the bacterial cells to two kanamycin concentrations (20 or 30 µg ml^{-1}) during biofilm development in two different culture media, a diluted medium (DM) and the lysogeny broth (LB).

Chapter 7 presents a simple and accurate method using fluorescence imaging for quantifying the leaky expression of eGFP within a biofilm population at bulk and single-cell levels.

In **Chapter 8**, the effects of IPTG induction on *E. coli* biofilm cells producing a heterologous model protein were determined. The 96-well microtiter plate was used to determine the IPTG concentration and the induction day that yields the highest specific eGFP fluorescence in order to use these parameters in the flow cell experiments. A complete characterization of induction effects in both planktonic and biofilm cells was made, including experimental data on plasmid stability, recombinant protein transcription and translation, and cellular metabolic activity. This molecular analysis was complemented with the theoretical determination of IPTG levels in suspension and on the liquid/biofilm interface.

In **Chapter 9**, two different techniques based on fluorescence - fluorometry and epifluorescence microscopy - were used to analyse the impact of IPTG induction on the eGFP production at bulk and single-cell levels, respectively. Analysis at single-cell scale enabled the identification of the production bottleneck in this system.

Finally, **Chapter 10** contains the main conclusions of this work and some suggestions for future work identified within the course of this thesis.

1.3. References

Baneyx F. 1999. Recombinant protein expression in *Escherichia coli*. Curr Opin Biotechnol. 10:411-421.

Bridier A, Sanchez-Vizuete P, Guilbaud M, Piard JC, Naïtali M, Briandet R. 2015. Biofilm-associated persistence of food-borne pathogens. Food Microbiol. 45, Part B:167-178.

Bryers JD. 2008. Medical biofilms. Biotechnol Bioeng. 100:1-18.

Bryers JD, Huang C-T. 1995. Recombinant plasmid retention and expression in bacterial biofilm cultures. Wat Sci Tech. 31:105-115.

Cook LCC, Dunny GM. 2014. The influence of biofilms in the biology of plasmids. Microbiol Spectr. 2:1-9.

Cristiani P, Carvalho ML, Guerrini E, Daghio M, Santoro C, Li B. 2013. Cathodic and anodic biofilms in Single Chamber Microbial Fuel Cells. Bioelectrochemistry. 92:6-13.

Edwards SJ, Kjellerup BV. 2013. Applications of biofilms in bioremediation and biotransformation of persistent organic pollutants, pharmaceuticals/personal care products, and heavy metals. Appl Microbiol Biotechnol. 97:9909-9921.

Folch J, Lees M, Sloane Stanley G. 1957. A simple method for the isolation and purification of total lipides from animal tissues. J Biol Chem. 226:497-509.

Huang C-T, Peretti SW, Bryers JD. 1993. Plasmid retention and gene expression in suspended and biofilm cultures of recombinant *Escherichia coli* DH5α(pMJR1750). Biotechnol Bioeng. 41:211-220.

Huang C-T, Peretti SW, Bryers JD. 1994a. Effects of inducer levels on a recombinant bacterial biofilm formation and gene expression. Biotechnol Lett. 16:903-908.

Mergulhão FJM, Taipa MA, Cabral JMS, Monteiro GA. 2004a. Evaluation of bottlenecks in proinsulin secretion by *Escherichia coli*. J Biotechnol. 109:31-43.

Mergulhão FJM, Summers DK, Monteiro GA. 2005. Recombinant protein secretion in *Escherichia coli*. Biotechnol Adv. 23:177-202.

Mergulhão FJM, Monteiro GA, Cabral JMS, Taipa MA. 2004b. Design of bacterial vector systems for the production of recombinant proteins in *Escherichia coli*. J Microbiol Biotechnol. 14:1-14.

Nicolella C, van Loosdrecht MCM, Heijnen JJ. 2000. Wastewater treatment with particulate biofilm reactors. J Biotechnol. 80:1-33.

O'Connell HA, Niu C, Gilbert ES. 2007. Enhanced high copy number plasmid maintenance and heterologous protein production in an *Escherichia coli* biofilm. Biotechnol Bioeng. 97:439-446.

Pines O, Inouye M. 1999. Expression and secretion of proteins in *E. coli*. Mol Biotechnol. 12:25-34.

Pogiatzis TA, Vassiliadis VS, Mergulhão FJM, Wilson DI. 2015. Choosing when to clean and how to clean biofilms in heat exchangers. Heat Transfer Eng. 36:676-684.

Qureshi N, Annous BA, Ezeji TC, Karcher P, Maddox IS. 2005. Biofilm reactors for industrial bioconversion processes: employing potential of enhanced reaction rates. Microb Cell Fact. 4:24.

Qureshi N, Brining H, Iten L, Dien B, Nichols N, Saha B, Cotta M. 2004. Adsorbed cell dynamic biofilm reactor for ethanol production from xylose and corn fiber hydrolysate. Paper presented at: The 36th Great Lakes Regional Meeting of the American Chemical Society, Peoria, IL.

Rosano GL, Ceccarelli EA. 2014. Recombinant protein expression in *Escherichia coli*: advances and challenges. Front Microbiol. 5:172.

Sanchez-Garcia L, Martín L, Mangues R, Ferrer-Miralles N, Vázquez E, Villaverde A. 2016. Recombinant pharmaceuticals from microbial cells: a 2015 update. Microb Cell Fact. 15:1-7.

Simões LC, Simões M, Vieira M. 2010a. Adhesion and biofilm formation on polystyrene by drinking water-isolated bacteria. Antonie van Leeuwenhoek. 98:317-329.

Singh R, Paul D, Jain RK. 2006. Biofilms: implications in bioremediation. Trends Microbiol. 14:389-397.

Teodósio JS, Simões M, Mergulhão FJ. 2012a. The influence of nonconjugative *Escherichia coli* plasmids on biofilm formation and resistance. J Appl Microbiol. 113:373-382.

Venkata Mohan S, Falkentoft C, Venkata Nancharaiah Y, Sturm BSM, Wattiau P, Wilderer PA, Wuertz S, Hausner M. 2009. Bioaugmentation of microbial communities in laboratory and pilot scale sequencing batch biofilm reactors using the TOL plasmid. Bioresour Technol. 100:1746-1753.

2.

Literature review

2.1. What is a biofilm?

Bacteria and other organisms tend to attach to solid surfaces where they grow and produce a polymeric matrix, forming a biofilm comprised either of single or multiple species (Costerton et al. 1999, Davey & O'Toole 2000, Stoodley et al. 2002). The definition of biofilm has changed significantly from the first description of the phenomenon more than 70 years ago (Zobell 1943). Currently, biofilm is defined as a multicellular population characterized by their spatial order, formation of extracellular polymeric substances (EPS) and increased tolerance to antimicrobial agents. More than 90% of the wet biofilm mass is water, and the EPS containing polysaccharides and glycoproteins correspond to more than 70% of the dry biofilm mass (Melo & Oliveira 2001). The EPS matrix plays an important role in biofilm maintenance since it delays or prevents biocides and other antimicrobial agents from reaching microorganisms within the biofilm, and modulates the nutrient concentration necessary for their survival (Allison 2003, Sutherland 2001). The thickness of the biofilm varies from a few microns to a few centimeters, depending on the microbial species, biofilm age, nutrient availability and environmental liquid shear stress.

Biofilms are often unwanted and have severe effects in industrial and biomedical settings. Besides causing additional problems in cleaning and disinfection, biofilms may cause energy losses and blockages in membrane systems and heat exchangers, a phenomenon known as biofouling. Biofouling costs can represent up to 30% of the entire plant operating costs in membrane systems (Melo & Flemming 2010) and, in specific cases such as power and desalination plants, they may exceed $15 billion per year (Melo

& Flemming 2010). However, the biofilms enjoying the worst reputation are undoubtedly those found in the health sector (Bryers 2008) since they are responsible for more than 60% of all microbial infections (Shunmugaperumal 2010). Overall, a large percentage of biofilm-related infections are associated with indwelling medical devices (Hancock et al. 2007). For instance, catheter-associated urinary tract infection (UTI) accounts for more than 1 million cases in United States hospitals and nursing homes (Tambyah & Maki 2000) and the estimated annual cost of caring for patients with these infections is around $2 billion (Foxman 2003). However, biofilms can be used in many applications, such as water purification and wastewater treatment (Nicolella et al. 2000), bioremediation (Edwards & Kjellerup 2013, Singh et al. 2006), and enhanced production of added-value products like ethanol, organic acids, enzymes, antibiotics and polysaccharides (Cheng et al. 2010, Demirci et al. 2007). Unlike the applications for wastewater treatment and bioremediation, which have been intensively studied, biofilm reactors which are implemented to produce added-value products remained in bench- or pilot-scale during the last decades. In spite of this, biofilm reactors have been demonstrated to enhance the production of such products because they can attain increased volumetric productivity rates by maintaining high biomass concentration (Demirci et al. 2007). With high stability and low nutrient requirement, biofilm reactors can be used for the development of continuous fermentation and to be applied in the industrial-scale production of added-value products.

From all the microorganisms that form biofilms, bacteria are the predominant group. Many *E. coli* isolates have the ability to form biofilms either *in vivo* or *in vitro* (Beloin et al. 2008) and, in recent years, the need to gain more knowledge on the molecular mechanisms underlying biofilm initiation and development led to the emergence of *E. coli* as a model organism due to its well characterized genetics (Beloin et al. 2004, Hancock et al. 2007, Prigent-Combaret et al. 1999, Wood 2009). This bacterium is an important member of the intestinal microflora, acting as a harmless gut commensal, or as an intra- or extra-intestinal pathogen (Beloin et al. 2008). Furthermore, *E. coli* is a highly versatile bacterium, with over 250 serotypes, associated to contamination of medical devices or to the primary cause of recurrent urogenital infections (Dorel et al. 2006, Jacobsen et al. 2008). In terms of its impact on industrial processes, *E. coli* is a typical indicator of the sanitary quality of water (Van Houdt & Michiels 2005) and forms biofilms in food processing environments (Marouani-Gadri et al. 2009) and on water distribution systems (Juhna et al. 2007).

2.1.1. Biofilm formation process

The accumulation of biofilm is a natural process, which follows a sigmoidal pattern (Figure 2.1) as a result of the balance between physical, chemical and biological processes that occur simultaneously (Bott 1993).

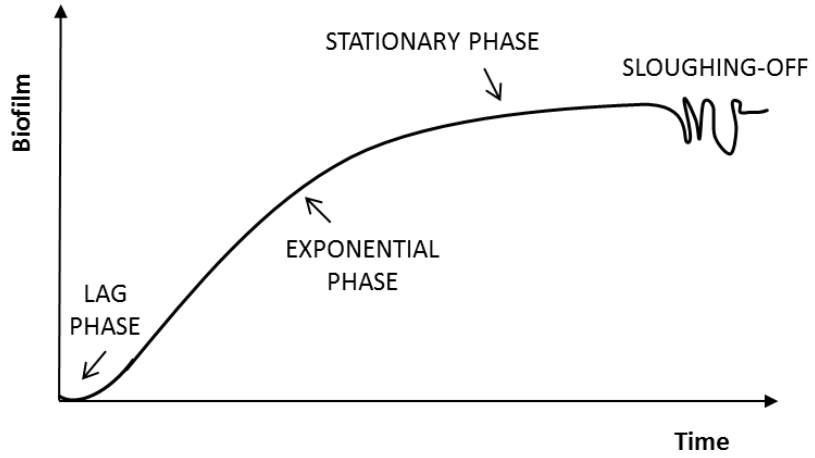

Figure 2.1. Biofilm accumulation through time [based on Melo & Flemming (2010)].

A common model for the formation of a differentiated and mature biofilm has been proposed and includes five different stages: (1) initial reversible attachment to a pre-conditioned surface, (2) transition from reversible to irreversible attachment, (3) early development of biofilm architecture, (4) development of microcolonies into a mature biofilm, and (5) dispersion of cells from the biofilm into the surrounding environment (Stoodley et al. 2002). Biofilm formation steps are represented in Figure 2.2.

It is known that the initial conditioning film is a very thin monolayer formed on the adhesion surface, which will be the docking place for the first reversibly attached cells. The rate at which the conditioning film forms depends on the concentration of organic molecules in the culture medium that contact with the surface, the affinity of those molecules to the support and the hydrodynamic features of the fluid, such as velocity and turbulence (Chamberlain 1992). The physical properties of the surface are also of capital importance for the adhesion of organic molecules, namely the surface charge, free energy and roughness (Boulange-Petermann et al. 2004, Tsibouklis et al. 1999).

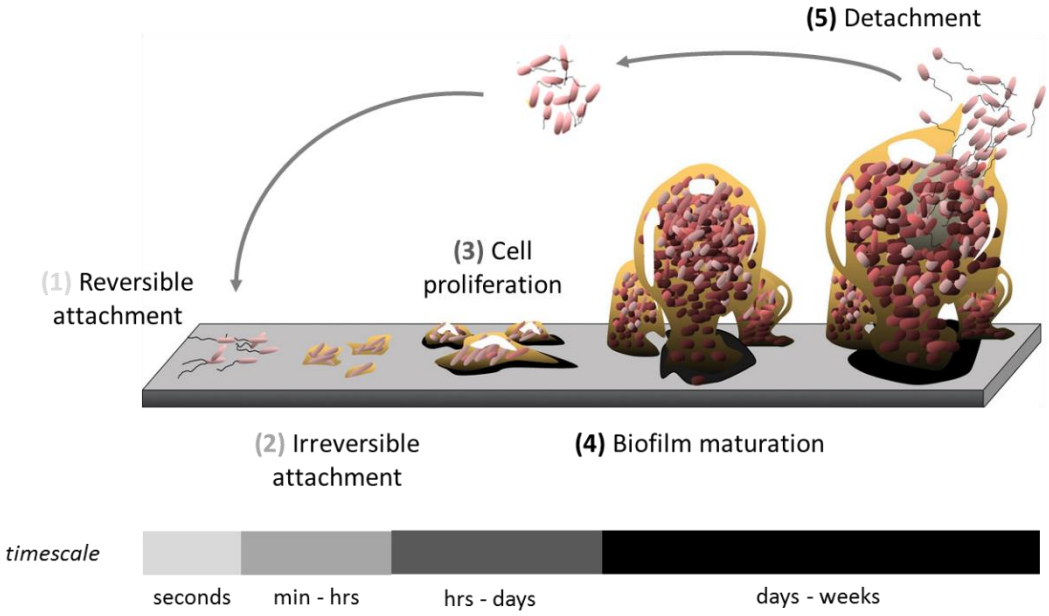

Figure 2.2. Schematic representation of biofilm development: (1) initial reversible attachment, (2) irreversible attachment, (3) cell proliferation, (4) maturation, and (5) dispersion of cells from the biofilm into the surrounding environment [based on Monroe (2007)].

After the initial conditioning film is established, there is the transport of microbial cells from the aqueous medium to the solid surface. The molecules present in the initial development of biofilm may provide a strong and stable adhesion through the formation of polymeric chains with the exopolymers on the surface of microorganisms, or through the external filamentous appendages, such as flagella, pili and fimbriae, that some bacteria as *E. coli* present (Van Houdt & Michiels 2005). Once the first microbial layer is formed, the subsequent adhesion of other cells and abiotic material is favoured.

With the substrate molecules reaching the cells inside the matrix, the production of biomass and extracellular polymers increases, as well as the dry mass and thickness of the biofilm. Complex architectures with pedestal-like structures, water channels and pores are formed to enable the convective and diffusive transport of oxygen and nutrients into the biofilm (Melo 2003).

Simultaneously, erosion or sloughing-off occurs in response to fluid shear forces, weak internal cohesion and depletion of nutrients or oxygen supplied in the biofilm. Erosion, a continuous process resulting from liquid shear forces, is defined as the removal of single cells or small portions of biofilm. Sloughing, in contrast, is the random detachment of large portions of biofilm as a result of rapid change or depletion of nutrients

(Donlan 2002, Gjaltema 1996). It is believed that detached cells migrate to a new surface and form new biofilms. Finally, when the balance between growth and detachment is achieved, the maximum average thickness of biofilm is reached and the system is considered at the pseudo-steady state.

Biofilm establishment and development are dynamic and complex processes that are strongly influenced by the properties of the adhesion surface, the characteristics of the aqueous medium and the properties of the cell surface (Table 2.1). Among these factors, the hydrodynamics and the nutrient levels will be considered in detail in this thesis.

Table 2.1. Variables involved in cell attachment and biofilm formation [based on Donlan (2002)]

Properties of the adhesion surface	**Properties of the bulk liquid**	**Properties of the cell**
Texture or roughness	Flow velocity	Cell surface hydrophobicity
Hydrophobicity	Nutrient availability	Extracellular appendages
Conditioning film	pH	Signaling molecules
	Temperature	

2.1.1.1. The effect of hydrodynamics

Biofilms in different environments are subjected to a very wide range of hydrodynamic conditions. It is known that hydrodynamics has impact on biofilm formation (Liu & Tay 2002, Stoodley et al. 2002, Wäsche et al. 2002), not only in terms of nutrients and oxygen supply (Moreira et al. 2013a), but also by the shear forces, which can modulate microbial cell adhesion to a given surface (Busscher & van der Mei 2006, Simões et al. 2007, Teodósio et al. 2013b). Shear force has been considered as one of the most important factors in the formation of biofilms when the liquid flows at high velocities (high Reynolds numbers, usually in turbulent flow regime) over the biofilm surface (Liu & Tay 2002, Melo & Flemming 2010, Vieira et al. 1993). There is evidence that the shear force has influence on the structure, mass transfer, production of exopolysaccharides and metabolic/genetic behaviours of biofilms (Liu & Tay 2002). As such, higher shear stresses result in a thinner, denser and stronger biofilm (Rochex et al. 2008). The high turbulence can cause two phenomena of opposite nature: it favours the

transport of nutrients to the surface, contributing to the growth and replication of cells in the microbial layer and to the production of exopolymers; on the other hand, with increasing flow velocity, the shear stress forces also increase and that can cause further erosion and detachment of biofilm portions, thus decreasing the amount of biomass attached to the solid support (Percival et al. 1999, Pereira & Vieira 2001, Vieira et al. 1993). However, the reduction in biofilm biomass originates thinner biofilms, which may benefical for the transport of nutrients within the biofilm.

2.1.1.2. The effect of nutrient availability

Several papers have been published during the last years concerning the effect of nutrient levels on the formation and behaviour of biofilms. The first studies observed that high concentrations of nutrients in drinking water distribution systems increased the number of cells in biofilms (Frias et al. 2001, Volk & LeChevallier 1999). Work carried out in a paper mill water stream also revealed that by increasing nutrient levels (nitrogen and phosphorous), the biofilm amount also increased (Klahre & Flemming 2000). The importance of this parameter was furthermore underlined by the conclusions that maintaining low levels of nutrients is an effective way of controlling regrowth in the system (van der Kooji 1992).

Most of the work has been done by independent groups with different members of *Pseudomonas* species. For instance, for *Pseudomonas aeruginosa* it is known that an increase in nutrient concentration promotes biofilm formation (Peyton 1996) and that starvation leads to detachment (Delaquis et al. 1989, Hunt et al. 2004). For *Pseudomonas putida*, Rochex & Lebeault (2007) observed an increase in biofilm thickness when increasing glucose concentration up to a certain limit (0.5 g l^{-1}), above which an additional increase of substrate reduced the biofilm accumulation rate as a consequence of a higher detachment. It has also been reported for *Pseudomonas* species that an increase in flow velocity or in nutrient concentration is associated with an increase of cell attachment.

Despite the lack of information on *E. coli* biofilms, contradictory results have been reported. Dewanti & Wong (1995) found that biofilms developed faster when *E. coli* O157:H7 was grown in low nutrient media. Later, Jackson et al. (2002) noted that the addition of glucose to media inhibited *E. coli* biofilm formation, an effect that may be due to the classical repression system of *E. coli*. Eboigbodin et al. (2007) findings revealed

that the relative presence of glucose in the media at the beginning of the growth phase limits aggregation of *E. coli* MG1655 by altering the concentration of functional groups from macromolecules present on the bacterial surface. It has also been shown that the presence of starved, stationary-phase like zones is important for biofilm formation (Ito et al. 2008). On the other hand, other authors demonstrated that the total yield of *E. coli* B54 (ATCC) growing in a biofilm increased linearly with increase of glucose up to 10 mmol l^{-1} (Bühler et al. 1998), indicating that higher glucose concentrations may be beneficial.

Although there is some information about the effect of glucose levels on biofilm formation, little is known about the effect of varying nitrogen concentrations in the same process. In biofilm reactors for ethanol production, low nitrogen media encouraged the growth of yeast cells on plastic composite supports (Demirci et al. 1997). However, in trickle-bed reactors for biological waste gas treatment, biofilm growth seems to respond strongly to the amount of available nitrogen (Holubar et al. 1999). A similar behaviour was observed for *P. putida* strain isolated from a paper machine; the rate and extent of biofilm accumulation increased with nitrogen concentration (from carbon/nitrogen = 90 to carbon/nitrogen = 20) (Rochex & Lebeault 2007). Additionally, it is known that when the carbon/nitrogen ratio on the nutrient supply is increased, the polysaccharide/protein ratio is also increased (Huang et al. 1994b). Delaquis et al. (1989) showed that nitrogen depletion led to the active detachment of cells from a *Pseudomonas fluorescens* biofilm, similarly to what was observed under glucose limitation.

2.2. Recombinant protein production in *E. coli*

Besides being an excellent model for biofilm studies (Wood 2009), *E. coli* has been extensively used for recombinant protein production (Mergulhão et al. 2004b, Sanchez-Garcia et al. 2016) due to its well characterized genetics and completed genome sequence, and to the availability of a large number of cloning vectors and mutant host strains (Baneyx 1999). In addition, *E. coli* is a cost-effective host for recombinant protein production and is recognized by drug regulatory authorities (Overton 2014). This bacterium has the ability to accumulate recombinant proteins to at least 20% of the total cell protein (Pines & Inouye 1999) and, in some cases, to translocate them from the cytoplasm to the periplasm (Mergulhão et al. 2005).

The first recombinant human protein to be generated in *E. coli* was somatostatin in 1977 (Itakura et al. 1977). Six years later, the human insulin, also made in *E. coli*, was the first recombinant drug to be launched on the market (Johnson 1983). Although this recombinant system cannot be used to produce proteins that require post-translational modifications like glycosylation, many recombinant drugs like thrombolytics, hormones, growth factors, interferons and antibody fragments have been successfully produced in *E. coli*. Currently, approximately 30% of approved recombinant therapeutic proteins are manufactured in *E. coli* (Overton 2014).

The recombinant protein production process in *E. coli* is outlined in Figure 2.3. The gene encoding the desired protein is first cloned into the multiple cloning site of an expression vector under the control of a promoter that will regulate the gene expression. The plasmid vector is then transformed into a strain of *E. coli* that is capable of recombinant protein production, and the transformants are grown in liquid culture. At a

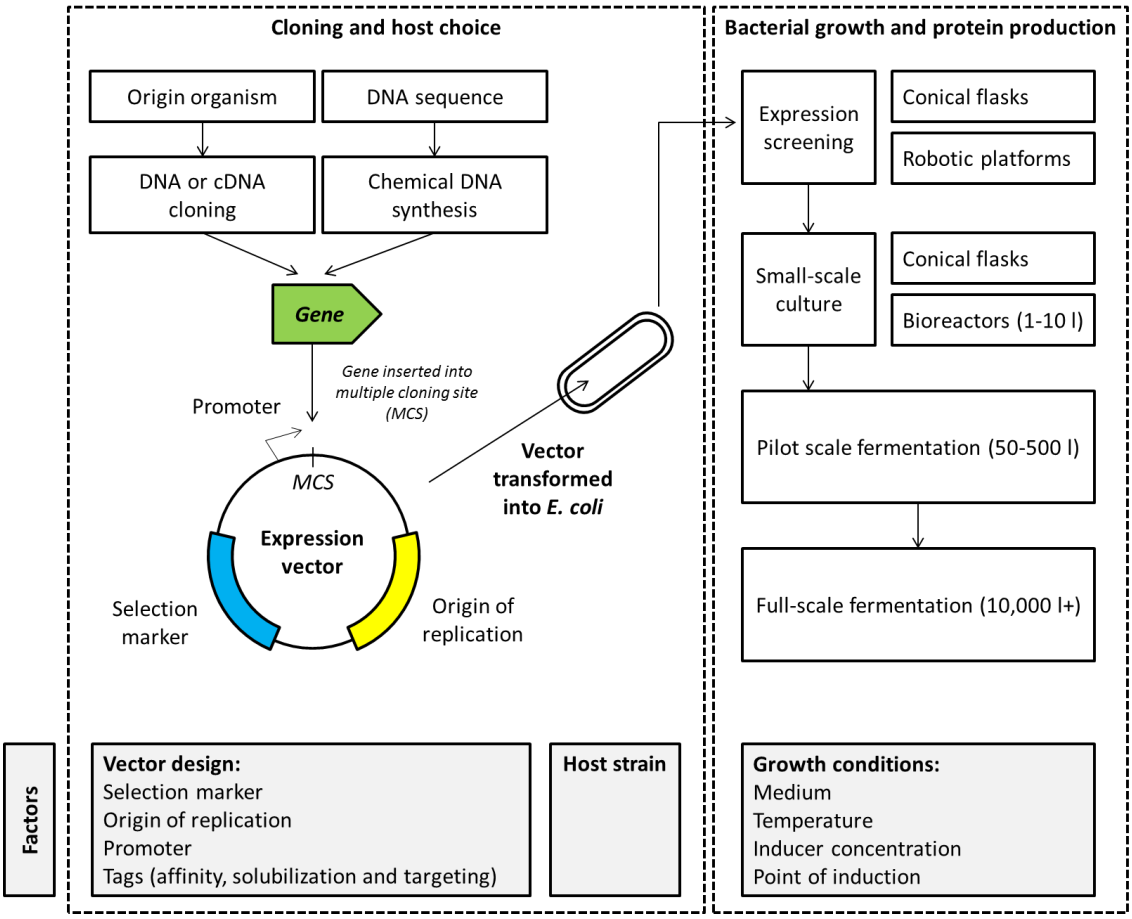

Figure 2.3. Outline and factors influencing recombinant protein production in *E. coli* [based on Overton (2014)].

specific stage of growth, production of the recombinant protein may be induced by the addition of a chemical inducer that will activate the promoter on the expression vector. After the recombinant gene is expressed, the protein of interest can be released from the cell, captured and purified. The successful production of recombinant proteins in *E. coli* depends on a great number of factors, namely the type of expression vector, the host strain and the cultivation conditions (Figure 2.3).

2.2.1. Plasmids as vectors for recombinant protein production

In most situations, recombinant protein production in *E. coli* is achieved by using a plasmid vector harbouring the gene coding for the protein of interest. Basically, a plasmid is an extrachromosomal, circular and double-stranded DNA molecule (with 1-100 kb in size) that carries its own origin of replication. Beyond the origin of replication, the plasmid vector contains a set of genetic elements that affect both transcriptional and translational steps of protein production (Mergulhão et al. 2004b), therefore optimal configuration of these elements should be followed. The essential architecture of an expression vector includes: (1) a origin of replication, (2) a promoter region (including an inducible or constitutive promoter, a start codon and a ribosome binding site), (3) a coding sequence for the target protein, (4) a transcription terminator and (5) a selection marker (Mergulhão et al. 2004b).

High-copy number plasmids [e.g. pUC, 500-700 copies per cell, (Sambrook & Russell 2001)] have been extensively used as vectors for recombinant protein expression. The use of these plasmids can be advantageous due to the gene dosage effect since multiple copies of the gene will be present on the cell under transcriptional regulation of the same promoter (Mergulhão et al. 2004b). Theoretically, the higher the copy number of a plasmid that contains a target gene, the higher will be the gene dosage effect (Choi et al. 1999, Herman-Antosiewicz et al. 2001). However, it is known that the net gain in protein synthesis from low to high-copy plasmids is not always proportional to the copy number increase (Kim & Shuler 1990, Smolke & Keasling 2002) due to the plasmid metabolic burden that may contribute to gene expression limitations (Carrier et al. 1998). Indeed, low-copy plasmids may have a number of advantages over high-copy plasmids

such as tight control of gene expression, ability to replicate large pieces of DNA and low metabolic burden on the host strains (Carrier et al. 1998).

Although the origin of replication regulates the number of copies of the plasmid in each host cell, it has been reported that some physiological states like the stringent response (Gautam & Bastia 2001) or the cell growth rate (Lee & Bailey 1984) may also influence plasmid replication.

Choosing an appropriate vector system is largely dictated by the strength and the control of its promoter. For example, the promoter has to be strong to allow the recombinant protein production to account for 10-30% of total cellular protein (Mergulhão et al. 2004b). Promoters are usually regulated by a chemical inducer, which activates transcription when added to the culture. This enables temporal control of protein production, as well as separation of cell growth and protein production phases (Overton 2014). Preferred characteristics of promoters are tight control, so that the promoter is switched "off" in the absence of inducer, and regulatable expression levels that are dependent upon the concentration of inducer molecule added to the culture medium.

The pET system (Figure 2.4), based on the T7 RNA polymerase, is commonly used in recombinant protein production (Novagen 2005, Studier & Moffatt 1986). The pET system relies upon an engineered *E. coli* host that carries a chromosomal copy of the gene encoding the RNA polymerase of bacteriophage T7. This RNA polymerase gene is usually under the control of an IPTG inducible promoter, such as *lac*UV5. This construct is incorporated into the bacterial chromosome at the DE3 locus. In the absence of IPTG, the *lac* promoter is bound by the *lac* repressor lacI, which represses transcription, preventing the synthesis of the T7 RNA polymerase (T7 RNAP). Upon addition of IPTG, lacI is released from the *lac* promoter region and the T7 RNA polymerase gene is transcribed and translated. The T7 RNAP is then able to activate transcription from the T7 promoter located on the pET plasmid, downstream of which the recombinant gene of interest is cloned. Since the T7 promoter on the pET expression plasmid is not strongly activated by the *E. coli* RNA polymerase, the recombinant protein expression is dependent upon IPTG (Novagen 2005). However, "leaky" expression of the target gene can be obtained resulting from the uninduced expression of T7 polymerase from the *lac*UV5 promoter (Novagen 2005).

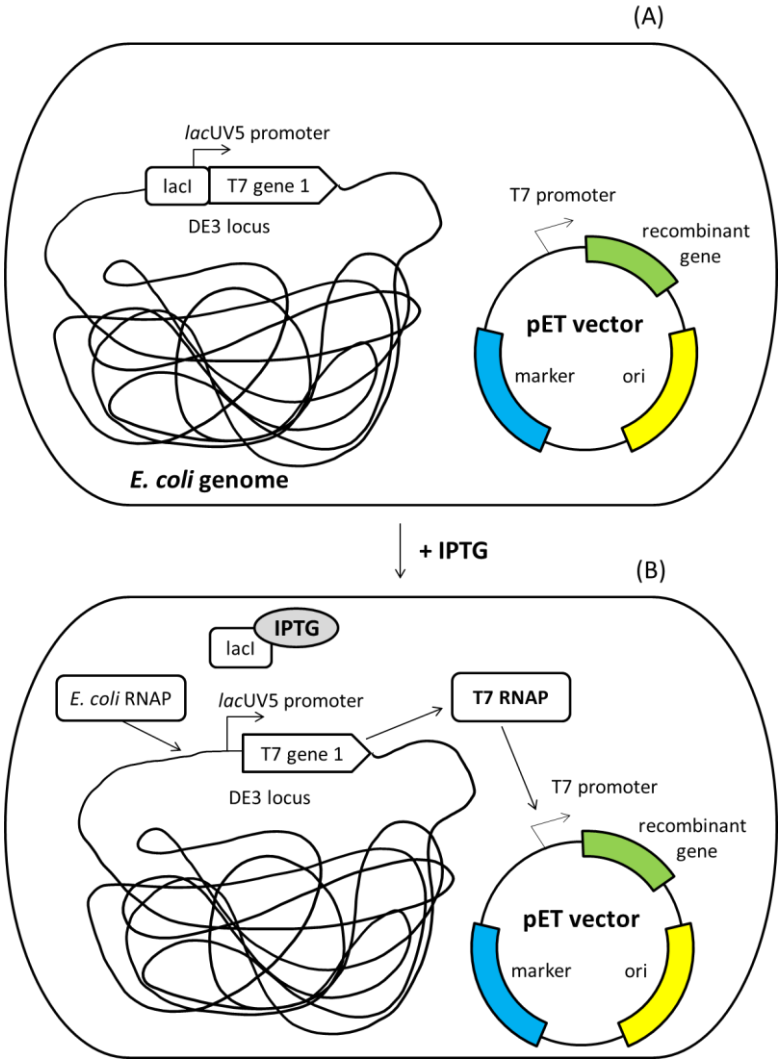

Figure 2.4. The pET system. The recombinant gene of interest is carried on a plasmid vector under the control of a T7 promoter, which cannot be activated by the native *E. coli* RNA polymerase. The T7 RNA polymerase (RNAP) enzyme is required for transcription; this is encoded on a portion of the host genome known as the DE3 locus. (A) Expression of the T7 RNAP is regulated by the *lac*UV5 promoter, which is repressed by the *lac* repressor lacI. (B) To express the recombinant gene, IPTG is added to the culture medium, which is a ligand for the *lac* repressor lacI. When bound to IPTG, lacI empties the *lac*UV5 promoter, enabling *E. coli* RNAP to transcribe the T7 gene 1, encoding the T7 RNAP. The T7 RNAP is then able to activate the promoter on the expression vector and transcribe the recombinant gene. Ori - origin of replication [based on Overton (2014)].

Engineered plasmids are often lost in culture (Summers 1998), and therefore selection markers are used for plasmid maintenance in the cell so that under selective conditions only cells that contain plasmids can survive. In *E. coli* systems, antibiotic resistance genes are the most commonly used selectable markers. Nevertheless, the

expression of these resistance genes has been recognized as the major cause for metabolic burden exerted on the host cell during recombinant protein production (Cunningham et al. 2009). In fact, it has been shown that the marker protein can represent up to 20% of total cellular protein (Birnbaum & Bailey 1991, Rozkov et al. 2004), which greatly exceeds the levels required for plasmid maintenance and selection. Figure 2.5 presents the resistance mechanisms of bacteria against antibiotics. Some are directed at the antibiotic itself: enzymes such as β-lactamases destroy penicillins, and modifying enzymes inactivate chloramphenicol and aminoglycosides such as kanamycin (Sambrook & Russell 2001). Other mechanisms target how the drug is transported; for example, an active efflux of drug mediates resistance to tetracyclines and fluoroquinolones (Levy & Marshall 2004). In any case, protein synthesis is involved and precursors such as amino acids and energy are consumed.

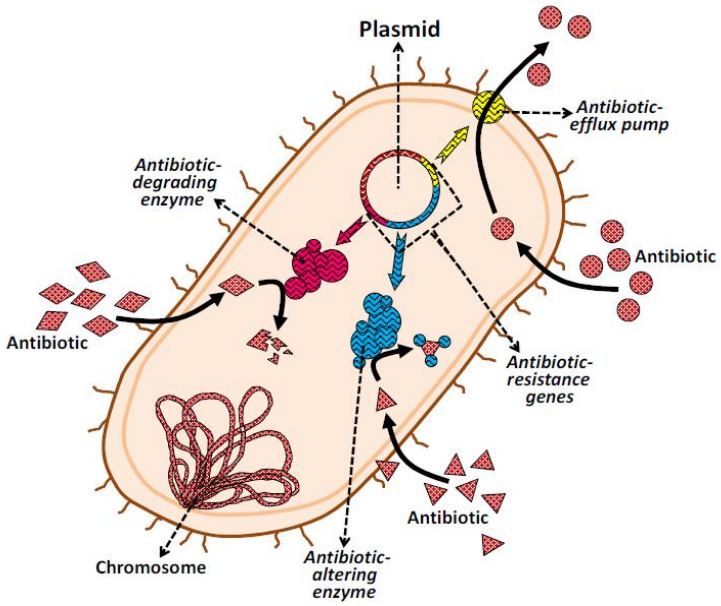

Figure 2.5. Schematic representation of the resistance mechanisms of bacteria against antibiotics [based on Levy & Marshall (2004)].

2.2.2. The impact of plasmids on planktonic cultures

The field of plasmid biology has historically focused on bacteria growing in liquid culture, hence there is much information available on plasmid effects in *E. coli* planktonic cells (Diaz Ricci & Hernández 2000, Silva et al. 2012).

Plasmid presence can have a variety of effects on host physiology. Some investigations have considered plasmids as "cellular parasites" (Diaz Ricci & Hernández 2000) since it was recognized that the introduction and expression of foreign DNA in a host organism often change the metabolism of that organism as a consequence of the metabolic burden (Glick 1995). The term "metabolic burden" is defined as the amount of host cell's resources (raw material and energy) that is required to maintain and express foreign DNA (Glick 1995). Concerning the physiological alterations at culture level, several studies with *E. coli* have shown that plasmid-bearing cells exhibited lower specific growth rates than plasmid-free cells (Birnbaum & Bailey 1991, Cheah et al. 1987, Flores et al. 2004, Khosravi et al. 1990, Ow et al. 2006, Ryan et al. 1989, Seo & Bailey 1985), resulting in lower biomass yields at the end of fermentation (Ow et al. 2006). The larger the plasmid size (Cheah et al. 1987, Khosravi et al. 1990, Ryan et al. 1989) or higher the copy number (Birnbaum & Bailey 1991, Seo & Bailey 1985), the more severe will be the impact on cell growth. Growth retardation in plasmid-bearing cells is possibly caused by the redirection of intracellular resources such as amino acids, nucleotides and metabolic energy to support plasmid-related activities and by inhibitory mechanisms on host cell metabolism (Andersson et al. 1996). At cellular level, alterations in the amount of *E. coli* cell proteins and ribosomal components have been shown to occur after the introduction of multicopy vectors (Birnbaum & Bailey 1991). The levels of stress proteins were higher for recombinant strains, while metabolic enzymes showed lower values. Cell filamentation can also occur during plasmid DNA production in *E. coli*, causing a decrease in growth rate or even no further cell division, leading to lower biomass and plasmid DNA productivity (Silva et al. 2009). Another detrimental effect of the metabolic burden is a reduced cellular viability of plasmid-bearing cells (Diaz Ricci & Hernández 2000), possibly as a result of the increased stress suffered by these cells. Nonetheless, it is clear that the metabolic burden associated with the plasmid alone is small when compared to the effect of recombinant protein expression (Andersson et al. 1996, Bentley et al. 1990, Sørensen & Mortensen 2005, Yang et al. 2016). The metabolic burden resulting from recombinant protein expression promotes segregational and structural plasmid instability (Yu et al. 2003) and several metabolic changes in the host cell (Haddadin & Harcum 2005) which may, in turn, affect the yield and activity of the recombinant protein.

We may think that plasmids will always affect hosts negatively because they rarely encode functions that are absolutely necessary for their growth, but that is not

necessarily true. In nature, plasmids usually provide cells with a growth advantage, showing that under certain culture conditions plasmids can positively affect host performance (Diaz Ricci & Hernández 2000). Rhee et al. (1994) observed that *E. coli* JM109 displays a better growth and a higher metabolic activity in a minimal media when carrying three plasmids than without plasmids. Diaz Ricci & Hernández (2000) have confirmed those results using different culture conditions and other plasmids. An additional report suggested that the presence of a low-copy number plasmid encoding multiple antibiotic resistance genes did not affect the maximum growth rate of *E. coli* (Klemperer et al. 1979).

2.2.3. The impact of plasmids on biofilms

The proximity of bacterial cells in biofilms provides an excellent environment for the exchange of genetic material carried by the plasmid (Ong et al. 2009). Thereby, the effects of *E. coli* plasmids on biofilm formation have been described on numerous studies, the vast majority of which have used conjugative plasmids (Ghigo 2001, Król et al. 2011, May & Okabe 2008, Norman et al. 2008, Reisner et al. 2006, Reisner et al. 2003, Yang et al. 2008). Ghigo (2001) provided the first evidence that natural conjugative plasmids induce the biofilm formation of different *E. coli* K-12 strains, despite that most laboratory *E. coli* K-12 strains are poor biofilm formers. Interestingly, Ghigo's results suggest that the conjugative pili responsible for the horizontal transfer of the plasmid may also act as cell adhesins, which connect the cells and stabilize biofilm structures in hydrodynamic biofilm systems (Ghigo 2001). These results were supported by Reisner et al. (2003, 2006) who showed that the transmission of a conjugative F plasmid induced biofilm formation by a mixed population of laboratory and wild isolates of *E. coli*, and played a role in the overall structure of the biofilm. Addition of an F-like conjugative plasmid (R1*drd*19) which constitutively synthesizes pili also induced greater biofilm formation in *E. coli* cultures. Interestingly, the presence of the R1*drd*19 plasmid increased the expression of numerous chromosomal genes, including those related to envelope stress, motility, and other genes known to be involved in biofilm formation (Yang et al. 2008). May & Okabe (2009) also demonstrated that the F pilus caused increased colonic acid and curli production during biofilm development, which promoted cell-surface adherence (Castonguay et al. 2006). Other conjugative plasmids of *E. coli*, including pOLA52 and

pMAS2027, have been shown to enhance biofilm formation through type 3 fimbriae (Burmølle et al. 2008, Ong et al. 2009).

Few studies have addressed the effect of non-conjugative plasmids on biofilm formation. *E. coli* O157:H7 cells carrying a 92kb virulent and non-conjugative plasmid (pO157) (Burland et al. 1998, Lim et al. 2010a) influenced biofilm formation and architecture (Lim et al. 2010b). Under smooth flow conditions, pO157 enabled biofilm development through increased EPS production and generation of hyperadherent variants (Lim et al. 2010b). It was also reported (Huang et al. 1993, Huang et al. 1994b) that when a plasmid containing a mutated pMB1 origin was transformed into *E. coli* DH5α, the plasmid-bearing cells formed biofilms with a higher cell density when compared to non-transformed cells. Similarly, Teodósio et al. (2012a) found that the addition of non-conjugative plasmids (pET28A and pUC8) to *E. coli* JM109(DE3) increased the concentration of cells growing in a biofilm under turbulent flow conditions compared with non-transformed cells. In opposition, Gallant et al. (2005) revealed that strains of *E. coli* carrying TEM-1-encoding plasmid vectors grew normally, but showed reduced adhesion and biofilm formation.

All the studies previously indicated assessed the impact of non-expression plasmids on biofilm formation. The recombinant protein expression in *E. coli* biofilms was initiated by Huang et al. (1993, 1994a, 1995), who have studied the production of β-galactosidase in *E. coli* DH5α cells carrying a plasmid with the *tac* promoter. These authors found that the recombinant protein was successfully produced in biofilm cells, but at a lower level than in planktonic cells (Bryers & Huang 1995, Huang et al. 1993). Later, O'Connell et al. (2007) have described the first system for high level heterologous protein production in *E. coli* biofilm cells using a pUC-based vector for the expression of eGFP. These authors showed that the biofilm environment enhanced the eGFP production when compared to planktonic cells. Furthermore, the continuous biofilm cultures for heterologous protein production were beneficial for retention of plasmid-bearing cells when compared to chemostats (O'Connell et al. 2007).

2.3. Platforms for biofilm studies

Intensive studies on the mechanisms of biofilm formation and resistance have encouraged the development of different *in vitro* platforms (Coenye & Nelis 2010) to be used in the study of such complex communities under controlled conditions. The focus of this thesis is on microtiter plates and flow cells, which are two of the most used platforms for *in vitro* biofilm studies.

2.3.1. Microtiter plates

The concept of microtiter plate was introduced in 1951 mainly for analytical purposes (Manns 2003). A microtiter plate is a flat plate with multiple wells used as small test tubes. Usually, it has 6, 12, 24, 48, 96 or 384 wells arranged in a 2:3 rectangular matrix. The bottoms of the wells are round or flat in shape and the wells are deep or shallow. The typical culture volume used in microtiter plate varies from 25 µl to 5 ml (Kumar et al. 2004), depending on the number of wells. Microtiter plates are manufactured in a variety of materials, being the most common the transparent polystyrene (PS).

In these systems, biofilms are formed on the bottom and wall of the plate wells (most commonly a 96-well microtiter plate) (Gomes et al. 2014), or they are grown on the surface of a coupon placed inside the wells (most commonly in a 6, 12 or 24-well plate) (Gomes et al. 2015). Illustrative pictures of PS microtiter plates with 96 wells and 12 wells containing coupons can be observed in Figure 2.6. Microtiter plates are closed (batch reactor-like) systems, in which there is no flow into or out of the reactor during the

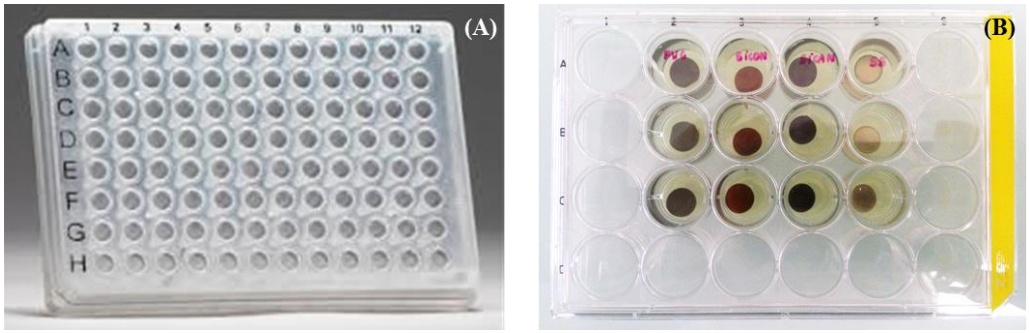

Figure 2.6. Illustrative photographs of PS microtiter plates used on biofilm formation: (A) 96-well microtiter plate and (B) 12-well microtiter plate with coupons of different materials.

experiment. As a result, the environment in the well will change (e.g. nutrients become depleted, toxic products accumulate, etc.), unless the fluid is regularly replaced.

The large number of advantages offered by these straightforward and user-friendly systems explains their widespread use among biofilm researchers. Indeed, microtiter plates provide a large number of parallel and miniaturized reactors with identical geometry and fluid dynamics in a small space (Kumar et al. 2004), allowing "multiplexing", i.e., multiple organisms and/or treatments can be included in a single run (Coenye & Nelis 2010). These devices are easy to handle with the use of multichannel micropipettes, pipetting robots, microplate readers and autosamplers (Duetz, 2007). Another advantage is that microtiter plate-based assays are fairly rapid and cheap as only small volumes of reagents are required (Coenye & Nelis 2010). Additionally, several well established protocols are available for determination of macroscopic parameters related to the biofilm (Table 2.2). As biofilm model systems, microtiter plates have been used for the screening of antimicrobial compounds (Pitts et al. 2003, Quave et al. 2008, Shakeri et al. 2007), to study microbial adhesion (Simões et al. 2010a) and to quantify biofilm inhibition (Cady et al. 2012, Lee et al. 2011).

2.3.2. Flow cell system

Flow cells have been used for more than 30 years for the study of dynamic biofilms. Although they exist in a variety of shapes and sizes, these systems can be divided in two main groups: those that contain removable coupons, usually referred as large-scale flow cells (Figure 2.7A), and those that are particularly well-suited for real-time non-destructive microscopic analysis of biofilms, usually small-scale flow cells designated by parallel plate flow chambers (Figure 2.7B). Many of the flow cell systems are custom-made and are typically composed by pumps and tubes required to circulate the growth medium and/or the cellular suspension to a chamber where the biofilms are formed, and a vessel for waste collection [e.g. Barros et al. (2013) and Teodósio et al. (2011a)]. Therefore, in contrast to microtiter plate-based systems, the flow cell systems are "open" systems in which growth medium is (semi-)continuously added and waste products are (semi-)continuously removed (Coenye & Nelis 2010).

The large-scale flow cells, like that shown in Figure 2.7A, are most suitable to the simulation of industrial biofilms since they have a large number of coupons or adhesion

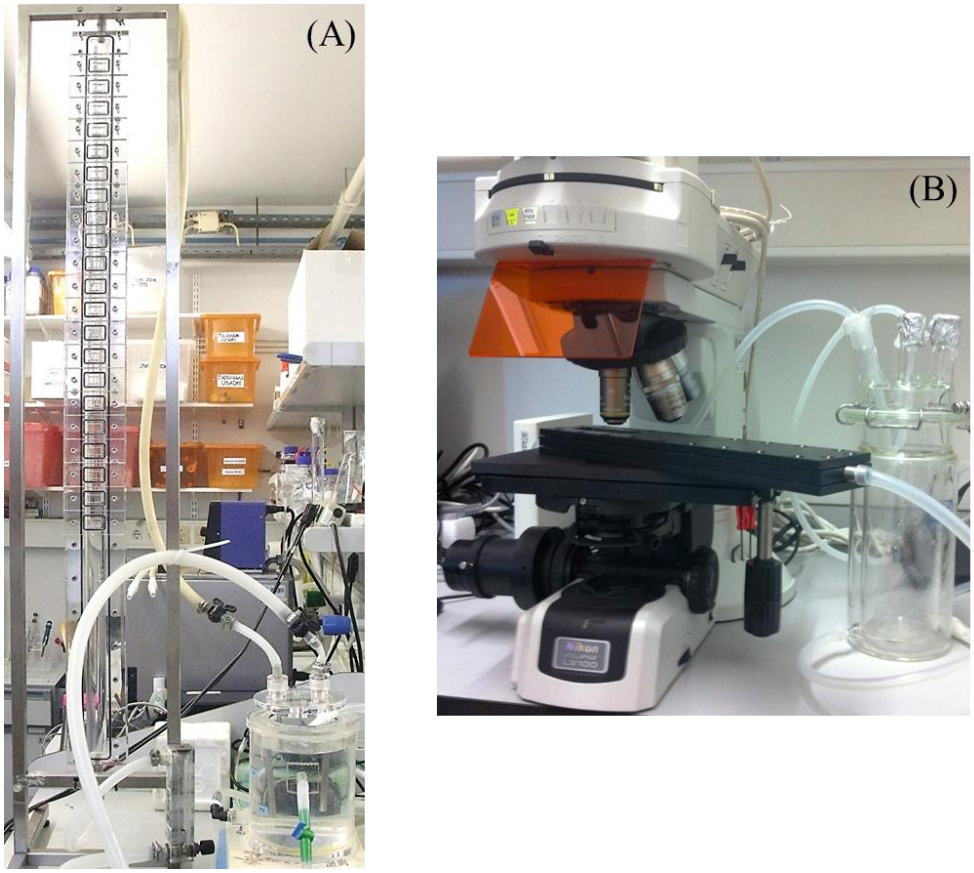

Figure 2.7. Illustrative photographs of flow cell systems: (A) large-scale flow cell and (B) parallel plate flow chamber [described by Moreira et al. (2014)].

surfaces for biofilm formation during days or weeks, and can be operated at high flow rates in regimes of high turbulence and shear stress (Melo & Vieira 1999). Additionally, their dimensions (usually in meters) are closer to the ones commonly found in industrial settings. Most of these large-scale flow cells are based on the design introduced by Jim Robbins and later modified by McCoy et al. (1981), creating what is commonly described as the Modified Robbins Device. These flow cells are square channel pipes with coupons fixed to sampling plugs that can be unscrewed from the walls. Several materials like glass, silicone rubber, polyvinyl chloride (PVC) or stainless steel can be used to make the coupons. Other designs include flow cells with a half-pipe geometry that more closely resemble the circular section of the tubes found in industrial piping systems (Pereira et al. 2002b, Teodósio et al. 2013). Also in order to mimic the high flow rates that are common in industrial processes (Melo & Vieira 1999), a recirculation system can be used in which nutrients are supplied onto a mixing vessel and then recirculated through the flow cell

(Teodósio et al. 2011a). In this case, the flow velocity in the flow cell is independent of the dilution rate of the system and higher shear rates can be achieved. Basically, these systems are "chemostats with irregular geometries" (Stoodley & Warwood 2003). To prevent gradient formation along the system, the recirculation flow rate must be high and the volume of the recycle loop must be minimized, thus decreasing the residence time. Ideally, the residence time in the entire recycle loop and flow cell should not exceed few minutes so that the whole system can be assumed to be completely mixed (Stoodley & Warwood 2003).

2.4. Biofilm analysis

Following biofilm growth in microtiter plates and flow cell systems, the extent of biofilm formation can be measured in a variety of ways. In this section, a brief overview of the different macroscopic and microscopic approaches available for these two laboratorial platforms is provided.

2.4.1. Macroscopic methods

The traditional approach to microbial quantification is based on plate counting. To this end, biofilm cells are removed from the surface by sonication (e.g. when biofilms are grown on the bottom and the walls of the microtiter plate) or they can be detached from the surface by scraping and vortexing (e.g. when biofilms are grown on coupons placed in the wells of the microtiter plate or screwed onto the flow cell). Then, the detached cells can be diluted and plated. However, conventional plating is labour-intensive and time-consuming (requiring at least 24 h before results may be interpreted), and can underestimate the number of viable cells due to the presence of viable but non-culturable cells (VBNCs).

Alternative techniques have been developed for the quantification of biofilms formed in microtiter plates, including techniques to determine the total biofilm biomass (i.e., matrix and both living and dead cells), the number of viable sessile cells only, or the amount of extracellular polymers in the biofilm matrix (Table 2.2).

Table 2.2. Macroscopic methods used for biofilm quantification in microtiter plates [based on Azevedo et al. (2009)]

Parameter	Method	Reference
Biofilm biomass	CV assay	(Costerton et al. 1999, Stepanović et al. 2000)
Microbial physiological activity	Fluorescein diacetate assay	(Honraet et al. 2005, Peeters et al. 2008)
	Resazurin assay	(Peeters et al. 2008)
	XTT[1] assay	(Honraet et al. 2005, Peeters et al. 2008)
Microbial cells in the biofilm	Syto9 assay	(Honraet et al. 2005, Peeters et al. 2008)
Biofilm matrix	Dimethylmethylene blue assay	(Toté et al. 2008)

[1]2,3-bis (2-methoxy-4-nitro-5-sulfophenyl)-5-[(phenylamino)carbonyl]-2*H*-tetrazolium hydroxide

In the early ages of biofilm research, much focus was placed on analysis of the amount and thickness of biofilms (Denkhaus et al. 2007). These parameters are still of interest in current research using flow cell systems, however in combination with the study of biofilm components (such as EPS), function and structure. Table 2.3 summarizes some of the most widely used techniques for analysis of biofilms formed in flow cell reactors. The epifluorescence-based methods will be addressed in detail in section 2.4.2.1.

Table 2.3. Methods used for biofilm quantification in flow cell systems

Parameter	Method	References
Biofilm thickness	Digital micrometer	(Pereira et al. 2008, Pereira et al. 2002a, Teodósio et al. 2011a)
	Light microscope	(Bakke & Olsson 1986)
	Confocal microscope	(Hentzer et al. 2001, Pereira et al. 2002b)
	Optical coherence tomography (OCT)	(Xi et al. 2006)
Biofilm wet weight	Pre and post weight quantification using analytical balance	(Teodósio et al. 2011a)

Table 2.3. (Continued)

Parameter	Method	References
Biofilm dry weight	Total volatile solids (TVS)	(Simões et al. 2007)
Biofilm cells	Plate counting	(Manuel et al. 2009, Moreira et al. 2016, Pereira et al. 2002a, Simões et al. 2006)
	ATP[1] bioluminescence assay	(Maezono et al. 2011, Mattila et al. 2002)
	Epifluorescence microscope (DAPI[2], CTC[3] and Live/Dead® *Bac*Light™ bacterial viability kit)	(Manuel et al. 2007, Manuel et al. 2009, Pereira et al. 2002a, Simões et al. 2006, Simões et al. 2007, Teodósio et al. 2012a)
Microbial activity	Respirometer	(Pereira et al. 2002a, Simões et al. 2007)
	Calorimeter	(von Rège & Sand 1998)
	XTT assay[4]	(Al-Fattani & Douglas 2006)
Biofilm processes and mass transfer	Microsensors (O_2, CO_2, Ca^{2+}; glucose, temperature, pH, etc.)	(Hartley et al. 1996, von Ohle et al. 2010)
EPS extraction	Cation-exchange resin - Dowex resin	(Simões et al. 2007)
EPS analysis	Phenol-sulfuric acid method (polysaccharide quantification)	(Simões et al. 2007)
	Lowry modified method (protein quantification)	(Simões et al. 2007)

[1] adenosine triphosphate; [2] 4'-6-diamidino-2-phenylindole; [3] 5-cyano-2,3-ditolyl tetrazolium chloride; [4] 2,3-bis (2-methoxy-4-nitro-5-sulfophenyl)-5-[(phenylamino)carbonyl]-2*H*-tetrazolium hydroxide

2.4.2. Microscopic methods

Despite the emergence of techniques for the macroscopic characterization of biofilms, the combination of microscopy with various labelling techniques and digital image acquisition/analysis software is extremely useful for the study of biofilms (Stewart & Franklin 2008), especially those formed in flow cells and microtiter plates. Basic light or phase contrast microscopy can only be used on samples of biofilm grown on thin transparent substrates since these techniques rely on the passage of a light beam through the sample. Therefore, more appropriate techniques for the study of biofilms include

epifluorescence microscopy, confocal laser scanning microscopy (CLSM), scanning electron microscopy (SEM), environmental scanning electron microscopy (ESEM), transmission electron microscopy (TEM) and atomic force microscopy (AFM). Table 2.4 presents a summary of the type of information provided by each of these microscopic methods, as well as their advantages and limitations.

2.4.2.1. Epifluorescence microscopy and CLSM

CLSM in combination with fluorescent labelling of the sample is probably the most widely used method for biofilm analysis since it is a three-dimensional technique that allows the examination of living fully hydrated biofilms in real time (Bridier et al. 2013, Bridier et al. 2010). In confocal microscopes, laser excitation and the introduction of a pinhole enable to block out-of-focus light, and thus to obtain images with a depth resolution around 0.3 µm (Palmer Jr & Sternberg 1999). By collecting a "stack" (series of digital xy optical sections) through the depth of the sample (z dimension), three-dimensional biofilm structures can be reconstructed (Figure 2.8). Most confocal image acquisition software has the ability to link multiparameter quantitative data sets of fluorescence intensity to each image, which can be translated into measurements, including cell counts, biofilm thickness and roughness, species identification and quantitative gene expression within biofilms (Bridier et al. 2010, Heydorn et al. 2000). Due to its non-destructive nature, researchers have used CLSM to investigate biofilm morphology and physiology, and the relationship between biofilm structure, adaptation, reactivity and response to external stress (Palmer Jr et al. 2006). This microscopic technique is widely applied in characterizing the antimicrobial resistance mechanisms of biofilms (Bridier et al. 2011a), the EPS matrix (Stewart & Franklin 2008) and the metabolite production in biofilms (Yawata et al. 2008). CLSM has also been extensively used with fluorescence *in situ* hybridization (FISH) techniques (Figure 2.8B) to enable the taxonomic identification and localization of bacteria within biofilms (Almeida et al. 2011, Azevedo et al. 2016).

Contrariwise, in epifluorescence microscopy, the biofilm is uniformly illuminated by a cone of light and the fluorescence emitted from the whole thickness is collected, not allowing the observation of a particular depth in the biofilm (Bridier & Briandet 2014).

Table 2.4. Relevant microscopic techniques for biofilm analysis

Technique	Acquired information	Advantages	Limitations	References
Epifluorescence microscopy	Distribution and enumeration of biofilm cells on surface	Fast and easy Less expensive	Two-dimensional imaging only Not applicable to thick biofilms The use of fluorochromes is necessary for viewing bacteria	(An et al. 1995)
CLSM	Three-dimensional structure of biofilms Biofilm physiology	Living fully hydrated sample Non-invasive Quantitative evaluation Reflection and fluorescence mode	Low resolution Narrow range of magnifications Use of fluorochromes or oligonucleotide probles	(Bridier et al. 2013, Bridier et al. 2010, Palmer Jr et al. 2006, Stewart et al. 1995)
SEM	Biofilm structure	High resolution Wide range of magnifications Good comparative information Ability to image complex shapes	Not real-time Requires additional sample preparation Limited quantification Expensive equipment	(Hannig et al. 2010, Norton et al. 1998, Serra et al. 2013, Stewart et al. 1995)
ESEM	Sub-micron biofilm structure EPS matrix	High resolution Examination of partially hydrated sample	Contrast effect caused by condensed water Expensive equipment	(Muscariello et al. 2005, Priester et al. 2007)
AFM	Topographical and morphological biofilm analysis	Non-invasive Nanometer resolution Three-dimensional images Qualitative and quantitative	Sample damage by the tip Time consuming Expensive equipment	(Wright et al. 2010)

(A)

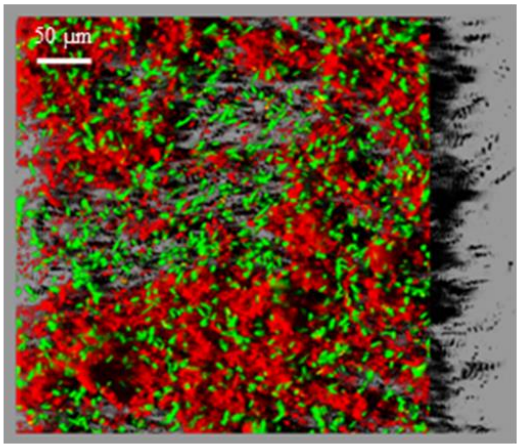

(B)

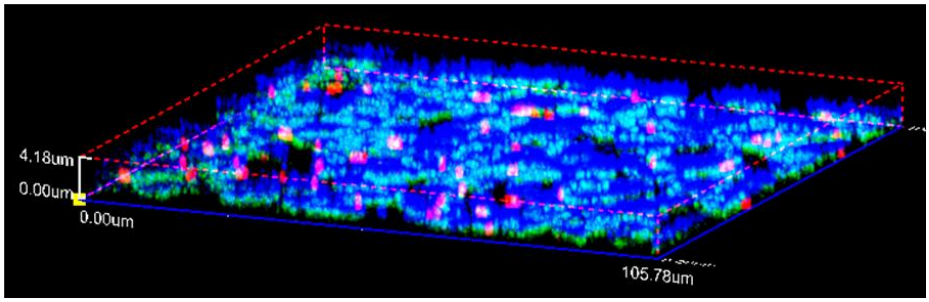

Figure 2.8. CLSM showing the three-dimensional spatial distribution of biofilms. (A) Dual-species biofilms formed by GFP-tagged *E. coli* SS2 (green) and Syto61-stained *Pantoea agglomerans* 19V1 (red); (B) three-species biofilm formed by *E. coli* (blue), *Salmonella enterica* (red) and *Listeria monocytogenes* (green) analysed by peptide nucleic acid (PNA) FISH (image courtesy of Dr. Carina Almeida, Centre of Biological Engineering, Universidade do Minho).

Although epifluorescence microscopy only allows two-dimensional imaging, it makes direct observation and enumeration possible for attached bacteria on an opaque surface. Moreover, it is a relatively fast and easy method that is especially suitable for a large set of samples (An et al. 1995).

Both epifluorescence microscopy and CLSM require staining of non-fluorescent specimens (Andersson & Rajarao 2013). The Syto stains (Invitrogen, USA) can efficiently stain cells in virtually any color of the rainbow. In combination with propidium iodide (PI), it is possible to specifically stain live and dead cells. The dye Syto9 stains all cells green regardless if they are dead or alive, while it is assumed that only cells with damaged membrane will be stained by the red PI dye, indicating dead cells (Figure 2.9A). On the other hand, 4'-6-diamidino-2-phenylindole (DAPI) is commonly used to stain all

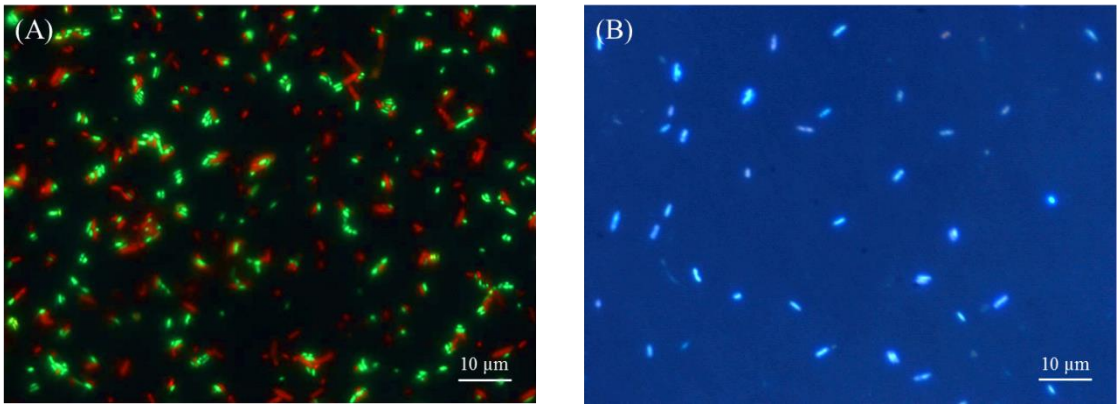

Figure 2.9. Epifluorescence images of detached biofilm cells of *E. coli* JM109(DE3) + pFM23. (A) Cells stained with the Live/Dead® *Bac*Light™ bacterial viability kit (live and dead cells represented in green and red, respectively); (B) cells stained with 4'-6-diamidino-2-phenylindole (DAPI).

nucleic acid-containing cells (Figure 2.9B). Stains targeting the extracellular matrix, such as lectins or calcofluor white (for polysaccharides), fluoresceine isothiocyanate or congo red (for proteins) and nile red (for lipids), can also be employed to visualize the surrounding of biofilm cells (Andersson & Rajarao 2013).

If genetic manipulation of biofilm cells is possible, chromosomal tagging with a gene cassette encoding the GFP can be a valuable tool for the fluorescent labeling of sessile cells. Alternatively, plasmids encoding the GFP might be introduced into the cells prior to biofilm examination. Depending on the construction, this fluorescent labeling can be used to verify the location of cells in a biofilm or, by selecting suitable variants of GFP genes and promoters, it can be used for monitoring gene expression and thereby to have access to the metabolic/physiological activity in biofilms (Bagge et al. 2004, Bridier et al. 2011b, Serra et al. 2013, Walters et al. 2003, Werner et al. 2004). GFP from the jellyfish *Aequorea victoria* has been studied from the early 1960s and has been used in biology since its cloning (Chalfie et al. 1994). It is a small protein (238 amino acids; 27 kDa) which is excited by ultraviolet (UV) to blue light and that can be expressed in many bacteria (Niwa et al. 1996). Small amounts of oxygen are needed for the newly synthesized protein to become fluorescent in a maturation process that requires several hours, after which it remains largely stable for days (Tombolini et al. 1997). It is this stability that precludes the use of wild-type GFP for dynamic gene expression studies. However, mutations of the GFP gene sequence were developed to reduce the protein maturation times.

2.4.2.2. SEM

SEM is a well-established microscopic technique to observe the morphology of bacteria adhered on a material, the material surface morphology and the relationship between both. SEM yields a three-dimensional rendering of the biofilm surface (lacking the vertical resolution), which reveals the overall shape of the microorganisms composing the biofilm, as well as their organization relative to each other and to the extracellular matrix (Hannig et al. 2010). It is an extremely useful tool for comparative analysis in biofilm research (Figure 2.10), especially when evaluating the anti-biofilm effects of a compound/treatment (Gomes et al. 2015) and the kinetic formation of biofilms (Janjaroen et al. 2013). SEM can be used to produce high resolution images of sessile cells on opaque substrata (from 50 to 100 nm) across a wide range of magnifications (Norton et al. 1998), from 20× (general view of biofilm) to approximately 30,000× (fine structure). At higher magnifications (up to 100,000×), individual cells are readily distinguished (Serra et al. 2013, Stewart et al. 1995).

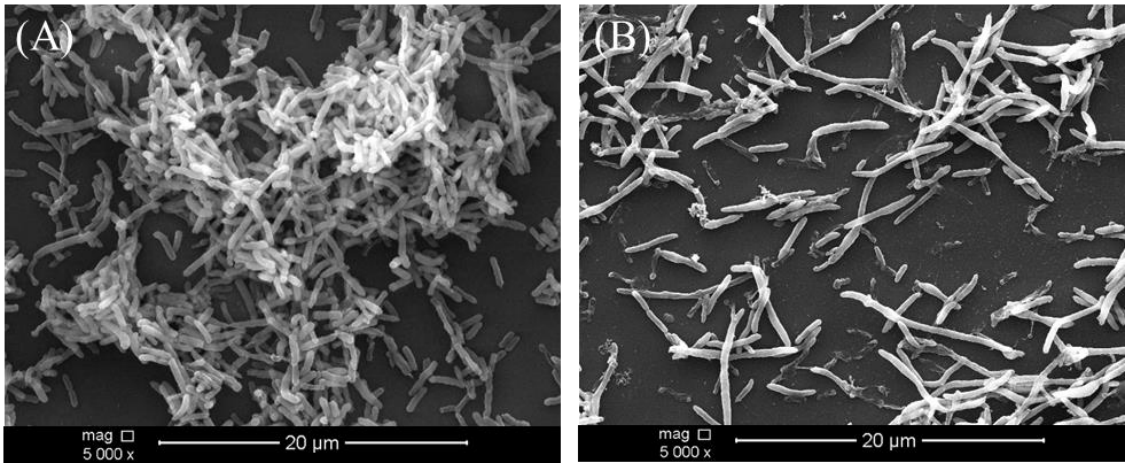

Figure 2.10. Scanning electron micrographs of *E. coli* JM109(DE3) biofilms formed on glass surfaces. (A) Biofilm not exposed to ampicillin; (B) biofilm exposed to ampicillin.

2.5. References

Al-Fattani MA, Douglas LJ. 2006. Biofilm matrix of *Candida albicans* and *Candida tropicalis*: chemical composition and role in drug resistance. J Med Microbiol. 55:999-1008.

Allison DG. 2003. The biofilm matrix. Biofouling. 19:139-150.

Almeida C, Azevedo NF, Santos S, Keevil CW, Vieira MJ. 2011. Discriminating multi-species populations in biofilms with peptide nucleic acid fluorescence *in situ* hybridization (PNA FISH). PLoS ONE. 6:e14786.

An YH, Friedman RJ, Draughn RA, Smith EA, Nicholson JH, John JF. 1995. Rapid quantification of staphylococci adhered to titanium surfaces using image analyzed epifluorescence microscopy. J Microbiol Methods. 24:29-40.

Andersson L, Yang S, Neubauer P, Enfors S-O. 1996. Impact of plasmid presence and induction on cellular responses in fed batch cultures of *Escherichia coli*. J Biotechnol. 46:255-263.

Andersson S, Rajarao GK. 2013. Methods for Biofilm Characterization. In: Mergulhão F, Simões M, editors. Biofilms in Bioengineering. New York: Nova Science Publishers. p. 27-43.

Azevedo AS, Almeida C, Pereira B, Melo LF, Azevedo NF. 2016. Impact of *Delftia tsuruhatensis* and *Achromobacter xylosoxidans* on *Escherichia coli* dual-species biofilms treated with antibiotic agents. Biofouling. 32:227-241.

Azevedo NF, Lopes SP, Keevil CW, Pereira MO, Vieira MJ. 2009. Time to "go large" on biofilm research: advantages of an omics approach. Biotechnol Lett. 31:477-485.

Bagge N, Hentzer M, Andersen JB, Ciofu O, Givskov M, Høiby N. 2004. Dynamics and spatial distribution of β-lactamase expression in *Pseudomonas aeruginosa* biofilms. Antimicrob Agents Chemother. 48:1168-1174.

Bakke R, Olsson PQ. 1986. Biofilm thickness measurements by light microscopy. J Microbiol Methods. 5:93-98.

Baneyx F. 1999. Recombinant protein expression in *Escherichia coli*. Curr Opin Biotechnol. 10:411-421.

Barros J, Grenho L, Manuel CM, Ferreira C, Melo LF, Nunes OC, Monteiro FJ, Ferraz MP. 2013. A modular reactor to simulate biofilm development in orthopedic materials. Int Microbiol. 16:191-198.

Beloin C, Roux A, Ghigo J-M. 2008. *Escherichia coli* Biofilms. In: Romeo T, editor. Bacterial Biofilms: Current topics in microbiology and immunology. Berlin: Springer-Verlag. p. 249-289.

Beloin C, Valle J, Latour-Lambert P, Faure P, Kzreminski M, Balestrino D, Haagensen JAJ, Molin S, Prensier G, Arbeille B, et al. 2004. Global impact of mature biofilm lifestyle on *Escherichia coli* K-12 gene expression. Mol Microbiol. 51:659-674.

Bentley WE, Mirjalili N, Andersen DC, Davis RH, Kompala DS. 1990. Plasmid-encoded protein: the principal factor in the "metabolic burden" associated with recombinant bacteria. Biotechnol. Bioeng. 35:668-681.

Birnbaum S, Bailey JE. 1991. Plasmid presence changes the relative levels of many host cell proteins and ribosome components in recombinant *Escherichia coli*. Biotechnol Bioeng. 37:736-745.

Bott TR. 1993. Aspects of biofilm formation and destruction. Corros Rev. 11:1-24.

Boulange-Petermann L, Jullien C, Dubois P, Benezech T, Faille C. 2004. Influence of surface chemistry on the hygienic status of industrial stainless steel. Biofouling. 20:25-33.

Bridier A, Briandet R. 2014. Contribution of Confocal Laser Scanning Microscopy in Deciphering Biofilm Tridimensional Structure and Reactivity. In: Donelli G, editor. Microbial Biofilms: Methods and Protocols. New York: Springer Science + Business Media. p. 255-266.

Bridier A, Meylheuc T, Briandet R. 2013. Realistic representation of *Bacillus subtilis* biofilms architecture using combined microscopy (CLSM, ESEM and FESEM). Micron. 48:65-69.

Bridier A, Dubois-Brissonnet F, Boubetra A, Thomas V, Briandet R. 2010. The biofilm architecture of sixty opportunistic pathogens deciphered using a high throughput CLSM method. J Microbiol Methods. 82:64-70.

Bridier A, Dubois-Brissonnet F, Greub G, Thomas V, Briandet R. 2011a. Dynamics of the action of biocides in *Pseudomonas aeruginosa* biofilms. Antimicrob Agents Chemother. 55:2648-2654.

Bridier A, Le Coq D, Dubois-Brissonnet F, Thomas V, Aymerich S, Briandet R. 2011b. The spatial architecture of *Bacillus subtilis* biofilms deciphered using a surface-associated model and *in situ* imaging. PLoS ONE. 6:e16177.

Bryers JD. 2008. Medical biofilms. Biotechnol Bioeng. 100:1-18.

Bryers JD, Huang C-T. 1995. Recombinant plasmid retention and expression in bacterial biofilm cultures. Wat Sci Tech. 31:105-115.

Bühler T, Ballestero S, Desai M, Brown MRW. 1998. Generation of a reproducible nutrient-depleted biofilm of *Escherichia coli* and *Burkholderia cepacia*. J Appl Microbiol 85:457-462.

Burland V, Shao Y, Perna NT, Plunkett G, Blattner FR, Sofia HJ. 1998. The complete DNA sequence and analysis of the large virulence plasmid of *Escherichia coli* O157:H7. Nucleic Acids Res. 26:4196-4204.

Burmølle M, Bahl MI, Jensen LB, Sørensen SJ, Hansen LH. 2008. Type 3 fimbriae, encoded by the conjugative plasmid pOLA52, enhance biofilm formation and transfer frequencies in Enterobacteriaceae strains. Microbiology. 154:187-195.

Busscher HJ, van der Mei HC. 2006. Microbial adhesion in flow displacement systems. Clin Microbiol Rev. 19:127-141.

Cady NC, McKean KA, Behnke J, Kubec R, Mosier AP, Kasper SH, Burz DS, Musah RA. 2012. Inhibition of biofilm formation, quorum sensing and infection in *Pseudomonas aeruginosa* by natural products-inspired organosulfur compounds. PLoS ONE. 7:e38492.

Carrier T, Jones KL, Keasling JD. 1998. mRNA stability and plasmid copy number effects on gene expression from an inducible promoter system. Biotechnol Bioeng. 59:666-672.

Castonguay MH, van der Schaaf S, Koester W, Krooneman J, van der Meer W, Harmsen H, Landini P. 2006. Biofilm formation by *Escherichia coli* is stimulated by synergistic interactions and co-adhesion mechanisms with adherence-proficient bacteria. Res Microbiol. 157:471-478.

Chalfie M, Tu Y, Euskirchen G, Ward WW, Prasher DC. 1994. Green fluorescent protein as a marker for gene expression. Science. 263:802-805.

Chamberlain AHL. 1992. The Role of Adsorbed Layers in Bacterial Adhesion. In: Melo LF, Bott TR, Fletcher M, Capdeville B, editors. Biofilms - Science and Technology. Springer Netherlands. p. 59-67.

Cheah UE, Weigand WA, Stark BC. 1987. Effects of recombinant plasmid size on cellular processes in *Escherichia coli*. Plasmid. 18:127-134.

Cheng K-C, Demirci A, Catchmark JM. 2010. Advances in biofilm reactors for production of value-added products. Appl Microbiol Biotechnol. 87:445-456.

Choi JW, Ra KS, Lee YS. 1999. Enhancement of bovine growth hormone gene expression by increasing the plasmid copy number. Biotechnol Lett. 21:1-5.

Coenye T, Nelis HJ. 2010. *In vitro* and *in vivo* model systems to study microbial biofilm formation. J Microbiol Methods. 83:89-105.

Costerton JW, Stewart PS, Greenberg EP. 1999. Bacterial biofilms: a common cause of persistent infections. Science. 284:1318-1322.

Cunningham DS, Koepsel RR, Ataai MM, Domach MM. 2009. Factors affecting plasmid production in *Escherichia coli* from a resource allocation standpoint. Microb Cell Fact. 8:1475-2859.

Davey ME, O'Toole GA. 2000. Microbial biofilms: from ecology to molecular genetics. Microbiol Mol Biol R. 64:847-867.

Delaquis PJ, Caldwell DE, Lawrence JR, McCurdy AR. 1989. Detachment of *Pseudomonas fluorescens* from biofilms on glass surfaces in response to nutrient stress. Microbial Ecol. 18:199-210.

Demirci A, Pometto AL 3rd, Ho KLG. 1997. Ethanol production by *Saccharomyces cerevisiae* in biofilm reactors. J Ind Microbiol Biotechnol. 19:299-304.

Demirci A, Pongtharangkul T, Pometto AL. 2007. Applications of Biofilm Reactors for Production of Value-Added Products by Microbial Fermentation. In: Blaschek HP, Wang HH, Agle ME, editors. Biofilms in the Food Environment. Oxford: Blackwell Publishing Ltd. p. 167-190.

Denkhaus E, Meisen S, Telgheder U, Wingender J. 2007. Chemical and physical methods for characterisation of biofilms. Microchim Acta 158:1-27.

Dewanti R, Wong ACL. 1995. Influence of culture conditions on biofilm formation by *Escherichia coli* O157:H7. Int J Food Microbiol. 26:147-164.

Diaz Ricci JC, Hernández ME. 2000. Plasmid effects on *Escherichia coli* metabolism. Crit Rev Biotechnol. 20:79-108.

Donlan RM. 2002. Biofilms: microbial life on surfaces. Emerg Infect Dis. 8:881-890.

Dorel C, Lejeune P, Jubelin G. 2006. Role of biofilms in infections caused by *Escherichia coli*. In: Pace JL, Rupp ME, Finch R, editors. Biofilms, infection, and antimicrobial therapy. Boca Raton: Taylor & Francis. p. 73-80.

Eboigbodin KE, Ojeda JJ, Biggs CA. 2007. Investigating the surface properties of *Escherichia coli* under glucose controlled conditions and its effect on aggregation. Langmuir. 23:6691-6697.

Edwards SJ, Kjellerup BV. 2013. Applications of biofilms in bioremediation and biotransformation of persistent organic pollutants, pharmaceuticals/personal care products, and heavy metals. Appl Microbiol Biotechnol. 97:9909-9921.

Flores S, de Anda-Herrera R, Gosset G, Bolívar FG. 2004. Growth-rate recovery of *Escherichia coli* cultures carrying a multicopy plasmid, by engineering of the pentose-phosphate pathway. Biotechnol Bioeng. 87:485-494.

Foxman B. 2003. Epidemiology of urinary tract infections: incidence, morbidity, and economic costs. Dis Mon. 49 53-70.

Frias J, Ribas F, Lucena F. 2001. Effects of different nutrients on bacterial growth in a pilot distribution system. Antonie van Leeuwenhoek. 80:129-138.

Gallant CV, Daniels C, Leung JM, Ghosh AS, Young KD, Kotra LP, Burrows LL. 2005. Common β-lactamases inhibit bacterial biofilm formation. Mol Microbiol. 58:1012-1024.

Gautam A, Bastia D. 2001. A replication terminus located at or near a replication checkpoint of *Bacillus subtilis* functions independently of stringent control. J Biol Chem. 276:8771-8777.

Ghigo J-M. 2001. Natural conjugative plasmids induce bacterial biofilm development. Nature. 412:442-445.

Gjaltema A. 1996. Biofilm Development: Growth versus Detachment [PhD]. TU Delft.

Glick BR. 1995. Metabolic load and heterologous gene expression. Biotechnol Adv. 13:247-261.

Gomes LC, Silva LN, Simões M, Melo LF, Mergulhão FJ. 2015. *Escherichia coli* adhesion, biofilm development and antibiotic susceptibility on biomedical materials. J Biomed Mater Res A. 103:1414-1423.

Gomes LC, Moreira JMR, Teodósio JS, Araújo JDP, Miranda JM, Simões M, Melo LF, Mergulhão FJ. 2014. 96-well microtiter plates for biofouling simulation in biomedical settings. Biofouling. 30:535-546.

Haddadin F, Harcum S. 2005. Transcriptome profiles for high-cell-density recombinant and wild-type *Escherichia coli*. Biotechnol Bioeng. 90:127-153.

Hancock V, Ferrières L, Klemm P. 2007. Biofilm formation by asymptomatic and virulent urinary tract infectious *Escherichia coli* strains. FEMS Microbiol Lett. 267:30-37.

Hannig C, Follo M, Hellwig E, Al-Ahmad A. 2010. Visualization of adherent micro-organisms using different techniques. J Med Microbiol. 59:1-7.

Hartley AM, House WA, Leadbeater BSC, Callow ME. 1996. The use of microelectrodes to study the precipitation of calcite upon algal biofilms. J Colloid Interface Sci. 183:498-505.

Hentzer M, Teitzel GM, Balzer GJ, Heydorn A, Molin S, Givskov M, Parsek MR. 2001. Alginate overproduction affects *Pseudomonas aeruginosa* biofilm structure and function. J Bacteriol. 183:5395-5401.

Herman-Antosiewicz A, Obuchowski M, Wegrzyn G. 2001. A plasmid cloning vector with precisely regulatable copy number in *Escherichia coli*. Mol Biotechnol. 17:193-199.

Heydorn A, Nielsen AT, Hentzer M, Sternberg C, Givskov M, Ersbøll BK, Molin S. 2000. Quantification of biofilm structures by the novel computer program COMSTAT. Microbiology. 146:2395-2407.

Holubar P, Andorfer C, Braun R. 1999. Effects of nitrogen limitation on biofilm formation in a hydrocarbon-degrading trickle-bed filter. Appl Microbiol Biotechnol. 51:536-540.

Honraet K, Goetghebeur E, Nelis HJ. 2005. Comparison of three assays for the quantification of *Candida* biomass in suspension and CDC reactor grown biofilms. J Microbiol Methods. 63:287-295.

Huang C-T, Peretti SW, Bryers JD. 1993. Plasmid retention and gene expression in suspended and biofilm cultures of recombinant *Escherichia coli* DH5α(pMJR1750). Biotechnol Bioeng. 41:211-220.

Huang C-T, Peretti SW, Bryers JD. 1994a. Effects of inducer levels on a recombinant bacterial biofilm formation and gene expression. Biotechnol Lett. 16:903-908.

Huang C-T, Peretti SW, Bryers JD. 1994b. Effects of medium carbon-to-nitrogen ratio on biofilm formation and plasmid stability. Biotechnol Bioeng. 44:329-336.

Hunt SM, Werner EM, Huang B, Hamilton MA, Stewart PS. 2004. Hypothesis for the role of nutrient starvation in biofilm detachment. Appl Environ Microbiol. 70:7418-7425.

Itakura K, Hirose T, Crea R, Riggs A, Heyneker H, Bolivar F, Boyer H. 1977. Expression in *Escherichia coli* of a chemically synthesized gene for the hormone somatostatin. Science. 198:1056-1063.

Ito A, May T, Kawata K, Okabe S. 2008. Significance of rpoS during maturation of *Escherichia coli* biofilms. Biotechnol Bioeng. 99:1462-1471.

Jackson DW, Simecka JW, Romeo T. 2002. Catabolite Repression of *Escherichia coli* Biofilm Formation. J Bacteriol. 184:3406-3410.

Jacobsen SM, Stickler DJ, Mobley HLT, Shirtliff ME. 2008. Complicated catheter-associated urinary tract infections due to *Escherichia coli* and *Proteus mirabilis*. Clin Microbiol Rev. 21:26-59.

Janjaroen D, Ling F, Monroy G, Derlon N, Mogenroth E, Boppart SA, Liu W-T, Nguyen TH. 2013. Roles of ionic strength and biofilm roughness on adhesion kinetics of *Escherichia coli* onto groundwater biofilm grown on PVC surfaces. Water Res. 47:2531-2542.

Johnson I. 1983. Human insulin from recombinant DNA technology. Science. 219:632-637.

Juhna T, Birzniece D, Larsson S, Zulenkovs D, Sharipo A, Azevedo NF, Ménard-Szczebara F, Castagnet S, Féliers C, Keevil CW. 2007. Detection of *Escherichia coli* in

biofilms from pipe samples and coupons in drinking water distribution networks. Appl Environ Microbiol. 73:7456-7464.

Khosravi M, Ryan W, Webster DA, Stark BC. 1990. Variation of oxygen requirement with plasmid size in recombinant *Escherichia coli*. Plasmid. 23:138-143.

Kim BG, Shuler ML. 1990. Analysis of pBR322 replication kinetics and its dependency on growth rate. Biotechnol Bioeng. 36:233-242.

Klahre J, Flemming HC. 2000. Monitoring of biofouling in papermill process waters. Water Res. 34:3657-3665.

Klemperer R, Ismail N, Brown M. 1979. Effect of R plasmid RPI on the nutritional requirements of *Escherichia coli* in batch culture. J Gen Microbiol. 115:325 - 331.

Król JE, Nguyen HD, Rogers LM, Beyenal H, Krone SM, Top EM. 2011. Increased transfer of a multidrug resistance plasmid in *Escherichia coli* biofilms at the air-liquid interface. Appl Environ Microbiol. 77:5079-5088.

Kumar S, Wittmann C, Heinzle E. 2004. Review: Minibioreactors. Biotechnol Lett. 26:1-10.

Lee J-H, Park J-H, Kim J-A, Neupane GP, Cho MH, Lee C-S, Lee J. 2011. Low concentrations of honey reduce biofilm formation, quorum sensing, and virulence in *Escherichia coli* O157:H7. Biofouling. 27:1095-1104.

Lee S, Bailey J. 1984. Analysis of growth rate effects on productivity of recombinant *Escherichia coli* populations using molecular mechanism models. Biotechnol Bioeng. 26:66-73.

Levy SB, Marshall B. 2004. Antibacterial resistance worldwide: causes, challenges and responses. Nat Med. 10:S122-S129.

Lim JY, Yoon J, Hovde CJ. 2010a. A brief overview of *Escherichia coli* O157:H7 and its plasmid O157. J Microbiol Biotechnol. 20:5-14.

Lim JY, La HJ, Sheng H, Forney LJ, Hovde CJ. 2010b. Influence of plasmid pO157 on *Escherichia coli* O157:H7 Sakai biofilm formation. Appl Environ Microbiol. 76:963-966.

Liu Y, Tay J-H. 2002. The essential role of hydrodynamic shear force in the formation of biofilm and granular sludge. Water Res. 36:1653-1665.

Maezono H, Noiri Y, Asahi Y, Yamaguchi M, Yamamoto R, Izutani N, Azakami H, Ebisu S. 2011. Antibiofilm effects of azithromycin and erythromycin on *Porphyromonas gingivalis*. Antimicrob Agents Chemother. 55:5887-5892.

Manns RL. 2003. Necessity is the Mother of Invention - The History of Microplates. Business Briefing: Future Drug Discovery - PolyPops Development Foundation.108-112.

Manuel CM, Nunes OC, Melo LF. 2007. Dynamics of drinking water biofilm in flow/non-flow conditions. Water Res. 41:551-562.

Manuel CM, Nunes OC, Melo LF. 2009. Unsteady state flow and stagnation in distribution systems affect the biological stability of drinking water. Biofouling. 26:129-139.

Marouani-Gadri N, Chassaing D, Carpentier B. 2009. Comparative evaluation of biofilm formation and tolerance to a chemical shock of pathogenic and nonpathogenic *Escherichia coli* O157:H7 strains. J Food Prot. 72:157-164.

Mattila K, Weber A, Salkinoja-Salonen SM. 2002. Structure and on-site formation of biofilms in paper machine water flow. J Ind Microbiol Biotechnol. 28:268-279.

May T, Okabe S. 2008. *Escherichia coli* harboring a natural IncF conjugative F plasmid develops complex mature biofilms by stimulating synthesis of colanic acid and curli. J Bacteriol. 190:7479-7490.

May T, Ito A, Okabe S. 2009. Induction of multidrug resistance mechanism in *Escherichia coli* biofilms by interplay between tetracycline and ampicillin resistance genes. Antimicrob Agents Chemother. 53:4628-4639.

McCoy WF, Bryers JD, Robbins J, Costerton JW. 1981. Observations of fouling biofilm formation. Can J Microbiol. 27:910-917.

Melo FL, Vieira JM. 1999. Physical stability and biological activity of biofilms under turbulent flow and low substrate concentration. Bioprocess Eng. 20:363-368.

Melo L, Oliveira R. 2001. Biofilm Reactors. In: Cabral JMS, Mota MM, Tramper J, editors. Multiphase Bioreactor Design. New York: Taylor & Francis. p. 271-308.

Melo L, Flemming H-C. 2010. Mechanistic Aspects of Heat Exchanger and Membrane Biofouling and Prevention. In: Amjad Z, editor. The Science and Technology of Industrial Water Treatment. CRC Press. p. 365-380.

Melo LF. 2003. Biofilm Formation and its Role in Fixed Film Processes. In: Mara D, Horan NJ, editors. Handbook of Water and Wastewater Microbiology. London: Academic Press. p. 337-349.

Mergulhão FJM, Summers DK, Monteiro GA. 2005. Recombinant protein secretion in *Escherichia coli*. Biotechnol Adv. 23:177-202.

Mergulhão FJM, Monteiro GA, Cabral JMS, Taipa MA. 2004b. Design of bacterial vector systems for the production of recombinant proteins in *Escherichia coli*. J Microbiol Biotechnol. 14:1-14.

Monroe D. 2007. Looking for chinks in the armor of bacterial biofilms. PLoS Biol. 5:e307.

Moreira JMR, Teodósio JS, Silva FC, Simões M, Melo LF, Mergulhão FJ. 2013a. Influence of flow rate variation on the development of *Escherichia coli* biofilms. Bioprocess Biosyst Eng. 36:1787-1796.

Moreira JMR, Araújo JD, Miranda JM, Simões M, Melo LF, Mergulhão FJ. 2014. The effects of surface properties on *Escherichia coli* adhesion are modulated by shear stress. Colloids Surf B Biointerfaces. 123:1-7.

Moreira JMR, Fulgêncio R, Alves P, Machado I, Bialuch I, Melo LF, Simões M, Mergulhão FJ. 2016. Evaluation of SICAN performance for biofouling mitigation in the food industry. Food Control. 62:201-207.

Muscariello L, Rosso F, Marino G, Giordano A, Barbarisi M, Cafiero G, Barbarisi A. 2005. A critical overview of ESEM applications in the biological field. J Cell Physiol. 205:328-334.

Nicolella C, van Loosdrecht MCM, Heijnen JJ. 2000. Wastewater treatment with particulate biofilm reactors. J Biotechnol. 80:1-33.

Niwa H, Inouye S, Hirano T, Matsuno T, Kojima S, Kubota M, Ohashi M, Tsuji FI. 1996. Chemical nature of the light emitter of the *Aequorea* green fluorescent protein. Proc Natl Acad Sci USA. 93:13617-13622.

Norman A, Hansen LH, She Q, Sørensen SJ. 2008. Nucleotide sequence of pOLA52: a conjugative IncX1 plasmid from *Escherichia coli* which enables biofilm formation and multidrug efflux. Plasmid. 60:59-74.

Norton TA, Thompson RC, Pope J, Veltkamp CJ, Banks B, Howard CV, Hawkins SJ. 1998. Using confocal laser scanning microscopy, scanning electron microscopy and phase contrast light microscopy to examine marine biofilms. Aquat Microbial Ecol. 16:199-204.

Novagen. 2005. pET system manual. 11th edition.

O'Connell HA, Niu C, Gilbert ES. 2007. Enhanced high copy number plasmid maintenance and heterologous protein production in an *Escherichia coli* biofilm. Biotechnol Bioeng. 97:439-446.

Ong C-LY, Beatson SA, McEwan AG, Schembri MA. 2009. Conjugative plasmid transfer and adhesion dynamics in an *Escherichia coli* biofilm. Appl Environ Microbiol. 75:6783-6791.

Overton TW. 2014. Recombinant protein production in bacterial hosts. Drug Discov Today. 19:590-601.

Ow D, Nissom P, Philp R, Oh S, Yap M. 2006. Global transcriptional analysis of metabolic burden due to plasmid maintenance in *Escherichia coli* DH5α during batch fermentation. Enzyme Microb Technol. 39:391-398.

Palmer Jr RJ, Sternberg C. 1999. Modern microscopy in biofilm research: confocal microscopy and other approaches. Curr Opin Biotechnol. 10:263-268.

Palmer Jr RJ, Haagensen JJ, Neu T, Sternberg C. 2006. Confocal Microscopy of Biofilms - Spatiotemporal Approaches. In: Pawley JB, editor. Handbook of Biological Confocal Microscopy. US: Springer. p. 870-888.

Peeters E, Nelis HJ, Coenye T. 2008. Comparison of multiple methods for quantification of microbial biofilms grown in microtiter plates. J Microbiol Methods. 72:157-165.

Percival SL, Knapp JS, Wales DS, Edyvean RGJ. 1999. The effect of turbulent flow and surface roughness on biofilm formation in drinking water. J Ind Microbiol Biotechnol. 22:152-159.

Pereira A, Mendes J, Melo LF. 2008. Using nanovibrations to monitor biofouling. Biotechnol Bioeng. 99:1407-1415.

Pereira MO, Vieira MJ. 2001. Effects of the interactions between glutaraldehyde and the polymeric matrix on the efficacy of the biocide against *Pseudomonas fluorescens* biofilms. Biofouling. 17:93-101.

Pereira MO, Morin P, Vieira MJ, Melo LF. 2002a. A versatile reactor for continuous monitoring of biofilm properties in laboratory and industrial conditions. Lett Appl Microbiol. 34:22-26.

Pereira MO, Kuehn M, Wuertz S, Neu T, Melo LF. 2002b. Effect of flow regime on the architecture of a *Pseudomonas fluorescens* biofilm. Biotechnol Bioeng. 78:164-171.

Peyton BM. 1996. Effects of shear stress and substrate loading rate on *Pseudomonas aeruginosa* biofilm thickness and density. Water Res. 30:29-36.

Pines O, Inouye M. 1999. Expression and secretion of proteins in *E. coli*. Mol Biotechnol. 12:25-34.

Pitts B, Hamilton MA, Zelver N, Stewart PS. 2003. A microtiter-plate screening method for biofilm disinfection and removal. J. Microbiol. Methods. 54:269-276.

Priester JH, Horst AM, Van de Werfhorst LC, Saleta JL, Mertes LA, Holden PA. 2007. Enhanced visualization of microbial biofilms by staining and environmental scanning electron microscopy. J Microbiol Methods. 68:577-587.

Prigent-Combaret C, Vidal O, Dorel C, Lejeune P. 1999. Abiotic surface sensing and biofilm-dependent regulation of gene expression in *Escherichia coli*. J. Bacteriol. 181:5993-6002.

Quave CL, Plano LRW, Pantuso T, Bennett BC. 2008. Effects of extracts from Italian medicinal plants on planktonic growth, biofilm formation and adherence of methicillin-resistant *Staphylococcus aureus*. J. Ethnopharmacol. 118:418-428.

Reisner A, Höller BM, Molin S, Zechner EL. 2006. Synergistic effects in mixed *Escherichia coli* biofilms: conjugative plasmid transfer drives biofilm expansion. J Bacteriol. 188:3582-3588.

Reisner A, Haagensen JAJ, Schembri MA, Zechner EL, Molin S. 2003. Development and maturation of *Escherichia coli* K-12 biofilms. Mol Microbiol. 48:933-946.

Rhee J, Diaz Ricci JC, Bode J, Schügerl K. 1994. Metabolic enhancement due to plasmid maintenance. Biotechnol Lett. 16:881-884.

Rochex A, Lebeault JM. 2007. Effects of nutrients on biofilm formation and detachment of a *Pseudomonas putida* strain isolated from a paper machine. Water Res. 41:2885-2892.

Rochex A, Godon J-J, Bernet N, Escudié R. 2008. Role of shear stress on composition, diversity and dynamics of biofilm bacterial communities. Water Res. 42:4915-4922.

Rozkov A, Avignone-Rossa C, Ertl P, Jones P, O'Kennedy R, Smith J, Dale J, Bushell M. 2004. Characterization of the metabolic burden on *Escherichia coli* DH1 cells imposed by the presence of a plasmid containing a gene therapy sequence. Biotechnol Bioeng. 88:909-915.

Ryan W, Parulekar SJ, Stark BC. 1989. Expression of β-lactamase by recombinant *Escherichia coli* strains containing plasmids of different sizes - effects of pH, phosphate, and dissolved oxygen. Biotechnol Bioeng. 34:309-319.

Sambrook J, Russell DW editors. 2001. Molecular cloning: a laboratory manual. 3rd ed. New York: Cold Spring Harbor Laboratory Press.

Sanchez-Garcia L, Martín L, Mangues R, Ferrer-Miralles N, Vázquez E, Villaverde A. 2016. Recombinant pharmaceuticals from microbial cells: a 2015 update. Microb. Cell Fact. 15:1-7.

Seo J-H, Bailey JE. 1985. Effects of recombinant plasmid content on growth properties and cloned gene product formation in *Escherichia coli*. Biotechnol Bioeng. 27:1668-1674.

Serra DO, Richter AM, Klauck G, Mika F, Hengge R. 2013. Microanatomy at cellular resolution and spatial order of physiological differentiation in a bacterial biofilm. mBio. 4:e100103-100113.

Shakeri S, Kermanshahi RK, Moghaddam MM, Emtiazi G. 2007. Assessment of biofilm cell removal and killing and biocide efficacy using the microtiter plate test. Biofouling. 23:79-86.

Shunmugaperumal T. 2010. Introduction and Overview of Biofilm. In: Shunmugaperumal T, editor. Biofilm Eradication and Prevention: A Pharmaceutical Approach to Medical Device Infections. Hoboken: John Wiley & Sons, Inc. p. 36-72.

Silva F, Queiroz JA, Domingues FC. 2012. Evaluating metabolic stress and plasmid stability in plasmid DNA production by *Escherichia coli*. Biotechnol Adv. 30:691-708.

Silva F, Passarinha L, Sousa F, Queiroz JA, Domingues FC. 2009. Influence of growth conditions on plasmid DNA production. J Microbiol Biotechnol. 19:1408-1414.

Simões LC, Simões M, Vieira M. 2010a. Adhesion and biofilm formation on polystyrene by drinking water-isolated bacteria. Antonie van Leeuwenhoek. 98:317-329.

Simões LC, Azevedo N, Pacheco A, Keevil CW, Vieira MJ. 2006. Drinking water biofilm assessment of total and culturable bacteria under different operating conditions. Biofouling. 22:91-99.

Simões M, Pereira MO, Sillankorva S, Azeredo J, Vieira MJ. 2007. The effect of hydrodynamic conditions on the phenotype of *Pseudomonas fluorescens* biofilms. Biofouling. 23:249-258.

Singh R, Paul D, Jain RK. 2006. Biofilms: implications in bioremediation. Trends Microbiol. 14:389-397.

Smolke CD, Keasling JD. 2002. Effect of copy number and mRNA processing and stabilization on transcript and protein levels from an engineered dual-gene operon. Biotechnol Bioeng. 78:412-424.

Sørensen HP, Mortensen KK. 2005. Advanced genetic strategies for recombinant protein expression in *Escherichia coli*. J Biotechnol. 115:113-128.

Stepanović S, Vuković D, Dakić I, Savić B, Švabić-Vlahović M. 2000. A modified microtiter-plate test for quantification of staphylococcal biofilm formation. J Microbiol Methods. 40:175-179.

Stewart PS, Franklin MJ. 2008. Physiological heterogeneity in biofilms. Nat Rev Micro. 6:199-210.

Stewart PS, Murga R, Srinivasan R, de Beer D. 1995. Biofilm structural heterogeneity visualized by three microscopic methods. Water Res. 29:2006-2009.

Stoodley P, Warwood BK. 2003. Use of Flow Cells an Annular Reactors to Study Biofilms. In: Lens P, O'Flaherty V, Moran AP, Stoodley P, Mahony T, editors. Biofilms in Medicine, Industry and Environmental Biotechnology: Characteristics, Analysis and Control. Cornwall: IWA Publishing. p. 197-213.

Stoodley P, Sauer K, Davies DG, Costerton JW. 2002. Biofilms as complex differentiated communities. Annu Rev Microbiol. 56:187-209.

Studier FW, Moffatt BA. 1986. Use of bacteriophage T7 RNA polymerase to direct selective high-level expression of cloned genes. J Mol Biol. 189:113-130.

Summers D. 1998. Timing, self-control and a sense of direction are the secrets of multicopy plasmid stability. Mol Microbiol. 29:1137-1145.

Sutherland IW. 2001. The biofilm matrix - an immobilized but dynamic microbial environment. Trends Microbiol. 9:222-227.

Tambyah P, Maki D. 2000. Catheter-associated urinary tract infection is rarely symptomatic: a prospective study of 1497 catheterized patients. Arch Intern Med. 160:678-682.

Teodósio JS, Simões M, Mergulhão FJ. 2012a. The influence of nonconjugative *Escherichia coli* plasmids on biofilm formation and resistance. J Appl Microbiol. 113:373-382.

Teodósio JS, Simões M, Melo LF, Mergulhão FJ. 2011a. Flow cell hydrodynamics and their effects on *E. coli* biofilm formation under different nutrient conditions and turbulent flow. Biofouling. 27:1-11.

Teodósio JS, Silva FC, Moreira JMR, Simões M, Melo LF, Alves MA, Mergulhão FJ. 2013. Flow cells as quasi ideal systems for biofouling simulation of industrial piping systems. Biofouling. 29:953-966.

Tombolini R, Unge A, Davey ME, de Bruijn FJ, Jansson JK. 1997. Flow cytometric and microscopic analysis of GFP-tagged *Pseudomonas fluorescens* bacteria. FEMS Microbiol Ecol. 22:17-28.

Toté K, Berghe DV, Maes L, Cos P. 2008. A new colorimetric microtitre model for the detection of *Staphylococcus aureus* biofilms. Lett Appl Microbiol. 46:249-254.

Tsibouklis J, Stone M, Thorpe AA, Graham P, Peters V, Heerlien R, Smith JR, Green KL, Nevell TG. 1999. Preventing bacterial adhesion onto surfaces: the low-surface-energy approach. Biomaterials. 20:1229-1235.

van der Kooji D. 1992. Assimilable organic-carbon as an indicator of bacterial regrowth. J Am Water Works Assoc. 84:57-65.

Van Houdt R, Michiels CW. 2005. Role of bacterial cell surface structures in *Escherichia coli* biofilm formation. Res Microbiol. 156:626-633.

Vieira MJ, Melo LF, Pinheiro MM. 1993. Biofilm formation: hydrodynamic effects on internal diffusion and structure. Biofouling. 7:67-80.

Volk CJ, LeChevallier MW. 1999. Impacts of the reduction of nutrient levels on bacterial water quality in distribution systems. Appl Environ Microbiol. 65:4957-4966.

von Ohle C, Gieseke A, Nistico L, Decker EM, deBeer D, Stoodley P. 2010. Real-time microsensor measurement of local metabolic activities in ex vivo dental biofilms exposed to sucrose and treated with chlorhexidine. Appl Environ Microbiol. 76:2326-2334.

von Rège H, Sand W. 1998. Evaluation of biocide efficacy by microcalorimetric determination of microbial activity in biofilms. J Microbiol Methods. 33:227-235.

Walters MC, Roe F, Bugnicourt A, Franklin MJ, Stewart PS. 2003. Contributions of antibiotic penetration, oxygen limitation, and low metabolic activity to tolerance of *Pseudomonas aeruginosa* biofilms to ciprofloxacin and tobramycin. Antimicrob Agents Chemother. 47:317-323.

Wäsche S, Horn H, Hempel DC. 2002. Influence of growth conditions on biofilm development and mass transfer at the bulk/biofilm interface. Water Res. 36:4775-4784.

Werner E, Roe F, Bugnicourt A, Franklin MJ, Heydorn A, Molin S, Pitts B, Stewart PS. 2004. Stratified growth in *Pseudomonas aeruginosa* biofilms. Appl Environ Microbiol. 70:6188-6196.

Wood TK. 2009. Insights on *Escherichia coli* biofilm formation and inhibition from whole-transcriptome profiling. Environ Microbiol. 11:1-15.

Wright CJ, Shah MK, Powell LC, Armstrong I. 2010. Application of AFM from microbial cell to biofilm. Scanning. 32:134-149.

Xi C, Marks D, Schlachter S, Luo W, Boppart SA. 2006. High-resolution three-dimensional imaging of biofilm development using optical coherence tomography. J Biomed Opt. 11:34001.

Yang X, Ma Q, Wood TK. 2008. The R1 conjugative plasmid increases *Escherichia coli* biofilm formation through an envelope stress response. Appl Environ Microbiol. 74:2690-2699.

Yang Y-X, Qian Z-G, Zhong J-J, Xia X-X. 2016. Hyper-production of large proteins of spider dragline silk MaSp2 by *Escherichia coli* via synthetic biology approach. Process Biochem. 51:484-490.

Yawata Y, Nomura N, Uchiyama H. 2008. Development of a novel biofilm continuous culture method for simultaneous assessment of architecture and gaseous metabolite production. Appl Environ Microbiol. 74:5429-5435.

Yu H, Shi Y, Sun X, Luo H, Shen Z. 2003. Effect of poly(β-hydroxybutyrate) accumulation on the stability of a recombinant plasmid in *Escherichia coli*. J Biosci Bioeng. 96:179-183.

Zobell CE. 1943. The effect of solid surfaces upon bacterial activity. J Bacteriol. 46:39-56.

3.

96-well microtiter plates for biofouling simulation: effect of hydrodynamics and nutrient concentration[a]

Abstract

Microtiter plates with 96 wells are routinely used in biofilm research mainly because they enable high-throughput assays. These platforms are used in a variety of conditions ranging from static to dynamic operation, but without proper knowledge of the flow behavior inside them.

In this chapter, the influence of flow conditions and nutrient concentration on *E. coli* biofilm formation in microtiter plates was assessed, and the operational conditions to be used in order to simulate relevant biomedical scenarios were defined. It was also intended to verify if the 96-well microtiter plate can reproduce the shear forces experienced in a flow cell operated under turbulent regime in order to use it for screening purposes.

Assays were performed in static mode and in incubators with distinct orbital diameters using different concentrations of glucose, peptone and yeast extract. CFD was used to simulate the flow inside the wells for shaking frequencies ranging from 50 to 200 rpm and orbital diameters from 25 to 100 mm. Numerical simulations were conducted by

[a] The content of this chapter was adapted from the following publication(s):

Gomes LC, Moreira JMR, Teodósio JS, Araújo JDP, Miranda JM, Simões M, Melo LF, Mergulhão FJ. 2014. 96-well microtiter plates for biofouling simulation in biomedical settings. Biofouling. 30:535-546.

Dr. João Miranda and Dr. José Araújo from the Transport Phenomena Research Center (CEFT - FEUP).

Higher glucose concentrations enhanced *E. coli* adhesion in the first 24 hours, but variation of peptone and yeast extract concentration had no significant impact on biofilm formation. Numerical simulations indicate that 96-well microtiter plates can be used to simulate a variety of biomedical scenarios if the operating conditions are carefully set. Nevertheless, these microplates fail to achieve the same average shear stress value obtained in the flow cell system (operating at Re = 4,600).

3.1. Introduction

Biofilm establishment and development are dynamic and complex processes regulated by intrinsic biological properties and also by many environmental conditions (Donlan 2002). It is known that hydrodynamics influence biofilm formation (Liu & Tay 2002, Stoodley et al. 2001, Wäsche et al. 2002), not only in terms of nutrient and oxygen supply (Moreira et al. 2013a), but also by the shear forces, which can modulate microbial cell adhesion to a given surface (Busscher & van der Mei 2006, Simões et al. 2007, Teodósio et al. 2013a, van Loosdrecht et al. 1995). One of the key parameters affecting cell adhesion to a surface is the shear rate at that surface (Busscher & van der Mei 2006, Teodósio et al. 2013a). Table 3.1 lists commonly found shear strain rates in biomedical and miscellaneous settings where bacterial adhesion can occur. In medical devices, molecules and microorganisms are constantly exposed to shear conditions caused by liquid flow (Fux et al. 2004, Mukherjee et al. 2009). Urinary catheters and the human urinary tract are submitted to significant hydrodynamic shear forces (adult humans produce 1-2 liters of urine per day, which is expelled at average flow rates of 40-80 ml h^{-1}) (Vejborg & Klemm 2008), but adhesion to surfaces enables *E. coli* to resist removal by urine flow and establish infection (Hancock et al. 2007, Ulett et al. 2007). Besides the hydrodynamic conditions, the nutrient/substrate concentration can have impact on biofilm growth, development and detachment behavior (Rochex & Lebeault 2007, Stoodley et al. 2001, Telgmann et al. 2004).

Microtiter plates are often used for biofilm studies because small media volumes are needed (Coenye & Nelis 2010), replicate tests are easily prepared using multichannel

Table 3.1. Characteristic shear strain rates found in biomedical and other settings

	Phenomenon	Shear strain rate (s^{-1})	Reference
Eyes	Blinking of an eye	0.35	(Bakker et al. 2003, Tranoudis & Efron 2004)
	On-eye contact lens motion	1,000	(Tran et al. 2011)
Mouth	Fluid on oral cavity	0.1-50	(Bakker et al. 2003)
	On teeth, while biting an apple	200	
Urinary tract	Urinary flow in a catheter	15	(Bakker et al. 2003, Velraeds et al. 1998)
Cardiovascular system	Blood flow in veins	20-800	(Aleviadrou & McIntire 1995, Inauen et al. 1990, Michelson 2002)
	Blood flow in arteries	50-650	(Aleviadrou & McIntire 1995, Bark et al. 2012, Michelson 2002)
	Central venous hemodialysis catheters	1,900-2,400	(Mareels et al. 2007)
	Blood flow in little blood vessels	2,000-5,000	(Aleviadrou & McIntire 1995, Mareels 2007)
Brain	Cerebral circulation	> 100	(Singh et al. 2010)
Other	Flow of a film over a vertical plate	0.1	(Bakker et al. 2003)
	Annular space of a scraped surface heat exchanger	< 40	(Yataghene et al. 2008)
	Tumbling or pouring	10-100	(Bakker et al. 2003)
	Wall of a planetary mixer during cake batters	20-500	(Chesterton et al. 2011)
	Ship in harbor	50	(Bakker et al. 2003)
	Channels within a biofilm	60-300	

pipettors (Duetz 2007), and this closed (batch reactor-like) system lends itself to protocols where different media compositions are simultaneously tested (Coenye & Nelis 2010).

The main goals of this chapter were to assess the influence of nutrient concentration and flow conditions on *E. coli* biofilm formation in the 96-well microtiter plate and to verify if this biofilm platform can simulate the hydrodynamics of a flow cell system operating under turbulent regime. Additionally, it is intended to confirm if the hydrodynamic conditions that can be attained with 96-well microtiter plates are similar to those normally encountered in diverse biomedical scenarios. With this aim, CFD was used since it enables the simulation of fluid flow and/or heat/mass transfer problems, providing fast and detailed information of general flow phenomena and other parameters which are difficult to obtain experimentally (Xia & Sun 2002). CFD has the advantage of allowing a quick assessment of different alternatives and changes, including geometrical and flow parameters, without spending much time and resources (Hilgenstock & Ernst 1996).

A good comprehension of the hydrodynamics that are found in the areas where biofilms naturally occur is crucial for biofilm studies performed in laboratory-based devices. This enables the correct setting of operational conditions in the lab in order to obtain biofilms that resemble those found in natural environments.

3.2. Materials and methods

3.2.1. Numerical simulations

Numerical simulations were made in Ansys Fluent CFD package (version 13.0). A cylindrical well (diameter of 6.6 mm and height of 11.7 mm, Figure 3.1) was built in Design Modeller 13.0 and discretized into a grid of 18,876 hexahedral cells by Meshing 13.0. The average dimensions of a single hexahedral cell were 270 × 300 × 300 μm. A grid independence analysis was performed and the results showed that reducing the cell dimensions by half in all directions (corresponding to an 8 fold reduction of the cell volume) has a negligible effect (about 7.7%) when compared to the uncertainty associated with the biological data obtained in the experimental part of this work (Table 3.2). For each simulation, the volume of the liquid phase inside the well was set to 200 μl and the

remaining volume was filled with gas. The properties of water and air at 30 ºC were used for the liquid and gas phases, respectively (Table 3.3). The surface tension was set equal to the surface tension of an air/water system.

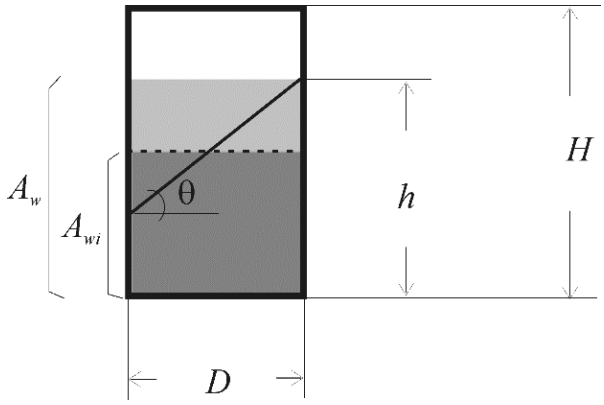

Figure 3.1. Schematic representation of a well. Dark grey area represents the wetted area in a stationary well (A_{wi}) and light grey area represents the area increase upon shaking (A_w). D is the well diameter, h is the maximum height of the interface, H is the well height and θ is the surface angle.

Table 3.2. Grid independence analysis for orbital diameter of 50 mm and shaking frequency of 150 rpm. Grid 1 was used throughout this work

	Grid 1	**Grid 2**
Cell number	18,876	151,008
Average cell dimensions (µm)	270 × 300 × 300	135 × 150 × 150
Average strain rate (s^{-1})	44.1	41.0
Difference	7.7%	

Table 3.3. Physical properties of the gas/liquid system used in the CFD simulations

	Density ($kg\ m^{-3}$)		**Viscosity ($kg\ m^{-1}s^{-1}$)**		**Surface tension (Nm^{-1})**	
	T = 30 ºC	T = 37 ºC	T = 30 ºC	T = 37 ºC	T = 30 ºC	T = 37 ºC
Air	1.15	1.14	1.86×10^{-5}	2.09×10^{-5}	0.071	0.070
Water	996	993	8.01×10^{-4}	6.94×10^{-4}		

The volume of fluid (VOF) methodology (Hirt & Nichols 1981) was used to track the liquid/gas interface and the precise locations of the interface were obtained by the Geo-Reconstruct method (Youngs 1982). The velocity-pressure coupled equations were solved by the PISO algorithm, the QUICK scheme was used for the discretization of the momentum equations and the PRESTO! scheme was chosen for pressure discretization.

In Ansys Fluent, the surface tension effects were modeled by the continuum surface force (Brackbill et al. 1992), which were introduced through a source term in the momentum equation. An accelerating reference frame was adopted, and the circular orbital motion was taken into account by introducing another source term that represents the effect of the force into the fluid resulting from this orbital motion. The no slip boundary condition and a contact angle of 83º were considered for all the walls (Simões et al. 2010a).

Simulations were made for different shaking frequencies (50 to 200 rpm) and orbital diameters (25 to 100 mm). For each case, 5 s of physical time were simulated with a fixed time step of 2.5×10^{-4} s. The primary numerical results were the instantaneous velocity components, the instantaneous pressure and the liquid or gas phase volume fractions. These results were used to determine the shear strain rate[b], the location of the interface and the air-liquid interfacial area. The magnitude of the shear rate was determined by Ansys Fluent with the help of a built-in expression. For each simulation, after the steady state is reached, the average shear strain rate was calculated by integrating an instantaneous solution over the wetted area. The time averaged shear strain rate was obtained by averaging the steady state shear rate of the liquid side during a complete orbit.

3.2.2. Bacterial strain

E. coli JM109(DE3) from Promega (USA) was used for biofilm formation. Its genotype is *end*A1, *rec*A1, *gyr*A96, *thi*, *hsd*R17 (r_k^-, m_k^+), *rel*A1, *sup*E44, λ^-, Δ(*lac-pro*AB), [F', *tra*D36, *pro*AB, *lac*$I^qZ\Delta M15$], λ(DE3). *E. coli* CECT 434 (ATCC 25922), a clinical isolate often used for antimicrobial susceptibility tests, was also used for

[b] The shear rate is the derivative of the velocity in the perpendicular direction from the wall. In this system, the shear rate gives an indication of the drag force felt by adhering cells and it is also a measurement of the frequency at which cells contact the wall. Mathematically, the shear stress in Newtonian fluids is proportional to the shear strain rate in the fluid, where the viscosity is the constant of proportionality.

confirmation of the results in selected conditions. An overnight culture of *E. coli* was obtained by inoculation of 500 µl of a glycerol stock (kept at -80 ºC) to a total volume of 0.2 l of inoculation media previously described by Teodósio et al (2011a). This consisted of 5.5 g l^{-1} glucose, 2.5 g l^{-1} peptone, 1.25 g l^{-1} yeast extract in phosphate buffer (1.88 g l^{-1} KH_2PO_4 and 2.60 g l^{-1} Na_2HPO_4), pH 7.0. The culture was grown on a 1 l shake-flask, incubated overnight at 30 ºC with orbital agitation (120 rpm). Cells were harvested by centrifugation (for 10 min at 3202 *g*) and appropriate dilutions in sterile saline (8.5 g l^{-1} NaCl) were performed to obtain an optical density (OD) of approximately 0.4 at 610 nm.

3.2.3. Culture conditions and biofilm quantitation

Different media formulations were assayed using a reference medium recipe that had already been tested for biofilm formation in a flow cell with the same strain (Teodósio et al. 2011a). This reference medium consisted of 0.5 g l^{-1} glucose, 0.25 g l^{-1} peptone, 0.125 g l^{-1} yeast extract and phosphate buffer (0.188 g l^{-1} KH_2PO_4 and 0.26 g l^{-1} Na_2HPO_4), pH 7.0. A glucose concentration of 0.15 g l^{-1} was also tested in that study and it was shown that there were no significant changes in the amount of biofilm formed (Teodósio et al. 2011a). In that work, when the glucose concentration was reduced to 0.15 g l^{-1}, the peptone and yeast concentrations were also reduced to 0.07 and 0.03 g l^{-1}, respectively. Since preliminary results (Moreira et al. 2013c) had shown that glucose concentration has a significant impact on the amount of biofilm formed in microtiter plates (concentrations of 0.25 and 1 g l^{-1} were assayed), an intermediate concentration (0.5 g l^{-1}) was also tested. Additionally, since it was shown that in turbulent flow conditions higher nutrient loads generally yield thicker biofilms (Teodósio et al. 2011b), the effect of increasing the peptone and yeast extract concentrations independently was assessed starting from their reference values of 0.25 and 0.125 g l^{-1}, respectively. Thus a concentration range of 0.25, 0.5 and 1 g l^{-1} was used for glucose and peptone, whereas for yeast extract concentrations of 0.125, 0.5 and 1 g l^{-1} were tested.

For each formulation, the reference culture medium (Teodósio et al. 2011a) was prepared without the compound under study and then the appropriate volume of a concentrated solution of that nutrient was added to obtain the desired concentration. 96-well microtiter plates were inoculated as described by Moreira et al. (2013c). Briefly, six wells of sterile 96-well PS, flat-bottomed microtiter plates (Orange Scientific, USA) were

filled with 180 µl of each media formulation and inoculated with 20 µl of the inoculum previously prepared (section 3.2.2). The plates were then incubated at 30 ºC in two separate orbital incubators operating at the same shaking frequency (150 rpm). One of the incubators had a 50 mm orbital shaking diameter (CERTOMAT® BS-1, Sartorius AG, Germany) and another had a 25 mm shaking diameter (AGITORB 200, Aralab, Portugal). An additional set of experiments was performed with no shaking (0 rpm) at 30 ºC. Biofilm formation was monitored for 60 h with plates being removed from the incubators every 12 h for biofilm quantification (for time zero the plates were not incubated at all). Three independent experiments were performed for each shaking condition. For control, quantifications were also conducted in the absence of bacteria, demonstrating that no biofilm growth occurred in the correspondent wells during the experimental time.

Biofilm quantitation by CV assay was performed as fully described by Moreira et al. (2013c). Concisely, the plate was inverted in a single quick movement, discarding the contents of the wells. To remove the non-adherent cells, all wells were washed with sterile water (200 µl per well). Bacterial biofilms were fixed with 250 µl of 96% ethanol per well (Shakeri et al. 2007) and, after 15 min, the content was removed by inverting the plate. Then the fixed bacteria were stained for 5 min with 200 µl of 1% (v/v) crystal violet (Merck, Portugal) per well. After that, the plate was again emptied and the dye bound to adherent cells was resolubilized with 200 µl of 33% (v/v) acetic acid (VWR, Portugal) per well (Simões et al. 2010a). The absorbance was measured at 570 nm using a microtiter plate reader (SpectraMax M2E, Molecular Devices, Inc., UK) and biofilm amount was expressed as absorbance (570 nm) values. The detection limit of this method was 0.005.

In order to confirm the results obtained by the CV method, biofilm quantitation in selected conditions was also performed using viable plate counting (Figure 3.2), as described by Moreira et al. (2015b). Both methods showed good correlation (r^2=0.988), as previously reported by Alnnasouri et al. (2011) and Sonak & Bhosle (1995).

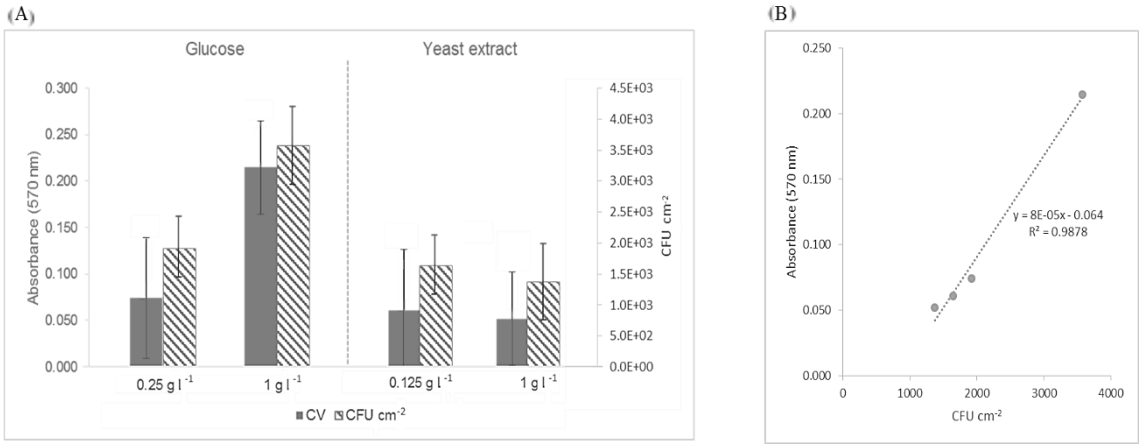

Figure 3.2. Comparison of the CV staining method ("Absorbance" y-scale) and the colony plating method ("CFU cm^{-2}" y-scale) for quantitation of 24 h biofilms formed in static conditions using two different concentrations of glucose or yeast extract. (A) Biofilm quantitation; (B) correlation between both methods.

3.2.4. Calculations and statistical analysis

The results presented in Figure 3.6 are an average of those obtained in three independent experiments for each shaking condition (50 and 25 mm orbital shaking diameter at 150 rpm and no shaking). For a single experiment, the final value is an average of the readings obtained in 6 replica wells within one plate. The following standard deviations (SDs) were obtained for the glucose experiments, 34%, 22% and 27% (50 mm, 25 mm and no shaking, respectively). For peptone 36%, 25% and 22%, and for yeast extract 19%, 25% and 26% (in the same order).

With the aim of ascertaining the statistical significance, data was analysed using IBM SPSS Statistics software version 19.0. The Post Hoc Multiple Comparisons Tests - Tukey and LSD - were used based on a confidence level of 95% (differences reported as significant for P values < 0.05). The following statistical analysis were conducted: a - comparison between 1 g l^{-1} and 0.5 g l^{-1} glucose or peptone or yeast extract, b - comparison between 1 g l^{-1} and 0.25 g l^{-1} glucose or peptone, c - comparison between 0.5 g l^{-1} and 0.25 g l^{-1} glucose or peptone, d - comparison between 0.5 g l^{-1} and 0.125 g l^{-1} yeast extract, e - comparison between 1 g l^{-1} and 0.125 g l^{-1} yeast extract (Figure 3.6). Paired *t*-test analysis was also performed when appropriate.

3.3. Results

3.3.1. CFD modelling of shaken 96-well microtiter plates

In an orbital shaker, the inclination of the air-liquid interface increases with the increase of the shaking frequency and the orbital diameter. This effect can be quantified by measuring the angle of the surface formed with the horizontal (Figure 3.3A). A maximum angle of 34º was obtained for the largest orbital diameter and shaking frequency. The maximum height of the interface (h), normalized by the height of the well (H), is represented in Figure 3.3B as a function of the shaking frequency for different orbital diameters. This dimensionless parameter is an indication of the volume of the well occupied by the liquid. Values ranging from 46 to 67% were obtained (with the highest values corresponding to the larger orbital diameter and shaking frequency), indicating that the liquid does not overflow from the well in any of the simulated situations. As the slope of the interface increased, the interfacial area also increased. Figure 3.3C shows the ratio between the specific surface area in a moving well (a_f) and the specific surface area in a stationary well (a_i) for several shaking frequencies and orbital amplitudes. When the a_f/a_i ratio is greater than 1, this means that an area gain is obtained with the orbital motion. The area gain was negligible (less than 2%) for the smaller orbital diameter regardless of the shaking frequency. For all the orbital diameters, area gains ranging from 0.4-2% were obtained for shaking frequencies up to 150 rpm (except for 75 and 100 mm at 150 rpm where the gains were of 5 and 8%, respectively). The highest area gain (of 31%) was obtained for the largest orbital diameter and shaking frequency. It is also possible to observe from Figure 3.3C that the slope of area gain increased significantly with the orbital diameter from 150 to 200 rpm. The evolution of the wetted area (A_w) normalized by the wetted area for a stationary well (A_{wi}) is represented on Figure 3.3D. It follows the same trend that was observed for the maximum height of the interface (Figure 3.3B), representing the available area for biofilm formation. At lower shaking frequencies (50 and 100 rpm), the wetted area remained practically constant at different orbital diameters (area gains less than 5%), but for higher frequencies area gains ranging from 4 to 34% were determined.

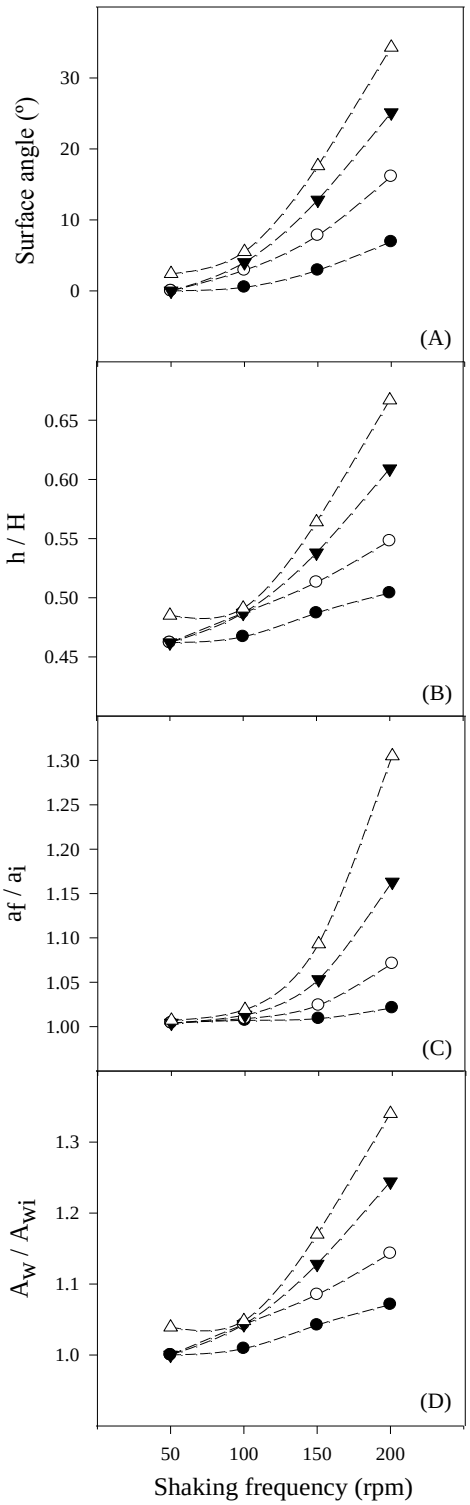

Figure 3.3. Simulation results of the effect of shaking frequency and amplitude on the (A) surface angle, (B) maximum height of the interface (h) normalized by the well height (H), (C) specific air-liquid surface area (a_f/a_i), (D) ratio between the wetted area for a dynamic (A_w) and a stationary well (A_{wi}). △ - 100 mm shaking diameter, ▼ - 75 mm shaking diameter, ○ - 50 mm shaking diameter, ● - 25 mm shaking diameter.

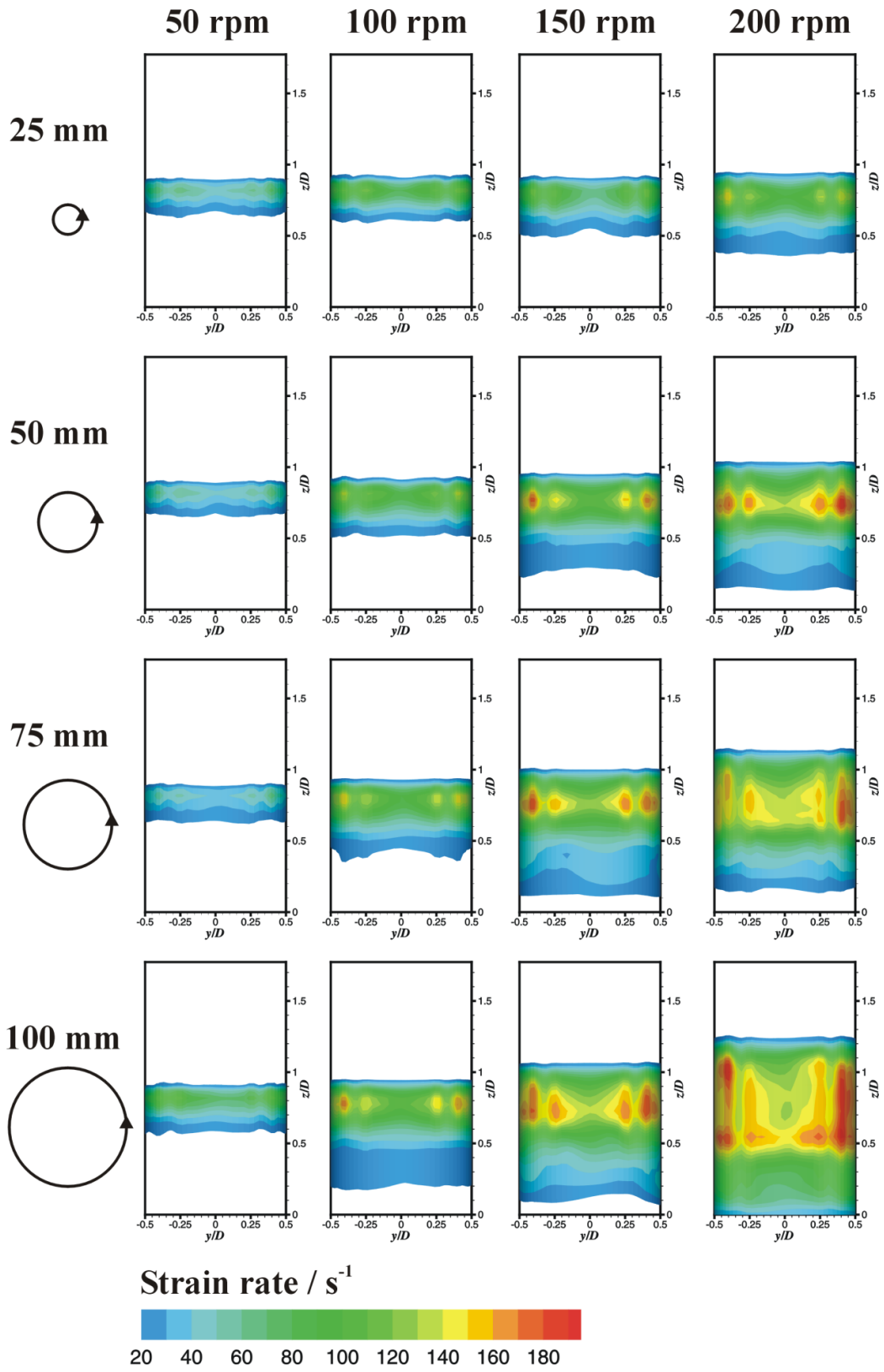

Figure 3.4. Time averaged strain rates on a 96-well microtiter plate at different orbital shaking diameters and shaking frequencies. The diameter of the circle is proportional to the diameter of the orbit described by each well of the plate when placed on an orbital incubator with the indicated orbital shaking diameter. Strain rates below 20 s^{-1} are not represented.

The increase of the amplitude of the interfacial surface oscillation led to an increase in the fluid velocity and, consequently, to an increase of the shear strain rate near the walls of the well. Figure 3.4 compares the time averaged wall strain rate distribution for several orbital diameters and shaking frequencies. The wall strain rate was not uniform, being much higher in the liquid side near the interface. A zone of wall strain rate above 30 s^{-1} was visible for all the systems shown in Figure 3.4, and was delimited by the region where the interface oscillates. The extension of this region increased as the shaking frequency and orbital diameter increased.

For all orbital diameters, the average strain rate is around 12 s^{-1} when a shaking frequency of 50 rpm is used (Figure 3.5). However, when an incubator with 25 mm of shaking amplitude is used, this value can be increased 3 fold under a shaking frequency of 200 rpm. A wider range of shear rate conditions can be experienced with incubators of 50 or 75 mm orbital diameters, where numerical simulations predicted an increase of 6 to 7 fold at the highest tested frequency when compared to the value obtained at 50 rpm. Indeed, as the orbital diameter increased the shear strain range widened, spanning from 10 to 142 s^{-1} (Figure 3.5).

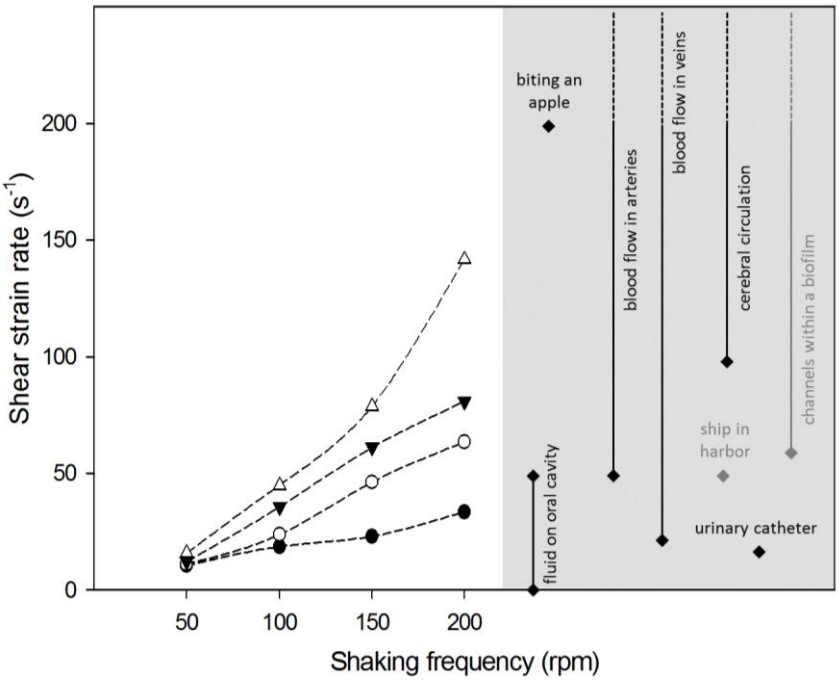

Figure 3.5. Numerical results of the shear strain rate as a function of the shaking frequency for different orbital shaking diameters: △ - 100 mm, ▼ - 75 mm, ○ - 50 mm, ● - 25 mm. The grey shading include some shear rates found in biomedical (◆) and other scenarios (◆) (references on Table 3.1).

3.3.2. Biofilm formation

The combined effects of shear forces and nutrient levels on biofilm formation were assessed by crystal violet assay (Figure 3.6). Polystyrene 96-well microtiter plates were placed in orbital incubators with shaking diameters of 25 and 50 mm (at the same shaking frequency of 150 rpm) and also without shaking (0 rpm). Simultaneously, the influence of three concentrations of the main nutrients (glucose, peptone and yeast extract) was studied.

Figures 3.6A, B and C, concerning the effect of glucose, show that the initial biofilm production (until 12 h) was 51% higher on the lower concentration media

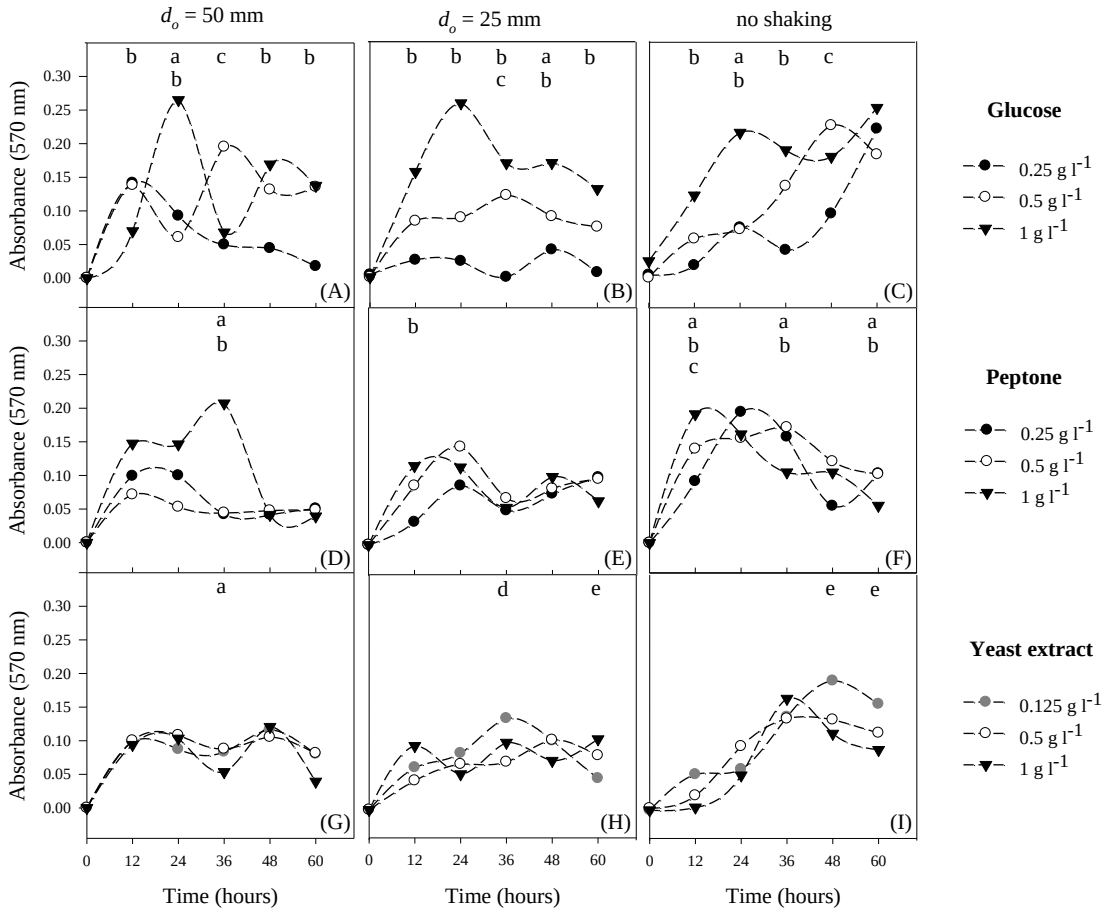

Figure 3.6. *E. coli* biofilm formation (absorbance at 570 nm) in 96-well microtiter plates under dynamic (d_o = 50 mm or 25 mm, 150 rpm) and static conditions: (A), (B) and (C) effect of glucose; (D), (E) and (F) effect of peptone; (G), (H) and (I) effect of yeast extract. Three nutrient concentrations were tested: ▼ - 1 g l^{-1} of glucose, peptone and yeast extract; ○ - 0.5 g l^{-1} of glucose, peptone and yeast extract; ● - 0.25 g l^{-1} of glucose and peptone; ● - 0.125 g l^{-1} of yeast extract. Results are an average of three independent experiments for each condition. Statistical analysis corresponding to each time point is represented for a

confidence level > 95% ($P < 0.05$): a - comparison between 1 g l^{-1} and 0.5 g l^{-1} glucose or peptone or yeast extract, b - comparison between 1 g l^{-1} and 0.25 g l^{-1} glucose or peptone, c - comparison between 0.5 g l^{-1} and 0.25 g l^{-1} glucose or peptone, d - comparison between 0.5 g l^{-1} and 0.125 g l^{-1} yeast extract, e - comparison between 1 g l^{-1} and 0.125 g l^{-1} yeast extract.

(0.25 and 0.5 g l^{-1}) for the highest shaking amplitude. Opposite results were observed for the lower amplitude and also for the static condition (statistically significant differences were obtained between the two extreme concentrations in all shaking conditions). For the highest glucose concentration (1 g l^{-1}), a maximum in biofilm formation was attained at 24 h in all shaking conditions. Above 24 h, whilst the biofilm amount decreased from the maximum in both shaking conditions (in particular for the higher shaking amplitude), this maximum amount was relatively the same on the static condition. Interestingly, approximately the same maximum amount of biofilm was formed in all hydrodynamic conditions ($P = 0.41$) for the highest glucose concentration tested.

When analysing the oscillatory behavior in detail for the highest shaking amplitude (Figure 3.6A), it is possible to see that the decrease in the biofilm amount in the culture medium with 1 g l^{-1} glucose was abrupt between 24 and 36 h, reaching the level obtained with the intermediate glucose concentration at the end of the experiment (60 h). For 0.5 g l^{-1} glucose, the fluctuations were also observed (the maximum was reached at 36 h), nevertheless with a smoother decrease than the one found for the most concentrated medium.

When an orbital shaker with 25 mm diameter at 150 rpm was used (Figure 3.6B), the general trend is that the amount of biofilm formed increased with increasing glucose concentrations. For this hydrodynamic condition and with 1 g l^{-1} glucose, the decrease of biofilm amount between 24 and 36 h was less pronounced than in the larger diameter incubator (35% versus 74% decrease, respectively). Then, the amount of biofilm stabilized until the end of the experiment, and similar values to those obtained with the larger shaking diameter were achieved ($P = 0.45$).

Concerning the effect of peptone concentrations (Figures 3.6D, E and F), the maximum biofilm amount was obtained at 36 h ($P < 0.05$) for the highest concentration (1 g l^{-1}) and shaking diameter (Figure 3.6D). From this moment onwards, the amount of biofilm obtained with this growth medium markedly decreased (80%) to the final level of the remaining media. Except for this maximum value, the differences found when varying

peptone concentrations were not statistically significant for the majority of the time points in both agitated conditions (Figures 3.6D and E). For the static condition (Figure 3.6F), it can be seen that increasing the concentration of this compound promoted biofilm growth in the early stages of biofilm development.

Figures 3.6G, H and I show the effect of yeast extract concentrations on biofilm formation under the tested hydrodynamic conditions. In terms of statistical significance, the results indicate that this is the nutrient for which less significant differences were obtained under the experimented concentrations (0.125, 0.25 and 1 g l^{-1}). Comparing the results for each concentration of yeast extract between both orbital shaking diameters, the growth profiles were very similar ($P > 0.05$ for 87% of time points), showing that the orbital shaking diameter had negligible impact on *E. coli* biofilm formation when different levels of yeast extract were used.

3.4. Discussion

3.4.1. CFD modelling of shaken 96-well microtiter plates

Because hydrodynamics have such a great impact on biofilm formation in terms of nutrient and oxygen transfer, and also influence cell attachment to and removal from surfaces (Simões et al. 2007, Stoodley et al. 1998, Teodósio et al. 2013a), it is interesting to estimate by CFD several hydrodynamic parameters such as the average shear strain rate, the specific air-liquid surface area and the wetted area available for cell adhesion.

As previously suggested by Hermann et al. (2003) and Kensy et al. (2005), the angle of the liquid surface in the wells increases exponentially with increasing shaking intensities (shaking diameters and shaking frequencies at constant filling volume), and an enlargement of the specific air-liquid mass transfer area ($\boldsymbol{a_f/a_i}$) is obtained. The numerical results also show that, at lower shaking frequency and especially for the lowest shaking amplitude tested, the surface tension force dominates and keeps the liquid surface nearly in the horizontal state. This corroborates the experimental results obtained by Ortiz-Ochoa et al. (2005) and Hermann et al. (2003). Images acquired with a CCD-camera for wells filled with 200 µl water and shaken at a shaking diameter of 25 mm showed no liquid movement below 200 rpm (Hermann et al. 2003). In this study, a change of the hydrodynamic flow was visible above 100 rpm (approximately the critical shaking

frequency) when the increased centrifugal force starts to gain relevance when compared to surface tension. With a further increase of shaking frequency, the maximum liquid height also increased and an expansion of the air-liquid mass transfer area was obtained (Hermann et al. 2003), providing better oxygen transfer to the liquid. From these results, it is reasonable to conclude that the surface tension has a strong influence on the hydrodynamic flow and likely on the mass transfer in 96-well microtiter plates.

The experimental shaking conditions chosen for the present work ($\boldsymbol{d_o}$= 25 and 50 mm, 150 rpm) can reproduce the hydrodynamics of urinary catheters where *E. coli* typically adheres. The shear strain rate found on these devices is of approximately 15 s^{-1} (Bakker et al. 2003, Velraeds et al. 1998), which is only slightly lower than the range obtained under the experimented conditions, according to the numerical results (23-46 s^{-1}). With the shaking amplitudes and frequencies used for biofilm formation in microtiter plates, it is also possible to attain the shear strain rates that are found in the oral cavity, arteries and veins (Table 3.1). For instance, the shear strain rate in the oral cavity can be simulated with the same incubators shaking at frequencies up to 150 rpm. In order to reproduce the shear rates resulting from the blood flow in arteries, it is vital to work with larger orbital diameters (75 or 100 mm) at shaking frequencies around 100 rpm or with shaking frequencies above the simulated ones for all shaking amplitudes. In this latter case, one must bear in mind that a splashing phenomenon can occur for larger diameters and frequencies above 200 rpm. This is not experimentally feasible due to contamination and loss of growth medium and cells. Regarding the non-biomedical scenarios, it is possible to attain the same shear rates encountered on a ship hull in a harbor with the 50 mm-incubator at 150 rpm or with the other incubators of larger diameter at velocities around 100 rpm. Finally, the liquid flow in biofilm channels should be simulated under the shaking conditions already indicated for the blood flow in arteries.

The average strain rates for the 25 and 50 mm shaking diameters (at 150 rpm) were 23.0 and 46.2 s^{-1}, respectively, which is equivalent to average shear stress values of 0.034 and 0.070 Pa (Moreira et al. 2013c). In turn, the flow cell system that will be used in the study of recombinant protein production (Chapters 5 to 9) reaches an average wall shear stress value of approximately 0.3 Pa (operating at $\boldsymbol{Re}$ = 4,600) (Moreira et al. 2015a), which is 4 fold higher than the maximum experimentally attainable in the 96-well microtiter plate. Therefore, the agitated microtiter plate does not mimic the shear stress conditions that are achieved in the flow cell.

Although microtiter plates have been extensively used for biofilm studies in the last years (Castelijn et al. 2012, Leroy et al. 2007, Rodrigues & Elimelech 2009, Shakeri et al. 2007), little is known about the flow pattern inside the wells. In fact, few papers have been published applying computational fluid dynamics to simulate flow in microtiter plates (Barrett et al. 2010, Zhang et al. 2008) during biofilm formation. Azevedo et al. (2006) simulated the flow inside 6-well plates to test the influence of shear stress, temperature and inoculation concentration on the adhesion of *Helicobacter pylori* to stainless steel and polypropylene coupons. Kostenko et al. (2010) studied *Staphylococcus aureus* deposition in the same plate format using different filling volumes and agitation frequencies. This latter system was further analysed by CFD by Salek et al. (2012) using a flow topology analysis to explain biofilm accumulation, morphology and orientation of endothelial cells. Since the 96-well format is currently one of the favorite platforms for biofilm studies, it is intriguing why such a lack of information exists for this system. Our research group started to study its hydrodynamics by monitoring the influence of two shaking conditions on *E. coli* biofilm development (Moreira et al. 2013c). This simulation was now extended in order to define which operational conditions should be chosen for each particular application. When trying to produce "artificial" biofilms in laboratory reactors one has to make sure that these biofilms resemble those that are formed in natural environments. If that is not the case, then important experiments regarding antibiotic susceptibilities, resistance to mechanical treatment, biocide efficacy assays and other tests will not produce reliable results that are indeed applicable to the "natural" biofilms that need to be controlled (Buckingham-Meyer et al. 2007). Since some knowledge about the hydrodynamics of the locations where "natural" biofilms form is already available, it is important that laboratory experiments are carried out in a way that mimics those conditions. The information presented on this work defines the applicability range of 96-well microtiter plates in the simulation of several natural scenarios where biofilms form.

3.4.2. Biofilm formation

In this work, the effects of glucose, peptone and yeast extract concentrations on biofilm development were tested. The reference concentration of each nutrient that was used on the previous study (Teodósio et al. 2011a) and higher concentrations of the three main nutrients were tested because it has been reported that high nutrient concentrations

can favour biofilm formation (Frias et al. 2001, Klahre & Flemming 2000, Volk & LeChevallier 1999).

A wide range of medical devices are currently used, including indwelling (Donlan 2001), partially implantable and external devices (Newman 2008). A temperature of 37 ºC is more appropriate for simulating indwelling devices in body core sites and temperatures closer to 25 ºC are best suited for external devices. Therefore, an average temperature of 30 ºC is a good approximation for a partially implantable device in body peripheral/skin sites (Andersen et al. 2010). On the other hand, as it is intended to use the 96-well microtiter plate as a screening platform for further experiments in a flow cell system working at 30 °C, it makes sense to choose this temperature. The influence of temperature (30 or 37 ºC) on the hydrodynamics was investigated. CFD simulations showed that the temperature is negligible and even when the average strain rates are compared at the two temperatures (Figure 3.7), the differences are on average below 5% (for the 150 rpm case used in the experimental part of this work, the difference is 0.4%).

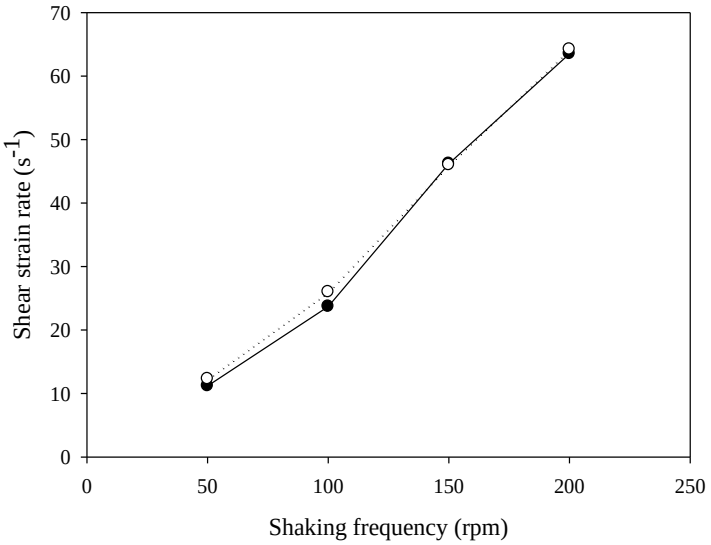

Figure 3.7. Comparison of the shear strain rate evolution as a function of the shaking frequency for 30 (—●—) and 37 ºC (···○···) in a 50 mm-incubator.

The overall results of the glucose experiments indicate that higher glucose concentrations may be beneficial for *E. coli* adhesion in the first 24 h, independently of the shaking conditions. Despite the lack of information on *E. coli* biofilms, it has been reported (Bühler et al. 1998) that the total yield of cells growing in a biofilm increased

linearly with increase of glucose up to 2 g l^{-1}. For *Pseudomonas* species, independent groups noted that an increase in nutrient concentration is associated with an increase of cell attachment (Peyton 1996, Simões et al. 2010b). For *P. putida*, Rochex & Lebeault (2007) observed an increase in biofilm thickness when increasing glucose concentration up to a certain limit (0.5 g l^{-1}), above which an additional increase of substrate reduced the biofilm accumulation rate as a consequence of a higher detachment.

In most cases, *E. coli* cells took more time to establish on the surface under static conditions. On the other hand, after the initial period of adhesion, the amount of biofilm formed under static conditions remained constant while that accumulated under shaking conditions dropped, in particular for the glucose experiments. This corroborates what has been postulated by several authors (Percival et al. 1999, Pereira & Vieira 2001, Vieira et al. 1993), that higher flow rates can cause two phenomena of opposite nature: on the one hand, they favour the transport of nutrients to the surface, contributing to cell growth in the microbial layer and to the production of exopolymers and, on the other hand, with increasing flow velocity the shear rates increase and that can cause further erosion and detachment of biofilm portions, and the consequent decrease in the amount of biomass attached to the surface. The interplay between these two effects (including the increase in surface area available for oxygenation) explains the higher growth followed by the more abrupt drop in biomass when the highest glucose concentration was used. Besides that, it is also known that *E. coli*, under certain conditions, adheres more strongly to surfaces with increasing fluid velocities due to the action of the lectin-like adhesin FimH (Thomas et al. 2002) or of the flagella (McClaine & Ford 2002).

Biofilms seemed to have entered a state of dynamic equilibrium at the highest shaking amplitude and for the two highest concentrations of glucose, probably as a consequence of the combined effects of hydrodynamics and carbon levels. The cyclical biofilm maturation and subsequent dispersal pattern probably occurred because it was no longer profitable for the bacterium to participate in the biofilm, due to several reasons such as shear forces, lack of nutrients and accumulation of toxic metabolic by-products (Dunne 2002).

The data presented in this work indicates that variation of peptone and yeast extract concentrations has no significant impact on the amount of attached cells, in the range of concentrations and hydrodynamic conditions tested. As glucose is the main carbon source in the tested culture media, peptone is the most important nitrogen source since its nitrogen content exceeds 13% (Merck, product information ref. 107214). Yeast

extract also provides nitrogen (> 10 %) to bacteria besides vitamins, amino acids and carbon (Merck, product information, ref. 103753). In reactors for biological waste gas treatment, biofilm growth seems to respond strongly to the amount of available nitrogen (Holubar et al. 1999). A similar behavior was observed for *P. putida* strain isolated from a paper machine (Rochex & Lebeault 2007). The rate and extent of biofilm accumulation increased with nitrogen concentration. Additionally, it is known that when the carbon/nitrogen ratio on the nutrient supply is increased, the polysaccharide/protein ratio generally increases (Huang et al. 1994b). Delaquis et al. (1989) showed that the depletion of nitrogen led to the active detachment of cells from *P. fluorescens* biofilm.

Since different *E. coli* strains are capable of causing UTI (Salo et al. 2009), selected experiments were performed to see if the results obtained with strain JM109(DE3) were also confirmed with another strain. *E. coli* CECT 434 (a clinical isolate) was used for this purpose, and in general there were no statistically significant differences between the results obtained for the two strains (Figure 3.8).

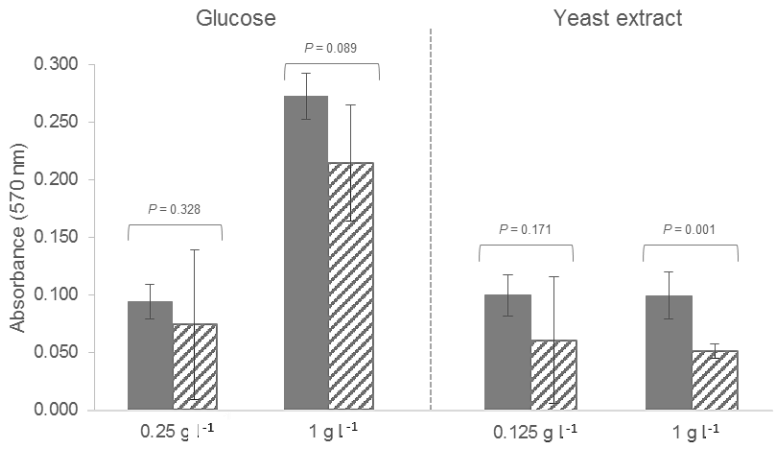

Figure 3.8. Comparison of 24-h biofilms formed by *E. coli* CECT 434 (■) and *E. coli* JM109(DE3) (▨) in static conditions using two different concentrations of glucose or yeast extract.

Although the wetted area predicted for cell adhesion was 2 fold higher for the 50 mm-incubator when compared to the 25-mm incubator (at 150 rpm), the maximum biofilm amount detected by the crystal violet assay was very similar for the three operational conditions used. Thus, an increase in wetted area did not cause an increase in the amount of biofilm.

The simulation results indicate that the strain rates under which the *E. coli* biofilms developed changed drastically along the cylindrical wall. The higher strain rates below the interface were associated with the formation of dispersed cell aggregates, while a decrease in the strain rate values resulted in a homogeneous distribution of single cells on the wall. Kostenko et al. (2010) also showed that biofilm deposition and morphology in microtiter plates is non-uniform and that the biofilm characteristics correlate strongly with local shear stress mean and fluctuation levels. It has been shown that biofilms in the human body are naturally heterogeneous as a result of the shear stress variations. Thus, microtiter plates are ideally suited to mimic these natural variations in the shear stress field in biomedical scenarios.

Taking together the results obtained from the numerical simulation and those obtained during biofilm formation studies, it is possible to conclude that if the right operational conditions are used, the microtiter plate is a powerful platform for biofilm simulation in a variety of applications including biomedical scenarios.

3.5. References

Aleviadrou BR, McIntire LV. 1995. Rheology. In: Loscalzo J, Schafer A, editors. Thrombosis and Hemorrhage. Cambridge: Blackwell Sciences. p. 369-384.

Alnnasouri M, Dagot C, Pons M-N. 2011. Comparison of four methods to assess biofilm development. Water Sci Technol. 63:432-439.

Andersen TE, Kingshott P, Palarasah Y, Benter M, Alei M, Kolmos HJ. 2010. A flow chamber assay for quantitative evaluation of bacterial surface colonization used to investigate the influence of temperature and surface hydrophilicity on the biofilm forming capacity of uropathogenic *Escherichia coli*. J Microbiol Methods. 81:135-140.

Azevedo NF, Pinto AR, Reis NM, Vieira MJ, Keevil CW. 2006. Shear stress, temperature, and inoculation concentration influence the adhesion of water-stressed *Helicobacter pylori* to stainless steel 304 and polypropylene. Appl Environ Microbiol. 72:2936-2941.

Bakker D, van der Plaats A, Verkerke G, Busscher H, van der Mei H. 2003. Comparison of velocity profiles for different flow chamber designs used in studies of microbial adhesion to surfaces. Appl Environ Microbiol. 69:6280-6287.

Bark DL, Para AN, Ku DN. 2012. Correlation of thrombosis growth rate to pathological wall shear rate during platelet accumulation. Biotechnol Bioeng. 109:2642-2650.

Barrett TA, Wu A, Zhang H, Levy MS, Lye GJ. 2010. Microwell engineering characterization for mammalian cell culture process development. Biotechnol Bioeng. 105:260-275.

Brackbill JU, Kothe DB, Zemach C. 1992. A continuum method for modeling surface tension. J Comput Phys. 100:335-354.

Buckingham-Meyer K, Goeres DM, Hamilton MA. 2007. Comparative evaluation of biofilm disinfectant efficacy tests. J Microbiol Methods. 70:236-244.

Bühler T, Ballestero S, Desai M, Brown MRW. 1998. Generation of a reproducible nutrient-depleted biofilm of *Escherichia coli* and *Burkholderia cepacia*. J Appl Microbiol. 85:457-462.

Busscher HJ, van der Mei HC. 2006. Microbial adhesion in flow displacement systems. Clin Microbiol Rev. 19:127-141.

Castelijn GAA, van der Veen S, Zwietering MH, Moezelaar R, Abee T. 2012. Diversity in biofilm formation and production of curli fimbriae and cellulose of *Salmonella* Typhimurium strains of different origin in high and low nutrient medium. Biofouling. 28:51-63.

Chesterton AKS, Moggridge GD, Sadd PA, Wilson DI. 2011. Modelling of shear rate distribution in two planetary mixtures for studying development of cake batter structure. J Food Eng. 105:343-350.

Coenye T, Nelis HJ. 2010. *In vitro* and *in vivo* model systems to study microbial biofilm formation. J Microbiol Methods. 83:89-105.

Delaquis PJ, Caldwell DE, Lawrence JR, McCurdy AR. 1989. Detachment of *Pseudomonas fluorescens* from biofilms on glass surfaces in response to nutrient stress. Microbial Ecol. 18:199-210.

Donlan RM. 2001. Biofilm formation: a clinically relevant microbiological process. Clin Infect Dis. 33:1387-1392.

Donlan RM. 2002. Biofilms: microbial life on surfaces. Emerg Infect Dis. 8:881-890.

Duetz WA. 2007. Microtiter plates as mini-bioreactors: miniaturization of fermentation methods. Trends Microbiol. 15:469-475.

Dunne WM, Jr. 2002. Bacterial adhesion: seen any good biofilms lately? Clin Microbiol Rev. 15:155-166.

Frias J, Ribas F, Lucena F. 2001. Effects of different nutrients on bacterial growth in a pilot distribution system. Antonie van Leeuwenhoek. 80:129-138.

Fux CA, Wilson S, Stoodley P. 2004. Detachment characteristics and oxacillin resistance of *Staphyloccocus aureus* biofilm emboli in an in vitro catheter infection model. J Bacteriol. 186:4486-4491.

Hancock V, Ferrières L, Klemm P. 2007. Biofilm formation by asymptomatic and virulent urinary tract infectious *Escherichia coli* strains. FEMS Microbiol Lett. 267:30-37.

Hermann R, Lehmann M, Büchs J. 2003. Characterization of gas-liquid mass transfer phenomena in microtiter plates. Biotechnol Bioeng. 81:178-186.

Hilgenstock A, Ernst R. 1996. Analysis of installation effects by means of computational fluid dynamics - CFD vs experiments? Flow Meas lnstrum. 7:161-171.

Hirt CW, Nichols BD. 1981. Volume of fluid (VOF) method for the dynamics of free boundaries. J Comput Phys. 39:201-225.

Holubar P, Andorfer C, Braun R. 1999. Effects of nitrogen limitation on biofilm formation in a hydrocarbon-degrading trickle-bed filter. Appl Microbiol Biotechnol. 51:536-540.

Huang C-T, Peretti SW, Bryers JD. 1994b. Effects of medium carbon-to-nitrogen ratio on biofilm formation and plasmid stability. Biotechnol Bioeng. 44:329-336.

Inauen W, Baumgartner H, Bombeli T, Haeberli A, Straub P. 1990. Dose- and shear rate-dependent effects of heparin on thrombogenesis induced by rabbit aorta subendothelium exposed to flowing human blood. Arterioscler Thromb Vasc Biol. 10:607-615.

Kensy F, Zimmermann HF, Knabben I, Anderlei T, Trauthwein H, Dingerdissen U, Büchs J. 2005. Oxygen transfer phenomena in 48-well microtiter plates: determination by optical monitoring of sulfite oxidation and verification by real-time measurement during microbial growth. Biotechnol Bioeng. 89:698-708.

Klahre J, Flemming HC. 2000. Monitoring of biofouling in papermill process waters. Water Res. 34:3657-3665.

Kostenko V, Salek MM, Sattari P, Martinuzzi RJ. 2010. *Staphylococcus aureus* biofilm formation and tolerance to antibiotics in response to oscillatory shear stresses of physiological levels. FEMS Immunol Med Microbiol. 59:421-431.

Leroy C, Delbarre C, Ghillebaert F, Compere C, Combes D. 2007. Effects of commercial enzymes on the adhesion of a marine biofilm-forming bacterium. Biofouling. 24:11-22.

Liu Y, Tay J-H. 2002. The essential role of hydrodynamic shear force in the formation of biofilm and granular sludge. Water Res. 36:1653-1665.

Mareels G. 2007. Experimental and numerical modeling of flow and mass transport in a bioartificial liver [PhD]. Ghent: Ghent University.

Mareels G, Kaminsky R, Eloot S, Verdonck PR. 2007. Particle image velocimetry-validated, computational fluid dynamics-based design to reduce shear stress and residence time in central venous hemodialysis catheters. ASAIO J. 53:438-446

McClaine JW, Ford RM. 2002. Characterizing the adhesion of motile and nonmotile *Escherichia coli* to a glass surface using a parallel-plate flow chamber. Biotechnol Bioeng. 78:179-189.

Michelson AD. 2002. Platelets. New York: Academic Press/Elsevier Science.

Moreira JMR, Simões M, Melo LF, Mergulhão FJ. 2015a. The combined effects of shear stress and mass transfer on the balance between biofilm and suspended cell dynamics. Desal Water Treat. 53:3348-3354.

Moreira JMR, Gomes LC, Simões M, Melo LF, Mergulhão FJ. 2015b. The impact of material properties, nutrient load and shear stress on biofouling in food industries. Food Bioprod Process. 95:228-236.

Moreira JMR, Teodósio JS, Silva FC, Simões M, Melo LF, Mergulhão FJ. 2013a. Influence of flow rate variation on the development of *Escherichia coli* biofilms. Bioprocess Biosyst Eng. 36:1787-1796.

Moreira JMR, Gomes LC, Araújo JDP, Miranda JM, Simões M, Melo LF, Mergulhão FJ. 2013c. The effect of glucose concentration and shaking conditions on *Escherichia coli* biofilm formation in microtiter plates. Chem Eng Sci. 94:192-199.

Mukherjee PK, Chand DV, Chandra J, Anderson JM, Ghannoum MA. 2009. Shear stress modulates the thickness and architecture of *Candida albicans* biofilms in a phase-dependent manner. Mycoses. 52:440-446.

Newman DK. 2008. Internal and external urinary catheters: a primer for clinical practice. Ostomy Wound Manag. 54:18-35.

Ortiz-Ochoa K, Doig SD, Ward JM, Baganz F. 2005. A novel method for the measurement of oxygen mass transfer rates in small-scale vessels. Biochem Eng J. 25:63-68.

Percival SL, Knapp JS, Wales DS, Edyvean RGJ. 1999. The effect of turbulent flow and surface roughness on biofilm formation in drinking water. J Ind Microbiol Biotechnol. 22:152-159.

Pereira MO, Vieira MJ. 2001. Effects of the interactions between glutaraldehyde and the polymeric matrix on the efficacy of the biocide against *Pseudomonas fluorescens* biofilms. Biofouling. 17:93-101.

Peyton BM. 1996. Effects of shear stress and substrate loading rate on *Pseudomonas aeruginosa* biofilm thickness and density. Water Res. 30:29-36.

Rochex A, Lebeault JM. 2007. Effects of nutrients on biofilm formation and detachment of a *Pseudomonas putida* strain isolated from a paper machine. Water Res. 41:2885-2892.

Rodrigues DF, Elimelech M. 2009. Role of type 1 fimbriae and mannose in the development of *Escherichia coli* K12 biofilm: from initial cell adhesion to biofilm formation. Biofouling. 25:401-411.

Salek M, Sattari P, Martinuzzi R. 2012. Analysis of fluid flow and wall shear stress patterns inside partially filled agitated culture well plates. Ann Biomed Eng. 40:707-728.

Salo J, Sevander JJ, Tapiainen T, Ikäheimo I, Pokka T, Koskela M, Uhari M. 2009. Biofilm formation by *Escherichia coli* isolated from patients with urinary tract infections. Clin Nephrol. 71:501-507.

Shakeri S, Kermanshahi RK, Moghaddam MM, Emtiazi G. 2007. Assessment of biofilm cell removal and killing and biocide efficacy using the microtiter plate test. Biofouling. 23:79-86.

Simões LC, Simões M, Vieira M. 2010a. Adhesion and biofilm formation on polystyrene by drinking water-isolated bacteria. Antonie van Leeuwenhoek. 98:317-329.

Simões M, Simões LC, Vieira MJ. 2010b. A review of current and emergent biofilm control strategies. LWT-Food Sci Technol. 43:573-583.

Simões M, Pereira MO, Sillankorva S, Azeredo J, Vieira MJ. 2007. The effect of hydrodynamic conditions on the phenotype of *Pseudomonas fluorescens* biofilms. Biofouling. 23:249-258.

Singh PK, Marzo A, Howard B, Rufenacht DA, Bijlenga P, Frangi AF, Lawford PV, Coley SC, Hose DR, Patel UJ. 2010. Effects of smoking and hypertension on wall shear stress and oscillatory shear index at the site of intracranial aneurysm formation. Clin Neurol Neurosurg. 112:306-313.

Sonak S, Bhosle NB. 1995. A simple method to assess bacterial attachment to surfaces. Biofouling. 9:31-38.

Stoodley P, Dodds I, Boyle JD, Lappin-Scott HM. 1998. Influence of hydrodynamics and nutrients on biofilm structure. J Appl Microbiol. 85:19S-28S.

Stoodley P, Wilson S, Hall-Stoodley L, Boyle JD, Lappin-Scott HM, Costerton JW. 2001. Growth and detachment of cell clusters from mature mixed-species biofilms. Appl Environ Microbiol. 67:5608-5613.

Telgmann U, Horn H, Morgenroth E. 2004. Influence of growth history on sloughing and erosion from biofilms. Water Res. 38:3671-3684.

Teodósio JS, Simões M, Melo LF, Mergulhão FJ. 2011a. Flow cell hydrodynamics and their effects on *E. coli* biofilm formation under different nutrient conditions and turbulent flow. Biofouling. 27:1-11.

Teodósio JS, Simões M, Melo LF, Mergulhão FJ. 2011b. The Influence of the Nutrient Load on the Formation of *Escherichia coli* Biofilms. In: Berhardt LV, editors. Advances in Medicine and Biology. New York: Nova Science Publishers. p. 153-168.

Teodósio JS, Silva FC, Moreira JMR, Simões M, Melo LF, Alves MA, Mergulhão FJ. 2013a. Flow cells as quasi ideal systems for biofouling simulation of industrial piping systems. Biofouling. 29:953-966.

Thomas WE, Trintchina E, Forero M, Vogel V, Sokurenko EV. 2002. Bacterial adhesion to target cells enhanced by shear force. Cell. 109:913-923.

Tran V, Fleiszig S, Evans D, Radke C. 2011. Dynamics of fagellum- and pilus-mediated association of *Pseudomonas aeruginosa* with contact lens surfaces. Appl Environ Microbiol. 77:3644-3652.

Tranoudis I, Efron N. 2004. Tensile properties of soft contact lens materials. Cont Lens Anterior Eye. 27:177-191.

Ulett GC, Mabbett AN, Fung KC, Webb RI, Schembri MA. 2007. The role of F9 fimbriae of uropathogenic *Escherichia coli* in biofilm formation. Microbiology. 153:2321-2331.

van Loosdrecht MCM, Eikelboom D, Gjaltema A, Mulder A, Tijhuis L, Heijnen JJ. 1995. Biofilm structures. Water Sci Technol. 32:35-43.

Vejborg RM, Klemm P. 2008. Blocking of bacterial biofilm formation by a fish protein coating. Appl Environ Microbiol. 74:3551-3558.

Velraeds MMC, van de Belt-Gritter B, van der Mei H, Reid G, Busscher HJ. 1998. Interface in initial adhesion of uropathogenic bacteria and yeasts to silicone rubber by a *Lactobacillus acidophilos* biosurfactant. J Med Microbiol. 47:1081-1085.

Vieira MJ, Melo LF, Pinheiro MM. 1993. Biofilm formation: hydrodynamic effects on internal diffusion and structure. Biofouling. 7:67-80.

Volk CJ, LeChevallier MW. 1999. Impacts of the reduction of nutrient levels on bacterial water quality in distribution systems. Appl Environ Microbiol. 65:4957-4966.

Wäsche S, Horn H, Hempel DC. 2002. Influence of growth conditions on biofilm development and mass transfer at the bulk/biofilm interface. Water Res. 36:4775-4784.

Xia B, Sun D-W. 2002. Applications of computational fluid dynamics (CFD) in the food industry: a review. Comput Electron Agr. 34:5-24.

Yataghene M, Pruvost J, Fayolle F, Legrand J. 2008. CFD analysis of the flow pattern and local shear rate in a scraped surface heat exchanger. Chem Eng Process. 47:1550-1561.

Youngs DL. 1982. Time-Dependent Multi-Material Flow With Large Fluid Distortion. In: Morton KW, Baibnes MJ, editors. Numerical Methods for Fluid Dynamics. New York: Academic Press. p. 273-285.

Zhang H, Lamping SR, Pickering SCR, Lye GJ, Shamlou PA. 2008. Engineering characterisation of a single well from 24-well and 96-well microtitre plates. Biochem Eng J. 40:138-149.

4.

Biofilm localization in the vertical wall of 96-well plates[c]

Abstract

Microtiter plates with 96 wells are being increasingly used for biofilm studies due to their high throughput, low cost, easy handling and easy application of several analytical methods to evaluate different biofilm parameters. These methods provide bulk information about the biofilm formed in each well but lack in detail, namely regarding the spatial location of the biofilms.

In this chapter, macroscale and microscale methods were used to study the impact of hydrodynamic conditions on the location of *E. coli* JM109(DE3) biofilms formed in microtiter plates. Biofilms were formed in shaking and static conditions, and two macroscale parameters were assayed: the total amount of biofilm was measured by the CV assay and the metabolic activity was determined by the resazurin assay. From the macroscale point of view, there were no statistically significant differences between the biofilms formed in static and shaking conditions. However, at a microscale level, the differences between both conditions were revealed using SEM. It was observed that

[c] The content of this chapter was adapted from the following publication(s):

Gomes LC, Moreira JMR, Miranda JM, Simões M, Melo LF, Mergulhão FJ. 2013. Macroscale *versus* microscale methods for physiological analysis of biofilms formed in 96-well microtiter plates. J Microbiol Methods. 95:342-349.

Gomes LC, Moreira JMR, Simões M, Melo LF, Mergulhão FJ. 2014. Biofilm localization in the vertical wall of shaking 96-well plates. Scientifica. 231083:13.

biofilm morphology and spatial distribution along the wall was different in these conditions. Additionally, it was shown that wall regions subjected to higher shear strain rates were associated with the formation of biofilms containing cells of smaller size. Conversely, regions with lower shear strain rate were prone to have a more uniform spatial distribution of adhered cells of larger size.

Location of sessile cells can be obtained by microscopy observation using electron microscopes, but this technique has lower throughput, higher cost and is subjected to equipment availability. Therefore, a differential CV staining method was developed to determine the spatial location of *E. coli* biofilms formed in the vertical wall of shaking 96-well plates. The results of this new procedure were corroborated by SEM visualization. The developed method is quicker, less expensive and has a higher throughput than the available methods for spatial location of biofilms in microtiter plates.

The results of this chapter highlight the wealth of information that may be gathered by complementing macroscale approaches with a microscale analysis of the experiments.

4.1. Introduction

Intensive studies on the mechanisms of biofilm formation and resistance have prompted the development of multiple *in vitro* platforms where biofilms are formed to simulate "real life" biofilms. When using these systems in the laboratory, it is important to choose the correct operational conditions in order to obtain biofilms that resemble those found in natural environments (Gomes et al. 2014). Microtiter plates with 96 wells enable high-throughput assays, are easy to handle and are cheap to use as only small volumes of reagents are required (Coenye & Nelis 2010, Duetz 2007). Moreover, multiple organisms and treatments can be included in a single run (Coenye & Nelis 2010), and several well established protocols are available for determination of macroscale parameters related to the biofilm (Table 2.2). Microtiter plates have been extensively used for biofilm studies addressing microbial adhesion (Moreira et al. 2013c, Simões et al. 2010a), biofilm inhibition (Cady et al. 2012, Lee et al. 2011) and screening of antimicrobial compounds (Pitts et al. 2003, Quave et al. 2008, Shakeri et al. 2007). However, the lack of detailed

knowledge of the hydrodynamics in microtiter plate systems has been, however, the major drawback of this technique in many reported studies (Gomes et al. 2014).

Despite the recent development of techniques for the macroscale characterization of biofilms, microscopy is still used to analyse morphological and structural details of biofilms *in vitro*, especially in flow cells and on coupons retrieved from microtiter plates (Hannig et al. 2010). The complexity and structural heterogeneity of biofilms has been unraveled by techniques such as SEM and CLSM. SEM can be used to produce clear images of microorganisms on opaque substrata across a wide range of magnifications (Norton et al. 1998). At higher magnifications (up to 100,000×), individual cells are readily distinguished (Serra et al. 2013, Stewart et al. 1995). For these reasons, it is recognized that SEM gives a detailed insight into the ultrastructure of bacteria and their environment (Alhede et al. 2012, Hannig et al. 2010), although it does not allow observation of the biofilm interior (Stewart et al. 1995). The main difficulty of SEM is that sample preparation might induce shrinkage and other structural changes due to dehydration (Hannig et al. 2010). Conversely, CLSM allows *in situ* and real-time examination of biofilms, but it provides much lower magnification and resolution (Fedel et al. 2007, Stewart et al. 1995). The use of the CLSM is also useful to obtain clear photomicrographs of densely packed microorganisms (Palmer Jr & Sternberg 1999). Mainly because of its excellent resolution properties, SEM will, in spite of its limitations, continue to be an important tool for biofilm research. The relative advantages and limitations of these two techniques are summarized in Table 2.4.

This study compares two well established macroscale techniques (crystal violet and resazurin assay), that provide bulk data from a biofilm, with SEM visualization for the analysis of biofilms formed in 96-well microtiter plates. Analysis of the hydrodynamics at a microscale using CFD provided additional information that can explain the results obtained with SEM. Prior to CFD simulation, a computational model must be generated and a meshing operation is performed. Meshing corresponds to the division of the region under study into numerous elements (also known as cells) where the equations from the computational model are solved (Xia & Sun 2002). CFD is a microscale fluid analysis technique that can be performed at different precision levels, much like microscopy, where the use of different magnifications can provide different levels of detail. In fact, in microscopy, the use of higher magnifications increases the detail, but this is obtained at a higher operational cost as the number of images that are required to analyse the same region of interest increases. Likewise, in CFD, the use of a

more refined mesh (with a higher number of cells of smaller volume) increases numerical accuracy, but also with an increased computational cost as the simulations will take longer to run.

The main objective of this work was to compare macroscale and microscale methods that can be used for biofilm analysis to see if the information that can be extracted from them is redundant or if they provide complementary data. Furthermore, a differential CV staining method was developed by combining the high throughput features of the usual CV staining with the determination of the spatial localization of the biofilm without the use of expensive equipment. The global information was used to assess the effect of hydrodynamics on biofilm location.

4.2. Materials and methods

4.2.1. Bacterial growth

E. coli JM109(DE3) from Promega (USA) was used to produce biofilms. An overnight culture was prepared as described in Chapter 3, section 3.2.2. Cells were harvested by centrifugation and appropriate dilutions in sterile saline (8.5 g l^{-1} NaCl) were performed to obtain an inoculum containing approximately 10^8 cells ml^{-1}.

4.2.2. Biofilm formation in 96-well microtiter plates

Biofilms were produced by pipetting 20 µl of inoculum into six wells of sterile 96-well PS microtiter plates (Orange Scientific, USA) filled with 180 µl of nutrient media. The media was previously described by Teodósio et al. (2011a) and consisted of 0.5 g l^{-1} glucose, 0.25 g l^{-1} peptone, 0.125 g l^{-1} yeast extract and phosphate buffer (0.188 g l^{-1} KH_2PO_4 and 0.26 g l^{-1} Na_2HPO_4), pH 7.0. Microtiter plates were placed for 24 h at 30 ºC in an orbital shaking incubator (50 mm of orbital diameter) at 150 rpm (CERTOMAT® BS-1, Sartorius AG, Germany) and without shaking.

4.2.3. Biofilm analysis

4.2.3.1. Macroscale assays

After 24 h of incubation, the total amount of biofilm formed was measured by CV assay and the metabolic activity was determined by the resazurin assay.

The CV procedure used in this work is fully described in Chapter 3, section 3.2.3.

Resazurin is a blue redox dye that can be reduced by viable bacteria in the biofilm to pink resofurin, and the extent of conversion from blue to pink is a reflection of metabolic activity (Pettit et al. 2009). This assay was described as a good alternative for microbial biofilm quantitation in microtiter plates (Peeters et al. 2008). Non-adherent bacteria were firstly removed according to the technique described for the CV assay. Fresh medium (190 µl) was added to the wells followed by the addition of 10 µl of 0.1 g l^{-1} resazurin (Sigma-Aldrich, USA) solution (Borges et al. 2014). Fluorescence (with the excitation filter of 570 nm and the emission filter of 590 nm) was measured after 20 min of incubation in darkness (Borges et al. 2014) using a microtiter plate reader (SpectraMax M2E, Molecular Devices, UK).

Three independent experiments were performed to characterize the biofilms formed under shaking and static conditions. For control, quantifications were also conducted in the absence of bacteria, demonstrating that no biofilm growth occurred in the corresponding wells during the experimental time.

4.2.3.2. Microscale assays

Microscopy

Microtiter plate wells containing biofilms were observed by SEM after 24 h of incubation. Prior to SEM observations, biofilm samples were fixed using 3% wt. glutaraldehyde in cacodylate buffer pH 7.2 (Manuel 2007) for 10 min and exposed to an ethanol dehydration series of 50, 60, 70, 80, 90 and 2 × 100% (v/v) ethanol, followed by a chemical dehydration series of 100% ethanol + hexamethyldisilazane (HMDS, Ted Pella, USA) at 50, 60, 70, 80, 90 and 2 × 100% (v/v) HMDS (Thorn & Greenman 2009), for 5 min at each concentration. The plate was air-dried for 1 day in a desiccator and

selected wells were cut out from the plate using a diamond blade. These wells were then cut longitudinally with the same blade and sputter-coated with a palladium-gold thin film (Simões et al. 2007) using the SPI Module Sputter Coater equipment for 80 s at 15 mA current. The biofilms were viewed with a SEM/EDS system (FEI Quanta 400FEG ESEM/EDAX Genesis X4M, FEI Company, USA) in high-vacuum mode at 10 kV to observe biofilm morphology and distribution. Ten view fields along the vertical wall section were analysed for three independent wells of each hydrodynamic condition and the cell length was determined using the microscope software (xT Microscope Control, FEI Company, USA).

CFD simulation

Numerical simulation was made in Ansys Fluent CFD package (version 13.0) for a shaking diameter of 50 mm and frequency of 150 rpm, as indicated in Chapter 3, section 3.2.1. The magnitude of the shear strain rate was determined with the help of a built-in expression. After the steady state is reached, the average shear strain rate was calculated by integrating an instantaneous solution over the wetted area. The time averaged shear strain rate was obtained by averaging the steady state shear strain rate of the liquid side during a complete orbit.

Differential CV staining

The amount of biofilm formed was also measured using the CV dye in a differential form: this means that the well has been divided into four different sections (Figure 4.1) and the corresponding vertical wall section was stained sequentially up to a maximum volume of 200 µl. Biofilm quantitation on the bottom of the well was performed by using 25 µl of CV for staining. Section 1 corresponded to a volume between 25 and 50 µl (and a height of 0.77 mm). Section 2 corresponded to a volume between 50 and 100 µl, section 3 corresponded to a volume between 100 and 150 µl and section 4 corresponded to a volume between 150 and 200 µl. Sections 2, 3 and 4 had an equivalent height of 1.54 mm.

Prior to CV staining, the microtiter plates were discarded and the wells were washed with 200 µl of sterile water to remove non-adherent bacteria (Stepanović et al.

2000). Then, the biofilms were fixed with 250 µl of 96% ethanol (Shakeri et al. 2007). The first section of the well to be quantified was the bottom (not represented in Figure 4.1), which corresponds to a volume of 25 µl and a height of 0.77 mm. The cells adhered to this region were stained for 5 min with the corresponding volume of 1% (v/v) crystal violet (Merck, Portugal) and the dye bound to this specific region was solubilized with 200 µl of 33% (v/v) acetic acid (VWR, Portugal). The absorbance was measured at 570 nm using a microtiter plate reader (SpectraMax M2E, Molecular Devices, UK). The biofilms formed in the successive sections of the well (sections 1 to 4 of Figure 4.1) were quantified using the described procedure, specifically using the CV volume equivalent to the maximum level of each section (section 1 - 50 µl; section 2 - 100 µl; section 3 - 150 µl; section 4 - 200 µl). The absorbance corresponding to each of the defined sections and presented on Figure 4.7D was calculated by subtracting the absorbances from the previous sections and considering the dilution factor. To quantify the biofilm formed in each of the well sections, six replica wells were used per experiment and three independent experiments were performed.

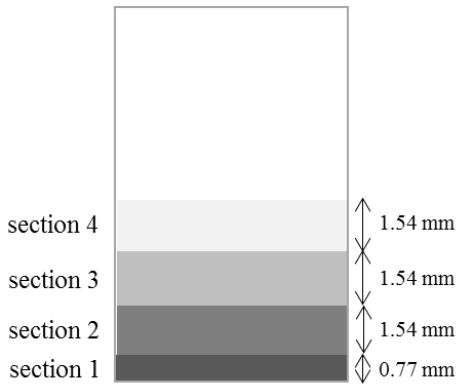

Figure 4.1. Schematic representation of the wall sections assayed by the differential CV staining.

4.2.4. Calculations and statistical analysis

The results presented in Figure 4.2 are an average of those obtained in three independent experiments for each hydrodynamic condition. For a single experiment, the final value is an average of the readings obtained in 6 replica wells within one plate. Cell length distribution in biofilms (Figure 4.6) was assessed by measurement of the lengths

of 100 randomly chosen cells adhered in the liquid side near the interface under shaking (Figure 4.5A) and static (Figure 4.5B) conditions. Paired *t*-test analyses were performed when appropriate based on a confidence level of 95% (differences reported as significant for P values < 0.05).

4.3. Results

4.3.1. Macroscale analysis of biofilm formation

The effect of orbital shaking on biofilm formation was firstly assessed by two macroscale parameters: the total amount of biofilm formed by the CV assay (Figure 4.2A) and the cell metabolic activity by the resazurin assay (Figure 4.2B). The amount of biofilm formed in agitated conditions was not significantly different (P = 0.42) from the amount formed in static conditions (Figure 4.2A). Also the differences found in the biofilm activity when varying shaking conditions (Figure 4.2B) were not statistically significant (P = 0.40).

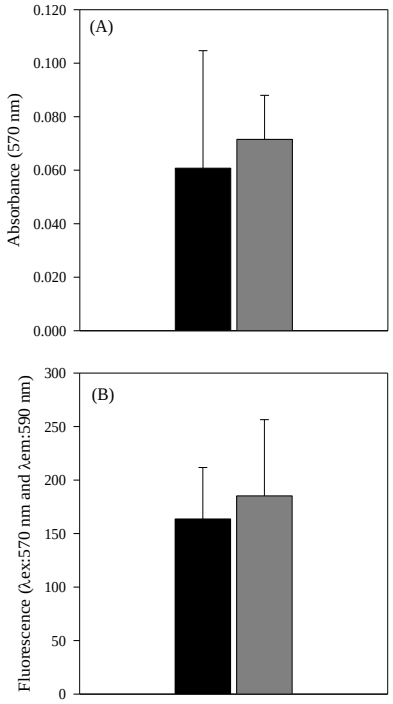

Figure 4.2. Biofilm quantification after 24 h of formation under shaking (■) and static (■) conditions. (A) Biofilm amount determined by the crystal violet assay; (B) biofilm metabolic activity determined by the resazurin assay. Mean values ± SD for three independent experiments are indicated.

4.3.2. Microscale analysis of biofilm formation

The shear strain rate distribution inside a 96-well microtiter plate during orbital shaking was determined by CFD (Figure 4.3). Then, these results were related to the biofilm distribution and morphology assessed by SEM (Figures 4.4 and 4.5). Each of the original SEM images obtained at a 1000× magnification covered an area of 250 × 200 µm (Figure 4.3 represents cropped sections of those images). The wall projected area of a single hexahedral cell that was used for the CFD simulation was of 270 × 300 µm. Thus, both methods were employed at similar scales.

Figure 4.3 presents the time averaged wall shear strain rate distribution in the internal wall of the well when an orbital shaker with 50 mm diameter at 150 rpm is used. The wall shear strain rate is unequally distributed in the cylindrical wall, spanning from 10 to 170 s^{-1}. Shear strain rate is much higher in the liquid side near the liquid-air interface, and there are spots where it has a relative maximum. These spots are associated with regions of unstable vortices near the wall (Moreira et al. 2013c). For this shaking condition, an average wall shear strain rate of 46 s^{-1} was predicted, which corresponds to a shear stress of 0.070 Pa.

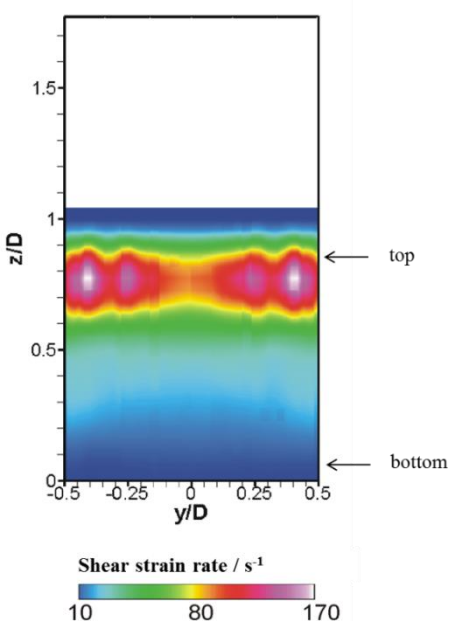

Figure 4.3. Time averaged shear strain rates on a 96-well microtiter plate when an orbital shaker with 50 mm diameter at 150 rpm is used. Scanning electron micrographs presented in Figure 4.4 were taken in the areas indicated with arrows: regions of higher (closer to the air-liquid interface, marked as top) and lower (closer to the bottom) shear strain rates.

Figures 4.4 and 4.5 display scanning electron micrographs representative of several fields observed in each well. They show that bacterial adhesion varied across the wall and that higher attachment occurred closer to the air-liquid interface (Figures 4.4A and B) compared to the bottom regions (Figures 4.4C and D). Concerning the morphology, the biofilms formed in the liquid side near the interface also differ from those found closer to the bottom. Biofilms consisting of cell aggregates were observed at the top for both hydrodynamic conditions (Figures 4.4A and B), whereas at the bottom of the walls there are only single cells homogeneously distributed along the surface (Figures 4.4C and D). Apart from being different along the vertical wall, it was observed by SEM that biofilm morphology is also different between static and shaking conditions. At equivalent locations, biofilms formed under the shaking situation have higher number of

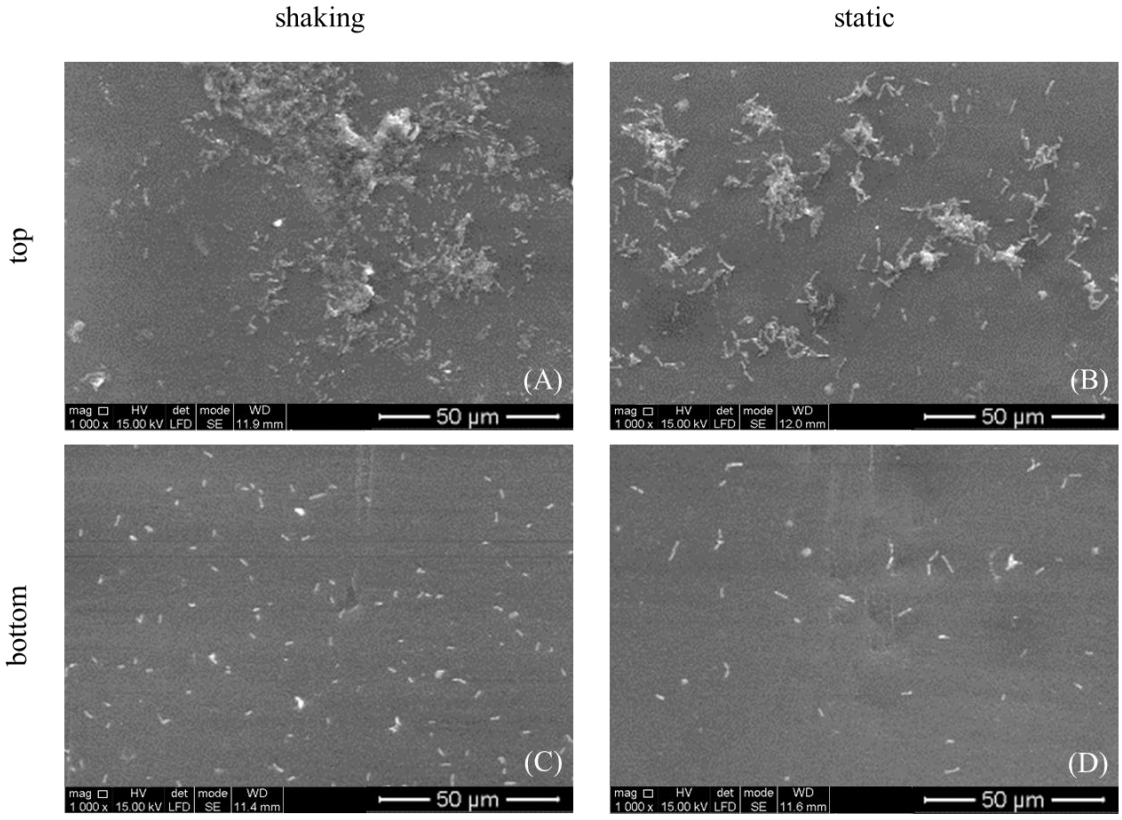

Figure 4.4. Scanning electron micrographs showing adhesion of *E. coli* to the vertical wall of 96-well microtiter plates. Images (A) and (C) were taken from the same well and are representative of cell distribution closer to the air-liquid interface (top) and closer to the bottom, respectively, for the shaking conditions (as indicated on Figure 4.3). Images (B) and (D) were taken from the same well and show cell adhesion closer to the air-liquid interface and closer to the bottom, respectively, in static conditions (images taken at equivalent locations to (A) and (C)). Magnification: 1000×; bars = 50 µm.

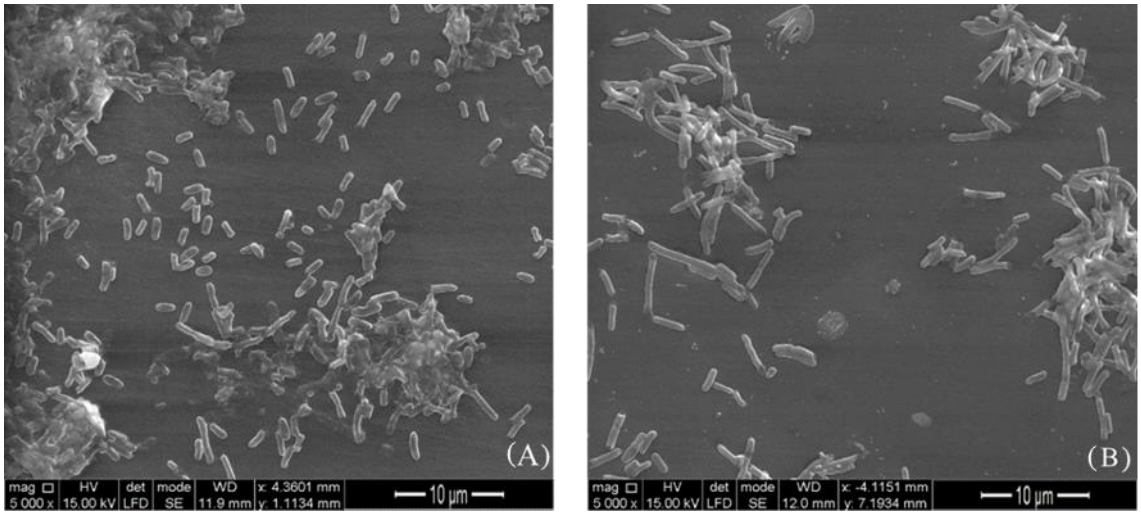

Figure 4.5. High-magnification scanning electron micrographs of *E. coli* adhesion in the liquid side near the interface for (A) shaking and (B) static conditions. Magnification: 5000×; bars = 10 µm.

cells (Figures 4.4A and C) than in the static condition (Figures 4.4B and D); besides, they seem to be embedded in EPS mostly in the area closer to the interface (Figure 4.4A). Furthermore, the length of the cells from biofilms grown in the shaking condition was smaller when compared to those formed in static, as shown by the 5000× magnification (Figure 4.5). Determination of the cell length in the higher magnification images (Figure 4.5) resulted in a bar chart showing the distribution of dimensions for both hydrodynamic conditions closer to the top (Figure 4.6). While *E. coli* cells had lengths ranging from 1 to 2.4 µm under shaking conditions (the average was 1.6 ± 0.3 µm), those which adhered without shaking measured up to 5 µm (the average was 3.0 ± 0.8 µm). Thus, this quantitative evaluation confirmed that *E. coli* cells had different lengths ($P < 0.001$) under the two conditions, being on average 2 fold longer in the static condition.

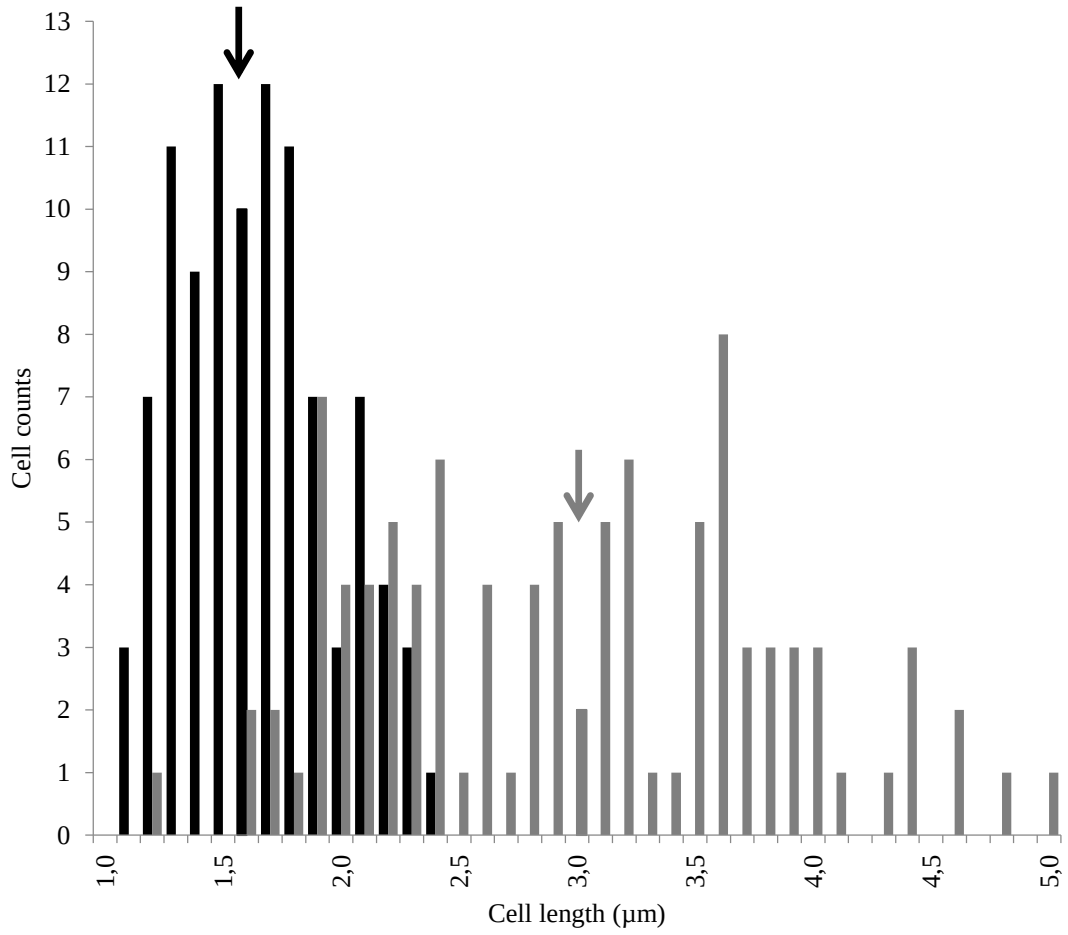

Figure 4.6. Cell length distribution in biofilms grown in the liquid side near the interface under shaking (■) and static (■) conditions. The arrows represent the average cell length for each condition.

4.3.2.1. Differential CV staining

Biofilm localization on the vertical walls of shaking 96-well microtiter plates was also determined by the differential CV staining (Figure 4.7D), a new microscale approach validated by SEM analysis (Figure 4.7E).

Through direct observation of the stained wells (prior to solubilization of the dye), it was possible to observe that biofilms were mainly formed on the wall and not on the bottom of the well. Moreover, since the amount of produced biofilm is proportional to the amount of CV adsorbed, it seemed that the biofilm was unevenly distributed in the cylindrical wall and higher amounts were formed closer to the air-liquid interface (Figure 4.7A). Similarly to what was observed in the photograph of the stained well, the CFD simulation revealed that the shear strain rate distribution was not uniform along the wall,

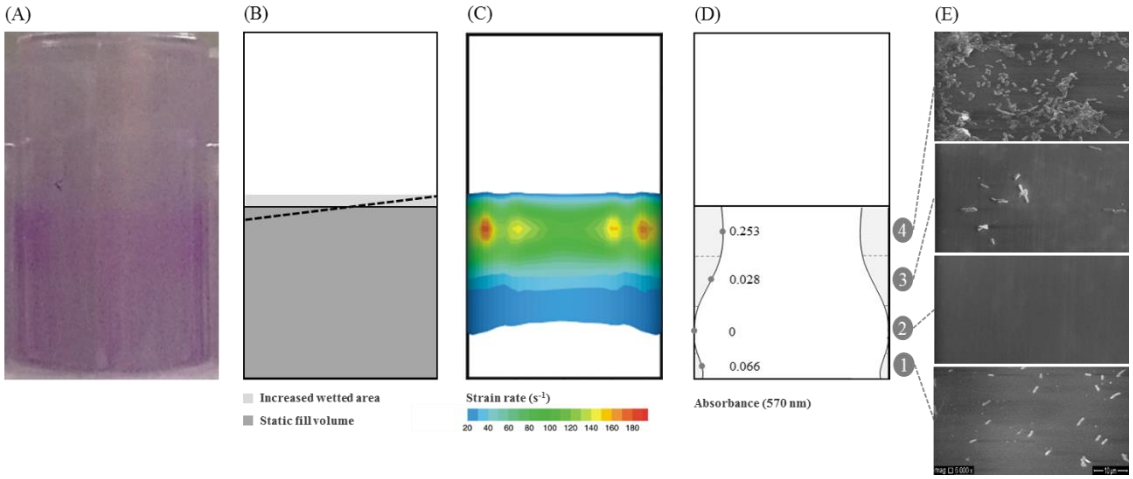

Figure 4.7. Biofilm localization in shaking 96-well microtiter plates placed in a 50 mm-incubator at 150 rpm. (A) Photograph of a well stained with crystal violet; (B) schematic representation of a well where the dark grey area corresponds to the wetted area without shaking, the light grey area represents the area increase upon shaking and the dotted line depicts the inclination of the air-liquid interface; (C) time averaged shear strain rates (values below 20 s^{-1} are not represented); (D) illustration of the biofilm distribution on the vertical wall assayed by the differential CV staining in the sections identified in Figure 4.1; (E) representative scanning electron micrographs of the wall sections defined in Figure 4.1 (magnification: 5000×; bar = 10 µm).

being much higher in the liquid side near the interface (Figure 4.7C). Also, for the shaking condition chosen for this work (50 mm of orbital diameter and 150 rpm), an area gain of 8.5% and a maximum angle of 7.8º was obtained (Figure 4.7B). Observing the results of the differential CV staining (Figure 4.7D), the amount of biofilm detected along the different sections of the wall was also not constant. The highest value of absorbance (corresponding to the highest amount of biofilm biomass) was measured in the region located immediately below the liquid level (section 4). In the intermediate sections of the well, the absorbance values were about 10 times lower than near the interface (section 3) or almost zero (section 2), increasing slightly in the section closer to the bottom of the well (section 1). In order to validate the results obtained by the differential CV staining, SEM analysis was performed on the vertical wall of the wells. Figure 4.6E shows scanning electron micrographs representative of the four sections defined in the application of the differential CV staining (Figure 4.7D). SEM analysis showed that *E. coli* adhesion varied across the wall and that higher attachment occurred closer to the air-

liquid interface (section 4) compared to the intermediate (sections 2 and 3) and near bottom (section 1) regions of the well.

4.4. Discussion

The influence of shaking conditions on *E. coli* biofilm formation in microtiter plates was analysed by a combination of macroscale and microscale methods. Although the macroscale techniques used - crystal violet and resazurin - did not reveal any bulk differences on the amount and metabolic state of the cells in different hydrodynamic conditions, microscale analysis revealed differences in the spatial distribution and cell length in biofilms when comparing shaking with static conditions. It was hypothesized that these variations in the microscopic appearance of biofilms may be correlated with the shear strain rate distribution on the well during agitation.

Under shaking conditions, zones of higher shear strain rate values as those closer to the air-liquid interface can be associated with the formation of higher cell density aggregates embedded in EPS, a type of biofilm typically observed under turbulent flow conditions (Paris et al. 2007). This higher cell density biofilms are supported by the higher oxygen and substrate mass transfer from the bulk liquid to the biofilm (Moreira et al. 2013a). In fact, when a 50 mm-incubator is rotating at 150 rpm, CFD simulations exhibited some spots of maximum shear strain rate near the interface, which were related to regions of unstable vortices (Moreira et al. 2013c) and hence more efficient liquid mixing. Additionally, the flow inside a vortex is characterized by a strong recirculation which may be able to trap bacteria entering this region (Salek et al. 2012). Low shear strain rate conditions, such as those found at the bottom of the vertical wall, were not favorable for *E. coli* adhesion and therefore single bacterial cells were observed uniformly distributed throughout the polystyrene surface. These results are in agreement with previous studies (Kwok et al. 1998, Rochex et al. 2008, Simões et al. 2007) that found that higher shear forces result in a denser biofilm.

Concerning the static condition, it would be expected that the biofilm distribution was more uniform along the wall because no shear forces were acting. An explanation for the higher number of cells observed near the liquid surface compared to the bottom can be a higher exposure to air that promoted cell adhesion and growth in that region.

Besides showing differences in the spatial distribution of biofilms, SEM analysis also revealed that biofilm cells had different sizes when subjected to different hydrodynamic conditions. On a previous work, Simões et al. (2007) demonstrated that *P. fluorescens* cells within turbulent and laminar flow-generated biofilms differed from each other in length. While cells from biofilms formed at lower shear strain rates had an equivalent cell radius of 0.408 μm, cells from biofilms formed at higher shear strain rates were smaller, with an equivalent cell radius of 0.201 μm (Simões et al. 2007). By microscopic observation, Paris et al. (2007) also showed that the wall shear strain rate in a flow chamber influenced the size of drinking water biofilms as cells were 5 fold longer when the shear strain rate was 5 fold smaller.

Both microscale methods have been applied in this work roughly at the same scale. In fact, when comparing the area covered by a SEM image taken at 1000× magnification with the projected area of a hexahedral CFD cell, the values were similar (250 × 200 μm and 270 × 300 μm, respectively). However, a higher magnification (5000×) was necessary to ascertain the cell size differences between the biofilms formed in different hydrodynamic conditions. This requirement for greater level of detail in the SEM analysis was obtained through a greater refinement of the surface area under analysis (a larger number of images was needed to cover the same area). In the CFD case, preliminary mesh tests indicated that a higher mesh refinement (using a higher number of hexahedral cells) would increase the required simulation time without significant improvement of the numerical accuracy (Table 3.2), and therefore a mesh with 18,876 hexahedral cells was used.

Although microtiter assays are broadly accepted by the biofilm community, there is a lack of information on the effect of hydrodynamics in the architecture of biofilms formed in this system. It was shown by Kostenko et al. (2010) that biofilm deposition and morphology in six-well plates is non-uniform and that the biofilm characteristics correlate strongly with local shear stress mean and fluctuation levels along the bottom face of a well. Berson et al. (2008) and Dardik et al. (2005) used these plates to study the effects of orbital shear stress on endothelial cells. The first study concluded that shear stress levels at the bottom of the plate were not uniform and that the rotational speed influenced the radial shear stress distribution. Dardik et al. (2005) demonstrated that the proliferation and orientation of endothelial cells at the well bottom differs between the static and shaking scenario. Similar to our findings, cells exposed to orbital shaking appear to have increased proliferation compared to cells exposed to static conditions (Dardik et al. 2005).

In the human body, biofilms are naturally heterogeneous as a result of the shear stress variations (Lantz et al. 2011, Potter et al. 2012). Thus, taking together the SEM visualizations and CFD simulations, it is possible to state that microtiter plates are probably well suited to mimic the natural variations in the shear stress field in biomedical scenarios.

Several macroscale protocols for biofilm quantitation in microtiter plates have been described. For CV and resazurin assays, the results are based on color and fluorescence intensity at a certain wavelength, respectively, which means that rapid, quantitative analysis can be obtained from a single equipment such as an automated multiplate reader (Azevedo et al. 2009). Another advantage of these macroscale methods is a broad and robust applicability for many microorganisms (Peeters et al. 2008). On the other hand, the results of CV staining can be correlated with conventional plate count, optical density, biofilm thickness and dry weight results (Alnnasouri et al. 2011), and resazurin assays correlate well with plate counting (Elkhatib & Noreddin 2009).

Unlike using spectrophotometric techniques, assessment of biofilms by microscopy not only can provide quantitative data on the total and active number of cells, but also enables a detailed structural characterization of biofilms for comparative purposes. Several electron microscopy methods have been used to investigate biofilms, being SEM the predominant choice (Alhede et al. 2012). Its main advantage is to offer excellent magnification (ranging from 20× to approximately 30,000×) and resolution (from 50 to 100 nm) with the ability to image complex shapes (Stewart et al. 1995, Surman et al. 1996). However, prior to imaging under high vacuum, biofilm specimens are prepared by fixation, dehydration and coating with a conductive material, which can destroy the structure of samples or cause artifacts (Hannig et al. 2010). Even though the distribution and/or morphology of the biofilms may have been slightly altered by these processes, SEM enables good comparative analysis between different experimental conditions (like the flow regimes analysed on this work), mainly at the biofilm surface. This analysis has shown clear differences between biofilms formed in shaking and static conditions that the macroscale methods failed to detect. According to Vertes et al. (2012), SEM has been used to verify if other types of assays are correlated with a real physical change in morphology and density of biofilms. Furthermore, it allows the estimation of the dimensions of microorganisms (Horath et al. 2006).

In recent years, CLSM has emerged as a method of choice for checking the three-dimensional structural characteristics of biofilms because it allows a non-destructive

analysis at a cell scale of their hydrated spatial arrangement (Bridier et al. 2013, Bridier et al. 2010). In addition to qualitative information, CLSM enables the determination of quantitative structural parameters on biofilms directly from three-dimensional image stacks (e.g. thickness, roughness, substrate coverage and surface to volume ratio) (Bridier et al. 2010, Heydorn et al. 2000). Nevertheless, real-time monitoring is not always possible, either because of the incompatibility of the biofilm platform with the microscope and/or practical problems associated with the use of CLSM for longer periods of time, thus "offline" visualization is often used (Coenye & Nelis 2010). This *ex-situ* preparation is time consuming and can alter the native biofilm spatial organization, possibly sharing some of the problems encountered by SEM. Another disadvantage of CLSM is that it may not be applicable to thick biofilms or those containing abiotic particulate matter if they are too opaque (Stewart et al. 1995). When biofilms are thick (> 50 µm), the optical sectioning provided by confocal microscopy is not sufficient to examine the sample in the *z*-dimension and biofilms must be embedded, physically sectioned, stained, and then examined (Palmer Jr et al. 2006). All these steps require sample manipulation and can disrupt the fine structure of biofilms, thereby making spatial analysis difficult. On the other hand, when water-immersible lens (dipping lens) are not available, the sample must have a coverslip placed on top of it, with the possibility of pressure distortion (Palmer Jr et al. 2006). Due to the intrinsic limitations of light microscopy, CSLM is also not indicated for the observation of the ultra-structure of cells or matrix constituents, which require higher resolution imaging (Bridier et al. 2013). The use of SEM overcomes some of these restrictions by using an electron beam instead of a photon beam that allows high magnification visualization of the cellular morphology, cell-to-cell interactions or matrix components within biofilms (Bridier et al. 2013).

Several papers have been recently published about the use of SEM for characterization of biofilms formed in microtiter plates, most of them using glass coupons or coverslips in the 6-well format (Kostenko et al. 2010, Martinez et al. 2010, Shields et al. 2013, Wang et al. 2011). Others reported the insertion of plastic (Bandara et al. 2009, Melo et al. 2011) and aluminum coupons (Bridier et al. 2013) in 6- or 24-well microtiter plates and the microscopic observation of biofilm developed on polystyrene pegs (Coraça-Hubér et al. 2012, Sanchez et al. 2013, Smith et al. 2008). Biofilm formation on the vertical wall of microtiter plate wells has always been neglected; thus, to the best of our knowledge, this is the first work that uses SEM visualization to provide rather detailed information about cell adhesion along the walls of 96-well microtiter plates and to relate

it to the local hydrodynamic patterns. This is of particular relevance because it was shown on a previous report that biofilm formation on the vertical wall can exceed the amount of biofilms formed on the bottom of the plate (Moreira et al. 2013c), particularly on the 96-well format due to the ratio of vertical wall area/ bottom area.

It is interesting to notice that the differential CV staining presented in this chapter corresponds to an intermediate scale between the traditional CV assay and SEM analysis. The traditional CV assay quantifies the biofilm formed on the wall and bottom of each well of a microtiter plate, which corresponds to an area of about 146 mm^2 (for a 96-well plate), while the method proposed here evaluates wall sections of about 14 and 28 mm^2. In comparison, the area covered by a SEM image taken at 5000× magnification was of 2×10^{-3} mm^2, and this technique enables detailed analysis of individual cells within the biofilm rather than simply determining their localization. However, one must bear in mind that most laboratories are not equipped with an electron microscope and this technique has a considerably lower throughput than macroscale methods such as CV and resazurin assays.

Observation of biofilms formed on the bottom of the wells of microtiter plates is very common using optical microscopes at magnifications of 100 to 200×, which typically cover areas of 0.3 mm^2 (Lizcano et al. 2010, Melo et al. 2007, Quave et al. 2012, White et al. 2011). These observations have provided some information about the architecture of the biofilms formed on the bottom of the wells (particularly when CLSM is used) but usually disregard the biofilm that forms on the vertical wall. Therefore, a method was developed to determine the spatial localization of these biofilms in a high throughput manner, using common laboratory equipment. The area under analysis in each of the four sections defined for the differential staining is equivalent to the area analysed by optical microscopy using a 15× magnification. This area could be further reduced (thus increasing the precision of the method) by dividing the well in sections of smaller height.

To conclude, it was demonstrated that SEM is an extremely useful tool for comparative analysis in biofilm research. When no differences were detected between biofilms formed under shaking and static conditions using macroscale methods, this microscale technique revealed differences in size and location of cells. On the other hand, the novel approach presented in this work demonstrated that the CV dye can be extremely useful in locating the adherent cells in microtiter plates when used in a differential way. The method is slightly more laborious and slower than the traditional staining procedure,

but it requires fewer resources and has higher throughput than SEM in determining the spatial location of biofilms.

The current trend for analytical methods is a shift towards high-throughput platforms that can provide meaningful information about bulk parameters. However, one must bear in mind that, if these high-throughput methodologies are the only ones to be used, a lot of relevant information may be lost simply because a detailed analysis using more precise techniques is still not amenable to this high-throughput format. Thus, the possibility of analysing bulk properties in large data-sets must not preclude the detailed analysis that is more likely to shed some light on the rationale of the observations that are being made at a macroscale level.

4.5. References

Alhede M, Qvortrup K, Liebrechts R, Høiby N, Givskov M, Bjarnsholt T. 2012. Combination of microscopic techniques reveals a comprehensive visual impression of biofilm structure and composition. FEMS Immunol Med Microbiol. 65:335-342.

Alnnasouri M, Dagot C, Pons M-N. 2011. Comparison of four methods to assess biofilm development. Water Sci Technol. 63:432-439.

Azevedo NF, Lopes SP, Keevil CW, Pereira MO, Vieira MJ. 2009. Time to "go large" on biofilm research: advantages of an omics approach. Biotechnol Lett. 31:477-485.

Bandara HMHN, Yau JYY, Watt RM, Jin LJ, Samaranayake LP. 2009. *Escherichia coli* and its lipopolysaccharide modulate *in vitro Candida* biofilm formation. J Med Microbiol. 58:1623-1631.

Berson RE, Purcell M, Sharp MK. 2008. Computationally Determined Shear On Cells Grown In Orbiting Culture Dishes. In: Kang K, Harrison D, Bruley D, editors. Oxygen Transport to Tissue XXIX. US: Springer. p. 189-198.

Borges A, Simões LC, Saavedra MJ, Simões M. 2014. The action of selected isothiocyanates on bacterial biofilm prevention and control. Int Biodeter Biodegr. 86:25-33.

Bridier A, Meylheuc T, Briandet R. 2013. Realistic representation of *Bacillus subtilis* biofilms architecture using combined microscopy (CLSM, ESEM and FESEM). Micron. 48:65-69.

Bridier A, Dubois-Brissonnet F, Boubetra A, Thomas V, Briandet R. 2010. The biofilm architecture of sixty opportunistic pathogens deciphered using a high throughput CLSM method. J Microbiol Methods. 82:64-70.

Cady NC, McKean KA, Behnke J, Kubec R, Mosier AP, Kasper SH, Burz DS, Musah RA. 2012. Inhibition of biofilm formation, quorum sensing and infection in *Pseudomonas aeruginosa* by natural products-inspired organosulfur compounds. PLoS ONE. 7:e38492.

Coenye T, Nelis HJ. 2010. *In vitro* and *in vivo* model systems to study microbial biofilm formation. J Microbiol Methods. 83:89-105.

Coraça-Hubér DC, Fille M, Hausdorfer J, Pfaller K, Nogler M. 2012. Evaluation of MBEC™-HTP biofilm model for studies of implant associated infections. J. Orthop. Res. 30:1176-1180.

Dardik A, Chen L, Frattini J, Asada H, Aziz F, Kudo FA, Sumpio BE. 2005. Differential effects of orbital and laminar shear stress on endothelial cells. J Vasc Surg. 41:869-880.

Duetz WA. 2007. Microtiter plates as mini-bioreactors: miniaturization of fermentation methods. Trends Microbiol. 15:469-475.

Elkhatib WF, Noreddin AM. 2009. A new fluorogenic assay for monitoring and determining planktonic and biofilm forms of *Pseudomonas aeruginosa* viable count *in vitro*. J Rapid Meth Aut Mic. 17:304-314.

Fedel M, Caciagli P, Chistè V, Caola I, Tessarolo F. 2007. Microbial biofilm imaging ESEM vs. HVSEM. Imaging & Microscopy. 9:44-47.

Gomes LC, Moreira JMR, Teodósio JS, Araújo JDP, Miranda JM, Simões M, Melo LF, Mergulhão FJ. 2014. 96-well microtiter plates for biofouling simulation in biomedical settings. Biofouling. 30:535-546.

Hannig C, Follo M, Hellwig E, Al-Ahmad A. 2010. Visualization of adherent micro-organisms using different techniques. J Med Microbiol. 59:1-7.

Heydorn A, Nielsen AT, Hentzer M, Sternberg C, Givskov M, Ersbøll BK, Molin S. 2000. Quantification of biofilm structures by the novel computer program COMSTAT. Microbiology. 146:2395-2407.

Horath T, Neu TR, Bachofen R. 2006. An endolithic microbial community in dolomite rock in central Switzerland: characterization by reflection spectroscopy, pigment analyses, scanning electron microscopy, and laser scanning microscopy. Microb Ecol. 51:353-364.

Kostenko V, Salek MM, Sattari P, Martinuzzi RJ. 2010. *Staphylococcus aureus* biofilm formation and tolerance to antibiotics in response to oscillatory shear stresses of physiological levels. FEMS Immunol Med Microbiol. 59:421-431.

Kwok WK, Picioreanu C, Ong SL, van Loosdrecht MCM, Ng WJ, Heijnen JJ. 1998. Influence of biomass production and detachment forces on biofilm structures in a biofilm airlift suspension reactor. Biotechnol Bioeng. 58:400-407.

Lantz J, Renner J, Karlsson M. 2011. Wall shear stress in a subject specific human aorta - influence of fluid structure interaction. Int. J. Appl. Mech. 3:759-778.

Lee J-H, Park J-H, Kim J-A, Neupane GP, Cho MH, Lee C-S, Lee J. 2011. Low concentrations of honey reduce biofilm formation, quorum sensing, and virulence in *Escherichia coli* O157:H7. Biofouling. 27:1095-1104.

Lizcano A, Chin T, Sauer K, Tuomanen EI, Orihuela CJ. 2010. Early biofilm formation on microtiter plates is not correlated with the invasive disease potential of *Streptococcus pneumoniae*. Microb Pathog. 48:124-130.

Manuel C. 2007. Biofilm Dynamics and Drinking Water Stability: Effects of Hydrodynamics and Surface Materials [PhD]. Faculty of Engineering: University of Porto.

Martinez LR, Mihu MR, Han G, Frases S, Cordero RJB, Casadevall A, Friedman AJ, Friedman JM, Nosanchuk JD. 2010. The use of chitosan to damage *Cryptococcus neoformans* biofilms. Biomaterials. 31:669-679.

Melo AS, Colombo AL, Arthington-Skaggs BA. 2007. Paradoxical growth effect of caspofungin observed on biofilms and planktonic cells of five different *Candida* species. Antimicrob Agents Chemother. 51:3081-3088.

Melo AS, Bizerra FC, Freymüller E, Arthington-Skaggs BA, Colombo AL. 2011. Biofilm production and evaluation of antifungal susceptibility amongst clinical *Candida* spp. isolates, including strains of the *Candida parapsilosis* complex. Med Mycol. 49:253-262.

Moreira JMR, Teodósio JS, Silva FC, Simões M, Melo LF, Mergulhão FJ. 2013a. Influence of flow rate variation on the development of *Escherichia coli* biofilms. Bioprocess Biosyst Eng. 36:1787-1796.

Moreira JMR, Gomes LC, Araújo JDP, Miranda JM, Simões M, Melo LF, Mergulhão FJ. 2013c. The effect of glucose concentration and shaking conditions on *Escherichia coli* biofilm formation in microtiter plates. Chem Eng Sci. 94:192-199.

Norton TA, Thompson RC, Pope J, Veltkamp CJ, Banks B, Howard CV, Hawkins SJ. 1998. Using confocal laser scanning microscopy, scanning electron microscopy and phase contrast light microscopy to examine marine biofilms. Aquat Microbial Ecol. 16:199-204.

Palmer Jr RJ, Sternberg C. 1999. Modern microscopy in biofilm research: confocal microscopy and other approaches. Curr Opin Biotechnol. 10:263-268.

Palmer Jr RJ, Haagensen JJ, Neu T, Sternberg C. 2006. Confocal Microscopy of Biofilms - Spatiotemporal Approaches. In: Pawley JB, editor. Handbook of Biological Confocal Microscopy. US: Springer. p. 870-888.

Paris T, Skali-Lami S, Block J-C. 2007. Effect of wall shear rate on biofilm deposition and grazing in drinking water flow chambers. Biotechnol Bioeng. 97:1550-1561.

Peeters E, Nelis HJ, Coenye T. 2008. Comparison of multiple methods for quantification of microbial biofilms grown in microtiter plates. J Microbiol Methods. 72:157-165.

Pettit R, Weber C, Pettit G. 2009. Application of a high throughput Alamar blue biofilm susceptibility assay to *Staphylococcus aureus* biofilms. Ann. Clin. Microbiol. Antimicrob. 8:28.

Pitts B, Hamilton MA, Zelver N, Stewart PS. 2003. A microtiter-plate screening method for biofilm disinfection and removal. J Microbiol Methods. 54:269-276.

Potter CMF, Schobesberger S, Lundberg MH, Weinberg PD, Mitchell JA, Gorelik J. 2012. Shape and compliance of endothelial cells after shear stress *in vitro* or from different aortic regions: scanning ion conductance microscopy study. PLoS ONE. 7:e31228.

Quave CL, Plano LRW, Pantuso T, Bennett BC. 2008. Effects of extracts from Italian medicinal plants on planktonic growth, biofilm formation and adherence of methicillin-resistant *Staphylococcus aureus*. J Ethnopharmacol. 118:418-428.

Quave CL, Estévez-Carmona M, Compadre CM, Hobby G, Hendrickson H, Beenken KE, Smeltzer MS. 2012. Ellagic acid derivatives from *Rubus ulmifolius* inhibit *Staphylococcus aureus* biofilm formation and improve response to antibiotics. PLOS One. 7:e28737.

Rochex A, Godon J-J, Bernet N, Escudié R. 2008. Role of shear stress on composition, diversity and dynamics of biofilm bacterial communities. Water Res. 42:4915-4922.

Salek M, Sattari P, Martinuzzi R. 2012. Analysis of fluid flow and wall shear stress patterns inside partially filled agitated culture well plates. Ann Biomed Eng. 40:707-728.

Sanchez C, Mende K, Beckius M, Akers K, Romano D, Wenke J, Murray C. 2013. Biofilm formation by clinical isolates and the implications in chronic infections. BMC Infect. Dis. 13:47.

Serra DO, Richter AM, Klauck G, Mika F, Hengge R. 2013. Microanatomy at cellular resolution and spatial order of physiological differentiation in a bacterial biofilm. mBio. 4:e100103-100113.

Shakeri S, Kermanshahi RK, Moghaddam MM, Emtiazi G. 2007. Assessment of biofilm cell removal and killing and biocide efficacy using the microtiter plate test. Biofouling. 23:79-86.

Shields RC, Mokhtar N, Ford M, Hall MJ, Burgess JG, ElBadawey MR, Jakubovics NS. 2013. Efficacy of a marine bacterial nuclease against biofilm forming microorganisms isolated from chronic rhinosinusitis. PLoS ONE. 8:e55339.

Simões LC, Simões M, Vieira M. 2010a. Adhesion and biofilm formation on polystyrene by drinking water-isolated bacteria. Antonie van Leeuwenhoek. 98:317-329.

Simões M, Pereira MO, Sillankorva S, Azeredo J, Vieira MJ. 2007. The effect of hydrodynamic conditions on the phenotype of *Pseudomonas fluorescens* biofilms. Biofouling. 23:249-258.

Smith K, Perez A, Ramage G, Lappin D, Gemmell CG, Lang S. 2008. Biofilm formation by Scottish clinical isolates of *Staphylococcus aureus*. J. Med. Microbiol. 57:1018-1023.

Stepanović S, Vuković D, Dakić I, Savić B, Švabić-Vlahović M. 2000. A modified microtiter-plate test for quantification of staphylococcal biofilm formation. J Microbiol Methods. 40:175-179.

Stewart PS, Murga R, Srinivasan R, de Beer D. 1995. Biofilm structural heterogeneity visualized by three microscopic methods. Water Res. 29:2006-2009.

Surman SB, Walker JT, Goddard DT, Morton LHG, Keevil CW, Weaver W, Skinner A, Hanson K, Caldwell D, Kurtz J. 1996. Comparison of microscope techniques for the examination of biofilms. J Microbiol Methods. 25:57-70.

Teodósio JS, Simões M, Melo LF, Mergulhão FJ. 2011a. Flow cell hydrodynamics and their effects on *E. coli* biofilm formation under different nutrient conditions and turbulent flow. Biofouling. 27:1-11.

Thorn RMS, Greenman J. 2009. A novel *in vitro* flat-bed perfusion biofilm model for determining the potential antimicrobial efficacy of topical wound treatments. J Appl Microbiol. 107:2070-2079.

Vertes A, Hitchins V, Phillips KS. 2012. Analytical challenges of microbial biofilms on medical devices. Anal Chem. 84:3858-3866.

Wang Y, Zhang W, Wu Z, Zhu X, Lu C. 2011. Functional analysis of luxS in *Streptococcus suis* reveals a key role in biofilm formation and virulence. Vet Microbiol. 152:151-160.

White MG, Piccirillo S, Dusevich V, Law DJ, Kapros T, Honigberg SM. 2011. Flo11p adhesin required for meiotic differentiation in *Saccharomyces cerevisiae* minicolonies grown on plastic surfaces. FEMS Yeast Res. 11:223-232.

Xia B, Sun D-W. 2002. Applications of computational fluid dynamics (CFD) in the food industry: a review. Comput Electron Agr. 34:5-24.

5.

Heterologous protein production in *E. coli* biofilms: a non-conventional form of high cell density cultivation[d]

Abstract

E. coli is one of the favourite hosts for recombinant protein production and has been recognized as an excellent model for biofilm studies. High cell density cultures (HCDC) of this bacterium enable attractive volumetric production yields and cells growing in biofilms share some of the challenges of conventional high cell density planktonic cultures.

This work assesses the production potential of *E. coli* JM109(DE3) biofilm cells expressing a model protein (eGFP) from a recombinant plasmid. A control strain harbouring the same plasmid backbone but lacking the *eGFP* gene was used to assess the impact of heterologous protein production on biofilm formation. Results showed that specific eGFP production from biofilm cells was about 30 fold higher than in planktonic state. Moreover, eGFP-expressing cells had enhanced biofilm formation compared to control cells. Volumetric production values were 2 fold higher than those previously reported with the same protein and are within the range of what can be obtained by conventional HCDC in the production of soluble proteins. Although the cellular density

[d] The content of this chapter was adapted from the following publication(s):

Gomes LC, Mergulhão FJ. Heterologous protein production in *Escherichia coli* biofilms: a non-conventional form of high cell density cultivation. Process Biochem (submitted).

that was obtained was lower than in conventional HCDC (0.5 fold), this system showed good production values which are likely to be improved by optimization of culture conditions.

5.1. Introduction

The Gram-negative bacterium *E. coli* is a preferred host for the production of recombinant proteins (Mergulhão et al. 2004b, Sanchez-Garcia et al. 2016) due to its fast growth at high cell densities, minimal nutrient requirements, well-known genetics and availability of a large number of cloning vectors and mutant host strains (Baneyx 1999). This bacterium has the ability to accumulate many recombinant proteins to at least 20% of the total cell protein (Pines & Inouye 1999) and to translocate them from the cytoplasm to the periplasm (Mergulhão et al. 2005). *E. coli* cultivation in HCDC presents many advantages such as reduced culture volume, enhanced downstream processing and lower production costs (Choi et al. 2006). Despite these advantages, there are still many challenges that have to be addressed in HCDC and these include insufficient oxygen transfer, specific culture medium requirements, reduced mixing efficiency in the reactor and accumulation of carbon dioxide which decreases growth rates and increases acetate production (Choi et al. 2006, Mergulhão et al. 2005). Recombinant protein production by biofilm cells shares some of the challenges of conventional HCDC, namely in diffusion of nutrients and oxygen through the biofilm and also in the accumulation of toxic waste products (Stewart 2003, Stewart & Franklin 2008).

Recombinant protein expression in *E. coli* biofilms was pioneered by Huang et al. (1993, 1994a, 1995) who have studied the production of β-galactosidase in *E. coli* DH5α carrying a plasmid containing the *tac* promoter. Later, O'Connell et al. (2007) have described the first system for high level heterologous protein production in *E. coli* biofilm cells using a pUC-based vector for the expression of eGFP. Despite the enormous potential of this expressing system, heterologous protein production from *E. coli* biofilm cells remains largely unexplored.

The expression of heterologous proteins in *E. coli* is commonly accomplished by inserting the gene of interest into a multicopy plasmid under the transcriptional control of either a constitutive or regulatable promoter (Mergulhão et al. 2004b). It is well

documented that plasmids impose a metabolic burden on the host cell, as cellular resources must be used for their replication as well for the expression of plasmid-encoded genes (Bentley et al. 1990, Glick 1995). In planktonic cells, this added metabolic burden decreases cellular growth rates (Cheah et al. 1987, Flores et al. 2004) and biomass yields (Ow et al. 2006), particularly when the plasmid vector is used to direct production of a recombinant protein (Andersson et al. 1996, Bentley et al. 1990, Sørensen & Mortensen 2005, Yang et al. 2016). This metabolic burden also promotes segregational and structural plasmid instability (Yu et al. 2003), and several metabolic changes in the host cell (Birnbaum & Bailey 1991, Haddadin & Harcum 2005) which may, in turn, affect the yield and activity of the product protein. In contrast to planktonic cells, the presence of plasmids was shown to increase biofilm formation and plasmid stability in many studies. However, most of these studies were performed with conjugative plasmids (Burmølle et al. 2008, Ghigo 2001, Król et al. 2011, May & Okabe 2008, Norman et al. 2008, Reisner et al. 2006, Yang et al. 2008). Although non-conjugative plasmids are commonly used for heterologous protein production in *E. coli*, information regarding their impact on biofilm formation remains scarce. It has been shown in flow conditions that when a plasmid (pTKW106 or pMJR1750) containing a mutated pMB1 origin was transformed into *E. coli* DH5α, the plasmid-bearing cells formed biofilms with higher cell density than non-transformed cells (Huang et al. 1993, Huang et al. 1994b). Lim et al. (2010b) also revealed that upon transformation of *E. coli* O157:H7 with a 92kb virulent and non-conjugative plasmid (pO157), biofilm formation and architecture were affected. Under smooth flow conditions, plasmid pO157 enabled biofilm development through increased production of EPS and generation of hyperadherent variants (Lim et al. 2010b). In a previous work, the effect of *E. coli* JM109(DE3) transformation with non-conjugative plasmids (pET28A and pUC8) on biofilm formation was assessed under turbulent flow conditions (Teodósio et al. 2012a). Plasmid-bearing cells formed biofilms with higher cell densities than non-transformed cells, which is an indication that biofilm cells may be a good platform for heterologous protein production unless the high-level expression of the foreign gene is detrimental for biofilm formation.

One of the major concerns about HCDC is that the specific productivity of recombinant protein that is obtained is often much lower than in flask culture (Choi et al. 2006). The aim of this work was to evaluate the specific production level of biofilm cells when compared to planktonic cells and to assess if heterologous protein expression was detrimental for biofilm development.

5.2. Materials and methods

5.2.1. Bacterial strain, plasmids and culture conditions

The *E. coli* strain JM109(DE3) from Promega (USA) was chosen because it is a well-characterized microorganism and recommended for protein expression with the pET system (Yanisch-Perron et al. 1985). Moreover, this strain has shown good biofilm forming ability in turbulent flow conditions (Teodósio et al. 2012a).

Competent *E. coli* cells were transformed by heat shock (Sambrook & Russell 2001) with the control plasmid pET28A (Novagen, USA) or with the expression plasmid pFM23 (Figure 5.1), which was obtained by cloning the *eGFP* gene into the pET28A vector as previously described by Mergulhão et al. (2004a). Transformants were selected on lysogeny broth (LB-Miller, Sigma, USA) agar supplemented with kanamycin (Eurobio, France).

Heterologous protein expression is obtained through the transcription of the *eGFP* gene, which is under the control of T7 promoter. Transcription is made by the chromosomally encoded T7 RNAP, which in turn is controlled by the *lac*UV5 inducible promoter (Novagen 2005). Induction can be achieved by the addition of IPTG although this compound was not added to the culture medium in this work.

Bacterial growth and reactor feeding was performed as described by Teodósio et al. (2012a). The recirculating tank of 1 l was continuously fed with 0.025 l h^{-1} of nutrient medium containing 0.55 g l^{-1} glucose, 0.25 g l^{-1} peptone, 0.125 g l^{-1} yeast extract and phosphate buffer (0.188 g l^{-1} KH_2PO_4 and 0.26 g l^{-1} Na_2HPO_4), pH 7.0. For maintenance of selective pressure, the antibiotic kanamycin was added to the growth and feeding media at a final concentration of 20 μg ml^{-1} (Teodósio et al. 2012a).

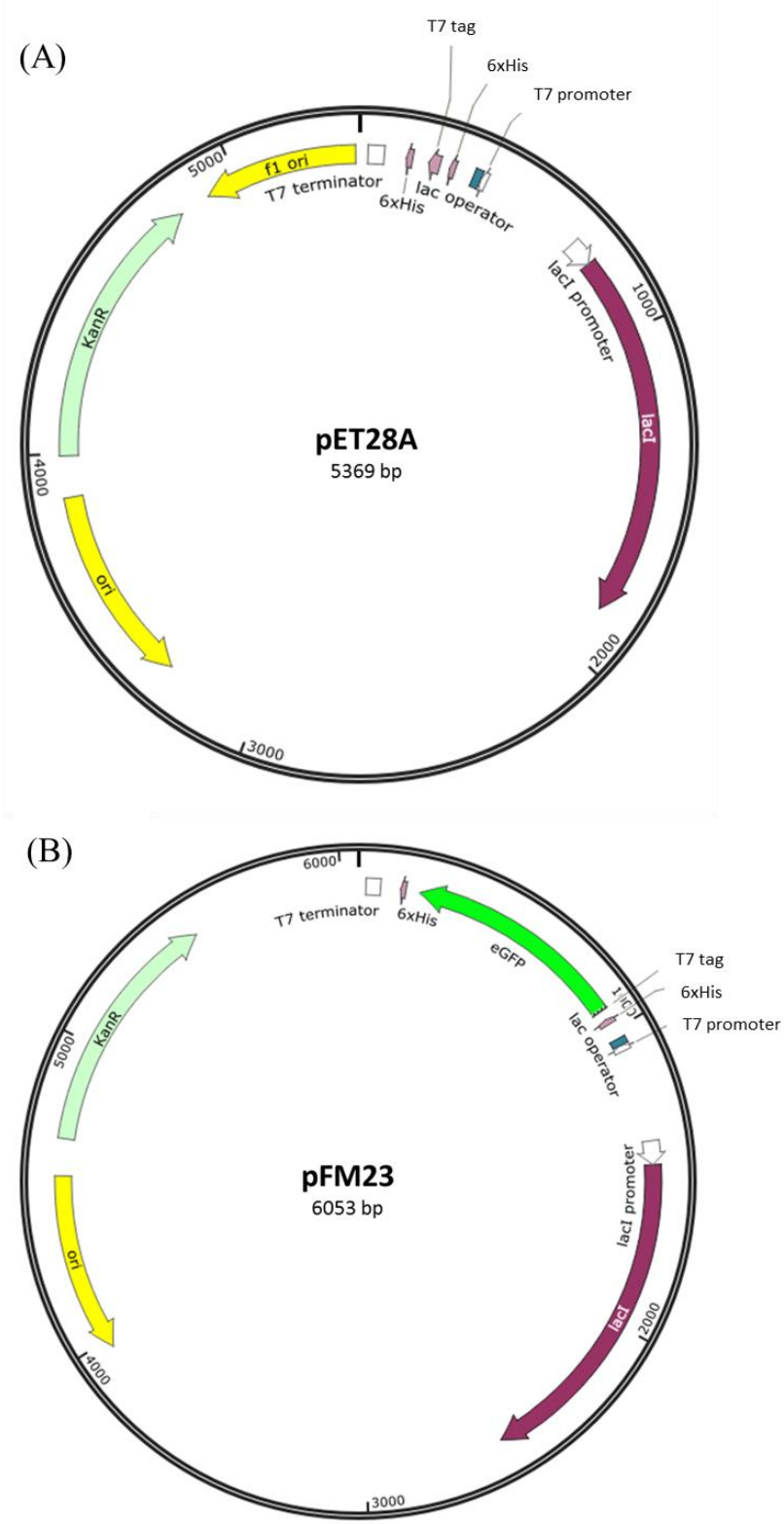

Figure 5.1. Maps of (A) plasmid pET28A and (B) plasmid pFM23. Both plasmids harbour (a) a pMB1 origin of replication (ori), (b) a repressor for the *lac* promoter (lacI), (c) a transcriptional promoter from the T7 phage (T7 promoter), (d) a lactose operator (*lac* operator), (e) an affinity purification tag (6×His), (f) a T7 transcriptional terminator (T7 terminator), and (g) a kanamycin resistance gene (*Kan*R). Plasmid pFM23 contains the *eGFP* gene (eGFP).

5.2.2. Biofilm formation system and sampling

To assess the eGFP expression in both biofilm and planktonic cells, a biofilm flow cell reactor connected to a recirculating tank (Figure 5.2) was used. The flow cell consists of a semi-circular Perspex duct (3.0 cm diameter and 1.2 m length) with 20 apertures on its flat wall to fit removable rectangular pieces of Perspex (coupons). PVC slides (2 x 1 cm) were glued onto the Perspex pieces and biofilms were formed on the upper faces that were in contact with the bacterial suspension circulating through the system. *E. coli* cells containing the pET28A or pFM23 plasmid were grown by recirculating the bacterial suspension at 30 ºC during 12 days under turbulent flow with a Reynolds number (Re) of 4,600 (flow rate of 255 l h^{-1}; average wall shear stress of approximately 0.3 Pa) (Moreira et al. 2015a, Teodósio et al. 2012a). This temperature was used since the *E. coli* strain JM109(DE3) had already demonstrated a good biofilm formation capacity at 30 ºC

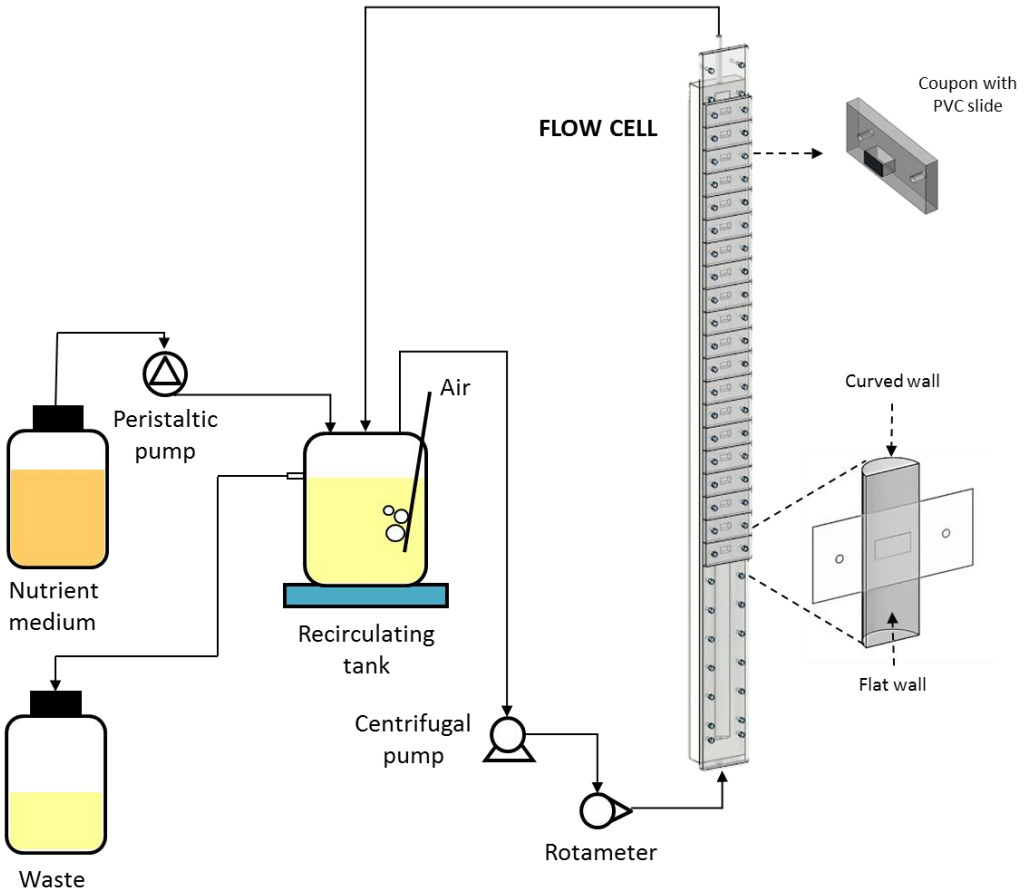

Figure 5.2. Schematic representation of the biofilm producing system comprising a recirculating tank, one vertical flow cell (with 20 coupons with PVC slides), peristaltic and centrifugal pumps.

in a similar culture medium and biofilm-producing system (Teodósio et al. 2011a). The recirculating tank of 1 l was aerated using an air pump (air flow rate of 108 l h^{-1}).

For biofilm sampling, the system was stopped to allow coupon removal and carefully started again maintaining the same flow conditions. Day 1 corresponds to the start of the reactor system and the sampling was initiated on day 3 of the experiment.

5.2.3. Analytical methods

Biofilm wet weight was determined by weighing each coupon before the experiment and subtracting this value from the weight of the same coupon at each sampling time. Biofilm thickness was also determined using a digital micrometer (Teodósio et al. 2011a) and afterwards the biofilm was resuspended and homogenized by vortexing in 25 ml of 8.5 g l^{-1} NaCl solution to assess total cell number and culturability.

Biofilm total cell counts were assessed by staining with DAPI as fully described by Gomes et al. (2015). Briefly, the cells were properly diluted, filtered through a nucleopore-etched (Whatman Int., Ltd., USA) black polycarbonate membrane (pore size 0.2 μm) and stained with 1 ml of DAPI reagent (0.5 mg l^{-1}) for 10 min in the dark (Saby et al. 1997). Stained bacterial observation and counting was performed using a Leica DM LB2 epifluorescence microscope connected to a Leica DFC300 FX camera (Leica Microsystems Ltd., Switzerland). Cell numbers on each membrane were estimated from counts of a minimum of 20 fields of view and the final values were presented as log cell cm^{-2}.

For biofilm culturability, samples were diluted to an appropriate cell density to yield > 10 and < 300 colony forming units (CFU) per plate of solid growth medium (PCA; Merck, Portugal) supplemented with kanamycin (20 μg ml^{-1}). Colony enumeration was carried out after 24 h incubation at 30 ºC and the final values were expressed as log CFU cm^{-2} of coupon area.

For planktonic cells, total cell number and culturability were assessed using the same methods as for biofilms. Results were presented as log cell ml^{-1} and log CFU ml^{-1}, respectively.

Glucose concentration and consumption in the whole system were determined as an indicator of metabolic activity (Teodósio et al. 2011a). Glucose consumption was

obtained by multiplying the difference between the glucose concentration entering the system and the glucose concentration in the tank by the feeding flow rate (0.025 l h^{-1}).

5.2.4. Heterologous protein expression

For *E. coli* cells containing the pFM23 expression vector, eGFP was analysed for both biofilm and planktonic cells. This analysis was performed as indicated in Mergulhão and Monteiro (2007). A sample volume corresponding to an equivalent $OD_{610\ nm}$ = 1 was used to harvest the cells by centrifugation (3202 *g* for 10 min). The pellet was resuspended in 100 µl of Buffer I (50 mM Na_2HPO_4, 300 mM NaCl, pH 8) and added to a 96-well microtiter plate (Orange Scientific, USA) already containing 100 µl of Buffer I. Fluorescence was measured using a microtiter plate reader (SpectraMax M2E, Molecular Devices, Inc., UK) with the excitation filter of 488 nm and the emission filter of 507 nm.

Calibration curves were constructed with purified eGFP standards (0 to 3.14 µg) mixed with 100 µl of washed JM109(DE3) cells harbouring the pET28A plasmid ($OD_{610\ nm}$ = 1). Buffer I was added to a final volume of 200 µl prior to measuring fluorescence and final values were expressed in specific eGFP production (fg $cell^{-1}$) using total cell values.

5.2.5. Quantification of EPS

The content of the main EPS found in biofilms (proteins and polysaccharides) was assessed for both strains after 7 days of growth. Matrix proteins and polysaccharides from biofilms were separated from cells using Dowex resin (50 X 8, Na^+ form, 20-50 mesh; Fluka Chemika, Switzerland) as described by Gomes et al. (2015). The biofilm was resuspended in 20 ml of extraction buffer (2 mM Na_3PO_4, 2 mM NaH_2PO_4, 9mM NaCl and 1 mM KCl, pH 7) and 2 g of Dowex resin per g of wet weight were added to the biofilm suspension. The extraction took place at 400 rpm for 4 h at 4 ºC, and ultimately the extracellular components (matrix) were separated from the cells through centrifugation.

Protein concentrations were determined for each strain using the Bicinchoninic Acid Protein Assay Kit - BCA™ Protein Assay Kit (Thermo Fisher Scientific, USA) and the polysaccharide concentrations by the phenol-sulphuric acid method of DuBois et al.

(1956). Protein and polysaccharide assays were performed using biofilm suspensions before EPS extraction (total constituents), and with cells (cellular constituents) and EPS (matrix constituents) after extraction. The final values were calculated taking into account the biofilm dry weight (Simões et al. 2007). The dry biofilm mass accumulated on the slides was assessed by the determination of the TVS of the homogenised biofilm suspensions according to the APHA, AWWA, WPCF Standard Methods (1989), method number 2540 A-D. According to this methodology, the TVS assessed at 550 + 5 ºC in a furnace for 2 h is equivalent to the amount of biological mass (cells and EPS). The dry biofilm mass accumulated was expressed in $mg_{biofilm}\ cm^{-2}$.

5.2.6. Statistical analysis

Results originated from averages of triplicate data sets obtained in independent experiments for each strain. Average SDs on the triplicate sets were calculated for all analysed parameters. For biofilm formation (Figure 5.3), the following averages were obtained: SD < 17% for glucose consumption, SD < 29% for biofilm wet weight, SD < 28% for biofilm thickness, SD < 9% for planktonic and biofilm culturability, and SD < 5% for planktonic and biofilm total cell counting. Regarding the fluorescence readings for eGFP quantitation (Figure 5.5), SD < 16% and SD < 10% were obtained for planktonic and biofilm cells, respectively.

In order to ascertain the statistical significance, paired *t*-test analysis was performed based on a confidence level of 90% (differences reported as significant for *P* values < 0.1 and marked with *) and 95% (differences reported as significant for *P* values < 0.05 and marked with $^{*}_{*}$).

5.3. Results

In order to assess if eGFP production was affecting biofilm development, the biofilm forming capacity of *E. coli* JM109(DE3) cells containing the pFM23 plasmid was compared to a strain harbouring the same plasmid backbone (pET28A) but devoid of the *eGFP* gene (Figures 5.3 to 5.5).

Figure 5.3A shows the glucose consumption profiles in the whole flow system (sessile plus planktonic cells). Higher glucose consumption values (on average 13%) were

obtained for the eGFP-expressing strain, although statistically significant differences were only obtained in 4 experimental points ($P < 0.05$ and $P < 0.1$). Additionally, glucose consumption increased over time for both strains until day 9. Thereafter, steady state was reached for the eGFP-expressing strain and a slight decrease was observed for *E. coli* cells bearing the pET28A plasmid.

Biofilm wet weight values (Figure 5.3B) were generally higher for the eGFP-expressing strain with statistically significant differences found mostly in the steady state (at days 8, 9 and 11, $P < 0.05$).

Planktonic culturability (Figure 5.3C) showed relatively little difference between the two strains. However, while the culturability of planktonic cells containing pET28A remained practically constant over time (around 7.9 log CFU ml^{-1}), culturability of the eGFP-expressing strain increased during the first half of the experiment before declining again after day 10. When comparing biofilm culturability, similar values were also obtained for both strains.

The number of planktonic total cells (Figure 5.3E) was higher for the eGFP-expressing cells (on average 62%) with statistically significant differences at days 4 and 5 ($P < 0.1$) and 9 and 12 ($P < 0.05$). The total planktonic cell number seemed to stabilize from day 6 onwards. The number of biofilm total cells (Figure 5.3F) was higher for the eGFP-expressing strain (on average 93%) for most of the experimental time (statistically significant differences were confirmed for all days, $P < 0.05$, with the exception of days 4 and 12), following the same trend of biofilm wet weight values (Figure 5.3B).

Biofilm thickness (Figure 5.3G) was higher for the eGFP-expressing strain, following the tendency of biofilm wet weight curve (Figure 5.3B), with statistically significant differences in most data points ($P < 0.05$). Considering the biofilm thickness in steady state, the cellular density of the biofilms producing eGFP was estimated to be 3.8×10^{10} cells ml^{-1}. Taking into account the average dry weight of the *E. coli* cell (Neidhardt 1996), this corresponds to an approximate cellular concentration of 11 g l^{-1}.

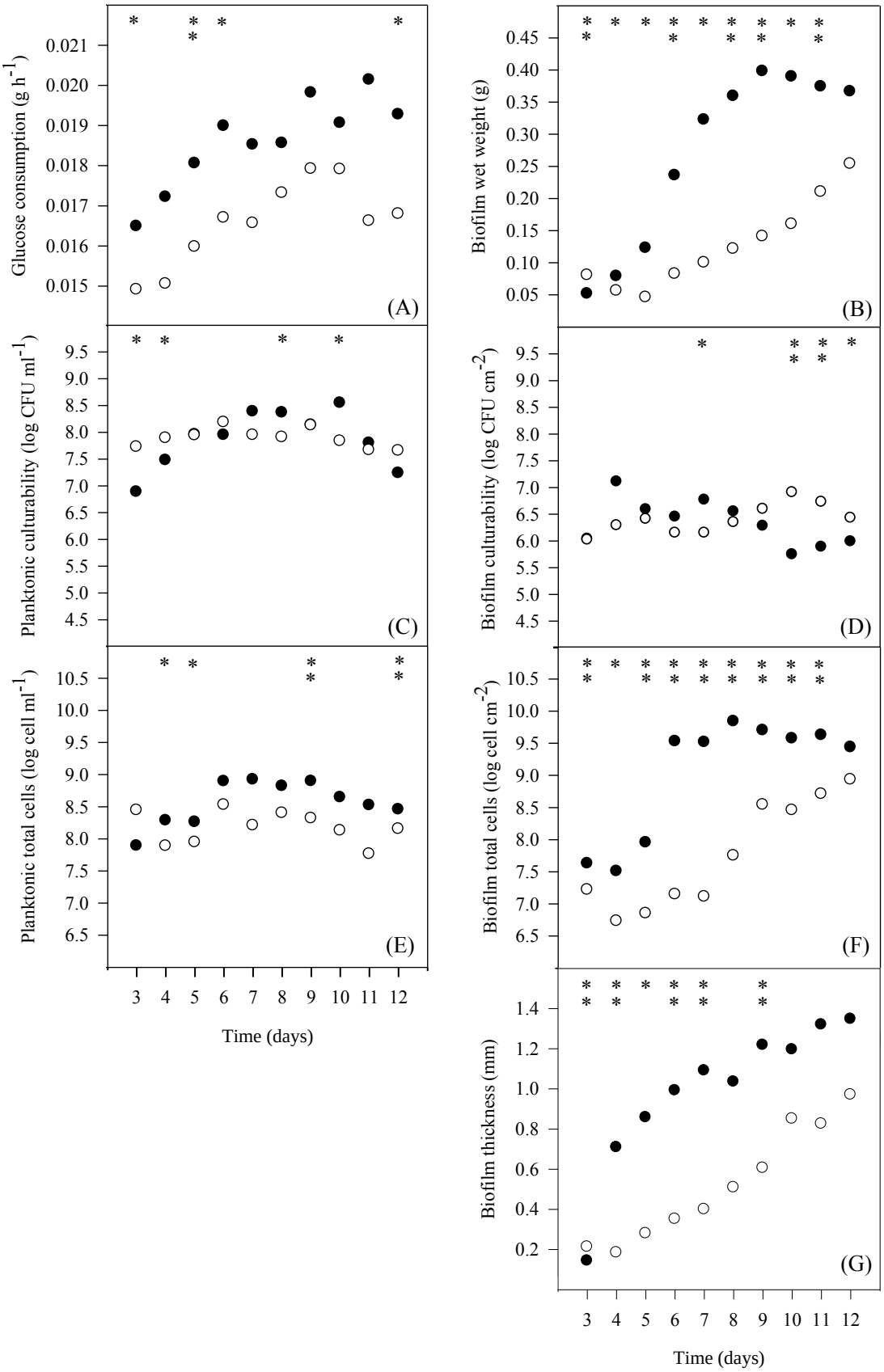

Figure 5.3. Time-course evolution of planktonic and biofilm assayed parameters: (A) glucose consumption in the system, (B) biofilm wet weight, (C) planktonic culturability, (D) biofilm culturability, (E) planktonic total cells, (F) biofilm total cells, (G) biofilm thickness. *E. coli* JM109(DE3) + pFM23 (●), *E. coli*

JM109(DE3) + pET28A (○). Results are an average of three independent experiments for each condition. Statistical analysis corresponding to each time point is represented with ∗ for a confidence level greater than 90% ($P < 0.1$) and with ∗∗ for a confidence level greater than 95% ($P < 0.05$).

Figure 5.4 shows photographs of wet biofilms formed by both strains in the flow cell reactor. It is evident from the images that the eGFP-producing strain showed greater biofilm formation than the pET28A-bearing strain, confirming the wet weight and thickness results presented on Figure 5.3B and G, respectively. After 7 days of growth, biofilms formed by the eGFP-producing strain appeared more homogenous and slimy, while those formed by the pET28A strain were more scattered on the PVC surface.

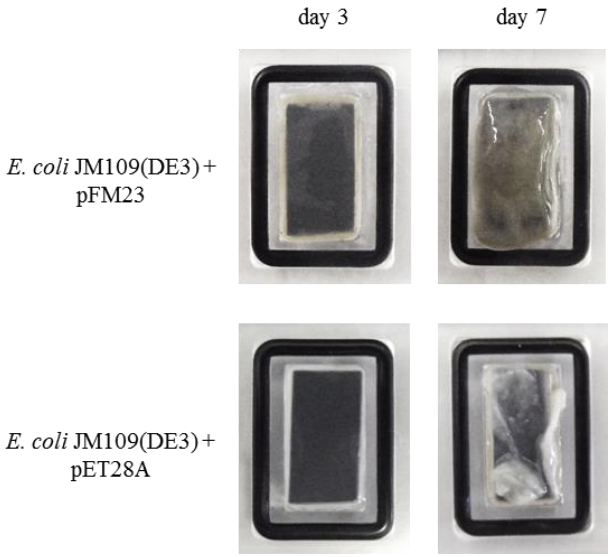

Figure 5.4. Photographs of coupons with wet biofilms formed by both strains (*E. coli* JM109(DE3) + pFM23 and *E. coli* JM109(DE3) + pET28A) on PVC slides after 3 and 7 days of growth.

Figure 5.5 presents the eGFP expression for planktonic and biofilm cells harbouring plasmid pFM23. Specific production in biofilm cells was very high on the first sampling day while biofilm formation had barely started. As the biofilm started to grow, specific production by these cells decreased, attaining a constant value around 5.8 fg cell^{-1} at steady state (from day 7 onwards). Heterologous protein production by planktonic cells remained constant at about 0.18 fg cell^{-1} until the end of the experiment.

Thus, the biofilm environment enhanced specific heterologous protein expression about 30 fold over the planktonic cells in steady state ($P < 0.05$).

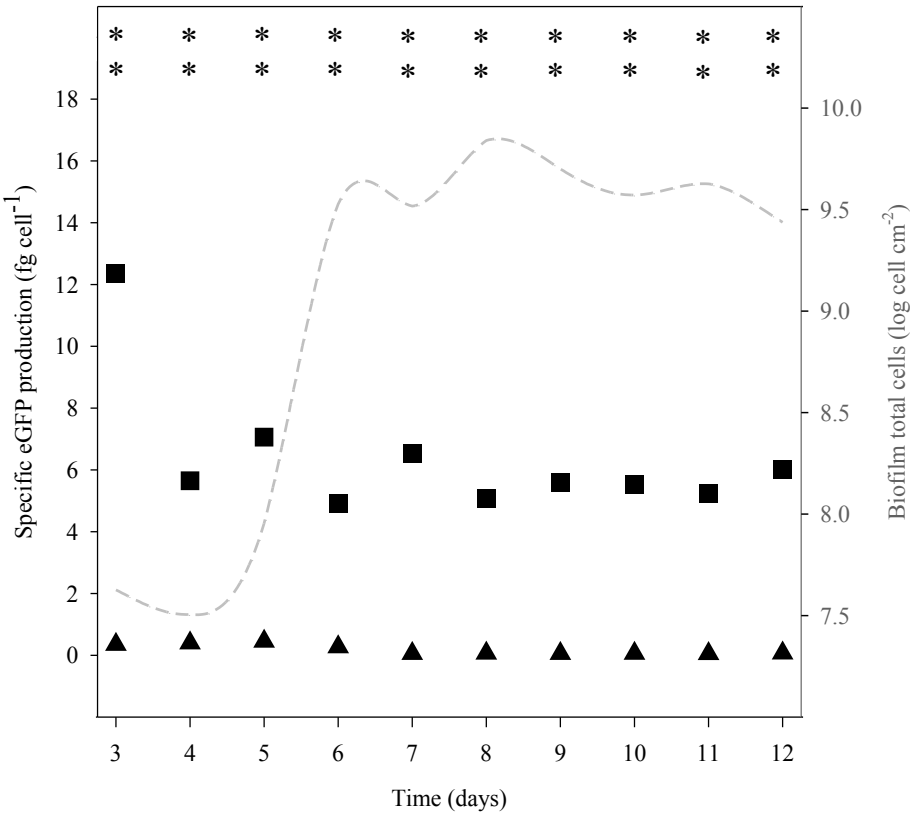

Figure 5.5. Time-course evolution of specific eGFP production for *E. coli* JM109(DE3) + pFM23 in planktonic (▲) and biofilm cells (■). The dotted line represents the evolution of biofilm total cell number assessed by staining with DAPI. Results are an average of three independent experiments. Statistical analysis for the results of specific eGFP production is pointed as * for a confidence level greater than 95% ($P < 0.05$).

The exopolymeric matrix of biofilms formed by both strains was extracted and quantified in terms of protein and polysaccharide content (Table 5.1). Although biofilms formed by the eGFP-producing strain had higher total protein content, the mass percentage of proteins localized at the matrix was similar (28% for the eGFP-producing strain and 25% for the pET28A-bearing strain). The eGFP-producing strain also produced biofilms with more polysaccharides, however the percentage of polysaccharides in the matrix of this biofilm was only 18% when compared to the 53% of the pET28A-bearing strain.

Table 5.1. Characteristics of the biofilm formed by both strains (*E. coli* JM109(DE3) + pFM23 and *E. coli* JM109(DE3) + pET28A) after 7 days of growth

Biofilm characteristics	***E. coli* JM109(DE3) + pFM23**	***E. coli* JM109(DE3) + pET28A**
Biofilm dry weight ($mg_{biofilm}\ cm^{-2}$)	8.00 ± 1.77	5.75 ± 1.06
Log cellular density (cells cm^{-2})	9.09 ± 0.745	7.08 ± 0.155
Total proteins ($mg\ g^{-1}_{biofilm}$)	97.4 ± 10.7	23.9 ± 5.52
Matrix proteins ($mg\ g^{-1}_{biofilm}$)	27.4 ± 2.01	6.09 ± 0.971
Total polysaccharides ($mg\ g^{-1}_{biofilm}$)	104 ± 19.2	24.6 ± 2.96
Matrix polysaccharides ($mg\ g^{-1}_{biofilm}$)	19.2 ± 1.68	13.1 ± 2.37

5.4. Discussion

The main goal of this chapter was to compare the specific production of a model heterologous protein by planktonic and biofilm cells. Additionally, it was important to verify if heterologous protein expression was not detrimental to biofilm development.

Results showed that biofilm production was enhanced for the eGFP-producing strain (assayed by wet weight, thickness and total cell number) when compared to the strain harbouring the pET28A plasmid. It is commonly recognized that different types of plasmids, including conjugative and non-conjugative plasmids, can enhance biofilm production (Ghigo 2001, Huang et al. 1993, Lim et al. 2010b, May & Okabe 2008, Teodósio et al. 2012a). In the present study, the expression of genes for heterologous protein production amplified this effect. Higher glucose consumption values were detected on eGFP-producing cells and this observation is probably a consequence of the metabolic burden triggered by the expression of the heterologous protein. It is documented that the production of stress proteins, elevated respiration rates and high-energy requirements are induced by recombinant protein synthesis (Hoffmann & Rinas 2004, Sørensen & Mortensen 2005). Since stress conditions can favour biofilm formation

(Landini 2009), the increased metabolic burden associated with recombinant protein expression may have stimulated biofilm formation by the eGFP-producing strain.

The cellular density that was possible to attain in steady state with the biofilm flow cell reactor was around 11 g l^{-1}. Although a maximum cellular limit of about 200 g l^{-1} was estimated for HCDC, a cell concentration range between 20 and 190 g l^{-1} has been reported in the expression of several proteins by different strains (Shiloach & Fass 2005). It is possible that the cellular density attained with this flow cell reactor can be increased by optimization of culture conditions such as nutrient level, surface properties and flow hydrodynamics (Moreira et al. 2015b, Teodósio et al. 2011a).

The high-level expression of recombinant proteins in *E. coli* biofilms was first reported by Huang et al. (1993, 1994a, 1995) using a flow cell reactor and a standard chemostat for the production of β-galactosidase. In those works, the authors attained specific productivities in the biofilms that were 25% lower than what they could obtain from the chemostat (Bryers & Huang 1995, Huang et al. 1993). The first report on high-level production of an heterologous protein in *E. coli* biofilms was published much later by O'Connell et al. (2007), who produced eGFP in a chemostat with planktonic cells and in a parallel plate flow reactor with biofilm cells. These authors have detected different populations of strongly producing cells (capable of producing 0.16 g l^{-1} of eGFP), moderately producing cells (with average eGFP productions of 0.01 g l^{-1}) and non-producing cells. In chemostat conditions, the population was equally divided between non-producing cells and moderately producing cells. In the biofilms, after the optimization of antibiotic concentration, the percentage of strongly producing cells reached 60%, whereas non-producing cells were not detected. In our work, the overall eGFP production that was obtained was around 0.22 g l^{-1}, which is 2 fold higher than previously reported (O'Connell et al. 2007). Comparing this production with other reported values for HCDC of *E. coli* cells, it is possible to see that higher production levels (from 4 to 10 g l^{-1}) have been obtain with different proteins, particularly when they are produced as inclusion bodies. For soluble cytoplasmic proteins or secreted proteins, these values drop down to 1 g l^{-1} or below (Choi et al. 2006).

It has been shown that continuous biofilm cultures for heterologous protein production can be beneficial for retention of plasmid-bearing cells when compared to chemostats (O'Connell et al. 2007). One reason is that cells in biofilms tend to grow more slowly than their planktonic counterparts (Williams et al. 1997), leading to fewer divisions and correspondingly less plasmid segregation. In this work, biofilms can be

compared to the quiescent-cell (Q-cell) expression system developed by Rowe & Summers (1999). The Q-cell system generates non-growing but metabolic active *E. coli* cells and since quiescent cells are no longer dividing, their metabolic resources are channelled towards the expression of plasmid-based genes (Chen et al. 2015, Rowe & Summers 1999). Here, slow growing biofilm cells also have a much higher specific production (about 30 fold) than planktonic cells.

Interestingly, the eGFP-producing strain presented higher specific concentrations of proteins and polysaccharides (mg g^{-1} biofilm) in the biofilm than the non-producing strain. It was expected that the biofilm cells from the eGFP-producing strain would use most of the intracellular resources involved in biosynthesis (such as amino acids, nucleotides and metabolic energy) towards heterologous gene expression, thus producing a lower amount of polysaccharides. Recombinant protein production can result in the synthesis of stress proteins at high rates (Hoffmann & Rinas 2004) and it is possible that some of these proteins are involved in adhesion and/or biofilm formation. As observed by Hoffmann & Rinas (2004), eGFP expression together with an increase in the synthesis of stress proteins may account for the higher glucose consumption observed for this strain when compared to the pET28A strain.

Conventional HCDC of planktonic *E. coli* cells presents many advantages over continuous or batch cultivation (Choi et al. 2006). However, this type of cultivation has its own challenges like limitations in oxygen transfer, acetate accumulation as well as the solubility and toxicity of medium components (Shiloach & Fass, 2005). A continuous culture of biofilm cells may be considered as a non-conventional form of HCDC and it is indeed a compromise between operating a continuous system with planktonic cells and a conventional fed-batch HCDC (O'Connell et al. 2007). Although mass transfer limitations also exist in biofilm cultures, the most significant mass transfer resistance occurs inside the biofilm, as external mass transfer limitations can be managed (Moreira et al. 2013a). It has been shown that the density of biofilm cultures (which affects internal mass transfer of nutrients, oxygen and toxic metabolites) can be regulated by careful optimization of the nutrient load and the hydrodynamic shear stress (Teodósio et al. 2011a). It is therefore likely that the volumetric yields that can be obtained during heterologous protein production can also be enhanced by optimization of culture conditions.

Using *E. coli* cells in HCDC is a very attractive way of producing heterologous proteins by improving volumetric productivities and reducing capital investment and operation costs in production facilities. Producing heterologous proteins in biofilm cells

shares some of the challenges of HCDC, but some studies have shown that biofilm cells have a superior producing capacity when compared to their planktonic counterparts. This work shows that *E. coli* biofilm cells can produce a model heterologous protein at much higher levels than planktonic cells and that the cellular densities and volumetric productivities are already within the range of what can be obtained by HCDC, even without optimization of culture conditions. Optimization of these conditions will be performed in the next chapters in order to harness the power of these productive biofilms.

5.5. References

Andersson L, Yang S, Neubauer P, Enfors S-O. 1996. Impact of plasmid presence and induction on cellular responses in fed batch cultures of *Escherichia coli*. J Biotechnol. 46:255-263.

APHA., AWWA., WPCF. 1989. Standard methods for the examination of water and wastewater. American Public Health Association.

Baneyx F. 1999. Recombinant protein expression in *Escherichia coli*. Curr Opin Biotechnol. 10:411-421.

Bentley WE, Mirjalili N, Andersen DC, Davis RH, Kompala DS. 1990. Plasmid-encoded protein: the principal factor in the "metabolic burden" associated with recombinant bacteria. Biotechnol Bioeng. 35:668-681.

Birnbaum S, Bailey JE. 1991. Plasmid presence changes the relative levels of many host cell proteins and ribosome components in recombinant *Escherichia coli*. Biotechnol Bioeng. 37:736-745.

Bryers JD, Huang C-T. 1995. Recombinant plasmid retention and expression in bacterial biofilm cultures. Wat Sci Tech. 31:105-115.

Burmølle M, Bahl MI, Jensen LB, Sørensen SJ, Hansen LH. 2008. Type 3 fimbriae, encoded by the conjugative plasmid pOLA52, enhance biofilm formation and transfer frequencies in Enterobacteriaceae strains. Microbiology. 154:187-195.

Cheah UE, Weigand WA, Stark BC. 1987. Effects of recombinant plasmid size on cellular processes in *Escherichia coli*. Plasmid. 18:127-134.

Chen C-C, Walia R, Mukherjee KJ, Mahalik S, Summers DK. 2015. Indole generates quiescent and metabolically active *Escherichia coli* cultures. Biotechnol J. 10:636-646.

Choi JH, Keum KC, Lee SY. 2006. Production of recombinant proteins by high cell density culture of *Escherichia coli*. Chem Eng Sci. 61:876-885.

DuBois M, Gilles KA, Hamilton JK, Rebers PA, Smith F. 1956. Colorimetric method for determination of sugars and related substances. Anal Chem. 28:350-356.

Glick BR. 1995. Metabolic load and heterologous gene expression. Biotechnol Adv. 13:247-261.

Gomes LC, Silva LN, Simões M, Melo LF, Mergulhão FJ. 2015. *Escherichia coli* adhesion, biofilm development and antibiotic susceptibility on biomedical materials. J Biomed Mater Res A. 103:1414-1423.

Haddadin F, Harcum S. 2005. Transcriptome profiles for high-cell-density recombinant and wild-type *Escherichia coli*. Biotechnol Bioeng. 90:127-153.

Hoffmann F, Rinas U. 2004. Stress Induced by Recombinant Protein Production in *Escherichia coli*. In: Enfors S-O, editor. Physiological Stress Responses in Bioprocesses. Berlin: Springer-Verlag. p. 73-92.

Huang C-T, Peretti SW, Bryers JD. 1993. Plasmid retention and gene expression in suspended and biofilm cultures of recombinant *Escherichia coli* DH5α(pMJR1750). Biotechnol Bioeng. 41:211-220.

Huang C-T, Peretti SW, Bryers JD. 1994a. Effects of inducer levels on a recombinant bacterial biofilm formation and gene expression. Biotechnol Lett. 16:903-908.

Huang C-T, Peretti SW, Bryers JD. 1994b. Effects of medium carbon-to-nitrogen ratio on biofilm formation and plasmid stability. Biotechnol Bioeng. 44:329-336.

Król JE, Nguyen HD, Rogers LM, Beyenal H, Krone SM, Top EM. 2011. Increased transfer of a multidrug resistance plasmid in *Escherichia coli* biofilms at the air-liquid interface. Appl Environ Microbiol. 77:5079-5088.

Landini P. 2009. Cross-talk mechanisms in biofilm formation and responses to environmental and physiological stress in *Escherichia coli*. Res Microbiol. 160:259-266.

Lim JY, La HJ, Sheng H, Forney LJ, Hovde CJ. 2010b. Influence of plasmid pO157 on *Escherichia coli* O157:H7 Sakai biofilm formation. Appl Environ Microbiol. 76:963-966.

May T, Okabe S. 2008. *Escherichia coli* harboring a natural IncF conjugative F plasmid develops complex mature biofilms by stimulating synthesis of colanic acid and curli. J Bacteriol. 190:7479-7490.

Mergulhão FJ, Monteiro GA. 2007. Analysis of factors affecting the periplasmic production of recombinant proteins in *Escherichia coli*. J Microbiol Biotechnol. 17:1236–1241.

Mergulhão FJM, Taipa MA, Cabral JMS, Monteiro GA. 2004a. Evaluation of bottlenecks in proinsulin secretion by *Escherichia coli*. J Biotechnol. 109:31-43.

Mergulhão FJM, Summers DK, Monteiro GA. 2005. Recombinant protein secretion in *Escherichia coli*. Biotechnol Adv. 23:177-202.

Mergulhão FJM, Monteiro GA, Cabral JMS, Taipa MA. 2004b. Design of bacterial vector systems for the production of recombinant proteins in *Escherichia coli*. J Microbiol Biotechnol. 14:1-14.

Moreira JMR, Gomes LC, Simões M, Melo LF, Mergulhão FJ. 2015b. The impact of material properties, nutrient load and shear stress on biofouling in food industries. Food Bioprod Process. 95:228-236.

Moreira JMR, Simões M, Melo LF, Mergulhão FJ. 2015a. The combined effects of shear stress and mass transfer on the balance between biofilm and suspended cell dynamics. Desal Water Treat. 53:3348-3354.

Moreira JMR, Teodósio JS, Silva FC, Simões M, Melo LF, Mergulhão FJ. 2013a. Influence of flow rate variation on the development of *Escherichia coli* biofilms. Bioprocess Biosyst Eng. 36:1787-1796.

Neidhardt FC. 1996. *Escherichia coli* and Salmonella: Cellular and Molecular Biology. 2nd edition. Washington: ASM Press.

Norman A, Hansen LH, She Q, Sørensen SJ. 2008. Nucleotide sequence of pOLA52: a conjugative IncX1 plasmid from *Escherichia coli* which enables biofilm formation and multidrug efflux. Plasmid. 60:59-74.

Novagen. 2005. pET system manual. 11th edition.

O'Connell HA, Niu C, Gilbert ES. 2007. Enhanced high copy number plasmid maintenance and heterologous protein production in an *Escherichia coli* biofilm. Biotechnol Bioeng. 97:439-446.

Ow D, Nissom P, Philp R, Oh S, Yap M. 2006. Global transcriptional analysis of metabolic burden due to plasmid maintenance in *Escherichia coli* DH5α during batch fermentation. Enzyme Microb Technol. 39:391-398.

Pines O, Inouye M. 1999. Expression and secretion of proteins in *E. coli*. Mol. Biotechnol. 12:25-34.

Reisner A, Höller BM, Molin S, Zechner EL. 2006. Synergistic effects in mixed *Escherichia coli* biofilms: conjugative plasmid transfer drives biofilm expansion. J Bacteriol. 188:3582-3588.

Rowe DC, Summers DK. 1999. The quiescent-cell expression system for protein synthesis in *Escherichia coli*. Appl Environ Microbiol. 65:2710-2715.

Saby S, Sibille I, Mathieu L, Paquin JL, Block JC. 1997. Influence of water chlorination on the counting of bacteria with DAPI (4',6-diamidino-2-phenylindole). Appl Environ Microbiol. 63:1564-1569.

Sambrook J, Russell DW editors. 2001. Molecular Cloning: a Laboratory Manual. 3rd edition. New York: Cold Spring Harbor Laboratory Press.

Sanchez-Garcia L, Martín L, Mangues R, Ferrer-Miralles N, Vázquez E, Villaverde A. 2016. Recombinant pharmaceuticals from microbial cells: a 2015 update. Microb Cell Fact. 15:1-7.

Simões M, Pereira MO, Sillankorva S, Azeredo J, Vieira MJ. 2007. The effect of hydrodynamic conditions on the phenotype of *Pseudomonas fluorescens* biofilms. Biofouling. 23:249-258.

Shiloach J, Fass R. 2005. Growing *E. coli* to high cell density - a historical perspective on method development. Biotechnol Adv. 23:345-357.

Sørensen HP, Mortensen KK. 2005. Advanced genetic strategies for recombinant protein expression in *Escherichia coli*. J Biotechnol. 115:113-128.

Stewart PS. 2003. Diffusion in biofilms. J Bacteriol. 185:1485-1491.

Stewart PS, Franklin MJ. 2008. Physiological heterogeneity in biofilms. Nat Rev Micro. 6:199-210.

Teodósio JS, Simões M, Mergulhão FJ. 2012a. The influence of nonconjugative *Escherichia coli* plasmids on biofilm formation and resistance. J Appl Microbiol. 113:373-382.

Teodósio JS, Simões M, Melo LF, Mergulhão FJ. 2011a. Flow cell hydrodynamics and their effects on *E. coli* biofilm formation under different nutrient conditions and turbulent flow. Biofouling. 27:1-11.

Williams I, Venables WA, Lloyd D, Paul F, Critchley I. 1997. The effects of adherence to silicone surfaces on antibiotic susceptibility in *Staphylococcus aureus*. Microbiology. 143:2407-2413.

Yang X, Ma Q, Wood TK. 2008. The R1 conjugative plasmid increases *Escherichia coli* biofilm formation through an envelope stress response. Appl Environ Microbiol. 74:2690-2699.

Yang Y-X, Qian Z-G, Zhong J-J, Xia X-X. 2016. Hyper-production of large proteins of spider dragline silk MaSp2 by *Escherichia coli* via synthetic biology approach. Process Biochem. 51:484-490.

Yanisch-Perron C, Vieira J, Messing J. 1985. Improved M13 phage cloning vectors and host strains: nucleotide sequences of the M13mpl8 and pUC19 vectors. Gene. 33:103-119.

Yu H, Shi Y, Sun X, Luo H, Shen Z. 2003. Effect of poly(β-hydroxybutyrate) accumulation on the stability of a recombinant plasmid in *Escherichia coli*. J Biosci Bioeng. 96:179-183.

6.

Effects of antibiotic concentration and nutrient medium composition on *E. coli* biofilm formation and GFP expression[e]

Abstract

Heterologous protein production from biofilm cells is dependent on many factors, including the composition of the culture medium. The aim of this study was to analyse the influence of two factors - the concentration of antibiotic used to maintain the selective pressure and the nutrient medium composition. *E. coli* JM109(DE3) cells transformed with plasmid pFM23 for eGFP expression and containing a kanamycin resistance gene were used. The 96-well microtiter plate was chosen for the initial screening of kanamycin concentration due to the high throughput of this biofilm formation platform. Then, a flow cell system was used to expose the *E. coli* cells to two kanamycin concentrations (20 or 30 μg ml^{-1}) during biofilm growth in two different culture media, a diluted medium (DM) or the lysogeny broth (LB).

A higher antibiotic concentration increased the specific eGFP production in planktonic cells, whereas no increase was detected in biofilm cells. Biofilm formation was increased in DM when compared to LB. Nevertheless, bacteria grown in LB had higher eGFP production than those grown in DM in both planktonic and sessile states (20

[e] The content of this chapter was adapted from the following publication(s):

Gomes LC, Mergulhão FJ. Effects of antibiotic concentration and nutrient medium composition on *Escherichia coli* biofilm formation and GFP expression. FEMS Microbiol Lett (submitted).

fold and 2 fold, respectively). Thus, among the conditions tested, LB supplemented with 20 μg ml^{-1} kanamycin is the most advantageous medium to obtain the highest specific eGFP production in biofilm cells.

6.1. Introduction

E. coli plasmids have been traditionally used as vectors for recombinant protein expression (Mergulhão et al. 2004b). Engineered plasmids are often lost in culture (Summers 1998) and therefore it is essential to impose a selective pressure to ensure plasmid stability, which is often achieved by adding antibiotics to the culture medium (Vandermeulen et al. 2011).

In suspended cultures, it is well documented that plasmids impose a metabolic burden on the host cell due to plasmid replication and consumption of precursor metabolites (Bentley et al. 1990, Glick 1995), being the expression of antibiotic resistance genes a major cause for this metabolic burden (Cunningham et al. 2009). In this case, the resistance agent is often an enzyme that will act upon reducing or eliminating the antibiotic activity. Therefore, protein synthesis is involved and precursors such as amino acids and energy are consumed. Studies involving non-expressing plasmids showed that the marker protein can represent up to 20% of total cellular protein (Birnbaum & Bailey 1991, Rozkov et al. 2004), which greatly exceeds the levels required for proper plasmid maintenance and selection. It has been reported that an *E. coli* strain expressing β-lactamase at a level of about 10% of total protein can suffer from a decrease in its maximum specific growth rate of about 40% (Birnbaum & Bailey 1991). Rozkov et al. (2004) concluded that the increased ATP synthesis requirements (24%) observed in *E. coli* DH1 cells containing a plasmid were also due to the expression of the kanamycin resistance gene, whose product accounted for 18% of the total cellular protein in plasmid-bearing cells.

Most publications addressing the metabolic load of plasmids were performed in planktonic conditions. However, since biofilm cells can have higher recombinant production levels than planktonic cells, it is interesting to explore the capabilities of the biofilm environment in recombinant bioprocesses. Concerning the particular effect of antibiotic markers, it is known that they can affect bacterial biofilm formation (Bagge et

al. 2004, Gallant et al. 2005, May et al. 2009, Teh et al. 2014). Some studies refer that the presence of the β-lactamase gene on a plasmid can reduce the amount of biofilm formed by *E. coli*, while the presence of other antibiotic resistance genes may not impair biofilm formation (Bagge et al. 2004, Gallant et al. 2005). May et al. (2009) found that marker genes on plasmids may play an important role in both biofilm formation and resistance of sessile cells to antibiotics, as they can trigger specific chromosomal resistance mechanisms that confer a high-level resistance during biofilm formation. The antibiotic marker also affects recombinant protein production due to its contribution to plasmid stability since maintaining a high concentration of plasmid-bearing cells may favour expression (Marini et al. 2014). An interesting work of Panayotatos (1988) demonstrated that by altering the promoter of the kanamycin resistance gene (*Kan*R), the synthesis of KanR protein was greatly reduced to the minimum required for host selection and, at the same time, the recombinant protein production was increased up to 2 fold.

Another important variable in both biofilm formation and recombinant protein expression is the nutrient composition of the culture medium. Several papers have been published during the last years concerning the effect of nutrient levels on biofilm formation (Frias et al. 2001, Gomes et al. 2014, Peyton 1996, Teodósio et al. 2011a). Some authors suggested that an increase in nutrient concentration enhances biofilm growth (Frias et al. 2001, Peyton 1996, Rochex & Lebeault 2007), while others have shown that a high nutrient media can inhibit biofilm formation (Dewanti & Wong 1995, Eboigbodin et al. 2007, Jackson et al. 2002). Regarding recombinant protein expression in suspended cultures, it was found that protein expression levels are dependent on the nutrient composition of the culture medium (Broedel et al. 2001). Although minimal media may sometimes be less expensive than complex media, the use of defined minimal media can lead to lower cell growth rates and product yields if the composition is sub-optimal (Donovan et al. 1996). On the other hand, when cells are grown on glucose as a carbon source, harmful by-products may also accumulate, thereby inhibiting cell growth and recombinant protein production (Chou et al. 1994). Furthermore, culture media may influence plasmid segregational stability (Goyal et al. 2009, Matsui et al. 1990, O'Kennedy & Patching 1997). Indeed, some authors argue that the use of complex nitrogen sources such as yeast extract or tryptone may result in increased plasmid stability (Matsui et al. 1990).

The challenges faced during the production of plasmid-derived recombinant proteins are to achieve the maximum yield of product using minimum resources. Thus, it

is important to understand the influence of culture conditions such as the antibiotic concentration and nutrient medium composition on the expression of heterologous proteins in *E. coli* biofilms. For this purpose, *E. coli* JM109(DE3) cells harbouring the plasmid pFM23 (expression vector for eGFP) was used. This vector contains a kanamycin resistance gene and bacterial cells were exposed to different concentrations of this antibiotic during biofilm development in different culture media.

6.2. Materials and methods

6.2.1. Bacterial strain

E. coli JM109(DE3) cells containing the plasmid pFM23 for the cytoplasmic production of eGFP were used (Mergulhão & Monteiro 2007).

6.2.2. High throughput screening of antibiotic concentration

An overnight culture of the *E. coli* strain was obtained as indicated in Chapter 3, section 3.2.2. Cells were then harvested by centrifugation and appropriate dilution in sterile saline was performed to obtain an OD of approximately 0.4 at 610 nm.

Eight kanamycin concentrations in the range of 0-100 μg ml^{-1} were tested for biofilm formation and eGFP expression in the 96-well microtiter plate. The wells (6 for each kanamycin concentration tested) were filled with 180 μl of DM (composition described in Chapter 5, section 5.2.1) containing the appropriate kanamycin amount, and inoculated with 20 μl of the inoculum previously prepared. For control, wells were inoculated with *E. coli* JM109(DE3) cells bearing the plasmid pET28A (Novagen, USA), which is the backbone of pFM23. Plates were incubated at 30 ºC for 24 h under the shaking conditions used for biofilm formation in Chapter 4 (section 4.2.2), i.e., an orbital diameter of 50 mm at 150 rpm. Then, the bacterial suspension was discarded and all the wells were washed to remove nonadherent cells. The biofilms were resuspended in 200 μl of Buffer I (50 mM Na_2HPO_4, 300 mM NaCl, pH 8) by pipetting up and down, and the OD was first measured using a microtiter plate reader (SpectraMax M2E, Molecular

Devices, USA). Then, the fluorescence was determined with the excitation filter of 488 nm and the emission filter of 507 nm. Three independent experiments were performed.

6.2.3. Biofilm formation system and experimental conditions

The kanamycin concentrations which have shown the most effective impact on biofilm formation and heterologous protein expression in the microtiter plate assay were chosen to be tested in the flow cell system described in Chapter 5, section 5.2.2. Thus, this biofilm platform was operated for 12 days with DM containing either 20 or 30 μg ml^{-1} kanamycin (Eurobio, France). This was the first culture medium to be tested since this *E. coli* strain previously demonstrated a good biofilm formation capacity in the same growth medium and biofilm reactor (Teodósio et al. 2012a, Teodósio et al. 2011a). The other medium tested for biofilm formation and eGFP production was LB supplemented with 20 μg ml^{-1} kanamycin. This commercial medium is composed of 10 g l^{-1} tryptone, 5 g l^{-1} yeast extract and 10 g l^{-1} NaCl (LB-Miller, Sigma, USA) and it is commonly used for recombinant protein expression with the pET system (Novagen 2005).

6.2.4. Analytical methods

On each experimental day, a coupon was removed from the flow cell and biofilm wet weight was quantified as indicated in Chapter 5, section 5.2.3. Biofilm thickness was also determined using a digital micrometer and afterwards the biofilm was resuspended and homogenized in NaCl solution for cell quantification. The biofilm culturability (log CFU cm^{-2}) was determined as described in Chapter 5, section 5.2.3. Biofilm total cells (viable plus non-viable) were assessed using the Live/Dead® *Bac*Light™ bacterial viability kit (Syto9/PI, Invitrogen Life Technologies, Alfagene, Portugal). Bacterial observations were performed after 10 min incubation with the fluorescent dyes in the dark (Gomes et al. 2015) using a Leica DM LB2 epifluorescence microscope connected to a Leica DFC300 FX camera (Leica Microsystems Ltd, Switzerland). The optical filter combination for optimal viewing of the stained preparations consisted of a 515-560-nm excitation filter combined with a dichromatic mirror at 580 nm and suppression filter at 590 nm. For capturing images, Leica IM50 Image Manager, Image Processing and Archiving software was used. Green cells labelled with Syto9 and red cells labelled with

PI were estimated on each membrane from counts of a minimum of 20 fields of view. Both types of cells were automatically quantified using the image processing software ImageJ v1.48 (NIH, USA). After background subtraction, the green and red cells were segmented and counted, and the results were expressed as log cell cm^{-2}.

The eGFP expression in biofilm cells was analysed as described in Chapter 5, section 5.2.4, and the final values were presented as specific eGFP production (fg $cell^{-1}$).

For planktonic cells, OD at 610 nm, cell number (log CFU ml^{-1}) and specific eGFP production (fg $cell^{-1}$) were assessed.

For the experiments with DM, glucose consumption in the whole system was determined as indicated in Chapter 5, section 5.2.3.

6.2.5. Quantification of EPS

The content of EPS found in biofilms (proteins and polysaccharides) was assessed for both DM and LB media supplemented with 20 µg ml^{-1} kanamycin after 7 days of growth. Matrix proteins and polysaccharides from biofilms were separated from the cells as described in Chapter 5, section 5.2.5, and determined using the BCA™ Protein Assay Kit (Thermo Fisher Scientific, USA) and the phenol-sulphuric acid method of DuBois et al. (1956), respectively. The final values were calculated taking into account the biofilm dry weight.

6.2.6. Calculations and statistical analysis

The results presented in Table 6.2 and Figures 6.2 to 6.4 originated from averages of triplicate sets obtained in three independent experiments for each culture condition (DM with 20 or 30 µg ml^{-1} kanamycin and LB with 20 µg ml^{-1} kanamycin). The results shown in Table 6.1 resulted from averages of eGFP production values obtained between days 7 and 12 (steady state) and presented as individual time points in panels (E) and (F) of Figures 6.2 and 6.4.

The following average SDs were obtained for all planktonic and biofilm parameters (Figures 6.2 and 6.4): SD < 15% for OD, SD < 32% for biofilm wet weight, SD < 7% for planktonic and biofilm cells, SD < 11% for planktonic and biofilm eGFP production, SD < 12% for glucose consumption and SD < 33% for biofilm thickness.

Paired *t*-test analysis was performed based on a confidence level of 90% (differences reported as significant for *P* values < 0.1) and 95% (differences reported as significant for *P* values < 0.05).

6.3. Results

6.3.1. High throughput screening of antibiotic concentration

The screening of the most relevant kanamycin concentrations affecting *E. coli* biofilm formation and eGFP expression was performed in agitated 96-well microtiter plates as this is a high throughput platform, unlike the flow cell system. Although it has been shown in Chapter 3 that the agitated microtiter plate does not reach the same average shear stress value obtained in the flow cell reactor, it is expected that the trends obtained with the 96-well microtiter plates are maintained in the flow cell.

The results obtained from the microtiter plate assays are plotted in Figure 6.1. It can be observed that there was a gradual decrease in the amount of biofilm formed from the concentration of 20 μg ml^{-1} onwards ($P < 0.05$, Figure 6.1A). Conversely, the eGFP fluorescence in the biofilm was similar to that verified in the absence of antibiotic until the concentration of 20 μg ml^{-1} ($P > 0.05$, Figure 6.1A), but an increase in eGFP production of approximately 50% was observed for the higher concentrations of kanamycin ($P < 0.05$, Figure 6.1B). Taking these results into account, it is interesting to test the antibiotic concentrations of 20 and 30 μg ml^{-1} kanamycin as they represent turning points in terms of biofilm formation and also specific eGFP production.

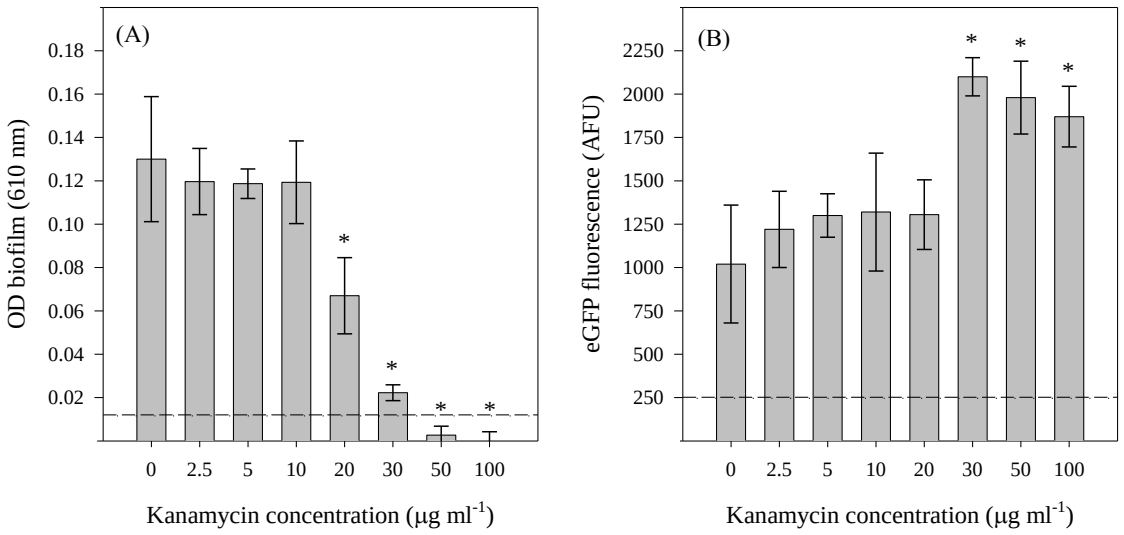

Figure 6.1. Screening of kanamycin concentration in 96-well microtiter plates: (A) biofilm growth and (B) eGFP fluorescence. The means ± SDs for three independent experiments are presented. ∗ indicates values that are significantly different (for a confidence level greater than 95%, $P < 0.05$) from the value of the same strain exposed to no antibiotic. The dashed lines correspond to the detection limits of the methods.

6.3.2. Effect of antibiotic concentration on biofilm formation and eGFP expression

The effect of antibiotic concentration on the dynamics of *E. coli* biofilm formation and eGFP expression in the flow cell reactor is presented in Figure 6.2, where two concentrations of kanamycin (20 and 30 μg ml^{-1}) in DM are compared.

The analysis of planktonic condition (Figures 6.2A and C) indicates that there were few differences in *E. coli* growth for both antibiotic concentrations ($P < 0.05$ for only 4 of 20 experimental points). The concentration of planktonic cells increased until day 5 and then decreased until the end of the experiment. The number of culturable biofilm cells (Figure 6.2D) was also similar in both antibiotic concentrations ($P < 0.05$ for only 2 of 10 experimental points). Regarding the biofilm wet weight and thickness measurements (Figures 6.2B and H), there was a strong increase (of about 85%) between days 3 and 8, and a sharp decrease after day 8 for the highest antibiotic concentration. In this later case, biofilm detachment may have occurred, as confirmed by a decrease in the total cell numbers (Figure 6.3).

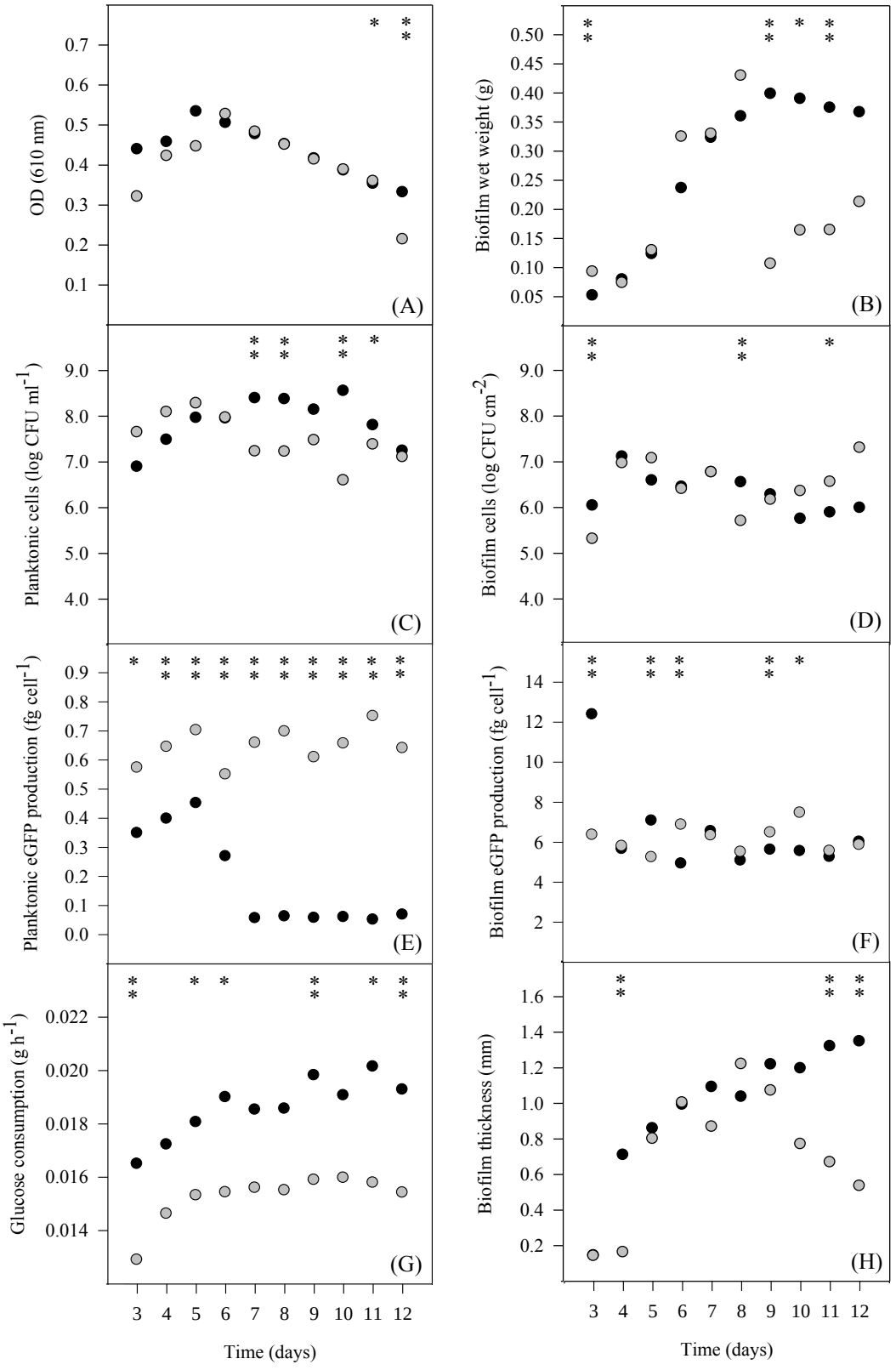

Figure 6.2. Time-course of planktonic and biofilm parameters in DM: (A) OD in the recirculating tank, (B) biofilm wet weight, (C) planktonic cells, (D) biofilm cells, (E) planktonic specific eGFP production, (F) biofilm specific eGFP production, (G) glucose consumption in the system, (H) biofilm thickness. Kanamycin concentration of 20 µg ml^{-1} (●) and 30 µg ml^{-1} (◍). Results are an average of three independent

experiments for each condition. Statistical analysis corresponding to each time point is represented with $*$ for a confidence level greater than 90% ($P < 0.1$) and with $\overset{*}{*}$ for a confidence level greater than 95% ($P < 0.05$).

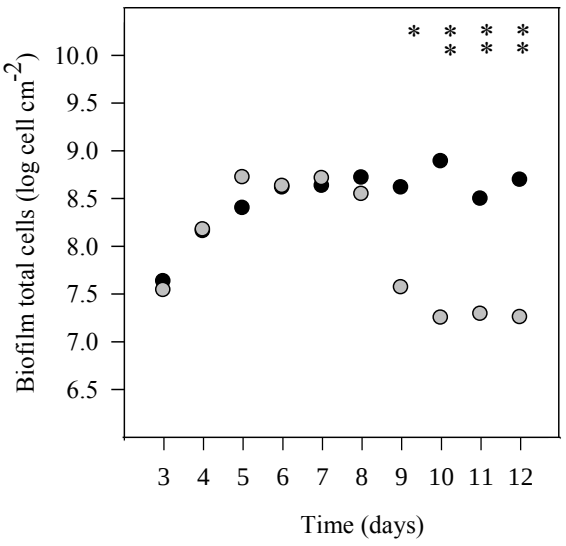

Figure 6.3. Time-course evolution of biofilm total cells in DM with 20 µg ml^{-1} (●) and 30 µg ml^{-1} of kanamycin concentration (○). Total cell counts (viable plus non-viable cells) were assessed with the live/dead staining for three independent experiments for each condition. Statistical analysis corresponding to each time point is represented with $*$ for a confidence level greater than 90% ($P < 0.1$) and with $\overset{*}{*}$ for a confidence level greater than 95% ($P < 0.05$).

Heterologous eGFP production in planktonic cells (Figure 6.2E) was higher for the highest antibiotic concentration ($P < 0.05$) and an average production value of 0.7 fg cell^{-1} was reached in this condition. For the lowest kanamycin concentration, the specific production was reduced 10 fold after day 5 (Figure 6.2E). For biofilm cells (Figure 6.2F), specific recombinant protein production was similar in both antibiotic concentrations and average values around 6 fg cell^{-1} were obtained.

Figure 6.2G presents the glucose consumption profiles in the whole system (suspended plus biofilm cells). Higher glucose consumption values (on average 18%) were obtained in DM containing 20 µg ml^{-1} kanamycin, with statistically significant differences in most experimental points ($P < 0.05$ and $P < 0.1$).

6.3.3. Effect of nutrient medium composition on biofilm formation and eGFP expression

Since the variation in antibiotic concentration had no effect on the specific eGFP production in biofilm cells of the flow cell system, a different medium (LB) was tested since it is widely used in recombinant protein expression studies. This medium was supplemented with the lowest concentration of kanamycin tested (20 μg ml^{-1}) in order to maintain the selective pressure without increasing the use of antibiotic in the bioprocess.

Comparing the DM with LB, higher optical density values (on average 33%) were always registered for LB ($P < 0.05$ and $P < 0.1$) (Figure 6.4A). The concentration of culturable planktonic cells (Figure 6.4C) was quite similar for both growth media and throughout the experiment. For biofilm cells (Figure 6.4D), a higher number of culturable cells was obtained in DM in most experimental points ($P < 0.05$ and $P < 0.1$). Biofilm wet weight (Figure 6.4B) was also higher in DM, whereas in LB the biofilm reached a constant value of about 0.08 g (5 fold lower than the average value obtained in DM after day 7). The evolution of biofilm thickness (Figure 6.4G) was similar to the wet weight and a 10 fold difference was obtained between DM and LB.

By analysing the specific eGFP production (Figures 6.4E and F), it can be seen that cells grown in LB produced more eGFP than those grown in DM in both planktonic and sessile states. When the flow cell system was in steady state (between days 7 and 12), the biofilm expression was 2 fold higher than in DM (Table 6.1). In LB medium and in DM supplemented with 30 μg ml^{-1} of kanamycin, specific eGFP production from biofilm cells was on average 10 fold higher than in planktonic cells. In DM supplemented with 20 μg ml^{-1} of kanamycin, a 95 fold higher production was obtained in biofilm cells when compared to their planktonic counterparts (Table 6.1).

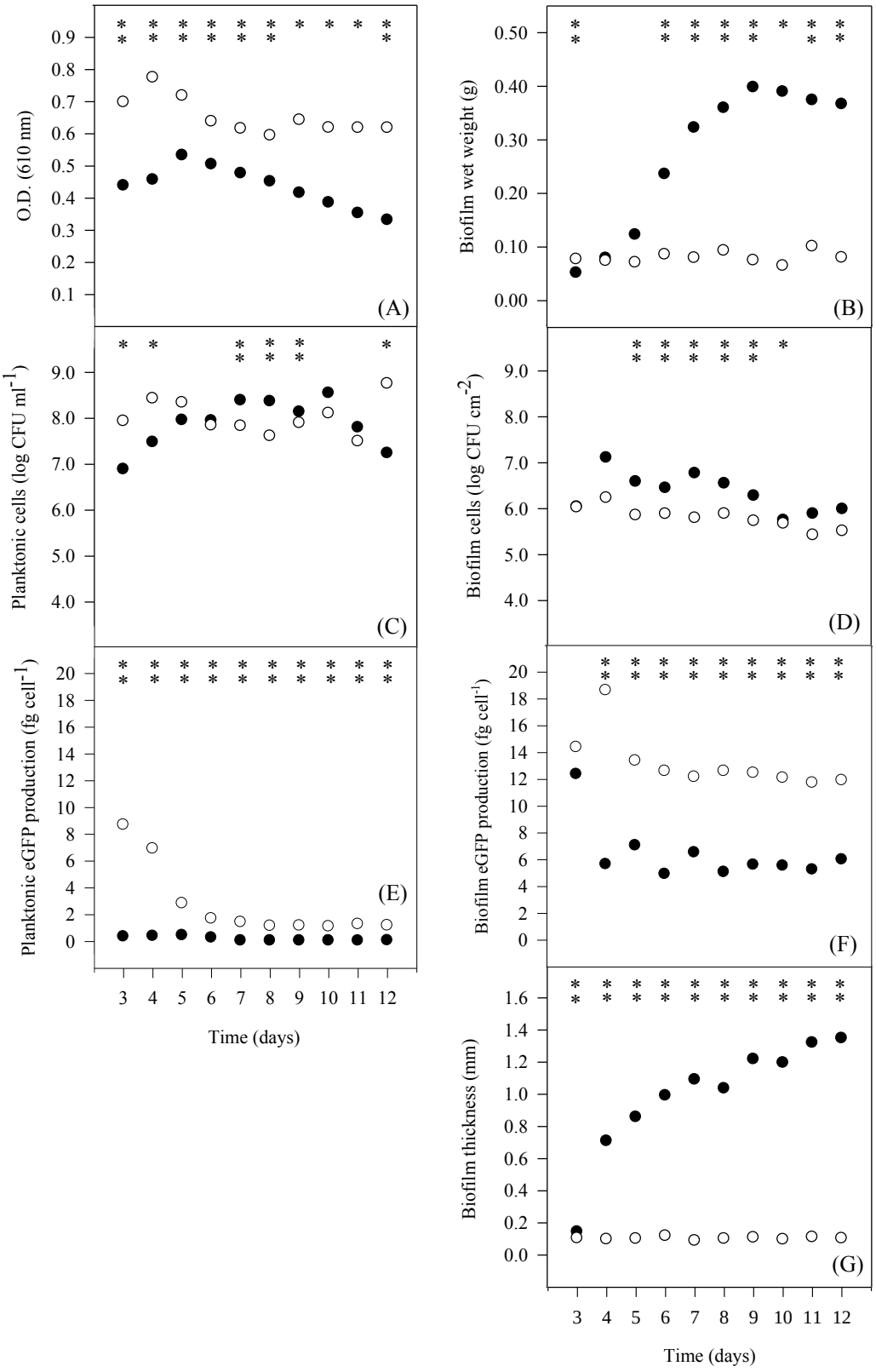

Figure 6.4. Time-course of planktonic and biofilm parameters: (A) optical density in the recirculating tank, (B) biofilm wet weight, (C) planktonic cells, (D) biofilm cells, (E) planktonic specific eGFP production, (F) biofilm specific eGFP production, (G) biofilm thickness. DM with 20 µg ml^{-1} kanamycin (●), LB with

20 μg ml^{-1} kanamycin (○). Results are an average of three independent experiments for each condition. Statistical analysis corresponding to each time point is represented with ∗ for a confidence level greater than 90% ($P < 0.1$) and with ∗∗ for a confidence level greater than 95% ($P < 0.05$).

Table 6.1. Specific eGFP production for planktonic and biofilm conditions in different growth media: DM with 20 and 30 μg ml^{-1} kanamycin and LB with 20 μg ml^{-1} kanamycin. The results presented were obtained under steady state (between days 7 and 12)

Medium	**Kanamycin concentration (μg ml^{-1})**	**Specific eGFP production (fg cell^{-1})**	
		Planktonic	Biofilm
DM	20	0.060	5.7
DM	30	0.67	6.2
LB	20	1.2	12

The influence of growth medium composition on EPS production of biofilms was also assessed (Table 6.2). It is interesting to observe that the matrix of *E. coli* biofilms formed in LB medium with 20 μg ml^{-1} kanamycin had a lower protein content (about 3 fold) compared to the biofilms developed in DM containing the same antibiotic concentration. On the contrary, the amount of matrix polysaccharides produced in LB was about 12 fold higher than in DM.

Table 6.2. Analysis of 7-day-old biofilms formed in DM and LB with 20 μg ml^{-1} kanamycin

Biofilm characteristics	**DM**	**LB**
Biofilm dry weight ($mg_{biofilm}$ cm^{-2})	8.00 ± 1.77	4.50 ± 0.870
Log cellular density (cells cm^{-2})	9.09 ± 0.740	7.76 ± 0.460
Matrix proteins (mg g$^{-1}_{biofilm}$)	27.4 ± 2.01	9.40 ± 1.70
Matrix polysaccharides (mg g$^{-1}_{biofilm}$)	19.2 ± 1.68	231 ± 35.0

6.4. Discussion

E. coli is a very interesting microorganism to study the biofilm development in environmental (Sambrook & Russell 2001), biomedical (Novagen 2005) and industrial settings (Perry & Green 1997). It is also one of the favourite hosts for recombinant protein production (Sanchez-Garcia et al. 2016) and in this case several variables, like the antibiotic concentration and the nutrient medium composition, are extremely important (Mergulhão et al. 2004b, Rosano & Ceccarelli 2014).

The screening assay for antibiotic concentration was conducted in agitated 96-well microtiter plates taking advantage of the high throughput of this platform. Two kanamycin concentrations - 20 and 30 μg ml^{-1} - were identified as the most important ones to test in the flow system. Furthermore, these concentrations are in the range recommended for selection of plasmids containing the kanamycin resistance gene (Sambrook & Russell 2001) and correspond to subinhibitory concentrations. In particular, 30 μg ml^{-1} kanamycin is the working concentration indicated for plasmids derived from pET vectors (Carapuça et al. 2007, Novagen 2005) and 20 μg ml^{-1} kanamycin, besides being a lower concentration and thus more suitable to reduce the risk of antibiotic resistance spread, maintains the stability of plasmid pFM23 in the flow cell system. In fact, the number of CFU on selective plates containing 20 μg ml^{-1} kanamycin was similar to that of nonselective plates (not shown).

In the flow cell system, when the antibiotic concentration was changed from 20 to 30 μg ml^{-1}, there was no change in the growth curves of planktonic cells. Identical results were reported by Marini et al. (2014), who studied the effect of kanamycin (in 10-50 μg ml^{-1} concentration range) on *E. coli* cell growth during the expression of recombinant pneumolysin. In the present work, the number of biofilm cells was also similar in both antibiotic conditions during most of the assay, although biofilm detachment occurred at a later stage for the highest antibiotic concentration.

It has been reported that subinhibitory concentrations of aminoglycoside antibiotics, such as kanamycin, can induce biofilm formation by Gram-negative bacteria (Boehm et al. 2009, Hoffman et al. 2005, Jones et al. 2013) and that these antibiotics may be used as signalling molecules rather than toxic compounds (Linares et al. 2006). An increase in biofilm formation was not observed in the current study when the antibiotic concentration was increased.

In the flow cell system, increasing the antibiotic concentration increased the specific eGFP production from planktonic cells, whereas no comparable benefit was detected in biofilm cells. It is possible that mass transfer limitations within the biofilm may have created a microenvironment where the effective antibiotic concentration was similar inside the biofilm for different bulk liquid concentrations (Stewart 2003). Planktonic cells are not subjected to this type of mass transfer limitations (Moreira et al. 2015a) and therefore the increase in kanamycin concentration may have exerted a higher selective pressure on these cells, which may have increased plasmid copy numbers and thus the production of recombinant protein. Yazdani & Mukherjee (2002) conducted continuous cultures for the expression of recombinant streptokinase in *E. coli* and showed that increasing the selective pressure by using high dosage of antibiotic concentration helped to increase the plasmid stability. Previously, Frenkel & Bremel (1986) also reported that high concentrations of chloramphenicol induced higher plasmid yields in minimal medium for an *E. coli* strain containing plasmid pBR322. To the best of our knowledge, the only work about the effect of antibiotic concentration in heterologous protein production in biofilms was published by O'Connell et al. (2007). Contrary to our findings, these authors showed that low concentrations of antibiotic enhanced protein production in *E. coli* biofilms developed in a flow cell reactor. These conflicting results seem to indicate that the profile of plasmid stability and heterologous protein expression is different for different host-vector systems.

Lower glucose consumption was detected in the medium containing the highest kanamycin concentration, which was also the medium where a higher eGFP concentration was found in planktonic cells. It is thought that these two phenomena may be related since a substantial decrease in the ribosome content can occur when *E. coli* cells accumulate higher amounts of gratuitous proteins (Dong et al. 1995). A degradation of rRNA may have decreased the biosynthetic capacity of the cells, with a consequent reduction in substrate consumption.

Using LB instead of DM favoured planktonic growth as indicated by the higher values of culture OD. LB contains higher levels of peptone and yeast extract, which often lead to higher cell culture densities (Studier 2005, Teodósio et al. 2011a).

Higher specific eGFP production was obtained in LB for both planktonic and biofilm conditions. Matsui et al. (1990) reported that the use of complex nitrogen sources such as tryptone and yeast extract found in LB resulted in higher plasmid stability. Furthermore, LB is a complex medium that provides an abundance of amino acids to

support the protein expression in *E. coli* (Donovan et al. 1996). On the other hand, it was reported that the addition of yeast extract increases the non-induced background expression from the *lac* promoter (Doran et al. 1990, Solaiman & Somkuti 1991). In the expression system used in this work, the *eGFP* gene is transcribed by the T7 RNAP whose expression is controlled by the *lac* promoter. It is foreseeable that if yeast extract induces T7 expression from the chromosome, a stronger transcription of the *eGFP* gene may occur and thus higher expression levels can be obtained.

Besides enhancing the specific production of eGFP, *E. coli* biofilms grown in LB also presented lower concentration of proteins within the extracellular matrix than the biofilms formed in DM. This observation is probably a consequence of the channelling of more resources normally involved in EPS-associated protein synthesis (such as amino acids, nucleotides and metabolic energy) towards the recombinant protein expression. In the expression system used in this thesis, the T7 RNAP is much more active than the *E. coli* RNAP (Studier & Moffatt 1986), which means that the expression of the *eGFP* gene under the control of T7 promoter will occur at a very high level. Additionally, the T7 RNAP is highly selective for its own promoter, so a small amount of T7 RNA polymerase is sufficient to direct high-level transcription from a T7 promoter in a multicopy plasmid (Studier & Moffatt 1986, Terpe 2006). Moreover, the half-time of the mRNA produced by T7 RNA polymerase is higher than the host mRNA because of its great length and/or stem-and-loop structures at 3' ends that help to protect it from exonucleolytic degradation (Studier & Moffatt 1986). Therefore, in some instances, the transcripts of T7 RNAP can saturate the translational machinery of *E. coli* cells in such a way that the target protein can accumulate to more than 50% of the total cell protein (Studier & Moffatt 1986). Due to the high T7 RNA polymerase activity and specificity and high mRNA stability, it is likely that the synthesis of other proteins (such as matrix proteins) may have been reduced in LB medium.

Compared to biofilms developed in DM, the amount of matrix polysaccharides in biofilms formed in LB increased with the simultaneous reduction of protein content. It is known that EPS composition is important in biofilm cohesion and adhesion to surfaces (Flemming & Wingender 2010), wherein higher polysaccharide concentrations are believed to contribute to biofilm cohesion (Ahimou et al. 2007). It is possible that biofilm cells grown in LB try to compensate for the low protein level in the matrix with a higher production of polysaccharides, in order to maintain the mechanical stability of biofilms.

In this work, increasing the antibiotic concentration from 20 to 30 μg ml^{-1} (50% increase) only had a modest effect on specific eGFP production by biofilm cells in the flow cell system (9% increase). Thus, using the lowest antibiotic concentration may be the best option if DM is chosen, not only due to the cost of antibiotic, but also because of the dissemination of antibiotic resistance, particularly in large-scale cultures (Rosano & Ceccarelli 2014). Specific heterologous production values were always higher in biofilm cells and the highest levels were obtained in LB medium. However, if the volumetric production values are analysed, a 60% increase can be obtained by using DM instead of LB due to the increased cell density of biofilms formed in DM. A deeper understanding of the operational parameters that maximise production is crucial to harness the power of these productive biofilms and this is the focus of the next chapters of this thesis.

6.5. References

Ahimou F, Semmens MJ, Haugstad G, Novak PJ. 2007. Effect of protein, polysaccharide, and oxygen concentration profiles on biofilm cohesiveness. Appl Environ Microbiol. 73:2905-2910.

Bagge N, Hentzer M, Andersen JB, Ciofu O, Givskov M, Høiby N. 2004. Dynamics and spatial distribution of β-lactamase expression in *Pseudomonas aeruginosa* biofilms. Antimicrob Agents Chemother. 48:1168-1174.

Bentley WE, Mirjalili N, Andersen DC, Davis RH, Kompala DS. 1990. Plasmid-encoded protein: the principal factor in the "metabolic burden" associated with recombinant bacteria. Biotechnol. Bioeng. 35:668-681.

Birnbaum S, Bailey JE. 1991. Plasmid presence changes the relative levels of many host cell proteins and ribosome components in recombinant *Escherichia coli*. Biotechnol Bioeng. 37:736-745.

Boehm A, Steiner S, Zaehringer F, Casanova A, Hamburger F, Ritz D, Keck W, Ackermann M, Schirmer T, Jenal U. 2009. Second messenger signalling governs *Escherichia coli* biofilm induction upon ribosomal stress. Mol Microbiol. 72:1500-1516.

Broedel SJ, Papciak S, Jones W. 2001. The selection of optimum media formulations for improved expression of recombinant proteins in *E. coli*. Technical Bulletin - Athena Enzyme Systems™ Group.

Carapuça E, Azzoni AR, Prazeres DM, Monteiro GA, Mergulhão FJ. 2007. Time-course determination of plasmid content in eukaryotic and prokaryotic cells using real-time PCR. Mol Biotechnol. 37:120-126.

Chou CH, Bennett GN, San KY. 1994. Effect of modified glucose uptake using genetic engineering techniques on high-level recombinant protein production in *Escherichia coli* dense cultures. Biotechnol Bioeng. 44:952-960.

Cunningham DS, Koepsel RR, Ataai MM, Domach MM. 2009. Factors affecting plasmid production in *Escherichia coli* from a resource allocation standpoint. Microb Cell Fact. 8:1475-2859.

Dewanti R, Wong ACL. 1995. Influence of culture conditions on biofilm formation by *Escherichia coli* O157:H7. Int J Food Microbiol. 26:147-164.

Dong H, Nilsson L, Kurland CG. 1995. Gratuitous overexpression of genes in *Escherichia coli* leads to growth inhibition and ribosome destruction. J Bacteriol. 177:1497-1504.

Donovan RS, Robinson CW, Glick BR. 1996. Review: Optimizing inducer and culture conditions for expression of foreign proteins under the control of the *lac* promoter. J Ind Microbiol Biotechnol. 16:145-154.

Doran JL, Leskiw BK, Petrich AK, Westlake DW, Jensen SE. 1990. Production of *Streptomyces clavuligerus* isopenicillin N synthase in *Escherichia coli* using two-cistron expression systems. J Ind Microbiol. 5:197-206.

DuBois M, Gilles KA, Hamilton JK, Rebers PA, Smith F. 1956. Colorimetric method for determination of sugars and related substances. Anal Chem. 28:350-356.

Eboigbodin KE, Ojeda JJ, Biggs CA. 2007. Investigating the surface properties of *Escherichia coli* under glucose controlled conditions and its effect on aggregation. Langmuir. 23:6691-6697.

Flemming HC, Wingender J. 2010. The biofilm matrix. Nat Rev Microbiol. 8:623-633.

Frenkel L, Bremer H. 1986. Increased amplification of plasmids pBR322 and pBR327 by low concentrations of chloramphenicol. DNA. 5:539-544.

Frias J, Ribas F, Lucena F. 2001. Effects of different nutrients on bacterial growth in a pilot distribution system. Antonie van Leeuwenhoek. 80:129-138.

Gallant CV, Daniels C, Leung JM, Ghosh AS, Young KD, Kotra LP, Burrows LL. 2005. Common β-lactamases inhibit bacterial biofilm formation. Mol Microbiol. 58:1012-1024.

Glick BR. 1995. Metabolic load and heterologous gene expression. Biotechnol Adv. 13:247-261.

Gomes LC, Silva LN, Simões M, Melo LF, Mergulhão FJ. 2015. *Escherichia coli* adhesion, biofilm development and antibiotic susceptibility on biomedical materials. J Biomed Mater Res A. 103:1414-1423.

Gomes LC, Moreira JMR, Teodósio JS, Araújo JDP, Miranda JM, Simões M, Melo LF, Mergulhão FJ. 2014. 96-well microtiter plates for biofouling simulation in biomedical settings. Biofouling. 30:535-546.

Goyal D, Sahni G, Sahoo DK. 2009. Enhanced production of recombinant streptokinase in *Escherichia coli* using fed-batch culture. Bioresour Technol. 100:4468-4474.

Hoffman LR, D'Argenio DA, MacCoss MJ, Zhang Z, Jones RA, Miller SI. 2005. Aminoglycoside antibiotics induce bacterial biofilm formation. Nature. 436:1171-1175.

Jackson DW, Simecka JW, Romeo T. 2002. Catabolite Repression of *Escherichia coli* Biofilm Formation. J Bacteriol. 184:3406-3410.

Jones C, Allsopp L, Horlick J, Kulasekara H, Filloux A. 2013. Subinhibitory concentration of kanamycin induces the *Pseudomonas aeruginosa* type VI secretion system. PLoS ONE. 8:e81132.

Linares JF, Gustafsson I, Baquero F, Martinez JL. 2006. Antibiotics as intermicrobial signaling agents instead of weapons. Proc Natl Acad Sci USA. 103:19484-19489.

Marini G, Luchese MD, Argondizzo AP, de Goes AC, Galler R, Alves TL, Medeiros MA, Larentis AL. 2014. Experimental design approach in recombinant protein expression: determining medium composition and induction conditions for expression of pneumolysin from *Streptococcus pneumoniae* in *Escherichia coli* and preliminary purification process. BMC Biotechnol. 14.

Matsui T, Sato H, Sato S, Mukataka S, Takahashi J. 1990. Effects of nutritional conditions on plasmid stability and production of tryptophan synthase by a recombinant *Escherichia coli*. Agric Biol Chem. 54:619-624.

May T, Ito A, Okabe S. 2009. Induction of multidrug resistance mechanism in *Escherichia coli* biofilms by interplay between tetracycline and ampicillin resistance genes. Antimicrob Agents Chemother. 53:4628-4639.

Mergulhão FJ, Monteiro GA. 2007. Analysis of factors affecting the periplasmic production of recombinant proteins in *Escherichia coli*. J Microbiol Biotechnol. 17:1236–1241.

Mergulhão FJM, Monteiro GA, Cabral JMS, Taipa MA. 2004b. Design of bacterial vector systems for the production of recombinant proteins in *Escherichia coli*. J Microbiol Biotechnol. 14:1-14.

Moreira JMR, Simões M, Melo LF, Mergulhão FJ. 2015a. The combined effects of shear stress and mass transfer on the balance between biofilm and suspended cell dynamics. Desal Water Treat. 53:3348-3354.

Novagen. 2005. pET system manual. 11th edition.

O'Connell HA, Niu C, Gilbert ES. 2007. Enhanced high copy number plasmid maintenance and heterologous protein production in an *Escherichia coli* biofilm. Biotechnol Bioeng. 97:439-446.

O'Kennedy RD, Patching JW. 1997. Effects of medium composition and nutrient limitation on loss of the recombinant plasmid pLG669-z and beta-galactosidase expression by *Saccharomyces cerevisiae*. J Ind Microbiol Biotechnol. 18:319-325.

Panayotatos N. 1988. Recombinant protein production with minimal-antibiotic-resistance vectors. Gene. 74:357-363.

Perry RH, Green DW, editors. 1997. Perry's Chemical Engineers' Handbook. 8th edition. New York: McGraw-Hill.

Peyton BM. 1996. Effects of shear stress and substrate loading rate on *Pseudomonas aeruginosa* biofilm thickness and density. Water Res. 30:29-36.

Rochex A, Lebeault JM. 2007. Effects of nutrients on biofilm formation and detachment of a *Pseudomonas putida* strain isolated from a paper machine. Water Res. 41:2885-2892.

Rosano GL, Ceccarelli EA. 2014. Recombinant protein expression in *Escherichia coli*: advances and challenges. Front Microbiol. 5:172.

Rozkov A, Avignone-Rossa C, Ertl P, Jones P, O'Kennedy R, Smith J, Dale J, Bushell M. 2004. Characterization of the metabolic burden on *Escherichia coli* DH1 cells imposed by the presence of a plasmid containing a gene therapy sequence. Biotechnol Bioeng. 88:909-915.

Sambrook J, Russell DW editors. 2001. Molecular Cloning: a Laboratory Manual. 3rd edition. New York: Cold Spring Harbor Laboratory Press.

Sanchez-Garcia L, Martín L, Mangues R, Ferrer-Miralles N, Vázquez E, Villaverde A. 2016. Recombinant pharmaceuticals from microbial cells: a 2015 update. Microb Cell Fact. 15:1-7.

Solaiman DK, Somkuti GA. 1991. Expression of streptomycete cholesterol oxidase in *Escherichia coli*. J Ind Microbiol. 8:253-258.

Stewart PS. 2003. Diffusion in biofilms. J Bacteriol. 185:1485-1491.

Studier FW. 2005. Protein production by auto-induction in high density shaking cultures. Protein Expr Purif. 41:207-234.

Studier FW, Moffatt BA. 1986. Use of bacteriophage T7 RNA polymerase to direct selective high-level expression of cloned genes. J Mol Biol. 189:113-130.

Summers D. 1998. Timing, self-control and a sense of direction are the secrets of multicopy plasmid stability. Mol Microbiol. 29:1137-1145.

Teh AH, Wang Y, Dykes GA. 2014. The influence of antibiotic resistance gene carriage on biofilm formation by two *Escherichia coli* strains associated with urinary tract infections. Can J Microbiol. 60:105-111.

Teodósio JS, Simões M, Mergulhão FJ. 2012a. The influence of nonconjugative *Escherichia coli* plasmids on biofilm formation and resistance. J Appl Microbiol. 113:373-382.

Teodósio JS, Simões M, Melo LF, Mergulhão FJ. 2011a. Flow cell hydrodynamics and their effects on *E. coli* biofilm formation under different nutrient conditions and turbulent flow. Biofouling. 27:1-11.

Terpe K. 2006. Overview of bacterial expression systems for heterologous protein production: from molecular and biochemical fundamentals to commercial systems. Appl Microbiol Biotechnol. 72:211-222.

Vandermeulen G, Marie C, Scherman D, Preat V. 2011. New generation of plasmid backbones devoid of antibiotic resistance marker for gene therapy trials. Mol Ther. 19:1942-1949.

Yazdani S, Mukherjee K. 2002. Continuous-culture studies on the stability and expression of recombinant streptokinase in *Escherichia coli*. Bioprocess Biosyst Eng. 24:341-346.

7.

Temporal variation of heterologous protein expression in *E. coli* biofilms analysed at single-cell level[f]

Abstract

Bioprocesses based on surface-associated microorganisms are emerging in environmental and industrial areas due to the physiological specificities and heterogeneities of biofilm cells. This chapter describes a simple and accurate method for evaluating the recombinant protein expression at a single-cell scale during *Escherichia coli* biofilm development. The model recombinant protein used was the eGFP as its intrinsic fluorescence allows us to quantify expression at both population and single-cell levels. The specific cell fluorescence intensity sharply increased during the first 4 days of biofilm cultivation. Thereafter, it decreased abruptly reaching a low-level plateau until the end of the experiment. During biofilm development, the population became increasingly heterogeneous with regard to eGFP expression. Three distinct biofilm types were observed over the course of the experiment: one with a homogeneous population (days 3-5), the second with a moderately heterogeneous population (days 6-8) and the third with a strongly heterogeneous population (days 9-11). Observation of *E. coli* biofilms by confocal laser scanning microscopy revealed marked spatial heterogeneity,

[f] The content of this chapter was adapted from the following publication(s):

Gomes LC, Carvalho D, Briandet R, Mergulhão FJ. Temporal variation of recombinant protein expression in *Escherichia coli* biofilms analysed at single-cell level. Process Biochem (in press).

with the cells actively producing eGFP restricted to the top layer of the biofilm. The proposed methodology allows a fine analysis of the recombinant protein expression within *E. coli* biofilms and it may be used to optimize the processing conditions.

7.1. Introduction

Several bacteria such as *E. coli* naturally grow in a community attached to a substratum and not in liquid cultures. The biocatalytic potential of these bacterial communities, termed biofilms, can be attributed to their high cell density; the former feature is widely exploited for wastewater treatment (Nicolella et al. 2000) and also for the production of industrial chemicals (Qureshi et al. 2005, Qureshi et al. 2004). Recombinant protein production in biofilms has been largely studied in the context of waste biodegradation (Bryers & Huang 1995, Venkata Mohan et al. 2009); however, this strategy could also be advantageous for other processes such as the biosynthesis of pharmaceutical intermediates (Panke & Wubbolts 2005) and catalysts for the food industry. In fact, using a recombinant *Aspergillus niger* strain, which contained a gene encoding the glucoamylase-GFP fusion protein, Talabardon & Yang (2005) showed that higher amounts of GFP and glucoamylase were produced in immobilized cells than in suspension culture. Moreover, a previous study with *E. coli* ATCC 33456 containing the plasmid pEGFP showed that the biofilm environment enhanced plasmid maintenance and GFP production (O'Connell et al. 2007).

During heterologous protein production, it is important to not only monitor the total amount of proteins produced by the culture using bulk methods such as fluorometry or standard fluorescence microscopy, but also evaluate the distribution of this protein in individual cells. For instance, knowing the fraction of protein-producing and non-producing cells may help to optimize the operational parameters for maximum strain performance. Bacteria grown in biofilms are normally distributed in a heterogeneous manner as they are exposed to local environmental conditions, which may vary on the micrometer scale (Stewart & Franklin 2008). The concentration gradients of chemicals dissolved in the interstitial fluid within the biofilm matrix promote differences in bacterial enzymatic activities in different areas of the biofilms (Huang et al. 1998, Werner et al.

2004) and they can create variation at the gene and protein levels (Beloin et al. 2004, Lenz et al. 2008, O'Connell et al. 2007, Rani et al. 2007).

In this chapter, a protocol using fluorescence imaging is proposed for quantifying the dynamics of protein expression within a biofilm population at both bulk and single-cell levels. It should be noted that the entire protocol required only an epifluorescence microscope and an open-source image analysis tool, both of which are available in most life science research and industrial laboratories (Webb & Brown 2013).

7.2. Materials and methods

7.2.1. Biofilm-producing system and culture conditions

E. coli cells harbouring the pFM23 plasmid for the cytoplasmic production of eGFP (Mergulhão & Monteiro 2007) were used and the biofilms were grown in the flow cell reactor as described in Chapter 5, section 5.2.2. The recirculating tank was continuously fed with 0.025 l h^{-1} of LB-Miller (Sigma, USA) supplemented with 20 µg ml^{-1} kanamycin (Eurobio, France). LB was the culture medium chosen since it was previously shown (Chapter 6) that the specific eGFP production in LB is higher than in DM in both planktonic and sessile environments. As it was demonstrated in Chapter 6 that changing the antibiotic concentration from 20 to 30 µg ml^{-1} did not affect the specific eGFP production of biofilm cells in the flow cell system, the lowest concentration was selected.

7.2.2. Biofilm monitoring

Biofilm cell populations were resuspended and homogenized into NaCl solution for total and viable cell assessment and eGFP analysis.

7.2.2.1. Quantification of total and viable cells by epifluorescence imaging on detached biofilm populations

Biofilm total (viable plus non-viable) and viable cell counts were assessed using the Live/Dead® *Bac*Light™ bacterial viability kit (Syto9/PI, Invitrogen Life Technologies, Alfagene, Portugal) as fully described in Chapter 6, section 6.2.4. Results were expressed as the mean of triplicate samples obtained in three independent experiments measured as log cell cm^{-2}.

7.2.2.2. Quantification of eGFP expression by epifluorescence microscopy

Biofilm cells were filtered through a nucleopore-etched (Whatman Inc., NJ, USA) black polycarbonate membrane (pore size 0.2 μm) and images were acquired using a Leica DM LB2 epifluorescence microscope (Leica Microsystems Ltd) coupled with a Leica DFC300 FX camera (Leica Microsystems Ltd). A 450-490-nm excitation filter was used in combination with a dichromatic mirror at 510 nm and suppression filter at 515 nm. Fifteen fields of view were photographed for each sample. A total of three biofilm samples originating from three independent experiments were used for each time point. The images were analysed in batch mode using ImageJ v1.48 (NIH). For each RGB (red, blue and green) image, the green channel was processed with a sliding paraboloid to reduce uneven background. Cell segmentation was performed using an automatic black and white threshold after convolution with a Laplacian of Gaussian (9 × 9 kernel) filter. The resulting binary image was then redirected to a background-reduced duplicate, and each cell was analysed with the size and circularity intervals defined as 0.52-4.16 μm and 0.25-1.00, respectively. For each image, the mean fluorescence intensity was expressed as the mean of the values of individual cells, which was in turn obtained by averaging each cell pixel intensity value. The mean fluorescence intensity is presented in arbitrary fluorescent units (AFUs).

7.2.3. Deciphering spatial heterogeneity of eGFP expression within biofilm by CLSM

For visualization by CLSM, 3-day-old biofilms were formed on sterile PVC coupons placed in a 24-well polystyrene, flat-bottomed TPP® tissue culture plate (Sigma-Aldrich, France) with LB. The plate was incubated at 30 ºC under defined shaking conditions to obtain the same average wall shear stress found in the sampling zone of the flow cell operating at a $Re = 4{,}600$ (Moreira et al. 2013c, Salek et al. 2012). Bacteria from the biofilms were counterstained with 5 µM Syto61 (Invitrogen, France), a cell-permeant red fluorescent nucleic acid marker. The biofilms in the PVC coupons were observed using a Leica SP2 AOBS CLSM (Leica Microsystems, France) at the INRA MIMA2 microscopy platform. The coupons were scanned using a 40× water immersion objective lens at excitation wavelengths of 488 nm (argon laser) and 633 nm (helium-neon laser). The emitted fluorescence was recorded within the range of 500-580 nm to collect the eGFP emission fluorescence and 640-730 nm to collect the Syto61 fluorescence. Two-dimensional projections of the biofilm structures were reconstructed using the Section function of the IMARIS 7.0 software (Bitplane, Switzerland). The Stack Profile tool provided by the LCS software (Leica Microsystems, France) was used to trace the intensity values of both fluorescent signals with regard to the z-position.

7.2.4. Calculations and statistical analysis

The coefficient of variation was chosen to express the extent of heterogeneity in the expression of eGFP by a cell population (Figure 7.3). For each image, the coefficient of variation for the specific fluorescence intensity (%) corresponds to the variability of the fluorescence signal of each bacterial cell in relation to the mean of the population. The coefficients of variation were calculated for each of the 45 images analysed for each experimental day and represented in the form of a typical graph of frequency distribution.

One-way ANOVA was performed using the Statgraphics v6.0 software (Manugistics, USA) for comparing the coefficients of variation between each pair of experimental days and between groups of days (Figure 7.3). Paired *t*-test analysis was also performed when appropriate. All tests were used based on a confidence level of 95% (differences reported as significant for P values < 0.05).

7.3. Results

Techniques based on epifluorescence microscopy were used to monitor the amount of heterologous protein expressed by biofilm cells and the physiological state of these cells during heterologous protein production (Figure 7.1). Figure 7.1A presents the temporal eGFP expression profile in the biofilm during its development in the flow cell system. The specific fluorescence intensity increased from day 3 to day 4, having reached a maximum on the latter day. From this day onward, a significant reduction of the specific cell fluorescence intensity (about 61%) was observed, and the values stabilized by the end of the experiment at about half of the value measured on day 3.

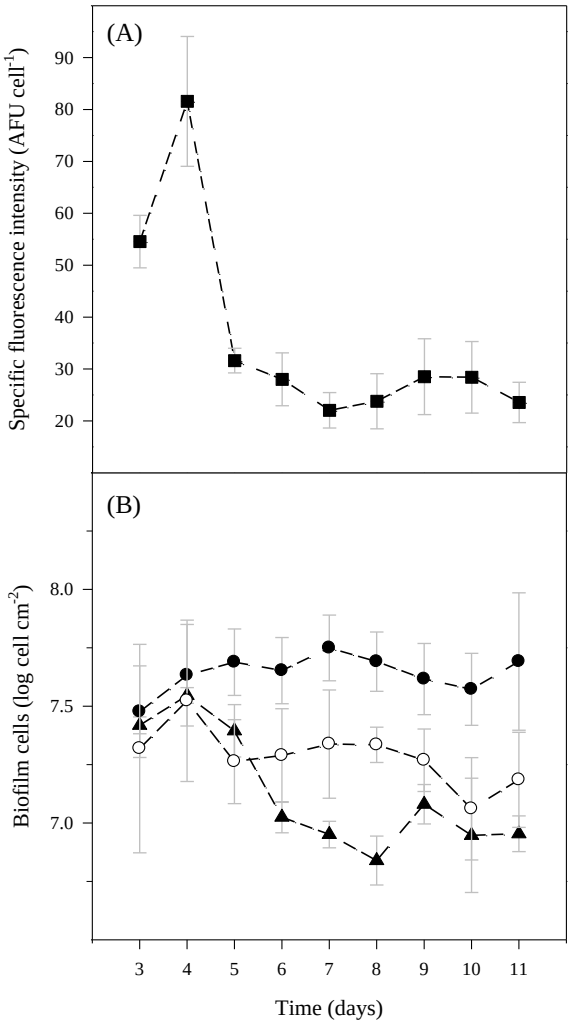

Figure 7.1. Temporal evolution of (A) specific fluorescence intensity (-■-) and (B) total cell (-●-), viable cell (-○-) and eGFP-expressing (-▲-) cell number for biofilms formed by *E. coli* JM109(DE3) + pFM23. The means ± SDs for three independent experiments are illustrated.

The physiology of the biofilm cells was evaluated during the course of the experiment by quantifying the number of total, viable and eGFP-expressing cells (Figure 7.1B). It can be seen that the total number of biofilm cells increased slightly between days 3 and 5 (39%), and it remained stable until the end of the experiment. Concerning biofilm cell viability, it is possible to observe that during days 3 and 4, the number of viable cells followed the increase in the number of total cells, corresponding to a viability percentage of 74%. From day 4, the fraction of viable cells decreased by 45% and was practically constant until the end of the experiment ($P < 0.05$). The number of eGFP-expressing cells followed the evolution of total and viable cells until day 4, and most of the total cells (82%) were found to express eGFP. However, between days 4 and 6, a strong reduction (of about 70%) in the number of eGFP-expressing cells was observed. By the end of the experimental time, the eGFP-expressing cells represented only 21% of the total cells. Figure 7.1B shows a gap between the biofilm cell viability (i.e., cells with intact cell membrane) and the sessile cells expressing eGFP, with a statistically significant difference between both curves at days 6, 7, 8, 9 and 11 ($P < 0.05$). This difference may be associated with the existence of a slow growth population of viable but non-expressing (VBNE) cells. The onset of this biofilm population was noticeable from day 6 onwards, and the fraction of VBNE cells remained almost constant until day 9.

The overall results of Figure 7.1 show some similarity between the curves for viable and eGFP-producing cells (Figure 7.1B) and the temporal evolution of recombinant protein production (Figure 7.1A). Both curves show a maximum at day 4 followed by a decrease in the next 24 h, which was more pronounced in the case of eGFP-expressing cells and specific fluorescent intensity.

Figure 7.2 shows illustrative images obtained by epifluorescence microscopy to quantify the total biofilm cells (Figures 7.2A, B and C) and the green fluorescence signal of each eGFP-expressing cell (Figures 7.2D, E and F) at selected days during the course of biofilm development in the flow cell system. Qualitatively, these sequences of epifluorescence images confirm the results presented on Figure 7.1. Although the total amount of cells forming the biofilm did not significantly differ between days 3, 7 and 11 ($P > 0.05$), the second sequence of images displays the reduction in the number of eGFP-expressing cells from day 3 to days 7 and 11 (Figures 7.2D, E and F). The number of eGFP-expressing cells as well as the fluorescence intensity of each expressing cell decreased. In addition, the cell population was more homogeneous on day 3 with regard

to eGFP production, as there was a lower variability in the intensity of the fluorescent signal emitted by each cell.

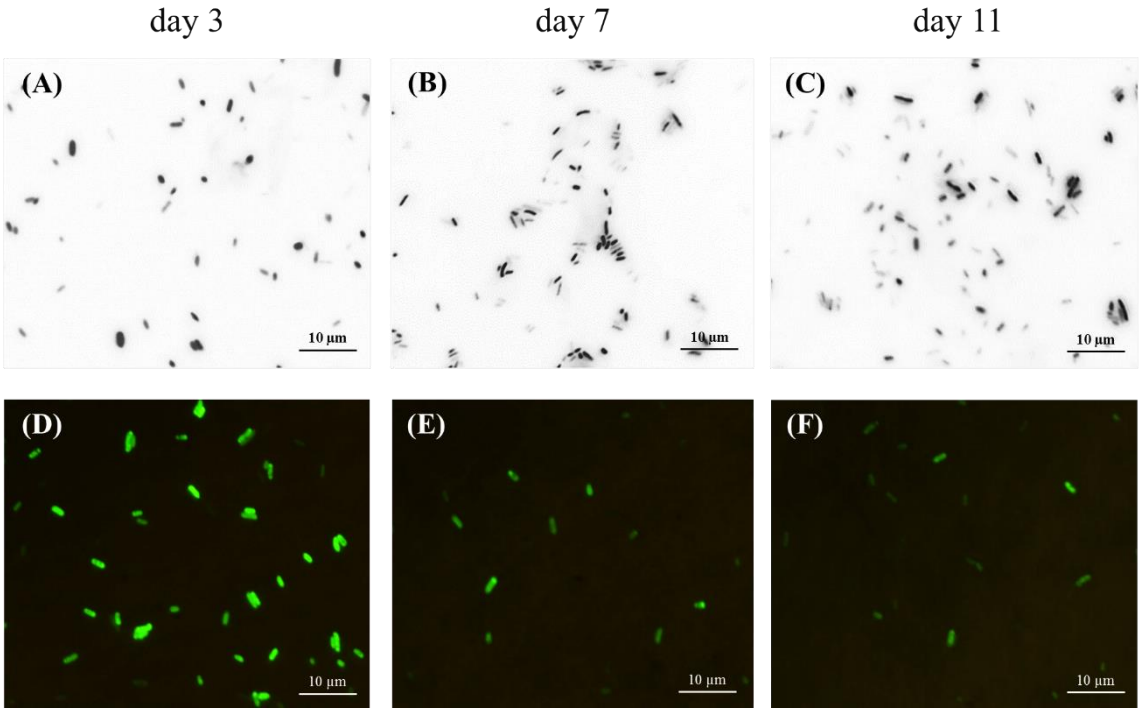

Figure 7.2. Illustrative epifluorescent micrographs of biofilm-detached cells after 3 ((A) and (D)), 7 ((B) and (E)) and 11 ((C) and (F)) days of operation of the flow cell system. Micrographs (A), (B) and (C) correspond to the representative colour-inverted images of the total *E. coli* cells stained with the Live/Dead® *Bac*Light™ bacterial viability kit. Micrographs (D), (E) and (F) are the representative fields of *E. coli* cells expressing eGFP (bars = 10 µm).

In addition to analysing the bulk eGFP expression levels obtained with biofilm cells (Figure 7.1A), analysis of the eGFP expression at a single-cell level was possible by image analysis. Figure 7.3 presents the coefficients of variation of the fluorescence intensity determined for each microscopic image obtained on each experimental day (a total of 45 images were obtained per day). The larger the coefficient of variation (shown in Figure 7.3 as vertical black line segments), the greater the difference in the eGFP levels among the individual cells within the same image. As the experiment progressed, a larger variation in cell fluorescence was obtained, indicating that the biofilm became increasingly heterogeneous during development. The temporal evolution of fluorescence heterogeneity shows three distinct groups: one with a homogeneous population (days 3-

5), the second with a moderately heterogeneous population (days 6-8) and the third with a strongly heterogeneous population (days 9-11). The statistical test performed revealed no significant differences in the average coefficients of variation within each group ($P > 0.05$), but the groups are statistically different from each other ($P < 0.05$).

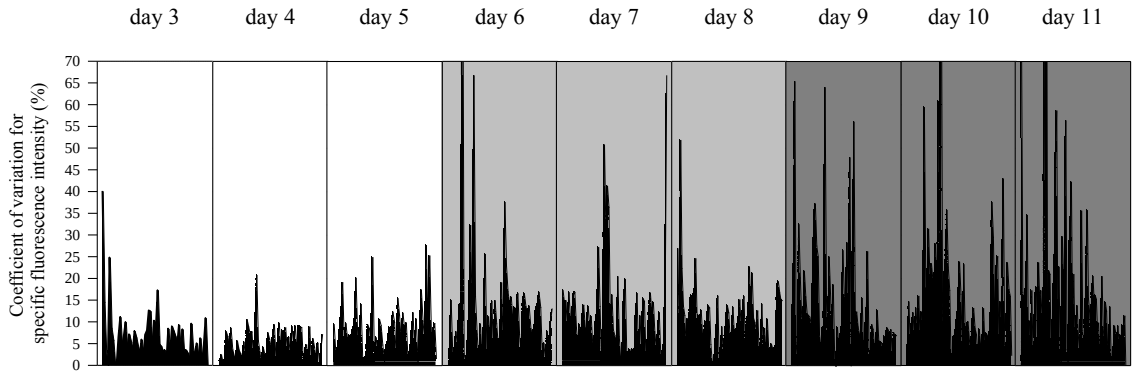

Figure 7.3. Temporal evolution of coefficients of variation for specific fluorescence intensity. Three distinct biofilm populations were identified: homogeneous (white), moderately heterogeneous (light grey) and strongly heterogeneous (dark grey).

Considering the average of coefficients of variation represented in Figure 7.3 for each experimental day, a good linear correlation was found between these two entities ($r = 0.92$) with most of the experimental points included within the 95% confidence interval (Figure 7.4). This clearly indicates that the biofilm heterogeneity increases over time.

To elucidate the rationale for this population heterogeneity, a confocal microscopy analysis was performed on a 3-day-old biofilm obtained on the same surface, with the same culture medium and at a similar shear stress and incubation temperature. A representative confocal image shows sharply stratified patterns of eGFP expression (Figure 7.5A). A zone of bright green fluorescence was observed at the liquid interface of the biofilm, whereas the interior regions of the biofilm lacked eGFP-expressing cells (non-expressing cells were marked in red). The qualitative assessment of the eGFP distribution in the verticality of the biofilm (Figure 7.5A) was confirmed by the quantitative results extracted from the *z*-stack acquisition. While the bottom layer of the biofilm (40 µm of dimension) consisted predominantly of non-expressing cells that emitted the red signal, the eGFP-expressing cells are predominantly located in the upper 90 µm of the biofilm (Figure 7.5B).

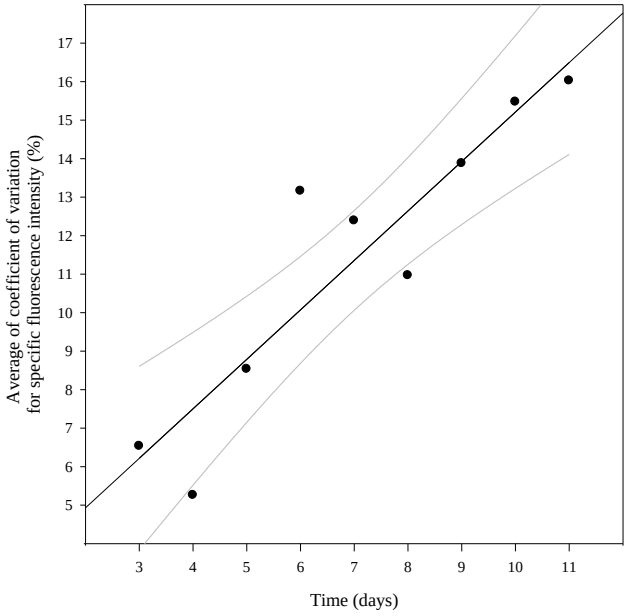

Figure 7.4. Correlation between the average of coefficient of variation for specific fluorescence intensity against time. The regression line is presented in black ($y = 1.28x + 2.36$; $r = 0.92$) and the 95% confidence band limits are presented in grey.

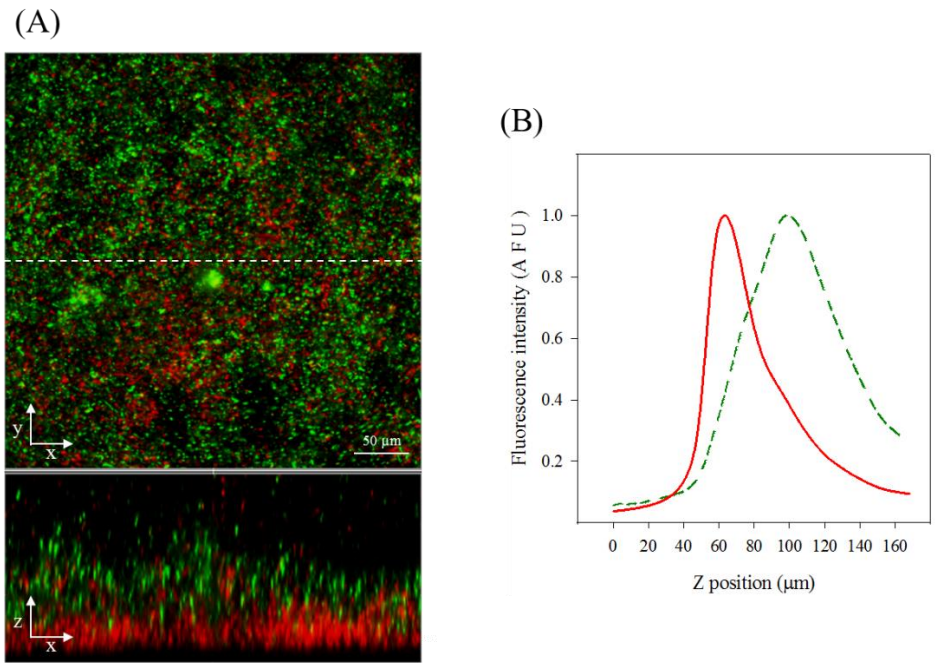

Figure 7.5. Spatial heterogeneity of a 3-day-old biofilm formed by *E. coli* JM109(DE3) + pFM23: (A) section view of the CLSM images and (B) distribution of red and green fluorescence intensities along the vertical (z) biofilm position. The eGFP-expressing cells are labelled in green and the non-expressing cells are countermarked in red with Syto61. The dotted white line indicates the vertical section (bar = 50 µm).

7.4. Discussion

This study demonstrates that epifluorescence microscopy is a powerful tool for assessing the features of recombinant protein expression in *E. coli* that are not routinely measured. Biofilm viability can be quantified with a simple staining procedure and the cells associated with the recombinant protein can be quantified in relative terms. Moreover, we report the application of an image analysis tool to fluorescence microscopy for the single-cell evaluation of recombinant protein expression during biofilm growth. The developed technique provides information on the population heterogeneity for eGFP production, which may be highly relevant for bioprocess monitoring, especially while using biofilms that are known to be heterogeneous and that contain several subsets of cells in different physiological states (Stewart & Franklin 2008). The temporal single-cell measurements showed that the biofilm heterogeneity increases over time. O'Connell et al. (2007) studied the dynamics of fluorescence during biofilm development by flow cytometry and detected three populations of *E. coli* cells with differing levels of GFP expression in 24-h biofilms. These authors also found changes in the distribution of GFP fluorescence along time (O'Connell et al. 2007), in agreement with the results obtained in this study. However, while O'Connell et al. (2007) reported the complete absence of non-fluorescent cells after 48 h of flow cell operation, in this work an increase in the number of such cells was detected between days 4 and 6, representing on average 79% of the total population from this moment until the end of the experiment. The different results presented by O'Connell et al. (2007) can be explained by the use of a high-copy-number plasmid (pUC19-based vector) and different cultivation and hydrodynamic conditions for biofilm growth in a parallel plate flow chamber.

Fluorometry is an easy, fast and common way of measuring GFP fluorescence of a bacterial population (Bongaerts et al. 2002). However, it measures the total sum of fluorescence intensities of all bacterial cells, which is not a good indicator of single-cell gene expression in the heterogeneous populations. By contrast, an epifluorescence microscope or a flow cytometer can be used to quantify the fluorescence of individual cells. The standard flow cytometers can rapidly determine the fluorescence of a large number of cells (Carneiro et al. 2009, Miyashiro & Goulian 2007). Nevertheless, using a microscope equipped with a high numerical aperture lens and a standard cooled charge-coupled device (CCD) camera, like that used in this work, cellular fluorescence can be

detected with much greater sensitivity and precision when compared to a flow cytometer (Miyashiro & Goulian 2007). This is consequently due to the efficient collection of the emitted photons and the long duration of exposure that can be achieved for a static field of cells on the microscope stage (Miyashiro & Goulian 2007, Shapiro 2000). In addition, epifluorescence microscopes are more common in the laboratory and industrial environments than the flow cytometers (Carneiro et al. 2009) due to their lower cost.

It should be noted that the low AFU values and the presence of a high fraction of non-expressing cells in the biofilm after day 5 are unlikely to be associated with plasmid loss. This is because the presence of antibiotics throughout the flow cell system ensured a strong selective pressure. In fact, the number of colonies on selective plates was found to be similar to that of the non-selective plates, indicating that the plasmid is maintained by the cells (data not shown). Furthermore, it is known that continuous biofilm cultures for recombinant protein production are advantageous in retaining plasmid-bearing cells (O'Connell et al. 2007). Cells in the biofilms tend to grow more slowly than their planktonic counterparts (Williams et al. 1997), leading to fewer divisions and hence less plasmid partitioning. The marked decline in the AFU values after day 4 may be due to the loss of the pre-existing eGFP molecules from cells due to lysis. This phenomenon may be explained by the decrease in the amount of viable cells after 4 days of biofilm development. Lowder et al. (2000) reported a strong correlation between cell death and leakage of GFP from cells due to the loss of membrane integrity. The decrease in biofilm viability was probably a result of the metabolic stress imposed by the high eGFP production levels (Kurland & Dong 1996) in the initial days of bioreactor operation. It is well documented that the production of recombinant proteins significantly affects cell metabolism by channelling resources towards producing foreign proteins, thereby imposing a metabolic burden and stress on the host cells (Glick 1995, Sørensen & Mortensen 2005, Xia et al. 2010, Yang et al. 2016). In particular, an increased protease activity and decreased growth rate and cell viability are some stress signals that can be induced during recombinant protein synthesis (Bentley et al. 1990, Dong et al. 1995, Georgiou et al. 1988, Kurland & Dong 1996). It has been shown that biofilm formation by itself is accompanied by the overexpression of many stress genes (Beloin et al. 2004, Heim et al. 1994, Stewart 2003). Therefore, it is likely that high-level recombinant protein expression may increase this cellular stress. The low fluorescence intensity values registered from day 5 may be due to the simultaneous effect of the drop in viability and in the number of eGFP-producing cells. In fact, a significant percentage of the total

biofilm cells were stained with propidium iodide (considered as non-viable cells) and therefore did not further participate in cell growth and eGFP formation.

Although confocal microscopes are not available in many biofilm research laboratories, a confocal microscopy analysis was introduced in this work for determining the association between the single-cell variations found within *E. coli* biofilms and the spatial distribution of eGFP-expressing cells inside biofilms. Gradients of pH, oxygen, nutrients and waste products are established at different depths in the biofilms. Further, it is widely recognized that such chemical heterogeneity can lead to cells in the biofilm exhibiting different metabolic activities (Stewart 2003, Stewart & Franklin 2008). In this work, staining with the Syto61 red fluorescent dye revealed that sessile cells expressing eGFP are confined to a single band at the top of the biofilm. These results are consistent with those of Werner et al. (2004) and Lenz et al. (2008) who observed spatially non-uniform patterns of GFP expression in *P. aeruginosa* colony biofilms and in biofilms grown under continuous flow conditions. GFP synthesis occurred in a relatively narrow zone (approximately 30-60 μm wide) at the interface between the biofilm and the source of oxygen (Werner et al. 2004), and the GFP mRNA levels correlated with this zone of active GFP fluorescence (Lenz et al. 2008). Rani et al. (2007) also demonstrated a stratified pattern of protein synthetic activity in *Staphylococcus epidermidis* drip-flow and capillary biofilms, with a single band of bright green fluorescence detected along the biofilm–fluid interface and rings of green fluorescence located at the periphery of cell clusters, respectively. It was hypothesized that the heterogeneous pattern of eGFP expression inside the *E. coli* biofilms may be a result of oxygen limitation. Prigent-Combaret et al. (1999) demonstrated oxygen limitation in *E. coli* K-12 biofilms via random insertion mutagenesis. This result was further corroborated by Schembri et al. (2003), who showed the induction of several genes commonly expressed during oxygen-limiting conditions in *E. coli* biofilm cells. Oxygen is the only requirement for GFP fluorescence, apart from gene expression by the host cells, which is necessary for the final stage of protein folding for the formation of fluorescent chromophore (Heim et al. 1994). Therefore, in this biofilm formation system, deeper biofilm zones may not be fluorescent due to the lack of oxygen, which is required for eGFP maturation, or due to mass transfer limitation of other nutrients (Stewart 2003, Stewart & Franklin 2008). In a previous study, it was shown that the density of biofilms formed with this strain is affected by the nutrient load of the system (Teodósio et al. 2011a). This increases the possibility of optimizing

the nutrient load for obtaining a more porous biofilm, thus facilitating the access to fresh nutrients in this bottom layer, which could then be shifted to a productive state.

The image analysis technique described in this work can be used not only to assess the expression levels of a fluorescent protein in order to optimize production yields, but it can also be used with different fluorescent proteins to study time-dependent processes using timer fluorescence proteins (with time-dependent chromophore maturation), for promoter tracking purposes (using split fluorescent proteins), or even to monitor physicochemical changes in microenvironments, among several other applications (Chudakov et al. 2010, Wuang et al. 2008). However, a limitation of this methodology is that it relies on the expression of fluorescent proteins. If the target protein is not fluorescent in a particular process, a translational fusion with a fluorescent protein tag may be used for quantification purposes (Shuman & Silhavy 2003). This strategy may require additional processing steps such as tag cleavage in order to obtain the native protein (Young et al. 2012). A different strategy is to use a transcriptional fusion between the protein of interest and the fluorescent protein (Shuman & Silhavy 2003), allowing the determination of protein expression levels without further processing steps. Furthermore, if the target protein is displayed on the cell surface it can be detected and quantitated using fluorescently labelled antibodies (Tang et al. 2008).

In conclusion, epifluorescence microscopy and the corresponding image analysis can be regarded as a valuable tool for determining certain production parameters that cannot be obtained by bulk methods such as fluorimetry, namely the distribution of fluorescent protein production within a cell population. The information extracted with such single-cell technique, combined with the biofilm physiological data, can be used to monitor the protein expression in biofilm cells and to further determine the best processing conditions for recombinant protein production in this type of cells.

7.5. References

Beloin C, Valle J, Latour-Lambert P, Faure P, Kzreminski M, Balestrino D, Haagensen JAJ, Molin S, Prensier G, Arbeille B, et al. 2004. Global impact of mature biofilm lifestyle on *Escherichia coli* K-12 gene expression. Mol Microbiol. 51:659-674.

Bentley WE, Mirjalili N, Andersen DC, Davis RH, Kompala DS. 1990. Plasmid-encoded protein: the principal factor in the "metabolic burden" associated with recombinant bacteria. Biotechnol Bioeng. 35:668-681.

Bongaerts RJ, Hautefort I, Sidebotham JM, Hinton JC. 2002. Green fluorescent protein as a marker for conditional gene expression in bacterial cells. Methods Enzymol. 358:43-66.

Bryers JD, Huang C-T. 1995. Recombinant plasmid retention and expression in bacterial biofilm cultures. Wat Sci Tech. 31:105-115.

Carneiro S, Amaral AL, Veloso AC, Dias T, Peres AM, Ferreira EC, Rocha I. 2009. Assessment of physiological conditions in *E. coli* fermentations by epifluorescent microscopy and image analysis. Biotechnol Prog. 25:882-891.

Chudakov DM, Matz MV, Lukyanov S, Lukyanov KA. 2010. Fluorescent proteins and their applications in imaging living cells and tissues. Physiol Rev. 90:1103-1163.

Dong H, Nilsson L, Kurland CG. 1995. Gratuitous overexpression of genes in *Escherichia coli* leads to growth inhibition and ribosome destruction. J Bacteriol. 177:1497-1504.

Georgiou G, Shuler ML, Wilson DB. 1988. Release of periplasmic enzymes and other physiological effects of β-lactamase overproduction in *Escherichia coli*. Biotechnol Bioeng. 32:741-748.

Glick BR. 1995. Metabolic load and heterologous gene expression. Biotechnol Adv. 13:247-261.

Heim R, Prasher DC, Tsien RY. 1994. Wavelength mutations and posttranslational autoxidation of green fluorescent protein. Proc Natl Acad Sci USA. 91:12501-12504.

Huang C-T, Xu KD, McFeters GA, Stewart PS. 1998. Spatial patterns of alkaline phosphatase expression within bacterial colonies and biofilms in response to phosphate starvation. Appl Environ Microbiol. 64:1526-1531.

Kurland CG, Dong H. 1996. Bacterial growth inhibition by overproduction of protein. Mol. Microbiol. 21:1-4.

Lenz AP, Williamson KS, Pitts B, Stewart PS, Franklin MJ. 2008. Localized gene expression in *Pseudomonas aeruginosa* biofilms. Appl Environ Microbiol. 74:4463-4471.

Lowder M, Unge A, Maraha N, Jansson JK, Swiggett J, Oliver JD. 2000. Effect of starvation and the viable-but-nonculturable state on green fluorescent protein (GFP) fluorescence in GFP-tagged *Pseudomonas fluorescens* A506. Appl Environ Microbiol. 66:3160-3165.

Miyashiro T, Goulian M. 2007. Single-cell analysis of gene expression by fluorescence microscopy. Methods Enzymol. 423:458-475.

Moreira JMR, Gomes LC, Araújo JDP, Miranda JM, Simões M, Melo LF, Mergulhão FJ. 2013c. The effect of glucose concentration and shaking conditions on *Escherichia coli* biofilm formation in microtiter plates. Chem Eng Sci. 94:192-199.

Nicolella C, van Loosdrecht MCM, Heijnen JJ. 2000. Wastewater treatment with particulate biofilm reactors. J Biotechnol. 80:1-33.

O'Connell HA, Niu C, Gilbert ES. 2007. Enhanced high copy number plasmid maintenance and heterologous protein production in an *Escherichia coli* biofilm. Biotechnol Bioeng. 97:439-446.

Panke S, Wubbolts M. 2005. Advances in biocatalytic synthesis of pharmaceutical intermediates. Curr Opin Chem Biol. 9:188-194.

Prigent-Combaret C, Vidal O, Dorel C, Lejeune P. 1999. Abiotic surface sensing and biofilm-dependent regulation of gene expression in *Escherichia coli*. J Bacteriol. 181:5993-6002.

Qureshi N, Annous BA, Ezeji TC, Karcher P, Maddox IS. 2005. Biofilm reactors for industrial bioconversion processes: employing potential of enhanced reaction rates. Microb Cell Fact. 4:24.

Qureshi N, Brining H, Iten L, Dien B, Nichols N, Saha B, Cotta M. 2004. Adsorbed cell dynamic biofilm reactor for ethanol production from xylose and corn fiber hydrolysate. Paper presented at: The 36th Great Lakes Regional Meeting of the American Chemical Society, Peoria, IL.

Rani SA, Pitts B, Beyenal H, Veluchamy RA, Lewandowski Z, Davison WM, Buckingham-Meyer K, Stewart PS. 2007. Spatial patterns of DNA replication, protein

synthesis, and oxygen concentration within bacterial biofilms reveal diverse physiological states. J Bacteriol. 189:4223-4233.

Salek M, Sattari P, Martinuzzi R. 2012. Analysis of fluid flow and wall shear stress patterns inside partially filled agitated culture well plates. Ann Biomed Eng. 40:707-728.

Schembri MA, Kjaergaard K, Klemm P. 2003. Global gene expression in *Escherichia coli* biofilms. Mol. Microbiol. 48:253-267.

Shapiro HM. 2000. Microbial analysis at the single-cell level: tasks and techniques. J. Microbiol. Methods. 42:3-16.

Shuman HA, Silhavy TJ. 2003. The art and design of genetic screens: *Escherichia coli*. Nat Rev Genet. 4:419-431.

Sørensen HP, Mortensen KK. 2005. Advanced genetic strategies for recombinant protein expression in *Escherichia coli*. J Biotechnol. 115:113-128.

Stewart PS. 2003. Diffusion in biofilms. J Bacteriol. 185:1485-1491.

Stewart PS, Franklin MJ. 2008. Physiological heterogeneity in biofilms. Nat Rev Micro. 6:199-210.

Talabardon M, Yang S-T. 2005. Production of GFP and glucoamylase by recombinant *Aspergillus niger*: effects of fermentation conditions on fungal morphology and protein secretion. Biotechnol Prog. 21:1389-1400.

Tang YQ, Han SY, Zheng H, Wu L, Ueda M, Wang XN, Lin Y. 2008. Construction of cell surface-engineered yeasts displaying antigen to detect antibodies by immunofluorescence and yeast-ELISA. Appl Microbiol Biotechnol. 79:1019-1026.

Teodósio JS, Simões M, Melo LF, Mergulhão FJ. 2011a. Flow cell hydrodynamics and their effects on *E. coli* biofilm formation under different nutrient conditions and turbulent flow. Biofouling. 27:1-11.

Venkata Mohan S, Falkentoft C, Venkata Nancharaiah Y, Sturm BSM, Wattiau P, Wilderer PA, Wuertz S, Hausner M. 2009. Bioaugmentation of microbial communities in laboratory and pilot scale sequencing batch biofilm reactors using the TOL plasmid. Bioresour Technol. 100:1746-1753.

Wang Y, Shyy JY, Chien S. 2008. Fluorescence proteins, live-cell imaging, and mechanobiology: seeing is believing. Annu Rev Biomed Eng. 10:1-38.

Webb DJ, Brown CM. 2013. Epi-Fluorescence Microscopy. In: Taatjes DJ, Roth J, editors. Methods Mol Biol. 931:29-59.

Werner E, Roe F, Bugnicourt A, Franklin MJ, Heydorn A, Molin S, Pitts B, Stewart PS. 2004. Stratified growth in *Pseudomonas aeruginosa* biofilms. Appl Environ Microbiol. 70:6188-6196.

Williams I, Venables WA, Lloyd D, Paul F, Critchley I. 1997. The effects of adherence to silicone surfaces on antibiotic susceptibility in *Staphylococcus aureus*. Microbiology. 143:2407-2413.

Xia X-X, Qian Z-G, Ki CS, Park YH, Kaplan DL, Lee SY. 2010. Native-sized recombinant spider silk protein produced in metabolically engineered *Escherichia coli* results in a strong fiber. Proc Natl Acad Sci USA. 107:14059-14063.

Yang Y-X, Qian Z-G, Zhong J-J, Xia X-X. 2016. Hyper-production of large proteins of spider dragline silk MaSp2 by *Escherichia coli* via synthetic biology approach. Process Biochem. 51:484-490.

Young CL, Britton ZT, Robinson AS. 2012. Recombinant protein expression and purification: a comprehensive review of affinity tags and microbial applications. Biotechnol J. 7:620-634.

8.

Heterologous protein expression in *E. coli* biofilms: gene dosage and induction effect[g]

Abstract

Despite the high production yields that can be attained with *E. coli* during cultivation of planktonic cells, heterologous protein production by biofilms remains largely unexplored. In this work, *E. coli* JM109(DE3) cells transformed with plasmid pFM23 for eGFP expression were used. The effect of chemical induction with IPTG was assessed in both planktonic and biofilm cells in order to evaluate their production potential.

It was shown that induction negatively affected the growth and viability of planktonic cultures, but eGFP production was not increased. Production was not limited by gene dosage or by transcriptional activity. Results suggest that plasmid maintenance at high copy number imposes a metabolic burden that precludes high level expression of the heterologous protein. In biofilm cells, the inducer avoided the overall decrease in the amount of expressed eGFP, however this result was also not correlated with gene dosage. Higher specific production levels were always attained with biofilm cells and it seems that while induction of biofilm cells shifts their metabolism towards the maintenance of heterologous protein concentration, in planktonic cells the cellular resources are directed towards plasmid replication and growth.

[g] The content of this chapter was adapted from the following publication(s):

Gomes LC, Monteiro GA, Mergulhão FJ. Heterologous protein expression in *Escherichia coli* biofilms: gene dosage and induction effect (manuscript in preparation).

8.1. Introduction

Successful recombinant protein production in *E. coli* is a combination of many good decisions involving the choice of the most appropriate strain, expression vector, cultivation and purification strategies (Mergulhão et al. 2004b). Plasmids are the most commonly used vectors for the expression of recombinant proteins in *E. coli*. Their design is crucial in order to maintain an equilibrium between the transcriptional and translational machinery of the host cell so that the deleterious effects of heterologous protein production can be managed (Mergulhão et al. 2005, Mergulhão et al. 2004b). A plasmid contains many elements that are essential for its use as an expression vector but some of the most important are the origin of replication and the promoter. The origin of replication controls the plasmid copy number (PCN) (Rosano & Ceccarelli 2014) and although it is often assumed that a high gene dosage is favorable for high level heterologous protein production, this is not always the case (Mergulhão et al. 2004b). It has been shown that a high PCN may impose a metabolic burden that decreases the bacterial growth rate and originates plasmid instability, thus reducing the number of healthy bacteria for protein synthesis (Bentley et al. 1990, Birnbaum & Bailey 1991, Carrier et al. 1998). The biofilm mode of growth affects plasmid maintenance and PCN control. In a first study, Davies & Geesey (1995) found that the PCN was approximately 1.5 fold higher in *P. aeruginosa* biofilms than in planktonic cells. Additionally, the PCN of plasmid pBR322, a plasmid carrying resistance genes against ampicillin and tetracycline, was 2 fold higher in *E. coli* cells growing in a biofilm (May et al. 2009). The results from O'Connell et al. (2007) also indicate that the biofilm environment favours plasmid maintenance. The potential of *E. coli* biofilm cells to retain high PCN's can be explained by the slower growth of sessile cells compared to planktonic cells (Donlan 2000), leading to fewer divisions and correspondingly less plasmid segregation. Recently, Cook & Dunny (2013) showed that four non-conjugative plasmids had increased PCN and copy-number heterogeneity in *Enterococcus faecalis* biofilm cells and this was correlated with increased expression of plasmid-borne resistance genes. Conversely, it has also been demonstrated that, for some plasmids, plasmid loss is more significant in biofilm populations (Huang et al. 1993, Ma et al. 2013) and that this can be affected by the age of the biofilm (Madsen et al. 2013).

In this work, the pET system was used for the expression of a heterologous model protein, the eGFP. This family of vectors contains a pMB1 origin of replication (medium-

copy number replicon) and uses the T7 promoter for transcription of the foreign gene, which can be induced by lactose or its non-hydrolyzable analogue IPTG (Rosano & Ceccarelli 2014). This system is one of the most widely used expression systems in *E. coli* mainly due to its very high expression levels as the target protein can represent up to 50% of the total cell protein. However, it suffers from some drawbacks like the leaky expression (Rosano & Ceccarelli 2014), which is particularly serious in the expression of toxic proteins.

Until now there is only one publication addressing heterologous protein production in *E. coli* biofilms (O'Connell et al. 2007). In that study, eGFP expression was achieved by using a pUC-based vector containing a mutated pMB1 origin of replication and an IPTG inducible promoter. However, the effect of induction was not addressed. The main aim of this chapter was to evaluate the effects of IPTG induction in the potential of biofilm cells to produce a heterologous model protein.

8.2. Materials and methods

8.2.1. Bacterial strain and culture conditions

E. coli JM109(DE3) harbouring the plasmid pFM23 was used in this work for the cytoplasmic production of eGFP (Mergulhão & Monteiro 2007). The strain was grown in LB-Miller (Sigma, USA) supplemented with 20 μg ml^{-1} kanamycin (Eurobio, France).

8.2.2. High throughput screening of IPTG concentration and induction time

An overnight culture of the *E. coli* strain was prepared as described in Chapter 3, section 3.2.2. Cells were harvested by centrifugation and appropriate dilution in sterile saline was performed to obtain an OD of approximately 0.4 at 610 nm.

Five IPTG concentrations (in the 0-4 mM range) and three induction days (3, 5 and 7) were tested for biofilm formation and eGFP expression in the 96-well microtiter plate. The wells (6 for each IPTG concentration tested) were filled with 180 μl of LB medium and 20 μl of the inoculum previously prepared. For control, wells with *E. coli*

JM109(DE3) cells bearing the pET28A plasmid (Novagen, USA), which is the backbone of pFM23, were prepared. A total of 3 microtiter plates were prepared per experiment so that one plate was retrieved from the incubator for addition of IPTG at each induction day. The plates were incubated at 30 ºC during 11 days under the shaking conditions used for biofilm formation in Chapter 4 (section 4.2.2), being removed from the incubator every 2 days for medium replacement (Azevedo et al. 2014) and IPTG addition (at day 9 only the culture medium was replaced). At day 11, the bacterial suspension was discarded from all the plates and the wells were washed to remove nonadherent bacterial cells. The biofilms were suspended in 200 µl of Buffer I (50 mM Na_2HPO_4, 300 mM NaCl, pH 8) by pipetting up and down, and the OD and eGFP fluorescence were determined as indicated in Chapter 6, section 6.2.2. Three independent experiments were performed and the final values were expressed in specific fluorescence intensity (AFU per $OD_{610\ nm}$).

8.2.3. Biofilm formation system

The biofilms were grown in the flow cell system as described in Chapter 5, section 5.2.2. After 5 days of flow cell operation, induction was carried out by adding a single pulse of IPTG (BIORON GmbH, Germany) in order to obtain a final concentration of 2 mM in the medium. The biofilm and planktonic samples corresponding to day 5 were collected 6 h after IPTG addition.

The system can be considered as a well-mixed chemostat with irregular geometry (Teodósio et al. 2012b), thus the concentration of any substance in the effluent stream is identical to the concentration inside the system (Fogler 2006). A mass balance for the IPTG that was introduced as a pulse at time $t = 0$ into the recirculating tank yields for $t > 0$

$$In - Out = Accumulation \quad (1)$$

$$0 - FC = V\frac{dC}{dt} \quad (2)$$

C in Equation (2) is the concentration of IPTG either in the effluent or inside the system. Also F is the volumetric flow rate and V is the volume of flow cell system. Separating the variables and integrating with $C = C_0$ at $t = 0$ yields

$$C(t) = C_0 e^{-t/\tau} \quad (3)$$

where τ is the average residence time, which is defined as being equal to V/F. Equation (3) gives the concentration of IPTG within the reactor at any time t, which is represented for the flow cell system operating for further 6 days after IPTG addition (see Figure 8.3). The dilution rate (DR) of the chemostat is given by

$$DR = \frac{F}{V} \quad (4)$$

8.2.4. Estimation of IPTG transfer rate

The rate of IPTG transport from the bulk liquid to the biofilm surface was quantified through the external mass transfer coefficient (K_m).

The Sherwood number (Sh) for a fully developed concentration profile in turbulent flow conditions was calculated by Equation (5) as a function of Re valid in the range between 2,100 and 35,000, and Schmidt number (Sc) in the range between 0.6 and 3,000 (Perry & Green 1997).

$$Sh = 0.023\, Re^{0.83} Sc^{1/3} \quad (5)$$

With the Sherwood number estimated from Equation (5), the external mass transfer coefficient was calculated from the definition

$$K_m = \frac{Sh\, D_{aq}}{d} \quad (6)$$

where D_{aq} is the diffusion coefficient of IPTG in water (8.7 x 10^{-10} m^2 s^{-1} at 30 °C) (Stewart 2003) and d is the hydraulic diameter.

Immediately after IPTG addition, the concentration at the top of the biofilm is approximately zero and therefore the mass transfer rate ($\dot{n}$) can be estimated by

$$\dot{n} = K_m A C \quad (7)$$

where *A* is the coupon area.

8.2.5. Analytical methods

On each experimental day, a coupon was removed from the flow cell and the biofilm thickness was immediately determined using a digital micrometer. Then, the biofilm was resuspended and homogenized in NaCl solution for assessment of total and viable cells, and for quantification of eGFP and plasmid content.

Biofilm total (viable plus non-viable) and viable cell counts were assessed with the Live/Dead® *Bac*Light™ bacterial viability kit (Syto9/PI, Alfagene, Portugal) as indicated in Chapter 6, section 6.2.4. Results of total cell and viable counts were expressed as log cell cm^{-2}.

For planktonic cells, total and viable cell numbers were determined using the same method as for biofilms. Results were presented as log cell ml^{-1}.

8.2.6. Quantification of EPS

The content of EPS in biofilms (proteins and polysaccharides) was determined after 7 days of growth as fully described in Chapter 6, section 6.2.5.

8.2.7. Quantification of eGFP production

The eGFP expression in both planktonic and biofilm cells was analysed as described in Chapter 5, section 5.2.4, and the final values were presented as specific eGFP production (fg $cell^{-1}$).

The remaining volume of planktonic and biofilm samples was centrifuged and the pellets were immediately frozen for subsequent quantification of PCN and evaluation of eGFP gene transcription.

8.2.8. Quantification of PCN

8.2.8.1. Preparation of plasmid DNA (pDNA) standards

Plasmid DNA standards were prepared by growing *E. coli* JM109(DE3) cells harbouring the plasmid pFM23 in LB supplemented with 20 µg ml^{-1} kanamycin. Plasmid extraction and isolation was performed according to the High Pure Plasmid Isolation Kit (Roche, Germany) protocol. The concentration of purified pDNA solution was determined with a NanoDrop Spectrophotomer (NanoVue™ Plus, GE Healthcare, Germany) and the plasmid quality was assessed by gel electrophoresis (agarose 1% in TAE buffer 1x). Serial dilutions of plasmid (1, 10, 100, 1000 and 10000 pg per capillary) were conducted in triplicates to establish the standard curve.

8.2.8.2. Real-time PCR (RT-PCR)

The quantification of plasmid copy number in planktonic and biofilm samples was performed with the Roche LightCycler™ detection system using the FastStart DNA Master SYBR Green I Kit™ (Roche, Germany) (Carapuça et al. 2007). The detection of pDNA was performed by amplification of a 108 bp sequence from the eGFP gene using the TCGAGCTGGACGGCGACGTAAA forward primer, and TGCCGGTGGTGCAGATGAAC reverse primer.

Each 20 µl of final reaction volume contained 2 µl of the 10× SYBR Green mixture, 1 µl of each primer (10 µM final concentration), 1.6 µl of $MgCl_2$ solution (3 mM final concentration), 2 µl of sample prepared as described below and 12.4 µl of PCR grade water. Reactions were incubated at 95 ºC for 10 min to activate FastStart DNA polymerase and lyse cells, followed by the amplification step consisting of 30 cycles of 15 s at 95 ºC, 10 s at 55 ºC and 14 s at 72 ºC. Following the final cycle, reactions were kept at 70 ºC for 30 s and heat-denatured over a temperature gradient of 0.1 ºC s^{-1} from 70 to 95 ºC.

8.2.8.3. Sample preparation

Plasmid DNA samples for the construction of calibration curve were prepared by spiking 2 µl of purified pDNA standards with non-transformed *E. coli* JM109(DE3) cells.

Appropriate dilutions of the frozen pellets were made with MilliQ water in order to maintain the same number of total cells per reaction (3 x 10^5 cells). Determination of pDNA concentration in planktonic and biofilm cells was done for triplicate sets by mixing 2 µl of suspension with 3 x 10^5 of cells, 2 µl of PCR grade water and the other PCR reagents as described above.

The calibration curve was established according to the method of Lee et al. (2006). Briefly, it includes the plot of the cycle threshold (C_T) values versus the log concentration of the plasmid DNA standard. For the unknown pDNA samples, the plasmid concentration was obtained by interpolating its C_T value against the calibration curve. The corresponding PCN was then calculated using the Equation (8) (Whelan et al. 2003):

$$PCN = \frac{6.02\times10^{23}\ (copy\ mol^{-1}) \times DNA\ amount\ (g)}{DNA\ length\ (bp)\times 660\ (g\ mol^{-1}bp^{-1})} \quad (8)$$

knowing that the plasmid pFM23 has length of 6053 bp.

8.2.8.4. Quantification of total RNA

For planktonic and biofilm samples from day 7 containing a fixed amount of total cells (4 x 10^7 cells), RNA extraction was performed according to the High Pure RNA Isolation Kit™ (Roche, Germany) protocol. The concentration of RNA solution was then determined using the NanoDrop Spectrophotomer and the final values were presented as specific total RNA concentration (fg $cell^{-1}$). The analysed samples were from two independent experiments.

8.2.9. Quantification of eGFP gene transcription

The total RNA was first denatured by heating at 65 ºC for 15 min, followed by rapid chilling on ice. The cDNA synthesis was carried out using the First Strand cDNA Synthesis Kit (Roche, Germany) according to the manufacturer's recommendations.

Briefly, each reaction contained 10x Reaction Buffer, 25 mM $MgCl_2$ solution, dNTPs, reverse primer (TGCCGGTGGTGCAGATGAAC), RNase inhibitor, AMV reverse transcriptase, gelatin, the total RNA sample and PCR grade water to complete 30 µl of reaction volume. The mixture was incubated at 25 ºC for 10 min and at 42 ºC for more 2 h. Then the AMV reverse transcriptase was denatured by incubating the reaction at 99ºC for 5 min and cooling to 4 ºC for more 5 min. The relative amount of cDNA (and consequently of eGFP mRNA) was determined by RT-PCR, as previously described for PCN quantification, taking into account that the C_T values obtained are inversely proportional to the amount of eGFP cDNA in the sample. The final values per cell are presented in arbitrary units (AU $cell^{-1}$) for comparative purposes.

8.2.10. Statistical analysis

Average SDs were calculated for all planktonic and biofilm parameters presented in Figures 8.2 and 8.4. For biofilm formation (Figure 8.2), the following averages were obtained: SD < 2% for planktonic and biofilm total cells, SD < 3% for planktonic and biofilm viable cells, and SD < 17% for biofilm thickness. Concerning eGFP quantitation (Figure 8.4A), SD < 16% and SD < 7% were obtained for planktonic and biofilm cells, respectively. Regarding plasmid copy number (Figure 8.4B), SD < 33% and SD < 40% were obtained for planktonic and biofilm cells, respectively. For eGFP mRNA and total RNA determination (Figure 8.5), SD < 8% and SD < 22% were obtained for planktonic and biofilm cells, respectively.

For biofilm formation (Figure 8.2) and analysis of transcription and total RNA (Figure 8.5), paired *t*-test analysis was performed based on a confidence level of 90% (differences reported as significant for *P* values < 0.1 and marked with $*$) and 95% (differences reported as significant for *P* values < 0.05 and marked with $\overset{*}{*}$ or $**$). Paired *t*-test analysis based on a confidence level of 95% was performed to compare biofilm and planktonic curves in Figure 8.4 (differences between biofilm conditions were marked with †, while differences between planktonic conditions were indicated with ‡).

8.3. Results

8.3.1. High throughput screening of IPTG concentration and induction time

The 96-well microtiter plate was used in this chapter to find the concentration of IPTG and the induction day that yields the higher specific eGFP fluorescence in order to use these optimal parameters in the flow cell experiments. Figure 8.1 presents the values of specific eGFP fluorescence for 11-day-old biofilms formed during exposure to different concentrations of IPTG from day 3, 5 or 7. It is clear that the highest specific fluorescence value was obtained when the 5-day-old biofilm was induced with 2 mM IPTG. Furthermore, it can be concluded that in order to attain high specific fluorescence in biofilms induced later is necessary to use a higher IPTG concentration.

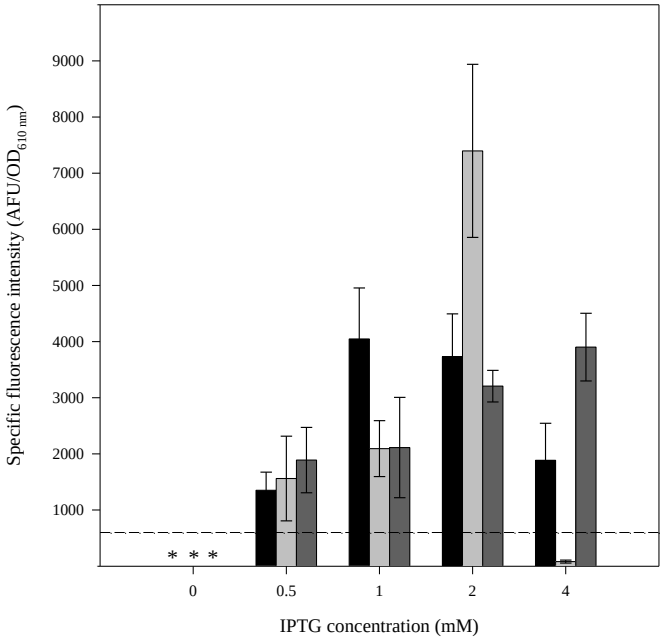

Figure 8.1. Screening of IPTG concentration and induction day in 96-well microtiter plates. Induction on day 3 (■), 5 (□) and 7 (■). The means ± SDs for three independent experiments are presented. * means that no fluorescence was detected. The dashed line corresponds to the detection limit of the method.

8.3.2. Effect of IPTG induction on planktonic and biofilm growth

The effect of IPTG induction on the dynamics of planktonic and biofilm growth in the flow cell system is presented in Figure 8.2. The growth of non-induced and induced planktonic cells was compared by determining the number of total (Figure 8.2A) and viable cells (Figure 8.2C). Planktonic cell concentration (Figure 8.2A) was practically constant throughout the experiment in the non-induced state, but a decrease was observed for the induced culture particularly towards the end of the experiment. A similar behaviour was observed for the number of viable cells (Figure 8.2C); however, statistically significant difference was found in the majority of experimental points ($P < 0.05$). Indeed, from day 5 onwards the values for the induced cells remained mostly lower (49%) than those determined in the non-induced culture. It is important to note that the IPTG decreased in the medium overtime, but it was present until the end of the experiment at concentrations above 0.24 mM (Figure 8.3).

The IPTG transport from the bulk medium to the top layer of the biofilm was also estimated. A maximum molar flux of 4.7 nmol s^{-1} was obtained by estimation of the external mass transfer coefficient (Equation 7) under the operational conditions. The impact of IPTG induction on biofilm development was also assessed by determining the amount of total (Figure 8.2B) and viable biofilm cells (Figure 8.2D), and the biofilm thickness (Figure 8.2E). The total cell and viable counts were very similar throughout the experiment and did not change significantly after exposure to IPTG. Nevertheless, the biofilm thickness was significantly higher for the induced biofilms from day 7 until the end of the experiment ($P < 0.05$, Figure 8.2E).

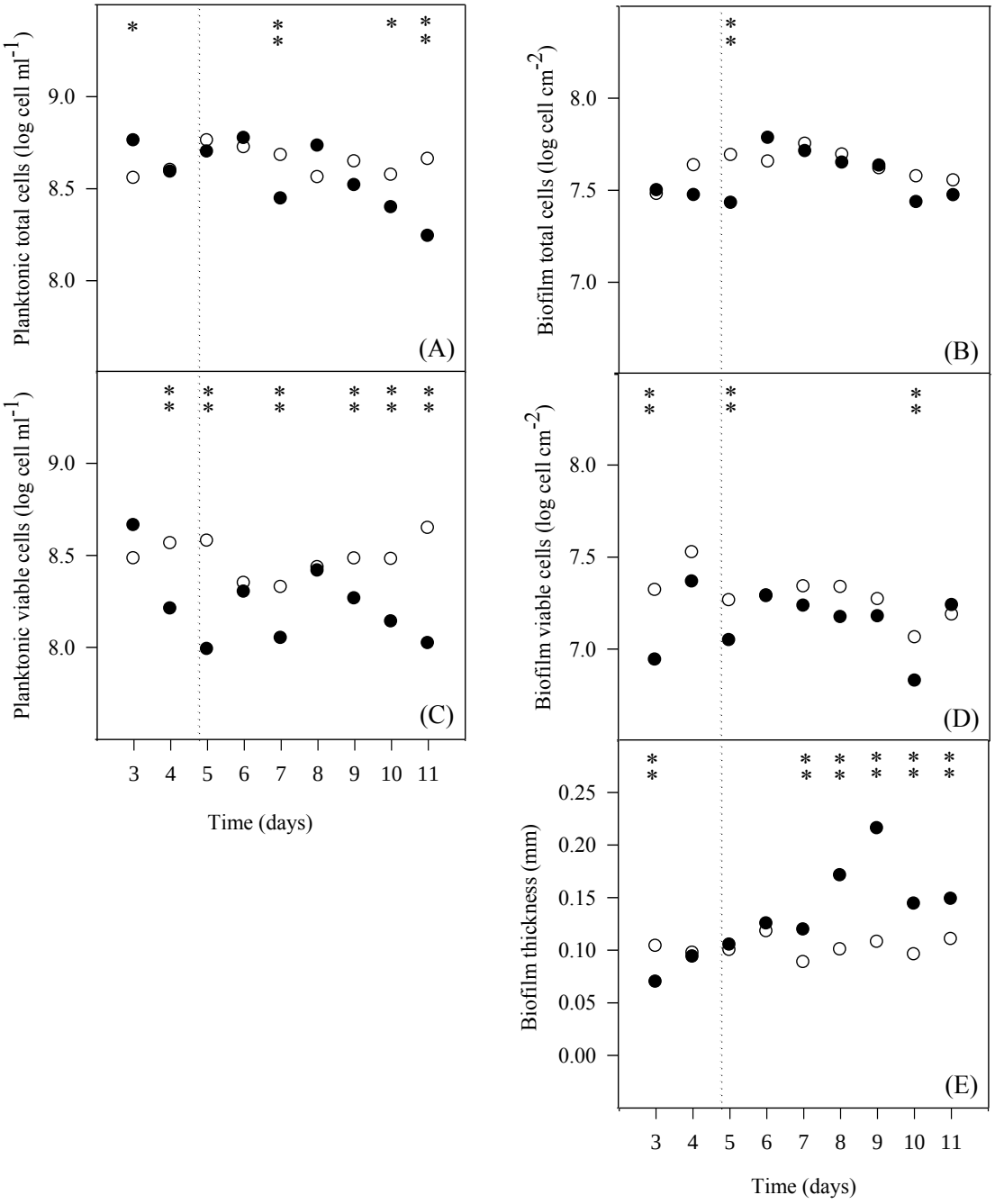

Figure 8.2. Time-course of planktonic and biofilm parameters: (A) planktonic total cells, (B) biofilm total cells, (C) planktonic viable cells, (D) biofilm viable cells, (E) biofilm thickness. Induced (●) and non-induced (○) LB culture. The dotted lines indicate the day on which the culture was induced with 2 mM IPTG. Results are an average of three independent experiments for each condition. Statistical analysis corresponding to each time point is represented with ∗ for a confidence level greater than 90% ($P < 0.1$) and with $\overset{*}{*}$ for a confidence level greater than 95% ($P < 0.05$).

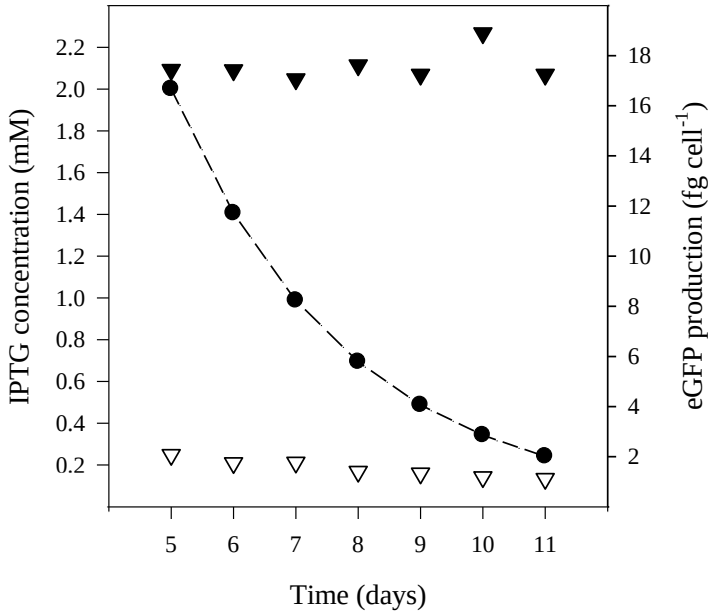

Figure 8.3. Time-course evolution of IPTG concentration within the flow cell system (−●−) and eGFP production in planktonic (▽) and biofilm (▼) cells. The culture was induced with 2 mM IPTG on day 5.

The EPS composition of 7-day-old biofilms was analysed (Table 8.1) and no significant differences were observed with IPTG induction as the dry mass, cell density and also the protein and polysaccharide levels of the matrix were similar ($P > 0.05$).

Table 8.1. EPS analysis of induced and non-induced biofilms after 7 days of growth

Biofilm characteristics	**Induced**	**Non-induced**
Biofilm dry weight ($mg_{biofilm}\ cm^{-2}$)	4.00 ± 1.17	4.50 ± 0.870
Log cellular density (cells cm^{-2})	7.83 ± 0.460	7.76 ± 0.460
Matrix proteins ($mg\ g^{-1}_{biofilm}$)	8.60 ± 1.80	9.40 ± 1.70
Matrix polysaccharides ($mg\ g^{-1}_{biofilm}$)	249 ± 41.0	231 ± 35.0

8.3.3. Determination of eGFP, PCN, mRNA and total RNA

The progression of specific eGFP production and plasmid copy number during planktonic and biofilm growth were monitored for non-inducing and inducing conditions (Figure 8.4). Comparing expression in planktonic and sessile cells (Figure 8.4A), it is clear that the biofilm state increased heterologous protein production (6- and 9-fold for non-induced and induced cultures, respectively). Specific eGFP production from planktonic cells decreased (approximately 87%) between days 3 and 8 in both induced and non-induced states. Furthermore, the eGFP levels in induced planktonic cells were similar to the leaky expression from the non-induced cells. The eGFP production from biofilm cells remained approximately constant for the induced culture (pre-induction levels were maintained at around 18 fg cell^{-1}), whereas a decrease in production (of about 30%) was observed on the non-induced cells. Thus, it seems that IPTG induction had a more pronounced effect on biofilm that in planktonic cells (Table 8.2).

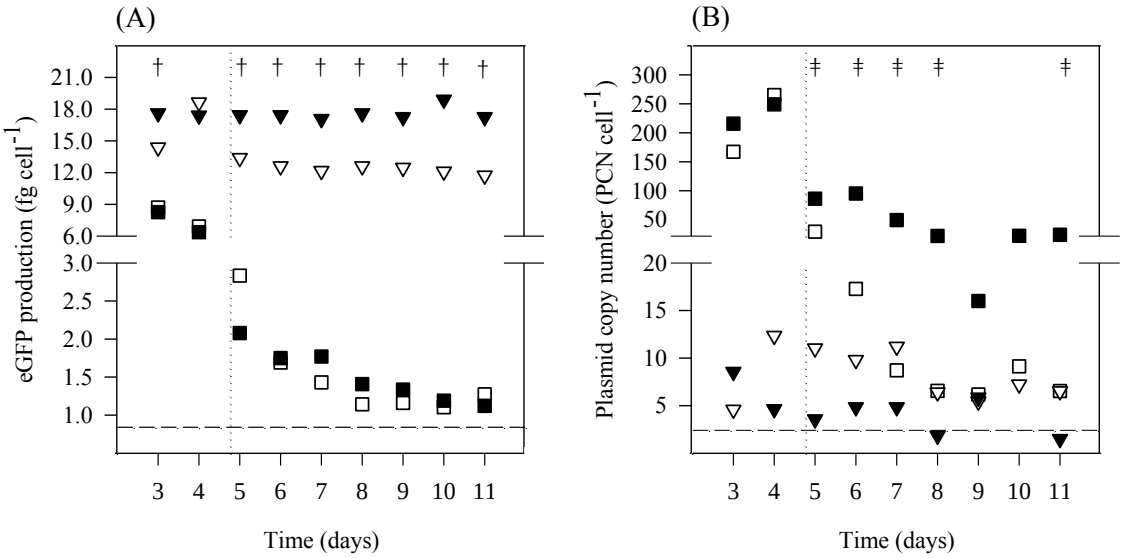

Figure 8.4. Time-course of (A) eGFP production and (B) plasmid copy number for planktonic and biofilm cells. Induced (▼) and non-induced (▽) biofilm cells; induced (■) and non-induced (□) planktonic cells. The vertical dotted lines indicate the day on which the culture was induced with 2 mM IPTG and the horizontal dashed lines correspond to detection limits of the methods. Results are an average of three independent experiments for each condition. Statistical analysis for a confidence level greater than 95% ($P < 0.05$) are pointed as † when induced biofilm cells are different from the non-induced biofilm cells, and as ‡ when induced planktonic cells are different from the non-induced planktonic cells.

Table 8.2. Specific eGFP production of planktonic and biofilm cells in the different cultivation conditions tested in this thesis: DM with 20 and 30 μg ml^{-1} kanamycin, LB with 20 μg ml^{-1} kanamycin, and LB with 20 μg ml^{-1} kanamycin and 2 mM IPTG. The results presented were obtained under steady state (between days 7 and 11)

Medium	Kanamycin concentration (μg ml^{-1})	IPTG concentration (mM)	Specific eGFP production (fg $cell^{-1}$)	
			Planktonic	Biofilm
DM[1]	20	0	0.060	5.7
DM[1]	30	0	0.67	6.2
LB[1]	20	0	1.2	12
LB	20	2	1.4	18

[1]values obtained in these conditions were originally reported in Table 6.1

The PCN (Figure 8.4B) was higher in planktonic than in sessile cells (7 and 20 fold higher for non-induced and induced cultures, respectively), showing that until day 3 the adhered cells lost most of the plasmid content. However, there was a strong loss of plasmid in planktonic cells after day 4 for both non-induced and induced cultures (around 95% and 80%, respectively). In the biofilms, these reductions were much smaller since the PCN reduced about 40% in the induced cultures and there was no loss of plasmid in the non-induced cultures.

The levels of mRNA and total RNA for day 7 are presented in Figure 8.5. Higher transcription of the *eGFP* gene occurred in planktonic cells when compared to biofilms (average $P < 0.1$), independently of the presence of IPTG (Figure 8.5A). Furthermore, transcription was more intense upon induction in both planktonic and biofilm environments (average $P < 0.05$) (Figure 8.5A). Observing the total RNA levels (Figure 8.5B), higher values were obtained for planktonic cells ($P < 0.1$) and total RNA levels in both types of cells decreased after induction.

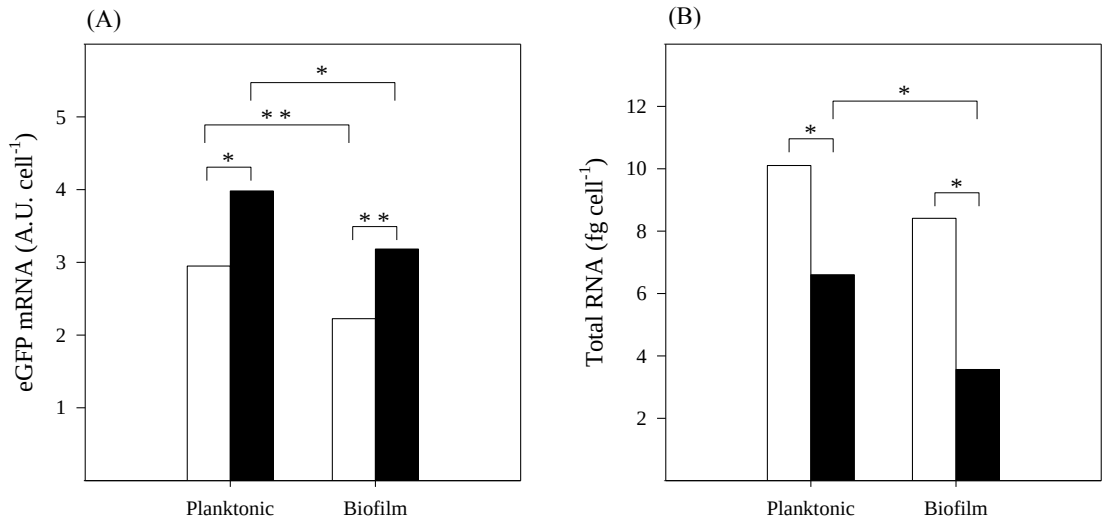

Figure 8.5. (A) Quantification of *eGFP* gene transcription and (B) total RNA concentration for planktonic and biofilm cells on day 7. Induced (■) and non-induced (□) cells. Results are an average of two independent experiments for each condition using the same quantity of cells. Statistical analysis corresponding to each time point is represented with ∗ for a confidence level greater than 90% ($P < 0.1$) and with ∗∗ for a confidence level greater than 95% ($P < 0.05$).

8.4. Discussion

The flow cell system used in this work can be considered as a chemostat with an irregular geometry (Stoodley & Warwood 2003, Teodósio et al. 2012b). For planktonic cells, under steady-state conditions, the dilution rate is equal to the specific growth rate of bacteria. A constant cellular concentration was reached for the non-induced planktonic culture, and therefore the specific *E. coli* growth rate was of 0.015 h^{-1}. Specific growth rates in batch culture were determined for this strain and values around 0.7 h^{-1} were obtained, indicating that the dilution rate used in these experiments was much lower than the critical dilution rate for non-induced conditions.

Since the planktonic cell concentration decreased for the induced culture, mostly towards the end of the experiment, its growth rate was below 0.015 h^{-1}. Taking into account that the non-induced culture can grow at this temperature and in this growth medium at specific growth rates that far exceed this value (as determined in batch cultivation), it is plausible to assume that IPTG induction had effect on the metabolism of planktonic cells. A reduction in cell growth rates upon induction had already been demonstrated for plasmid-bearing cells (Bentley et al. 1991, Neubauer et al. 1992, Wood

& Peretti 1991). It has been proposed that cell growth arrest is caused by the metabolic stress which an expression vector imposes upon induction, including sequestering of cellular resources for transcription and translation of the target gene. In the present study, since the amount of eGFP produced by induced and non-induced planktonic cells was similar, the reduction of cell density in the induced culture was possibly a consequence of the metabolic drain of biosynthetic precursors, energy and other cellular components for plasmid replication and transcription. IPTG induction had a negative effect not only on growth, but also on cellular viability of *E. coli* suspended cultures. Although IPTG was added in a single pulse, it was estimated that the inducer was present in the bulk medium at high concentrations (above 0.24 mM) until the end of the experiment. This long term exposure may explain the deleterious effects on growth and viability of planktonic cells.

IPTG addition had different effects on planktonic and biofilm cells. As far as biofilm development is concerned, there were no major observed effects on the biofilm cell number, viability or even EPS composition. It was therefore important to estimate if the IPTG that was added as a pulse to the bulk medium would reach the biofilm so that biofilm cells could be induced. A crude estimation of the external mass transfer coefficient allowed us to estimate that a molar flux of 4.7 nmol s^{-1} can reach the surface of the biofilm. Although this does not guarantee that the inducer reaches all the biofilm cells, previous studies have shown that this molecule readily penetrates biofilms and it has been estimated that it can take up to 7 minutes for IPTG to cross a 300-μm-thick biofilm (Stewart 2003, Werner et al. 2004). Heterologous protein expression levels in our system were maintained from day 6 onwards. On that day, biofilm thickness was around 100 μm and therefore it is very likely that IPTG was able to cross the biofilm effectively during the timescale of the experiment. Additionally, IPTG is not hydrolysed (Fernández-Castané et al. 2012), therefore there is no capture of this compound within sessile bacteria and it can get in and out of the cell at the same rate. It was recently demonstrated for high cell density cultures that the majority of inducer remains in the medium and that at high IPTG concentrations (40-1000 μM) only a minor amount of inducer is taken up by the biomass (Fernández-Castané et al. 2012). Hence, in the present work, the IPTG depletion from the growth medium is controlled by the average residence time in the whole system.

Regarding biofilm formation, the non-accumulation of bacterial cells after induction corroborates the results obtained by Huang et al. (1994a) using *E. coli* DH5α(pTKW106) cultures exposed to the highest IPTG concentration tested (0.51 mM).

However, the biofilm thickness was higher for the induced biofilms from day 7 onwards. Since the EPS content of induced and non-induced biofilms was similar, we believe that the increase of thickness was an architectural change of the biofilm itself in an attempt to adapt to the introduction of IPTG in the culture medium. In a previous work (Teodósio et al. 2011a), it was shown that biofilms adjust their architecture in order to cope with the hydrodynamic conditions and nutrient availability.

By comparing the eGFP concentrations in planktonic and biofilm cells, it is possible to conclude that the inducer had an instantaneous effect on sessile cells, preventing the overall decrease in the amount of expressed eGFP. A fast IPTG response was also obtained by Stewart (2003) and Lenz et al. (2008), who reported the appearance of a green fluorescent band in *P. aeruginosa* biofilms after only 4 h of induction, whether IPTG was applied from the bottom of colony biofilms or from the liquid medium in drip-flow cultivated biofilms. Other reports on *E. coli* biofilms (Bryers & Huang 1995, Huang et al. 1994a) confirmed the variation in recombinant protein concentration in the first hours of induction. In the present work, a lower amount of eGFP mRNA was detected after induction in biofilm cells than in planktonic cells. However, since lower levels of total RNA were also measured in biofilm cells and these are essentially ribosomal RNA (rRNA) (Berg et al. 2002), it is possible that the biofilm was metabolically less active and therefore more cellular resources were available to produce the heterologous protein. It is interesting to observe that upon induction, the total RNA levels of both planktonic and biofilm cells decrease. This effect was previously reported by Dong et al. (1995) and it can be an indication that the overall protein translation activity is decreased in induced cells. In our system, a relatively constant biofilm cell number was observed after induction. Thus, biofilm growth rate was similar to biofilm detachment rate. If cells are growing more slowly in biofilms (Donlan 2000), the production of housekeeping proteins also decreases and consequently more cellular resources will become available for heterologous protein production.

Contrary to what was expected, heterologous protein production from planktonic cells did not benefit from IPTG induction since expression levels were similar to the leaky expression from the non-induced culture. It was demonstrated that IPTG was present in the culture medium until the end of the experiment and it has been shown that a 6-fold lower concentration than what was determined may be enough for full induction (Fernández-Castané et al. 2012). Despite this fact, it has also been reported that omission of IPTG in the culture medium may be beneficial in the expression of some types of

recombinant proteins, particularly when LB medium is used (Zhang et al. 2015). It has also been suggested that IPTG addition can be deleterious in the expression of recombinant proteins when using high-copy plasmids (Jones et al. 2000). The pET plasmid contains a pMB1 origin of replication and is considered a medium-copy number plasmid with an expected PCN between 15 and 60 (Rosano & Ceccarelli 2014). Although we have shown that it can reach a PCN of about 200 copies, its steady state values are closer to 50 (for the induced planktonic culture) or around 10 or below for biofilm cells and non-induced planktonic cultures. It is interesting to observe that the most beneficial effects of induction were observed in the cells which contain a lower PCN.

Although a high concentration of IPTG was available in the growth medium, both induced and non-induced planktonic cells presented the same specific eGFP concentration. We have already concluded that heterologous protein production from induced planktonic cells is not limited by inducer concentration, gene dosage or transcriptional activity. The translational capacity of induced planktonic cells is probably higher than in induced biofilm cells as total RNA levels are also higher. Thus, the high level eGFP production from induced planktonic cells may be due to the high metabolic burden associated with plasmid replication since PCN in induced planktonic cultures is on average 5 fold higher than in non-induced cells. The plasmid replication probably causes a high metabolic drain not only in terms of the requirement of nucleotides, but also in the expression of the antibiotic resistance gene (Bentley et al. 1990). Thus, for producing the same amount of eGFP, the higher levels of total RNA in planktonic non-induced cells may compensate for the lower gene dosage effect of these cells when compared to planktonic induced cells. The absence of an increase in the eGFP concentration of induced cells may be related with the leakage of recombinant protein into the extracellular medium caused by the loss of membrane integrity, as previously reported by Lowder et al. (2000). This phenomenon of cell lysis is supported by the strong decline in the number of viable cells in suspended cultures immediately after IPTG addition.

It is well known that plasmid stability is a key issue in recombinant protein production (Mergulhão et al. 2004b). There is a considerable amount of information available on the plasmid stability in *E. coli* batch cultures (e.g. (Bentley et al. 1990, Birnbaum & Bailey 1991, Carrier et al. 1998), but little is known about the influence of biofilm development on the plasmid copy number and recombinant protein expression. In this work, higher specific eGFP concentrations were detected in biofilm cells, where a

smaller number of copies of plasmid pFM23 was found compared to planktonic cells. Even within biofilms cells, a higher PCN was obtained in non-induced cells, whereas higher eGFP production was achieved with induction. Thus, the gene dosage was not controlling the production of eGFP in both types of cells. The same phenomenon was observed by Bhattacharya & Dubey (1995) in *E. coli* suspensions where induced cultures had 17% more foreign protein, even though they only presented a PCN of 65 against 75 of non-induced cultures. Similarly to our results, the increased metabolic burden derived from the higher recombinant protein production in biofilm cells may have itself contributed to PCN depression, as observed by Ricci & Hernández (2000) for batch cultures.

From the PCN results, it can be established that the biofilm mode of growth had a beneficial effect on plasmid retention. This agrees with the results obtained in previous studies (Davies & Geesey 1995, May et al. 2009, O'Connell et al. 2007) and can be explained by the fact that cells in biofilms tend to grow more slowly than their planktonic counterparts (Donlan 2000), leading to fewer cell divisions and correspondingly less plasmid segregation.

This work presents a contribution to the study of IPTG induction on heterologous protein expression in planktonic and sessile cells. To the best of our knowledge, this is the first report that does a complete characterization of induction effects in both types of *E. coli* cells, including experimental data on plasmid stability, recombinant protein transcription and translation and cellular metabolic activity. This full molecular analysis was complemented with the theoretical determination of IPTG levels in suspension and on the liquid/biofilm interface. It is expected that the obtained results will be of value to elucidate the mechanisms of induction on heterologous protein production, especially in biofilm cells which have already shown potential to be used as protein factories.

8.5. References

Azevedo AS, Almeida C, Melo LF, Azevedo NF. 2014. Interaction between atypical microorganisms and *E. coli* in catheter-associated urinary tract biofilms. Biofouling. 30:893-902.

Bentley WE, Davis RH, Kompala DS. 1991. Dynamics of induced CAT expression in *E. coli*. Biotechnol Bioeng. 38:749-760.

Bentley WE, Mirjalili N, Andersen DC, Davis RH, Kompala DS. 1990. Plasmid-encoded protein: the principal factor in the "metabolic burden" associated with recombinant bacteria. Biotechnol Bioeng. 35:668-681.

Berg J, Tymoczko J, Stryer L. 2002. Gene Expression Is the Transformation of DNA Information Into Functional Molecules. Biochemistry. New York: W.H. Freeman and Company.

Bhattacharya S, Dubey A. 1995. Metabolic burden as reflected by maintenance coefficient of recombinant *Escherichia coli* overexpressing target gene. Biotechnol Lett. 17:1155-1160.

Birnbaum S, Bailey JE. 1991. Plasmid presence changes the relative levels of many host cell proteins and ribosome components in recombinant *Escherichia coli*. Biotechnol Bioeng. 37:736-745.

Bryers JD, Huang C-T. 1995. Recombinant plasmid retention and expression in bacterial biofilm cultures. Wat Sci Tech. 31:105-115.

Carapuça E, Azzoni AR, Prazeres DM, Monteiro GA, Mergulhão FJ. 2007. Time-course determination of plasmid content in eukaryotic and prokaryotic cells using real-time PCR. Mol Biotechnol. 37:120-126.

Carrier T, Jones KL, Keasling JD. 1998. mRNA stability and plasmid copy number effects on gene expression from an inducible promoter system. Biotechnol Bioeng. 59:666-672.

Cook LC, Dunny GM. 2013. Effects of biofilm growth on plasmid copy number and expression of antibiotic resistance genes in *Enterococcus faecalis*. Antimicrob Agents Chemother. 57:1850-1856.

Davies DG, Geesey GG. 1995. Regulation of the alginate biosynthesis gene algC in *Pseudomonas aeruginosa* during biofilm development in continuous culture. Appl Environ Microbiol. 61:860-867.

Diaz Ricci JC, Hernández ME. 2000. Plasmid effects on *Escherichia coli* metabolism. Crit Rev Biotechnol. 20:79-108.

Dong H, Nilsson L, Kurland CG. 1995. Gratuitous overexpression of genes in *Escherichia coli* leads to growth inhibition and ribosome destruction. J Bacteriol. 177:1497-1504.

Donlan RM. 2000. Role of biofilms in antimicrobial resistance. ASAIO J. 46:S47-52.

Fernández-Castané A, Caminal G, López-Santín J. 2012. Direct measurements of IPTG enable analysis of the induction behavior of *E. coli* in high cell density cultures. Microb Cell Fact. 11:1-9.

Fogler HS. 2006. Distributions of Residence Times for Chemical Reactors. In: Fogler HS, editor. Elements of Chemical Reaction Engineering. Upper Saddle River: Prentice Hall. p. 867-944.

Huang C-T, Peretti SW, Bryers JD. 1993. Plasmid retention and gene expression in suspended and biofilm cultures of recombinant *Escherichia coli* DH5α(pMJR1750). Biotechnol Bioeng. 41:211-220.

Huang C-T, Peretti SW, Bryers JD. 1994a. Effects of inducer levels on a recombinant bacterial biofilm formation and gene expression. Biotechnol Lett. 16:903-908.

Jones KL, Kim S-W, Keasling JD. 2000. Low-copy plasmids can perform as well as or better than high-copy plasmids for metabolic engineering of bacteria. Metab Eng. 2:328-338.

Lee C, Kim J, Shin SG, Hwang S. 2006. Absolute and relative QPCR quantification of plasmid copy number in *Escherichia coli*. J Biotechnol. 123:273-280.

Lenz AP, Williamson KS, Pitts B, Stewart PS, Franklin MJ. 2008. Localized gene expression in *Pseudomonas aeruginosa* biofilms. Appl Environ Microbiol. 74:4463-4471.

Lowder M, Unge A, Maraha N, Jansson JK, Swiggett J, Oliver JD. 2000. Effect of starvation and the viable-but-nonculturable state on green fluorescent protein (GFP) fluorescence in GFP-tagged *Pseudomonas fluorescens* A506. Appl Environ Microbiol. 66:3160-3165.

Ma H, Katzenmeyer KN, Bryers JD. 2013. Non-invasive in situ monitoring and quantification of TOL plasmid segregational loss within *Pseudomonas putida* biofilms. Biotechnol Bioeng. 110:2949-2958.

Madsen JS, Burmolle M, Sorensen SJ. 2013. A spatiotemporal view of plasmid loss in biofilms and planktonic cultures. Biotechnol Bioeng. 110:3071-3074.

May T, Ito A, Okabe S. 2009. Induction of multidrug resistance mechanism in *Escherichia coli* biofilms by interplay between tetracycline and ampicillin resistance genes. Antimicrob Agents Chemother. 53:4628-4639.

Mergulhão FJ, Monteiro GA. 2007. Analysis of factors affecting the periplasmic production of recombinant proteins in *Escherichia coli*. J Microbiol Biotechnol. 17:1236–1241.

Mergulhão FJM, Summers DK, Monteiro GA. 2005. Recombinant protein secretion in *Escherichia coli*. Biotechnol Adv. 23:177-202.

Mergulhão FJM, Monteiro GA, Cabral JMS, Taipa MA. 2004b. Design of bacterial vector systems for the production of recombinant proteins in *Escherichia coli*. J Microbiol Biotechnol. 14:1-14.

Neubauer P, Hofmann K, Holst O, Mattiasson B, Kruschke P. 1992. Maximizing the expression of a recombinant gene in *Escherichia coli* by manipulation of induction time using lactose as inducer. Appl Microbiol Biotechnol. 36:739-744.

O'Connell HA, Niu C, Gilbert ES. 2007. Enhanced high copy number plasmid maintenance and heterologous protein production in an *Escherichia coli* biofilm. Biotechnol Bioeng. 97:439-446.

Perry RH, Green DW. 1997. Perry's Chemical Engineers' Handbook. New York: McGraw-Hill.

Rosano GL, Ceccarelli EA. 2014. Recombinant protein expression in *Escherichia coli*: advances and challenges. Front Microbiol. 5:172.

Stewart PS. 2003. Diffusion in biofilms. J Bacteriol. 185:1485-1491.

Stoodley P, Warwood BK. 2003. Use of Flow Cells an Annular Reactors to Study Biofilms. In: Lens P, O'Flaherty V, Moran AP, Stoodley P, Mahony T, editors. Biofilms in Medicine, Industry and Environmental Biotechnology: Characteristics, Analysis and Control. Cornwall: IWA Publishing. p. 197-213.

Teodósio JS, Simões M, Melo LF, Mergulhão FJ. 2011a. Flow cell hydrodynamics and their effects on *E. coli* biofilm formation under different nutrient conditions and turbulent flow. Biofouling. 27:1-11.

Teodósio JS, Simões M, Alves MA, Melo LF, Mergulhão FJ. 2012b. Setup and validation of flow cell systems for biofouling simulation in industrial settings. Scientific World J. 2012:ID 361494.

Werner E, Roe F, Bugnicourt A, Franklin MJ, Heydorn A, Molin S, Pitts B, Stewart PS. 2004. Stratified growth in *Pseudomonas aeruginosa* biofilms. Appl Environ Microbiol. 70:6188-6196.

Whelan JA, Russell NB, Whelan MA. 2003. A method for the absolute quantification of cDNA using real-time PCR. J Immunol Methods. 278:261-269.

Wood TK, Peretti SW. 1991. Effect of chemically-induced, cloned-gene expression on protein synthesis in *E. coli*. Biotechnol Bioeng. 38:397-412.

Zhang Z, Kuipers G, Niemiec Ł, Baumgarten T, Slotboom DJ, de Gier J-W, Hjelm A. 2015. High-level production of membrane proteins in *E. coli* BL21(DE3) by omitting the inducer IPTG. Microb Cell Fact. 14:1-11.

9.

Monitoring heterologous protein production in *E. coli* biofilms using bulk and single-cell analysis[h]

Abstract

Heterologous protein production in *E. coli* has been established in the past decades and the development of new monitoring methods has been encouraged by the need to evaluate the influence of processing conditions during production and also for optimization purposes. In this work, two different techniques based on fluorescence were used to monitor the production of a model heterologous protein (eGFP) by *E. coli* biofilms. Bulk production levels were assayed by fluorometry, whereas single-cell analysis was performed by epifluorescence microscopy in induced and non-induced cultures. Both methods showed the same evolution in the bulk production of the model protein and the induction effect was clearly demonstrated by an increase in the specific production after only 6 h of IPTG induction. Induction not only increased specific production, but also increased the heterogeneity of eGFP production within the biofilms.

Analysis at single-cell level enabled the identification of the production bottleneck in this system, consisting in the low percentage of expressing cells in the biofilm population. Identification of this bottleneck allows the design of optimization strategies to increase the bulk production of heterologous protein during process development.

[h] The content of this chapter was adapted from the following publication(s):

Gomes LC, Mergulhão FJ. Monitoring heterologous protein production by *Escherichia coli* biofilms using bulk and single-cell analysis (manuscript in preparation).

9.1. Introduction

Over the past decades, remarkable progresses in recombinant protein technology have led to the development of many processes for the production of high-value proteins with a wide range of applications including cancer treatment, detergent production or food processing applications (Palomares et al. 2004). Although recombinant protein expression in mammalian systems is very attractive for the production of complex proteins that require post-translational modifications (Folsom et al. 2010), *E. coli* remains as one of the favourite hosts for heterologous protein production (Mergulhão et al. 2004b, Sanchez-Garcia et al. 2016). *E. coli* biofilms have a great potential to be used as microbial cell factories, but until now only few studies have addressed this expression system. Initial investigations on the productive power of *E. coli* biofilms were made by Huang et al. (1993, 1994a, 1995**)** in the expression of β-galactosidase. Much later, a study from O'Connell et al. (2007) has shown that the biofilm environment enhanced the production of eGFP when compared to planktonic cells. These authors have used relatively thin biofilms (30-45 μm) and this finding was confirmed in Chapter 5 with much thicker biofilms (1200 μm), enabling specific productivities of eGFP that are in the range that can be obtained by high cell density cultivation. The study made by O'Connell et al. (2007) was the first to include single-cell analysis of heterologous protein production in *E. coli* biofilms (assessed by flow cytometry), but recently it has been shown that epifluorescence microscopy can also be used for this purpose (Folsom et al. 2010).

During recombinant protein production, it is crucial to monitor the amount of target protein produced by the culture. If this protein exhibits fluorescence, like in the case of GFP and its derivatives, fluorometry is the method of choice because of its high sensitivity, specificity (Drees & Wu 2013, Naresh 2014), simplicity and low instrumental costs when compared to other analytical techniques (Bongaerts et al. 2002, Naresh 2014) like flow cytometry. A fluorometer generates the wavelength of light required to excite the fluorochrome and selectively transmits the wavelength of light emitted, measuring the intensity of this light. Since the emitted light is directly proportional to the concentration of the fluorochrome being measured (Bongaerts et al. 2002, Naresh 2014), its concentration can be readily determined using a calibration curve. This type of analysis is very important during heterologous protein expression in biofilms, but it may be insufficient since biofilms are known to be heterogeneous and contain several subsets of

cells in different physiological states (Stewart & Franklin 2008). In fact, the chemical gradients that are established at different depths in biofilms can promote differences in cell enzymatic activities (Huang et al. 1998, Werner et al. 2004) and create variation at gene and protein levels (Beloin et al. 2004, Lenz et al. 2008, O'Connell et al. 2007, Rani et al. 2007). As mentioned before, only a couple of studies have analysed the productive potential of *E. coli* biofilm cells (Bryers & Huang 1995, Huang et al. 1993, Huang et al. 1994a, O'Connell et al. 2007). Although some insights were obtained from these studies, none of them addressed the effect of chemical induction on *E. coli* biofilm cells at single-cell level.

The aim of this chapter was to analyse the effects of IPTG addition on *E. coli* biofilm cells using fluorometry as a bulk method (fluorometry) and epifluorescence microscopy at single-cell level. The type of information that can be gathered by each method will be compared, thus providing a more detailed analysis of the induction phenomenon and enabling the development of more efficient production strategies using inducible biofilm cells.

9.2. Materials and methods

9.2.1. Biofilm formation system and induction conditions

The biofilms of *E. coli* JM109(DE3) harbouring the plasmid pFM23 were grown on the flow cell system as described in Chapter 8, section 8.2.3. After 5 days of flow cell operation, induction was carried out by adding a single pulse of IPTG (BIORON GmbH, Germany) to the recirculating tank to a final concentration of 2 mM. The planktonic and biofilm samples corresponding to day 5 were collected 6 h after IPTG addition.

9.2.2. Biofilm analysis

The flow cell system was stopped each day to allow coupon removal, and the biofilm formed on it was resuspended and homogenized for eGFP analysis by fluorometry and epifluorescence microscopy. Biofilm total and eGFP-expressing cell counts were also assessed as indicated in Chapter 7, section 7.2.2.

9.2.2.1. Quantification of eGFP expression by fluorometry

The eGFP expression in both induced and non-induced biofilm cells was analysed as described in Chapter 5, section 5.2.4, and the final values were presented as specific eGFP production (fg $cell^{-1}$).

9.2.2.2. Quantification of eGFP expression by epifluorescence microscopy

The eGFP expression in induced and non-induced biofilm cells was determined by epifluorescence microscopy according to the procedure described in Chapter 7, section 7.2.2.2. For each microscopic image, the mean fluorescence intensity was expressed as the mean of the fluorescence values of individual cells, in turn obtained by averaging each cell pixel intensity value. The signal intensity of the most and less green fluorescent cell in each image was also extracted. The fluorescence intensity values are presented in AFUs.

9.2.3. Calculations and statistical analysis

The specific fluorescence intensity values (AFU $cell^{-1}$) presented in Figure 9.1 correspond to the average of the mean fluorescence intensity calculated for each of the 45 images analysed on each experimental day.

The percentage of eGFP-expressing cells in the biofilm (Figure 9.2B) was calculated by dividing the number of eGFP-expressing cells by the total number of cells.

The maximum and minimum single-cell fluorescence were chosen to express the temporal evolution of populations of maximum and minimum eGFP-producing cells, respectively, after IPTG induction (Figure 9.3). The maximum and minimum fluorescence values of the 45 images analysed each day were arranged in ascending order (Figure 9.3).

Paired *t*-test analysis was performed based on a confidence level of 90% (differences reported as significant for P values < 0.1) and 95% (differences reported as significant for P values < 0.05).

9.3. Results

In this work, two fluorescence-based techniques (fluorometry and epifluorescence microscopy) were firstly compared for the purpose of monitoring eGFP production in *E. coli* biofilms. Figure 9.1 presents the eGFP production values obtained during biofilm development by the non-induced culture. Both methods yield very similar results, although calibration of the fluorometer readout enables a more straightforward determination of the mass production from the bulk biofilm cells. The specific fluorescence intensity and eGFP production increased from day 3 to day 4, having reached a maximum on the latter day. A severe reduction in the specific production (about 30%) was observed between days 4 and 5, followed by a smother reduction (12%) towards the end of the experiment.

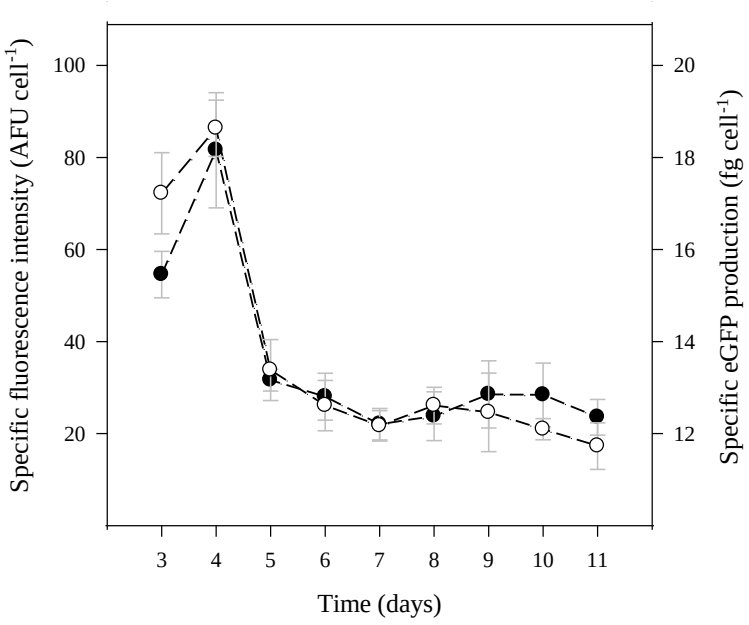

Figure 9.1. Comparison of time-course evolution of specific fluorescence intensity assayed by fluorometry (-●-) and eGFP production assayed by microscopy (-○-) for non-induced biofilms (secondary axis). The means ± SDs for three independent experiments are illustrated.

The effect of IPTG induction on eGFP concentration was analysed by fluorometry (Figure 9.2A) and the percentage of expressing cells was analysed by epifluorescence microscopy (Figure 9.2B). Results from Figure 9.2A seem to indicate that induction

avoided the decrease (of about 30%) in the eGFP concentration after day 4, maintaining the protein levels around 18 fg cell^{-1} until the end of experiment. However, Figure 9.2B shows that a strong reduction (of approximately 80%) in the percentage of eGFP-producing cells was observed upon induction and that this reduction is higher than the one observed in non-induced cells. Combining this information with the data from Figure 9.2A it is possible to conclude that if the percentage of expressing cells decreases after day 4 and the "bulk" production level stabilises, the specific production from expressing cells must be highly increased upon induction. Figure 9.2B also shows that from day 5 onwards, the percentage of expressing cells in induced conditions oscillated at a level of 10%, whereas for the non-induced state, expressing cells represented 23% of the biofilm population from day 6 onwards. The total number of biofilm cells was similar in both induced and non-induced cultures (4×10^7 cells cm^{-2}).

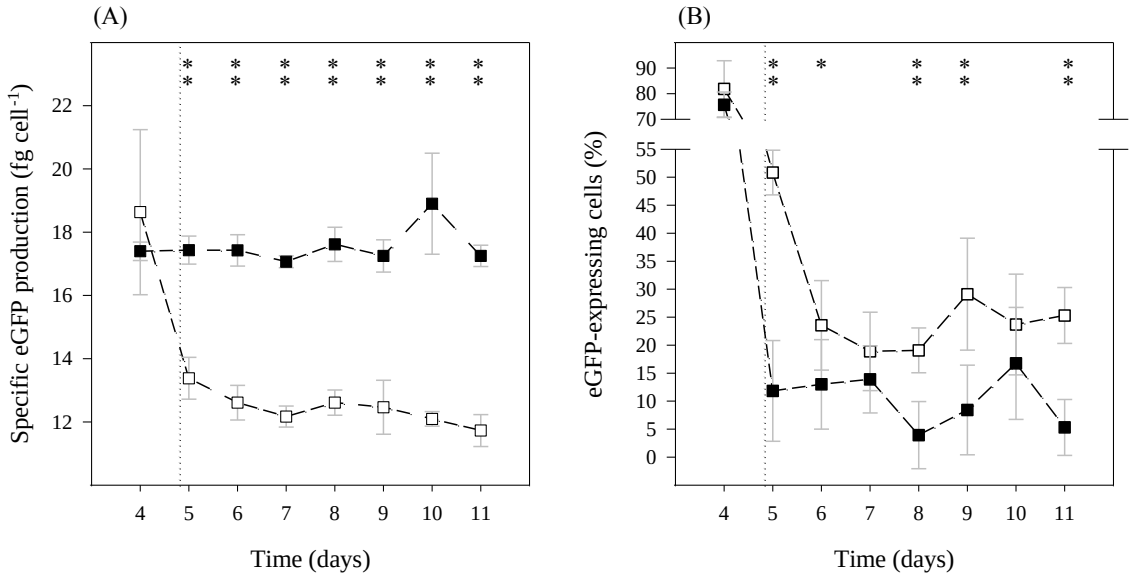

Figure 9.2. Time-course evolution of (A) specific eGFP production (assayed by fluorometry) and (B) percentage of eGFP-expressing cells (assayed by fluorescence microscopy) in induced (-■-) and non-induced (-□-) biofilms. The vertical dotted lines indicate the induction point. The means ± SDs for three independent experiments are indicated. Statistical analysis corresponding to each time point is represented with ∗ for a confidence level greater than 90% ($P < 0.1$) and with $\overset{*}{*}$ for a confidence level greater than 95% ($P < 0.05$).

The maximum and minimum values of fluorescence intensity obtained from each of the 45 microscopic images of each day for induced and non-induced conditions were ordered and represented in Figure 9.3. This analysis was performed 6 h after induction

(day 5) and on later representative days (day 6, 8 and 11). The results of day 5 show that 6 h after induction the amount of eGFP produced by the high- and low-level producing cells was higher than the leaky expression of both types of cells in non-induced biofilms (17% and 3%, respectively). Furthermore, as the experiment progressed, a gradual increase in the maximum and minimum fluorescence intensity of induced cells was observed when compared to the non-induced state. In fact, the difference in expression levels between induced and non-induced cultures (evidenced by the grey areas shown in Figure 9.3) seems to be progressively higher, reaching its maximum at the last day of experiment. On day 11, the maximum and minimum expression levels were higher than the correspondent values for non-induced cells (48% and 55%, respectively), and the highest gaps between both expression conditions were also obtained (40% for induced and 48% for non-induced cells). Thus, IPTG induction also increased the gap between high-level and low-level producers.

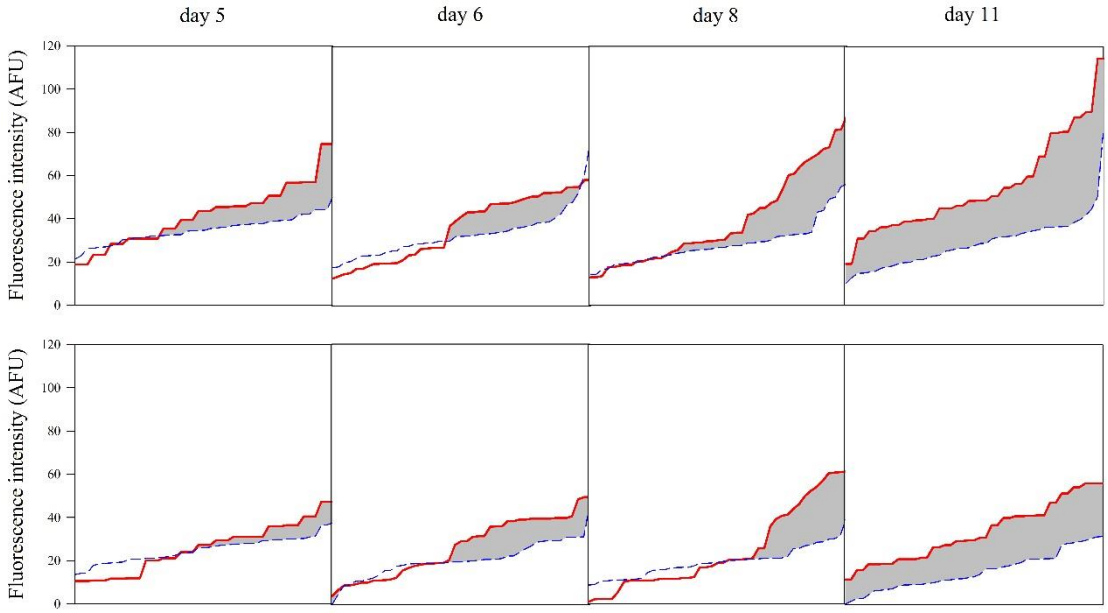

Figure 9.3. Evolution of the maximum (top) and minimum (bottom) fluorescence intensity of non-induced (----) and induced (——) expressing biofilm cells. The fluorescence values of 45 images analysed each day are arranged in ascending order. The grey areas represent the gap between induced and non-induced biofilms when the fluorescence intensities of the induced culture are higher than the non-induced culture.

9.4. Discussion

A model heterologous protein was produced in *E. coli* biofilm cells and the impact of chemical induction by IPTG was evaluated by fluorometry (a bulk method) and epifluorescence microscopy (a single-cell method). Both methods yielded similar results when the overall production by biofilm cells was assessed, thus providing an internal validation of the microscopy method. The fluorescence readings obtained from the fluorometer could be readily calibrated (using a calibration curve with purified eGFP standards), thus enabling an absolute quantification of the heterologous protein produced by biofilm cells. The main advantages of this method are its simplicity, speed and the ability to obtain an average production value for the biofilm cells (Bongaerts et al. 2002, Drees & Wu 2013, Naresh 2014). On the other hand, single-cell biofilm analysis is less simple, more time consuming and it is not straightforward to calibrate independently. However, despite these drawbacks, analysis of heterologous protein expression at single-cell level is particularly suited for biofilm systems since biofilms are known to be heterogeneous and contain several subsets of cells in different physiological states (Stewart & Franklin 2008).

The results of fluorometry indicated that induction prevented the decrease in heterologous protein production from biofilm cells and that the system was fully induced after only 6 h of IPTG addition. This observation is consistent with another report from Lenz et al. (2008) where *P. aeruginosa* PAO1(pAB1) biofilms were cultivated for 52 h in the absence of IPTG and increased fluorescence levels were observed after only 4 h of induction. Although not many studies have been performed addressing recombinant protein expression in *E. coli* biofilm cultures, a couple of reports from Huang et al. (1993, 1994a, 1995) have shown that an increase in β-galactosidase production from induced biofilm cells could be detected few hours after induction, although maximum production levels were attained 24 h after induction.

The results from the single-cell level analysis have shown that, in both induced and non-induced cultures, there was a decrease in the percentage of eGFP-expressing cells and that this decrease was more significant in the induced culture. Thus, in order to maintain the same "bulk" production level determined by fluorometry, the eGFP-producing cells had to produce the heterologous protein at much higher levels. Analysis of single-cell expression patterns has shown that both high-level producers and low-level

producers attained specific eGFP production levels which were higher in the induced state and that IPTG addition increased the gap between high-level and low-level producers. Another observation was that production heterogeneity increased with cultivation time. Recently, confocal laser microscopy analysis of *E. coli* biofilms producing eGFP under similar hydrodynamic conditions and on the same surface revealed that expressing cells were predominantly located in the upper region of the biofilm, while the bottom layer of the biofilm consisted predominantly of non-expressing cells (Gomes et al. 2016). This production heterogeneity may be caused by inefficient penetration of nutrients or oxygen (Stewart & Franklin 2008) since it has been shown that IPTG readily penetrates this type of biofilms (Stewart 2003, Werner et al. 2004). As far as nutrients are concerned, it has been shown in this reactor system that inefficient mass transfer to the biofilm cells is not due to external mass transfer limitations (Moreira et al. 2015a, Moreira et al. 2013b). In the case of oxygen transfer, it has been shown that both external and internal mass transfer limitations can be important in microbial aggregate systems, depending on the operational conditions (Wilen et al. 2004). Mass transfer inside biofilms occurs by diffusion, which in turn is dependent on architectural features like porosity and tortuosity. It has been shown in this reactor system that the hydrodynamic conditions affect external mass transfer (Moreira et al. 2013b) and that the biofilm architecture (thickness and density) is also affected by the hydrodynamic conditions and nutrient load (Teodósio et al. 2011a). These findings suggest that by careful optimization of the operational conditions, it may be possible to increase mass transfer to the bottom layers of the biofilm. With such optimization, it may be possible to increase the percentage of expressing cells and also to increase the specific production by low-level producers, attaining a substantial increase in the production of the target protein. Single-cell analysis allowed the identification of the production bottleneck in this system. The producing capacity is limited by the low percentage of expressing cells which represent only 10% of the biofilm population in steady state. The average difference between high-level producers and low-level producers was about 50% on day 11, indicating that optimization should be focused in increasing the percentage of expressing cells rather than in increasing the production levels of low-producing cells. However, as discussed above, it is likely that optimization of culture conditions may be beneficial in both aspects.

A variety of methods is available for monitoring the production of recombinant proteins and fluorescence-based methods have many advantages such as simplicity, sensitivity and low-cost (Bongaerts et al. 2002, Drees & Wu 2013, Naresh 2014). Bulk

methods provide crucial information as in most cases the contents of a production reactor will be pooled for downstream processing. However, analysis at single-cell level can help to identify cellular bottlenecks in biofilm systems, enabling the design of optimization strategies to increase the production of heterologous proteins.

9.5. References

Beloin C, Valle J, Latour-Lambert P, Faure P, Kzreminski M, Balestrino D, Haagensen JAJ, Molin S, Prensier G, Arbeille B, et al. 2004. Global impact of mature biofilm lifestyle on *Escherichia coli* K-12 gene expression. Mol Microbiol. 51:659-674.

Bongaerts RJ, Hautefort I, Sidebotham JM, Hinton JC. 2002. Green fluorescent protein as a marker for conditional gene expression in bacterial cells. Methods Enzymol. 358:43-66.

Bryers JD, Huang C-T. 1995. Recombinant plasmid retention and expression in bacterial biofilm cultures. Wat Sci Tech. 31:105-115.

Drees JC, Wu AHB. 2013. Analytical Techniques. In: Bishop ML, Fody EP, Schoeff LE, editors. Clinical Chemistry: Principles, Techniques, and Correlations. Baltimore: Lippincott Williams & Wilkins. p. 130-165.

Folsom J, Richards L, Pitts B, Roe F, Ehrlich G, Parker A, Mazurie A, Stewart P. 2010. Physiology of *Pseudomonas aeruginosa* in biofilms as revealed by transcriptome analysis. BMC Microbiol. 10:294.

Gomes LC, Carvalho D, Briandet R, Mergulhão FJ. 2016. Temporal variation of recombinant protein expression in *Escherichia coli* biofilms analysed at single-cell level. Process Biochem. (in press).

Huang C-T, Peretti SW, Bryers JD. 1993. Plasmid retention and gene expression in suspended and biofilm cultures of recombinant *Escherichia coli* DH5α(pMJR1750). Biotechnol Bioeng. 41:211-220.

Huang C-T, Peretti SW, Bryers JD. 1994a. Effects of inducer levels on a recombinant bacterial biofilm formation and gene expression. Biotechnol Lett. 16:903-908.

Huang C-T, Xu KD, McFeters GA, Stewart PS. 1998. Spatial patterns of alkaline phosphatase expression within bacterial colonies and biofilms in response to phosphate starvation. Appl Environ Microbiol. 64:1526-1531.

Lenz AP, Williamson KS, Pitts B, Stewart PS, Franklin MJ. 2008. Localized gene expression in *Pseudomonas aeruginosa* biofilms. Appl Environ Microbiol. 74:4463-4471.

Mergulhão FJM, Monteiro GA, Cabral JMS, Taipa MA. 2004b. Design of bacterial vector systems for the production of recombinant proteins in *Escherichia coli*. J Microbiol Biotechnol. 14:1-14.

Moreira JMR, Simões M, Melo LF, Mergulhão FJ. 2015a. The combined effects of shear stress and mass transfer on the balance between biofilm and suspended cell dynamics. Desal Water Treat. 53:3348-3354.

Moreira JMR, Teodósio JS, Silva FC, Simões M, Melo LF, Mergulhão FJ. 2013b. Influence of flow rate variation on the development of *Escherichia coli* biofilms. Bioprocess Biosyst Eng. 36:1-10.

Naresh K. 2014. Applications of fluorescence spectroscopy. J Chem Pharm Sci. 974:2115.

O'Connell HA, Niu C, Gilbert ES. 2007. Enhanced high copy number plasmid maintenance and heterologous protein production in an *Escherichia coli* biofilm. Biotechnol Bioeng. 97:439-446.

Palomares LA, Estrada-Mondaca S, Ramirez OT. 2004. Production of recombinant proteins: challenges and solutions. Methods Mol Biol. 267:15-52.

Rani SA, Pitts B, Beyenal H, Veluchamy RA, Lewandowski Z, Davison WM, Buckingham-Meyer K, Stewart PS. 2007. Spatial patterns of DNA replication, protein synthesis, and oxygen concentration within bacterial biofilms reveal diverse physiological states. J. Bacteriol. 189:4223-4233.

Sanchez-Garcia L, Martín L, Mangues R, Ferrer-Miralles N, Vázquez E, Villaverde A. 2016. Recombinant pharmaceuticals from microbial cells: a 2015 update. Microb Cell Fact. 15:1-7.

Stewart PS. 2003. Diffusion in biofilms. J Bacteriol. 185:1485-1491.

Stewart PS, Franklin MJ. 2008. Physiological heterogeneity in biofilms. Nat Rev Micro. 6:199-210.

Teodósio JS, Simões M, Melo LF, Mergulhão FJ. 2011a. Flow cell hydrodynamics and their effects on *E. coli* biofilm formation under different nutrient conditions and turbulent flow. Biofouling. 27:1-11.

Werner E, Roe F, Bugnicourt A, Franklin MJ, Heydorn A, Molin S, Pitts B, Stewart PS. 2004. Stratified growth in *Pseudomonas aeruginosa* biofilms. Appl Environ Microbiol. 70:6188-6196.

Wilen BM, Gapes D, Keller J. 2004. Determination of external and internal mass transfer limitation in nitrifying microbial aggregates. Biotechnol Bioeng. 86:445-457.

10.

Conclusions and suggestions for future work

10.1. Conclusions

The main goal of this thesis was to assess the effect of biofilm formation on recombinant protein expression using a model recombinant protein (eGFP) and biofilms formed by tranformed *E. coli* JM109(DE3).

This work started with the characterization of the hydrodynamics inside the wells of a 96-well microtiter plate under different orbital shaking conditions in order to validate the use of this platform for biofilm studies, including the screening for cultivation parameters involved in recombinant protein production in biofilm cells. Numerical simulations using CFD revealed that the 96-well microtiter plate is a powerful platform for biofilm simulation in a variety of applications, including biomedical scenarios, if the operating conditions are carefully set. However, it fails to achieve the same average shear stress value obtained in the flow cell system operating in turbulent conditions. Additionally, the combined effects of hydrodynamics and nutrient levels on *E. coli* biofilm formation were assessed by the crystal violet assay. The overall results of glucose experiments indicated that higher glucose concentrations may be beneficial for cell adhesion in the first 24 hours, independently of the shaking conditions. Neverthless, variation of peptone and yeast extract concentration had no impact on biofilm formation.

The shear strain rate distribution inside 96-well microtiter plates was then related to the biofilm localization assessed by SEM. Although the macroscale techniques used did not reveal any bulk differences on the amount and metabolic state of sessile cells in different hydrodynamic conditions, SEM analysis showed differences in the spatial distribution and cell length in biofilms when comparing shaking with static conditions.

Wall regions subjected to higher shear strain rates (such as those closer to the air-liquid interface) are associated with the formation of cell aggregates for both hydrodynamic conditions, while low shear strain rate conditions (such as those found at the wall bottom) were not favorable for bacterial adhesion and thus single cells were uniformly distributed throughout the surface. On the other hand, biofilms formed under the shaking condition had higher number of cells than in the static condition, and the cell length was smaller than in static. A differential CV staining method was also developed to determine the location of adherent cells in 96-well microtiter plates. This novel method is quicker, less expensive and has higher throughput than SEM in determining the spatial location of biofilms. These results highlight the wealth of information that may be gathered by complementing macroscale approaches with a microscale analysis of biofilms.

The impact of *E. coli* biofilm formation on recombinant protein expression was evaluated in a flow cell system, however the 96-well microtiter plate previously characterized was used for the screening of cultivation conditions. Biofilm formation was enhanced for the eGFP-producing strain when compared to the strain harbouring the pET28A plasmid. Moreover, it was demonstrated that the sessile cells can produce a model heterologous protein at much higher levels than planktonic cells and that the cellular densities and volumetric productivities are already within the range of that can be obtained by conventional HCDC, even without optimization of culture conditions.

Since heterologous protein production is dependent on the composition of the culture medium, the influence of the concentration of antibiotic used to maintain the selective pressure and the nutrient medium composition was assessed. Increasing the kanamycin concentration from 20 to 30 μg ml^{-1} had a modest effect on the specific eGFP production by biofilm cells. Thus, using the lowest antibiotic concentration may be the best option for recombinant protein, not only due to the cost of antibiotic, but also because of the dissemination of antibiotic resistance. The specific production values were always higher in the biofilm when compared to planktonic cells, albeit the highest levels were obtained in LB medium.

Later on, experiments were performed in order to understand the influence of IPTG induction in the potential of biofilm cells to produce the heterologous protein. There were no major effects on the biofilm cell number, viability and EPS composition. However, with regard to eGFP production, it is possible to conclude that the inducer had an instantaneous impact on sessile cells, preventing the decrease in the amount of expressed eGFP. Due to the analysis of heterologous protein transcription and cellular

metabolic activity, it was also possible to demonstrate that the expression profile was not related with the gene dosage. Also in inducing conditions, higher specific production levels were attained with biofilm cells and it seems that while induction of biofilm cells shifts their metabolism towards the maintenance of heterologous protein concentration, in planktonic cells the cellular resources are directed towards plasmid replication and growth. Additionally, it was established that the biofilm environment enhances plasmid retention.

The final accomplished task within this thesis dealt with the distribution of expressed eGFP at a single-cell scale during *E. coli* biofilm formation. The proposed methodology based on epifluorescence microscopy revealed that, during biofilm growth in a non-induced culture, the sessile population became increasingly heterogeneous with regard to eGFP expression. Moreover, confocal microscopy showed spatial heterogeneity, with the cells actively producing eGFP restricted to the top layer of the biofilm. Regarding induced cultures, IPTG addition not only increased the specific production, but also increased the heterogeneity of eGFP production within the biofilms. The analysis at single-cell level also enabled the identification of the production bottleneck in this system, consisting in a low percentage of expressing cells in the biofilm population.

Overall, this thesis demonstrates the potential of *E. coli* biofilms to be used as cell factories for the production of recombinant proteins. Among the cultivation conditions tested in the flow cell system, LB supplemented with 20 μg ml^{-1} kanamycin and 2 mM IPTG is the most advantageous medium to obtain the highest specific eGFP concentration in biofilm cells. Despite the high specific production yield that has already been achieved under this condition, single-cell analysis indicated that the producing capacity of the biofilm system was limited by the low percentage of expressing cells, which represented only 10% of the bacterial population in steady state. The indentification of this bottleneck allows the further design of optimization strategies to increase the bulk production of recombinant protein during process development.

10.2. Suggestions for future work

The 96-well microtiter plate has been used as a high throughput screening platform for antimicrobial compounds (Pitts et al. 2003, Quave et al. 2008, Shakeri et al. 2007) and to study cell adhesion and biofilm formation (Simões et al. 2010a, Stepanović et al. 2000). However, these studies have been made with little knowledge about the influence of hydrodynamic conditions and oxygen transfer on biofilm development in this system. In this thesis, the hydrodynamic characterization inside the 96-well microtiter plate was performed and its effect on biofilm formation was evaluated. Different studies have addressed the oxygen transfer in microtiter plates by numerical simulation (Doig et al. 2005, Ramirez-Vargas et al. 2014, Zhang et al. 2008) and it is known that oxygen transfer can affect bacterial growth, being a major factor in microbial processes (Garcia-Ochoa & Gomez 2009). Therefore, it would be interesting to study the gas-liquid mass transfer phenomena in a single well by determining the oxygen transfer rates at different orbital shaking intensities (different shaking frequencies and shaking diameters at constant filling volume). The simulation results can be further supported by the experimental determination of volumetric oxygen mass transfer coeficients ($k_L a$) using the sodium sulfite oxidation method (Hermann et al. 2003).

In this thesis, single-cell analysis of *E. coli* biofilms revealed that only 10% of the cells are producing eGFP in the best cultivation condition found. In addition, these expressing cells are predominantly located in the upper region of the biofilm, while the bottom layers consist mainly of non-expressing cells. This biofilm heterogeneity may be due to the lack of oxygen, which is required for eGFP maturation, or to mass transfer limitation of other nutrients. In the case of oxygen transfer, it has been shown that both external and internal mass transfer limitations are important in microbial aggregate systems (Wilen et al. 2004). Mass transfer inside biofilms occurs by diffusion, which is dependent on architectural features like porosity and tortuosity. Therefore, optimizing the hydrodynamic conditions for obtaining a more porous biofilm will facilitate the acess of the bottom layers of biofilm to oxygen and fresh nutrients. With such optimization, it may be possible to increase the percentage of eGFP-expressing cells, as well as the specific production of low-level producers, attaining a substantial increase in the global production of the target protein.

It is well documented that recombinant protein expression imposes a metabolic burden on *E. coli* (Bentley et al. 1990). Nevertheless, it is not understood how the metabolic burden associated with recombinant protein production disrupts or redirects gene regulation. *E. coli* was completely sequenced in 1997 (Haddadin & Harcum 2005), and this has allowed researchers to use DNA microarrays to globally quantify gene expression changes in this bacterium under different stress conditions such as biofilm formation, hydrogen peroxide exposure and high-cell density fermentations (Bolivar et al. 1977, del Solar & Espinosa 2000, Haddadin & Harcum 2005). Few researchers have examined the global gene expression in recombinant *E. coli* (Davies & Geesey 1995, Ehlers 2000, Haddadin & Harcum 2005, Madsen et al. 2013, Oh & Liao 2000, Ow et al. 2006). Furthermore, to the best of our knowledge, no reports determined the gene expression profile for biofilms producing a recombinant protein. Thus, it would be interesting to correlate the response of sessile cells to foreign protein expression with changes in the transcriptome. Another interesting approach would be to combine the global transcriptional expression analysis with a proteomic study using two-dimensional gel electrophoresis in order to determine the changes of synthesis of host cell proteins during recombinant protein production. Expressing a recombinant protein probably disturbs global gene expression and leads to significant changes in central metabolic pathways in the host. Hence further investigation at gene expression level would greatly contribute to the development of a better *E. coli* strain for protein production in biofilms.

10.3. References

Bentley WE, Mirjalili N, Andersen DC, Davis RH, Kompala DS. 1990. Plasmid-encoded protein: the principal factor in the “metabolic burden” associated with recombinant bacteria. Biotechnol Bioeng. 35:668-681.

Bolivar F, Rodriguez RL, Greene PJ, Betlach MC, Heyneker HL, Boyer HW, Crosa JH, Falkow S. 1977. Construction and characterization of new cloning vehicles. II. A multipurpose cloning system. Gene. 2:95-113.

Davies DG, Geesey GG. 1995. Regulation of the alginate biosynthesis gene algC in *Pseudomonas aeruginosa* during biofilm development in continuous culture. Appl Environ Microbiol. 61:860-867.

del Solar G, Espinosa M. 2000. Plasmid copy number control: an ever-growing story. Mol Microbiol. 37:492-500.

Doig SD, Pickering SCR, Lye GJ, Baganz F. 2005. Modelling surface aeration rates in shaken microtitre plates using dimensionless groups. Chem Eng Process. 60:2741-2750.

Ehlers LJ. 2000. Gene Transfer in Biofilms. In: DG A, P G, HM L-S, M W, editors. Community Structure and Co-operation in Biofilms. Cambridge: Cambridge University Press. p. 215-254.

Garcia-Ochoa F, Gomez E. 2009. Bioreactor scale-up and oxygen transfer rate in microbial processes: an overview. Biotechnol Adv. 27:153-176.

Haddadin F, Harcum S. 2005. Transcriptome profiles for high-cell-density recombinant and wild-type *Escherichia coli*. Biotechnol Bioeng. 90:127-153.

Hermann R, Lehmann M, Büchs J. 2003. Characterization of gas-liquid mass transfer phenomena in microtiter plates. Biotechnol Bioeng. 81:178-186.

Madsen JS, Burmolle M, Sorensen SJ. 2013. A spatiotemporal view of plasmid loss in biofilms and planktonic cultures. Biotechnol Bioeng. 110:3071-3074.

Oh M, Liao J. 2000. DNA microarray detection of metabolic responses to protein overproduction in *Escherichia coli*. Metab Eng. 2:201-209.

Ow D, Nissom P, Philp R, Oh S, Yap M. 2006. Global transcriptional analysis of metabolic burden due to plasmid maintenance in *Escherichia coli* DH5α during batch fermentation. Enzyme Microb Technol. 39:391-398.

Pitts B, Hamilton MA, Zelver N, Stewart PS. 2003. A microtiter-plate screening method for biofilm disinfection and removal. J Microbiol. Methods. 54:269-276.

Quave CL, Plano LRW, Pantuso T, Bennett BC. 2008. Effects of extracts from Italian medicinal plants on planktonic growth, biofilm formation and adherence of methicillin-resistant *Staphylococcus aureus*. J Ethnopharmacol. 118:418-428.

Ramirez-Vargas R, Vital-Jacome M, Camacho-Perez E, Hubbard L, Thalasso F. 2014. Characterization of oxygen transfer in a 24-well microbioreactor system and potential respirometric applications. J Biotechnol. 186:58-65.

Shakeri S, Kermanshahi RK, Moghaddam MM, Emtiazi G. 2007. Assessment of biofilm cell removal and killing and biocide efficacy using the microtiter plate test. Biofouling. 23:79-86.

Simões LC, Simões M, Vieira M. 2010a. Adhesion and biofilm formation on polystyrene by drinking water-isolated bacteria. Antonie van Leeuwenhoek. 98:317-329.

Stepanović S, Vuković D, Dakić I, Savić B, Švabić-Vlahović M. 2000. A modified microtiter-plate test for quantification of staphylococcal biofilm formation. J Microbiol Methods. 40:175-179.

Wilen BM, Gapes D, Keller J. 2004. Determination of external and internal mass transfer limitation in nitrifying microbial aggregates. Biotechnol Bioeng. 86:445-457.

Zhang H, Lamping SR, Pickering SCR, Lye GJ, Shamlou PA. 2008. Engineering characterisation of a single well from 24-well and 96-well microtitre plates. Biochem Eng J. 40:138-149.